AWARD NUMBER: W81XWH-12-1-0153

TITLE: Probing Androgen Receptor Signaling in Circulating Tumor Cells in Prostate Cancer

PRINCIPAL INVESTIGATOR: David T. Miyamoto, MD, PhD

RECIPIENT: Massachusetts General Hospital, Boston, MA 02114

REPORT DATE: October 2017

TYPE OF REPORT: Final Summary

PREPARED FOR: U.S. Army Medical Research and Materiel Command
Fort Detrick, Maryland 21702-5012

REPORT DOCUMENTATION PAGE

Form Approved
OMB No. 0704-0188

1. REPORT DATE	2. REPORT TYPE	3. DATES COVERED
October 2017	Final Summary	1 July 2012 – 30 June 2017

4. TITLE AND SUBTITLE

Probing Androgen Receptor Signaling in Circulating Tumor Cells in Prostate Cancer

5a. CONTRACT NUMBER

5b. GRANT NUMBER
W81XWH-12-1-0153

5c. PROGRAM ELEMENT NUMBER

6. AUTHOR(S)
David T. Miyamoto

E-Mail: dmiyamoto@partners.org

5d. PROJECT NUMBER

5e. TASK NUMBER

5f. WORK UNIT NUMBER

7. PERFORMING ORGANIZATION NAME(S) AND ADDRESS(ES)

Massachusetts General Hospital
55 Fruit Street
Boston, MA 02114-2621

8. PERFORMING ORGANIZATION REPORT NUMBER

9. SPONSORING / MONITORING AGENCY NAME(S) AND ADDRESS(ES)

U.S. Army Medical Research and Materiel Command
Fort Detrick, Maryland 21702-5012

10. SPONSOR/MONITOR'S ACRONYM(S)

11. SPONSOR/MONITOR'S REPORT NUMBER(S)

12. DISTRIBUTION / AVAILABILITY STATEMENT

Approved for Public Release; Distribution Unlimited

13. SUPPLEMENTARY NOTES

14. ABSTRACT

This Physician Research Training Award supports a mentored training program integrated with a research project focused on the study of circulating tumor cells (CTCs) in prostate cancer patients using a microfluidic device ("CTC-chip") to isolate CTCs from peripheral blood samples. During this award, we developed a quantitative immunofluorescence assay to measure AR activity in CTCs in patients with metastatic prostate cancer receiving treatment with hormonal therapy. We also developed methods for single CTC RNA-seq and digital gene expression profiling, and applied these techniques to single prostate CTCs. We analyzed single cell transcriptomes to reveal the heterogeneity of CTCs, and to identify key genes and molecular pathways enriched in CTCs that may contribute to treatment resistance in prostate cancer, including AR splice variants and the non-canonical Wnt pathway. Finally, this Award provided valuable protection of time for research and mentored training of the PI, and was essential in enabling his development towards a productive independent career in translational prostate cancer research.

15. SUBJECT TERMS
prostate cancer, circulating tumor cells, androgen receptor, castration-resistant prostate cancer, RNA sequencing, single cell

16. SECURITY CLASSIFICATION OF:			17. LIMITATION OF ABSTRACT	18. NUMBER OF PAGES	19a. NAME OF RESPONSIBLE PERSON
a. REPORT	b. ABSTRACT	c. THIS PAGE			USAMRMC
Unclassified	Unclassified	Unclassified	Unclassified	132	19b. TELEPHONE NUMBER *(include area code)*

Table of Contents

Page

INTRODUCTION

Castration-resistant prostate cancer (CRPC) is thought to arise from the persistence of androgen receptor (AR) signaling in cancer cells despite castrate levels of testosterone (1). As second line AR targeting therapies have entered clinical care for CRPC (e.g. abiraterone acetate and enzalutamide) in addition to cytotoxic therapeutics (e.g. docetaxel, cabazitaxel, Ra-223), no reliable biomarkers exist to target appropriate therapies to individual patients (2, 3). In the Research Project supported by this Physician Research Training Award, we used a novel microfluidic technology (the "CTC-chip") to interrogate the status of AR signaling and other signaling pathways in circulating tumor cells (CTCs) isolated from metastatic prostate cancer patients in an effort to develop novel biomarkers to guide therapy, as well as to understand the biology of CRPC. An AR activity signature developed in prostate cancer cell lines were applied to CTCs in patients with castration-resistant prostate cancer (CRPC) before and after secondary hormonal therapies to test the hypothesis that effective suppression of AR signaling in CTCs correlates with clinical response to hormonal therapy. To identify novel genes and pathways involved in the evolution of treatment resistant disease, digital gene expression profiling of single CTCs was performed. These studies provided initial validation of novel molecular biomarkers that can monitor and predict responses to second-line hormonal therapy in patients with CRPC, and also revealed insights into the mechanisms underlying treatment resistance in prostate cancer. In combination with this integrated research project, this Physician Research Training Award enabled the PI to have protected time for research and mentored training towards his development into an independent translational prostate cancer researcher.

Specific Aims

1. Define an AR activity score in CTCs and test the hypothesis that AR signaling activity in prostate CTCs correlates with response to second-line hormonal therapy in metastatic prostate cancer patients.

2. Perform digital gene expression (DGE) profiling of prostate CTCs to identify novel pathways that promote castration resistance.

Key Words

prostate cancer, circulating tumor cells, androgen receptor, castration-resistant prostate cancer, RNA sequencing, single cell

BODY

Accomplishments and Progress on Statement of Work (SOW).

In this Research Project, we developed a single cell immunofluorescence-based assay for measurement of AR activity in CTCs, and demonstrated feasibility of using this assay as a potential biomarker to monitor and predict response to second line hormonal therapy in patients with castration-resistant prostate cancer (CRPC) (4, 5). We also demonstrated feasibility of performing high throughput qRT-PCR and whole transcriptome RNA-sequencing of single prostate CTCs, using a 3rd generation CTC isolation platform, the CTC-iChip (6, 7). We demonstrated our ability to obtain high quality whole transcriptome RNA-seq data from single CTCs, and have applied this single cell RNA-seq technique to CTCs isolated from patients with prostate cancer. We completed extensive bioinformatic analyses to identify molecular pathways that are enriched in CTCs, resulting in identification of the non-canonical Wnt signaling pathway as significantly associated with treatment resistance (8). These studies have resulted in several manuscripts that have now been published (see Reportable Outcomes and Appendix).

Progress on Tasks related to the Research Project are outlined below.

Task 1. Regulatory review and approval of clinical protocol.

A minimal risk clinical research protocol for the collection of blood from patients with solid tumors for CTC analysis (DF/HCC 05-300) was initially received by the US Army Medical Research and Materiel Command (USAMRMC), Office of Research Protections (ORP), Human Research Protection Office (HRPO) on 9 May 2012, and reviewed for compliance with human subject protection requirements. A revised research consent form and clinical research protocol was approved by the HRPO on 7 June 2012, and this revised protocol was approved by the Dana-Farber Cancer Institute Institutional Review Board (DFCI IRB) on 12 July 2012. The final protocol received approval by the HRPO on 30 July 2012. Continuation of the subject protocol was approved by the DFCI IRB on 30 May 2013, 9 May 2014, 17 June 2015, 30 May 2016, and 1 March 2017. Since DF/HCC 05-300 is an umbrella minimal risk clinical research protocol for multiple other research projects funded by several different sponsors in addition to this DOD award, the protocol will remain active with the DFCI IRB following completion of this DOD award.

Task 2. (Aim 1) Recruitment of patients with castration-resistant prostate cancer for CTC AR activity analysis.

Patients with CRPC were recruited for the purposes of AR activity analysis in CTCs. Of note, the overall accrual rate was slower than initially anticipated due to a transition in CTC isolation technology in the laboratory from the 2nd generation HB CTC-chip technology (9) to the 3rd generation CTC iChip technology (6). However, once this technology was incorporated into the laboratory, the goal subject accrual was met during the remainder of this project.

Task 3. (Aim 1) CTC AR signature activity analysis in patients.

As part of this Research Project, we developed a novel CTC-based single cell immunophenotyping approach to measure AR activity in CTCs using two genes that we identified as most consistently upregulated and downregulated following AR modulation in prostate cancer cells: PSA (androgen driven) and PSMA (androgen suppressed). The details of this assay were published in *Cancer Discovery* during this reporting period (see Reportable Outcomes and Appendices) (4).

Briefly, after developing and testing our immunofluorescence-based AR activity assay using androgen responsive prostate cancer cell lines, we identified PSA+/PSMA- cells as androgen activated (AR-on) and PSA-/PSMA+ cells as androgen suppressed (AR-off). In transition between AR-on and AR-off states, we identified PSA+/PSMA+ (AR-mixed) cells. Application of this CTC-based assay in a small cohort of men with prostate cancer revealed several interesting findings. In treatment-naïve men with metastatic prostate cancer, the majority of CTCs were AR-on. Within 4 weeks of initiation of androgen deprivation therapy, these CTCs turned predominantly to AR-off, and CTC counts thereafter dropped below detection. In contrast, striking heterogeneity was evident in CRPC where some patients had only AR-on cells, some had only AR-off cells, and others had large numbers of dual positive AR-mixed cells. In a cohort of patients with CRPC treated with abiraterone acetate, the presence of AR-mixed cells prior to treatment or an increase in AR-on cells despite therapy were associated with decreased overall survival. Together, these studies point to a novel approach to measure the fraction of CTCs that are AR-driven and likely to be sensitive to hormonal therapy. These results are described in detail in the manuscript published in *Cancer Discovery* during this reporting period (4) (see Reportable Outcomes and Appendices).

Task 4. (Aim 2) Recruitment of patients with metastatic castration-resistant prostate cancer and metastatic castration-sensitive prostate cancer for digital gene expression profiling.

We recruited 24 patients with metastatic prostate cancer and 14 patients with localized untreated prostate cancer for the purposes of digital gene expression profiling of CTCs, isolated using the 3rd generation CTC iChip technology (6). Of these, 18 metastatic and 4 localized prostate cancer patients had detectable CTCs. Single CTC RNA-seq and digital gene expression profiling analysis of CTC samples from these patients have been described in our manuscript, published in *Science* during this reporting period (see Reportable Outcomes and Appendices) (8).

Task 5. (Aim 2) Digital gene expression profiling of CTCs including sample preparation and RNA sequencing.

One of the goals of this Research Project is to identify cellular pathways that underlie the acquisition of treatment resistance in prostate cancer by dissecting the transcriptome of CTCs. We demonstrated that the third generation CTC-chip technology (CTC-iChip) can be used to generate high purity CTC preparations in solution that can be micromanipulated for single cell analysis, enabling single cell whole transcriptome RNA-seq of CTCs from a mouse model of pancreatic cancer (7). We then used these techniques to isolate and sequence CTCs from blood acquired from human prostate cancer patients. The details of this work were published in *Science* during this reporting period (8) (see Reportable Outcomes and Appendix).

Briefly, untagged and unfixed CTCs were identified by cell surface staining for epithelial (EpCAM) and mesenchymal (CDH11) markers and absent staining for the common leukocyte marker CD45. A total of 221 single candidate prostate CTCs were isolated from 18 patients with metastatic prostate cancer and 4 patients with localized prostate cancer. Of these, 133 cells (60%) had RNA of sufficient quality for amplification and next generation RNA sequencing, and 122 (55%) had >100,000 uniquely aligned sequencing reads. In addition to candidate CTCs, we also obtained comprehensive transcriptomes for bulk primary prostate cancers from a separate cohort of 12 patients (macrodissected for >70% tumor content), 30 single cells derived from four different prostate cancer cell lines, and 5 patient-derived leukocyte controls. The leukocytes were readily distinguished by their expression of hematopoietic lineage markers and served to exclude any CTCs with potentially contaminating signals. Strict expression thresholds were used to define lineage-confirmed CTCs, scored by prostate lineage-specific genes (*PSA*, *PSMA*, *AMACR*, *AR*) and standard epithelial markers (*KRT7, KRT8*, *KRT18*, *KRT19*, *EPCAM*). Twenty-eight cells were excluded given the presence of leukocyte transcripts suggestive of cellular contamination or misidentification during selection, and 17 cells were excluded given low expression of both prostate lineage-specific genes and standard epithelial markers. The remaining 77 cells (from 13 patients; average of 6 CTCs per patient) were defined as lineage-confirmed CTCs. Further details are provided in our manuscript published in *Science* during this reporting period (see Reportable Outcomes and Appendices) (8).

Task 6. (Aim 2) Data analysis of CTC digital gene expression profiles.

During this reporting period, we completed analysis of the whole transcriptome digital gene expression profiles of the lineage-confirmed CTCs that were sequenced as described in Task 5. Details of this analysis are provided in our manuscript published in *Science* during this reporting period (see Reportable Outcomes and Appendices) (8).

Briefly, unsupervised hierarchical clustering analysis of single prostate CTCs, primary tumor samples, and cancer cell lines resulted in their organization into distinct clusters. Single CTCs from an individual patient showed considerably greater intercellular heterogeneity in their transcriptional profiles than single cells from prostate cancer cell lines (mean correlation coefficient 0.10 vs. 0.44, $P<1x10^{-20}$), but they strongly clustered according to patient of origin, indicating higher diversity in CTCs from different patients (mean correlation coefficient 0.10 for CTCs within patient vs. 0.0014 for CTCs between patients, $P=2.0x10^{-11}$).

We then performed differential gene expression analysis to identify genes that are upregulated in prostate CTCs compared to primary tumor samples. A total of 711 genes were highly expressed in CTCs compared to primary tumors, with the most enriched being the molecular chaperone *HSP90AA1*, which regulates the activation and stability of AR, among other functions (10), and the non-coding RNA transcript *MALAT1*, which has been implicated in alternative mRNA splicing and transcriptional control of gene expression (11) (FDR<0.1 and fold-change >2). We used the Pathway Interaction Database (PID) (12) to identify key molecular pathways upregulated in CTCs versus primary tumors, as well as those upregulated in metastatic versus primary prostate tumors based on analyses of previously published datasets. In total, 21 pathways were specifically enriched in prostate CTCs, with the majority implicated in growth factor, cell adhesion, and hormone signaling.

We then performed retrospective differential analyses in subsets of CTCs to identify mechanisms of resistance to enzalutamide. From eight patients with metastatic prostate cancer who had not received enzalutamide (group A), 41 CTCs were compared with 36 CTCs from five patients whose cancer exhibited radiographic and/or PSA progression during therapy (group B). Gene set enrichment analysis (GSEA) of candidate PID cellular signaling pathways showed significant enrichment for noncanonical Wnt signaling in group B compared with group A CTCs (P=0.0064; FDR = 0.239). This signaling pathway, activated by a subset of Wnt ligands, mediates multiple downstream regulators of cell survival, proliferation, and motility (13). A separate analysis using a metagene for the PID non-canonical Wnt signature confirmed enrichment of the signature in group B compared with group A CTCs, at the level of both individual CTCs and individual patients (P=0004 for CTCs). Among the downstream components of non-canonical Wnt, the most significantly enriched were *RAC1*, *RHOA*, and *CDC42*, signaling molecules involved in actin cytoskeleton and cell migration.

Although most studies of CRPC have focused on acquired *AR* gene abnormalities, an alternative pathway, glucocorticoid receptor (GR) signaling, has recently been shown to contribute to anti-androgen resistance in a prostate cancer mouse xenograft model (14). Interestingly, we noted an inverse relationship in our human prostate CTC data set between *GR* expression and non-canonical Wnt signaling. Among CTCs with low *GR* expression, GSEA analysis showed significant enrichment for non-canonical Wnt signaling in enzalutamide-progressing patients (group B) (P=0.025), which was absent in CTCs with high *GR* expression (P=0.34). Thus, these two AR-independent drug resistance pathways may predominate in different subsets of cancer cells. Further details are provided in our manuscript published in *Science* during this reporting period (see Reportable Outcomes and Appendices) (8).

Task 7. (Aim 2) Validation and follow-up studies of promising genes and pathways identified through CTC digital gene expression profiles.

We engaged in validation studies in the laboratory based on genes and pathways implicated in disease progression and treatment resistance through our analysis of CTC transcriptional profiles described above. Details of these studies are provided in our manuscript published in *Science* during this reporting period (see Reportable Outcomes and Appendices) (8).

Briefly, to test whether activation of non-canonical Wnt signaling modulates enzalutamide sensitivity, we ectopically expressed the non-canonical Wnt ligands *WNT4, WNT5A, WNT7B,* or *WNT11* in LNCaP androgen-sensitive prostate cancer cells, which express low endogenous levels (Appendix, Fig. S7A and S7B). Survival of the AR-positive LNCaP cells in the presence of enzalutamide was enhanced by the non-canonical Wnt ligands, particularly *WNT5A* (Appendix, Fig. 4A and Fig. S7C; $P=2.8 \times 10^{-5}$). Remarkably, endogenous *WNT5A* was acutely induced upon treatment with enzalutamide, suggestive of a feedback mechanism, and its depletion (knockdown) resulted in reduced cell proliferation (Appendix, Fig. 4B and Fig. S7D; $P=6.6 \times 10^{-4}$). We also generated stable enzalutamide-resistant LNCaP cells through prolonged in vitro selection (Appendix, Fig. S7E). These cells also exhibited increased expression of endogenous *WNT5A*, whose suppression reduced proliferation in enzalutamide-supplemented medium (Appendix, Fig. 4C and Fig. S7F). Finally, we tested the contribution of non-canonical

Wnt signaling to antiandrogen resistance in an independent data set, interrogating a previously published mouse LNCaP xenograft model, in which aberrant activation of GR contributes to enzalutamide resistance (14). A significant association between enzalutamide resistance and non-canonical Wnt signaling was evident (P=0.023), which again showed an inverse relation between *GR* expression and non-canonical Wnt signaling (P=0.032 for *GR* low versus P=0.11 for *GR* high; Appendix, Fig. 4D and Fig. S8, A and B). This independent data set further validates the independent contributions of GR and non-canonical Wnt signaling to anti-androgen resistance. Further details are provided in our manuscript published in *Science* during this reporting period (see Reportable Outcomes and Appendices) (8).

Task 8. Preparation of results, presentations, and manuscripts.

This Research Project has resulted in multiple publications and presentations, described in detail in the Reportable Outcomes section. We published a manuscript in Cancer Discovery in 2012 describing our results analyzing AR signaling activity in CTCs using the PSA/PSMA immunfluorescence-based assay (4). Pilot data demonstrating the isolation of single CTCs using the CTC-iChip followed by microfluidic multigene qRT-PCR was published as part of a manuscript in Science Translational Medicine in 2013 (6). We also published a manuscript in *Science* in 2015 describing our single cell RNA-sequencing whole transcriptome profiling of prostate CTCs, and our finding implicating the noncanonical Wnt signaling pathway in resistance to enzalutamide therapy (8). A critical review on the potential of CTCs for monitoring and predicting treatment response in prostate cancer was published in Nature Reviews Clinical Oncology in 2014 (5). In addition, the PI delivered several presentations at national and international meetings, as described in detail in the Reportable Outcomes section.

Training and Professional Development of PI.

This Physician Research Training Award combines a training plan for the PI consisting of mentorship, coursework, conferences, seminars, and patient care, together with an integrated research project to enable the PI to become an effective translational investigator in prostate cancer. During this award, I attended regular formal mentorship meetings with Dr. Daniel Haber and Dr. Shyamala Maheswaran to discuss my research progress and future research directions. I also met with Dr. Matthew Smith on a regular basis for continued guidance regarding clinical aspects of my research. I also received scientific guidance from key collaborators and advisors, including Dr. Mehmet Toner and Dr. Sridhar Ramaswamy.

With regard to coursework, conferences, and seminars, I have completed formal courses in clinical trial design, biostastistics, informed consent, and data safety and monitoring through the MGH Clinical Research Program Education Unit. I attended regularly scheduled educational conferences, including the biweekly MGH multi-disciplinary urologic oncology conference, the MGH Cancer Center Grand Rounds, and the MGH Radiation Oncology chart rounds. I also attended and presented at multiple national annual conferences directly relevant to my research, including the Annual Meeting of the American Association for Cancer Research (AACR) and the Annual American Society for Radiation Oncology (ASTRO) meetings.

Finally, as a component of my training as a physician scientist specialized in prostate cancer, I continued to engage in the clinical care of patients as a radiation oncologist specializing in genitourinary malignancies. I devoted 1 day a week to the care of patients undergoing or who have completed radiation therapy, and a half day per week providing new consultations for patients presenting to the MGH Multidisciplinary GU Oncology clinic together with Urology and Medical Oncology colleagues. My clinical responsibilities were limited to 20% to 30% of my total effort. Together, this training plan has been effective in enabling my growth as a translational prostate cancer investigator.

In recognition of my potential to be a successful independent investigator in translational prostate cancer research, I was promoted to the position of Assistant Professor of Radiation Oncology at Harvard Medical School and Assistant Radiation Oncologist at the Massachusetts General Hospital in 2015, as well as a Principal Investigator in the MGH Center for Cancer Research in 2017.

KEY RESEARCH ACCOMPLISHMENTS

- Development of an androgen receptor (AR) signaling assay in CTCs based on a two-color PSA/PSMA immunofluorescence assay.
- Demonstration of the ability of the immunofluorescence-based AR signaling assay to measure AR activity in CTCs in patients with prostate cancer, and potentially predict patient outcomes after abiraterone acetate treatment.
- Development of a methodology to isolate single CTCs for RNA analysis using the microfluidic CTC-iChip.
- Demonstration of the feasibility of microfluidic qRT-PCR to measure mRNA transcript levels in single prostate CTCs.
- Demonstration of feasibility of RNA-sequencing and digital gene expression profiling of whole transcriptomes in single prostate CTCs.
- Successful RNA-sequencing of single prostate CTCs.
- Analysis of genes and pathways upregulated in CTCs compared to metastatic and primary tumors in patients with prostate cancer.
- Identification of the noncanonical Wnt signaling pathway as a potential mechanism of resistance to antiandrogen therapy in prostate cancer.

REPORTABLE OUTCOMES

Manuscripts, Abstracts, and Presentations

- Manuscripts during this reporting period:

    - **Miyamoto, D.T.**, Lee, R.J., Stott, S.L., Ting, D.T., Wittner, B.S., Ulman, M., Smas, M.E., Lord, J.B., Brannigan, B.W., Trautwein, J., Bander, N.H., Wu, C.L., Sequist, L.V., Smith, M.R., Ramaswamy, S., Toner, M., Maheswaran, S., Haber, D.A. (2012).

Androgen receptor signaling in circulating tumor cells as a marker of hormonally responsive prostate cancer. *Cancer Discovery*, 2:995-1003.

- Ozkumur, E., Shah, A.M., Ciciliano, J.C., Emmink, B.L., **Miyamoto, D.T.**, Brachtel, E., Yu, M., Chen, P., Morgan, B., Trautwein, J., Kimura, A., Sengupta, S., Stott, S.L., Karabacak, N.M., Barber, T.A., Walsh, J.R., Smith, K., Spuhler, P., Sullivan, J., Lee, R., Ting, D.T., Luo, X., Shaw, A.T., Bardia, A., Sequist, L.V., Louis, D.N., Maheswaran, S., Kapur, R., Haber, D.A., Toner, M. (2013). Inertial Focusing for Positive and Negative Sorting of Rare Circulating Tumor Cells. *Science Translational Medicine*, 5:179ra47.
- **Miyamoto, D.T.**, Sequist, L.V., Lee, R.J. (2014). Circulating tumour cells – monitoring treatment response in prostate cancer. *Nature Reviews Clinical Oncology*, 11(7):401-12.
- Ting, D.T., Wittner, B.S., Ligorio, M., Vincent Jordan, N., Shah, A.M., **Miyamoto, D.T.**, Aceto, N., Bersani, F., Brannigan, B.W., Xega, K., Ciciliano, J.C., Zhu, H., MacKenzie, O.C., Trautwein, J., Arora, K.S., Shahid, M., Ellis, H.L., Qu, N., Bardeesy, N., Rivera, M.N., Deshpande, V., Ferrone, C.R., Kapur, R., Ramaswamy, S., Shioda, T., Toner, M., Maheswaran, S., Haber, D.A. Single-cell RNA sequencing identifies extracellular matrix gene expression by pancreatic circulating tumor cells. *Cell Reports* 2014; 8:1905-18. PMID: 25242334
- **Miyamoto, D.T.**, Zheng, Y., Wittner, B.S., Lee, R.J., Zhu, H., Broderick, K.T., Desai, R., Fox, D.B., Brannigan, B.W., Trautwein, J., Arora, K.S., Desai, N., Dahl, D.M., Sequist, L.V., Smith, M.R., Kapur, R., Wu, C.L., Shioda, T., Ramaswamy, S., Ting, D.T., Toner, M., Maheswaran, S., Haber, D.A. RNA-Seq of single prostate CTCs implicates noncanonical Wnt signaling in antiandrogen resistance. *Science* 2015; 349:1351-1356. PMID: 26383955
- **Miyamoto, D.T.** and Lee, R.J. Cell-free and circulating tumor cell-based biomarkers in men with metastatic prostate cancer: Tools for real-time precision medicine? *Urologic Oncology: Seminars and Original Investigations* 2016; 34:490-501. PMID 27771279
- Hwang, W.L., Hwang, K.L., **Miyamoto, D.T.** The promise of circulating tumor cells for precision cancer therapy. *Biomarkers in Medicine* 2016; 10:1269-1285. PMID 27924634
- **Miyamoto, D.T.**, Ting, D.T., Toner, M., Maheswaran, S., and Haber, D.A. Single-cell analysis of circulating tumor cells as a window into tumor heterogeneity. In: *Cold Spring Harbor Symposia on Quantitative Biology*, Volume LXXXI. Cold Spring Harbor Laboratory Press; 2017. p. 1-6.

- Abstracts:
  - **Miyamoto, D.T.**, Zheng, Y., Wittner, B.S., Lee, R.J., Zhu, H., Broderick, K.T., Desai, R., Fox, D.B., Brannigan, B.W., Trautwein, J., Arora, K.S., Desai, N., Dahl, D.M., Sequist, L.V., Smith, M.R., Kapur, R., Wu, C.L., Shioda, T., Ramaswamy, S., Ting, D.T., Toner, M., Maheswaran, S., Haber, D.A. (June, 2015). Single cell RNA-sequencing of circulating prostate tumor cells. 2015 HHMI Scientific Meeting, Janelia Research Campus, Ashburn, VA. (Poster Presentation).
  - **Miyamoto, D.T.**, Zheng, Y., Wittner, B.S., Lee, R.J., Zhu, H., Broderick, K.T., Desai, R., Brannigan, B.W., Arora, K.S., Dahl, D.M., Sequist, L.V., Smith, M.R.,

Kapur, R., Wu, C.L., Shioda, T., Ramaswamy, S., Ting, D.T., Toner, M., Maheswaran, S., Haber, D.A. (June, 2015). Single cell RNA-sequencing of circulating tumor cells. AACR Precision Medicine Series: Integrating Clinical Genomics and Cancer Therapy, Salt Lake City, UT. (Oral Presentation).

- **Miyamoto, D.T.**, Zheng, Y., Wittner, B.S., Lee, R.J., Zhu, H., Broderick, K.T., Desai, R., Brannigan, B.W., Arora, K.S., Dahl, D.M., Sequist, L.V., Smith, M.R., Kapur, R., Wu, C.L., Shioda, T., Ramaswamy, S., Ting, D.T., Toner, M., Maheswaran, S., Haber, D.A. (October, 2015). Single cell RNA profiling of circulating tumor cells in patients with prostate cancer. 2015 American Society for Radiation Oncology Annual Meeting, San Antonio, TX. (Oral Presentation).

- Presentations during this reporting period:

  - Local:
    - **Miyamoto, D.T.** "Monitoring Androgen Receptor Signaling in Circulating Tumor Cells in Prostate Cancer." Departmental Seminar, MGH Cancer Center, Massachusetts General Hospital, Boston, MA 12 December 2012.
    - **Miyamoto, D.T.** "Single Cell RNA-Seq of Circulating Prostate Tumor Cells." Department Seminar, Cancer Center, MGH, September, 2014.

  - National:
    - **Miyamoto, D.T.** "Microfluidic Isolation and Molecular Analysis of Circulating Tumor Cells." BIO International Convention, Chicago, IL, 22 April 2013.
    - **Miyamoto, D.T.** "Microfluidic Isolation and Molecular Analysis of Circulating Tumor Cells." Next Generation Diagnostics Summit, Washington DC, August 2013.
    - **Miyamoto, D.T.** "Microfluidic Isolation and Molecular Analysis of Circulating Tumor Cells." World CTC Summit, November 2013.
    - **Miyamoto, D.T.** "Microfluidic Isolation and Molecular Characterization of Circulating Tumor Cells." SELECTBIO Circulating Biomarkers Conference, May 2014.
    - **Miyamoto, D.T.** "Single cell RNA-sequencing of circulating tumor cells." Invited Plenary Lecture, American Association for Cancer Research Precision Medicine Series, Salt Lake City, UT, June, 2015.
    - **Miyamoto, D.T.** "Single cell RNA profiling of circulating tumor cells in patients with prostate cancer." Oral Presentation, American Society for Radiation Oncology 57th Annual Meeting, San Antonio, TX, October, 2015.
    - **Miyamoto, D.T.** "Molecular Analysis of CTCs in Prostate Cancer." Invited Lecture, Society for Translational Oncology, 2015 Chabner Colloquium, Boston, MA, October, 2015.
    - **Miyamoto, D.T.** "Molecular Profiling of Circulating Tumor Cells in Prostate Cancer." Invited Lecture, USC Norris Cancer Center Grand Rounds, University of Southern California, Los Angeles, CA, October, 2015.
    - **Miyamoto, D.T.** "RNA-Seq of Single Prostate CTCs Implicates Noncanonical Wnt Signaling in Antiandrogen Resistance." Oral Presentation,

Innovative Minds in Prostate Cancer Today (IMPaCT) Meeting, Towson, MD, 2016.
- **Miyamoto, D.T.** "Molecular Characterization of Circulating Tumor Cells." Invited Lecture, American Urological Association Annual Meeting, Boston, MA, 2017.

- International:
  - **Miyamoto, D.T.** "RNA-Seq of single prostate CTCs implicates noncanonical Wnt signaling in antiandrogen resistance." Global Summit on Genitourinary Malignancies, Banff Springs, Canada, October, 2015.

Inventions, Patents, and Licenses
Nothing to report during this reporting period.

Degrees obtained supported by this training grant
Nothing to report during this reporting period.

Development of cell lines, tissue, or serum repositories
Nothing to report during this reporting period.

Informatics such as databases and animal models
Single prostate CTC RNA-sequencing data has been deposited in GEO under accession number GSE67980.

Funding applied for based on work supported by this training grant
The PI received a Young Investigator Award from the Prostate Cancer Foundation in June of 2016.

Employment or research opportunities received based on experience/training supported by this grant
The PI was promoted to Assistant Professor of Radiation Oncology at Harvard Medical School in June 2015 and Assistant Radiation Oncologist at the Massachusetts General Hospital in September 2015 based on experience, training, and accomplishments supported by this Award. He was also appointed a Principal Investigator in the MGH Center for Cancer Research based on accomplishments supported by this grant in July 2017.

CONCLUSION

This Physician Research Training Award supported a mentored training program integrated with a research project focused on the study of circulating tumor cells (CTCs) in prostate cancer patients using a microfluidic device ("CTC-chip") to isolate CTCs from peripheral blood samples. During this award, we developed a quantitative immunofluorescence assay to measure AR activity in CTCs in patients with metastatic prostate cancer receiving treatment with hormonal therapy, and showed that dysregulation of AR signaling in CTCs correlated with

resistance to hormonal therapy. We also developed methods for single CTC RNA-seq and digital gene expression profiling, and applied these techniques to single prostate CTCs. We analyzed single cell transcriptomes to reveal the heterogeneity of CTCs, and to identify key genes and molecular pathways enriched in CTCs that may contribute to treatment resistance in prostate cancer, including AR splice variants and the non-canonical Wnt pathway. Thus, this Research Project successfully provided initial validation of novel molecular biomarkers that can monitor and predict responses to second-line hormonal therapy in patients with CRPC, and also revealed fundamental insights into the mechanisms underlying castration-resistance in prostate cancer. Finally, this Award provided valuable protection of time for research and mentored training of the PI, and was essential in enabling his development towards a productive career as an independent investigator in translational prostate cancer research.

REFERENCES

1. Chen Y, Clegg NJ, Scher HI. Anti-androgens and androgen-depleting therapies in prostate cancer: new agents for an established target. Lancet Oncol 2009; 10: 981-91.
2. de Bono JS, Logothetis CJ, Molina A, Fizazi K, North S, Chu L, et al. Abiraterone and increased survival in metastatic prostate cancer. N Engl J Med 2011; 364: 1995-2005.
3. Scher HI, Fizazi K, Saad F, Taplin ME, Sternberg CN, Miller K, et al. Increased survival with enzalutamide in prostate cancer after chemotherapy. N Engl J Med 2012; 367: 1187-97.
4. Miyamoto DT, Lee RJ, Stott SL, Ting DT, Wittner BS, Ulman M, et al. Androgen receptor signaling in circulating tumor cells as a marker of hormonally responsive prostate cancer. Cancer Discov 2012; 2: 995-1003.
5. Miyamoto DT, Sequist LV, Lee RJ. Circulating tumour cells-monitoring treatment response in prostate cancer. Nat Rev Clin Oncol 2014; 11: 401-12.
6. Ozkumur E, Shah AM, Ciciliano JC, Emmink BL, Miyamoto DT, Brachtel E, et al. Inertial focusing for tumor antigen-dependent and -independent sorting of rare circulating tumor cells. Sci Transl Med 2013; 5: 179ra47.
7. Ting DT, Wittner BS, Ligorio M, Vincent Jordan N, Shah AM, Miyamoto DT, et al. Single-Cell RNA Sequencing Identifies Extracellular Matrix Gene Expression by Pancreatic Circulating Tumor Cells. Cell reports 2014; 8: 1905-18.
8. Miyamoto DT, Zheng Y, Wittner BS, Lee RJ, Zhu H, Broderick KT, et al. RNA-Seq of single prostate CTCs implicates noncanonical Wnt signaling in antiandrogen resistance. Science 2015; 349: 1351-6.
9. Stott SL, Hsu CH, Tsukrov DI, Yu M, Miyamoto DT, Waltman BA, et al. Isolation of circulating tumor cells using a microvortex-generating herringbone-chip. Proc Natl Acad Sci U S A 2010; 107: 18392-7.
10. Trepel J, Mollapour M, Giaccone G, Neckers L. Targeting the dynamic HSP90 complex in cancer. Nat Rev Cancer 2010; 10: 537-49.
11. Gutschner T, Hammerle M, Diederichs S. MALAT1 -- a paradigm for long noncoding RNA function in cancer. Journal of molecular medicine 2013; 91: 791-801.
12. Schaefer CF, Anthony K, Krupa S, Buchoff J, Day M, Hannay T, et al. PID: the Pathway Interaction Database. Nucleic Acids Res 2009; 37: D674-9.
13. Katoh M, Katoh M. WNT signaling pathway and stem cell signaling network. Clin Cancer Res 2007; 13: 4042-5.
14. Arora VK, Schenkein E, Murali R, Subudhi SK, Wongvipat J, Balbas MD, et al. Glucocorticoid receptor confers resistance to antiandrogens by bypassing androgen receptor blockade. Cell 2013; 155: 1309-22.

APPENDICES

Includes the following:

Biosketch, David T. Miyamoto, October 2017

Miyamoto, D.T., et al. (2012). Androgen receptor signaling in circulating tumor cells as a marker of hormonally responsive prostate cancer. *Cancer Discovery*, 2:995-1003.

Ozkumur, E. et al. (2013). Inertial Focusing for Positive and Negative Sorting of Rare Circulating Tumor Cells. *Science Translational Medicine*, 5:179ra47.

Miyamoto, D.T., Sequist, L.V., Lee, R.J. (2014). Circulating tumour cells – monitoring treatment response in prostate cancer. *Nature Reviews Clinical Oncology*, 11(7):401-12.

Ting, D.T. et al. (2014). Single-cell RNA sequencing identifies extracellular matrix gene expression by pancreatic circulating tumor cells. *Cell Reports*, 8:1905-18.

Miyamoto et al. (2015). RNA-Seq of single prostate CTCs implicates noncanonical Wnt signaling in antiandrogen resistance. *Science*, 349:1351-56

Miyamoto, D.T. and Lee, R.J. (2016). Cell-free and circulating tumor cell-based biomarkers in men with metastatic prostate cancer: Tools for real-time precision medicine? *Urologic Oncology: Seminars and Original Investigations*, 34:490-501.

Hwang, W.L., Hwang, K.L., **Miyamoto, D.T.** (2016). The promise of circulating tumor cells for precision cancer therapy. *Biomarkers in Medicine*, 10:1269-1285.

Miyamoto, D.T., Ting, D.T., Toner, M., Maheswaran, S., and Haber, D.A. Single-cell analysis of circulating tumor cells as a window into tumor heterogeneity. In: *Cold Spring Harbor Symposia on Quantitative Biology*, Volume LXXXI. Cold Spring Harbor Laboratory Press; 2017. p. 1-6.

BIOGRAPHICAL SKETCH

Provide the following information for the Senior/key personnel and other significant contributors.
Follow this format for each person. DO NOT EXCEED FIVE PAGES.

NAME: Miyamoto, David T.

eRA COMMONS USER NAME (credential, e.g., agency login): DMIYAMOTO

POSITION TITLE: Assistant Professor of Radiation Oncology, Harvard Medical School; Assistant Radiation Oncologist, Massachusetts General Hospital

EDUCATION/TRAINING *(Begin with baccalaureate or other initial professional education, such as nursing, include postdoctoral training and residency training if applicable. Add/delete rows as necessary.)*

INSTITUTION AND LOCATION	DEGREE *(if applicable)*	Completion Date MM/YYYY	FIELD OF STUDY
Harvard College, Cambridge, MA	A.B.	06/1997	Chemistry
Harvard University, Cambridge, MA	Ph.D.	11/2004	Cell & Developmental Biology
Harvard Medical School, Boston, MA	M.D.	06/2006	Medicine
Brigham & Women's Hospital, Boston, MA	Intern	06/2007	Internal Medicine
Harvard Radiation Oncology Program, Boston, MA	Resident	06/2011	Radiation Oncology
Massachusetts General Hospital Cancer Center / Howard Hughes Medical Institute	Postdoctoral	06/2015	Cancer Genetics

A. Personal Statement

I am a translational physician scientist and a radiation oncologist with a strong research and clinical interest in prostate and bladder cancer. I serve as an Assistant Professor of Radiation Oncology at Harvard Medical School and Massachusetts General Hospital, devoting 80% of my effort to translational research and 20% to clinical activities specializing in genitourinary malignancies. I am the Principal Investigator of a translational research laboratory in the Mass General Hospital Cancer Center focused on the development of novel biomarkers to guide the treatment of patients with prostate and bladder cancer. I am dedicated to the mentorship of young physician scientists, residents, and medical students, in the laboratory and in the clinic.

A major focus of my laboratory is the investigation of rare circulating tumor cells (CTCs) in the blood of cancer patients. CTCs represent a "liquid biopsy" that may be performed repeatedly and non-invasively to monitor treatment efficacy and study tumor evolution during therapy. As part of the MGH Circulating Tumor Cell Center, we have applied novel microfluidic technologies to analyze CTCs from the blood of patients with a variety of solid tumors, with a focus on genitourinary cancers. We recently developed a sensitive, specific, and cost-effective method to detect CTC transcriptional signatures by coupling microfluidic negative selection with droplet digital PCR. I have the laboratory experience, clinical expertise, and access to clinical samples necessary to execute the goals of his project.

1. **Miyamoto, D.T.**, Zheng, Y., Wittner, B.S., Lee, R.J., Zhu, H., Broderick, K.T., Desai, R., Fox, D.B., Brannigan, B.W., Trautwein, J., Arora, K.S., Desai, N., Dahl, D.M., Sequist, L.V., Smith, M.R., Kapur, R., Wu, C.L., Shioda, T., Ramaswamy, S., Ting, D.T., Toner, M., Maheswaran, S., Haber, D.A. (2015). RNA-Seq of single prostate CTCs implicates noncanonical Wnt signaling in antiandrogen resistance. ***Science***, 349:1351-1356. PMID: 26383955

2. **Miyamoto, D.T.,** Lee, R.J., Stott, S.L., Ting, D.T., Wittner, B.S., Ulman, M., Smas, M.E., Lord, J.B., Brannigan, B.W., Trautwein, J., Bander, N.H., Wu, C.L., Sequist, L.V., Smith, M.R., Ramaswamy, S., Toner, M., Maheswaran, S., Haber, D.A. (2012). Androgen receptor signaling in circulating tumor cells as a marker of hormonally responsive prostate cancer. ***Cancer Discovery***, 2:995-1003. PMCID: PMC3508523 *(featured as cover article)*
3. **Miyamoto, D.T.** and Lee, R.J. (2016) Cell-free and circulating tumor cell-based biomarkers in men with metastatic prostate cancer: Tools for real-time precision medicine? ***Urologic Oncology: Seminars and Original Investigations***, 34:490-501. PMID 27771279.
4. **Miyamoto, D.T.**, Sequist, L.V., Lee, R.J. (2014). Circulating Tumor Cells – Monitoring Treatment Response in Prostate Cancer. ***Nature Reviews Clinical Oncology***, 11(7):401-12. PMID 24821215

B. Positions and Honors

Positions and Employment

2011 - 2015	Instructor in Radiation Oncology, Harvard Medical School, Boston, MA
2011 - 2015	Assistant in Radiation Oncology, Massachusetts General Hospital, Boston, MA
2015 -	Assistant Professor of Radiation Oncology, Harvard Medical School, Boston, MA
2015 -	Assistant Radiation Oncologist, Massachusetts General Hospital, Boston, MA

Other Professional Positions

1999 - 2006	Resident Tutor in Medicine, Leverett House, Harvard College, Cambridge, MA
2007	Visiting Physician, National Cancer Center Hospital, Tokyo, Japan
2011 -	Harvard-MIT Health Sciences and Technology MD Board of Advisors, HMS
2015 -	Member, Prostate Cancer Program, Dana-Farber / Harvard Cancer Center
2017 -	Investigator, Center for Cancer Research, Mass General Cancer Center

Honors

1993	National Merit Scholarship
1993 – 1997	John Harvard Scholarship
1996	Merck Undergraduate Research Fellow
1997	*Magna cum laude*, Harvard College
1997	High Honors in Chemistry, Harvard College
2001 – 2004	Howard Hughes Medical Institute Predoctoral Fellow
2009 – 2011	B. Leonard Holman Research Pathway, American Board of Radiology
2010	ASTRO Annual Meeting Scientific Abstract Award
2011 – 2013	A. David Mazzone Career Development Award, Dana-Farber/Harvard Cancer Center
2012 and 2014	Ira J. Spiro Translational Research Award, MGH
2012 – 2017	Physician Research Training Award, Department of Defense
2016 – 2019	Young Investigator Award, Prostate Cancer Foundation
2017	The One Hundred Honoree, Mass General Cancer Center

Licensure and Certification

2008 – present	Massachusetts Full License, Board of Registration in Medicine
2012 – present	Board Certification, Radiation Oncology, American Board of Radiology

Membership in Professional Societies

2013 – present	Member, American Association for Cancer Research
2009 – present	Member, American Society of Clinical Oncology
2008 – present	Member, American Society for Radiation Oncology
2003 – present	Member, American Society for Cell Biology

C. Contribution to Science

1. ***Molecular mechanisms of mitosis.*** My early publications in graduate school focused on the elucidation of fundamental mechanisms underlying mitotic spindle assembly and function. Proper function of the spindle is necessary for the faithful segregation of chromosomes during cell division, and components of this dynamic macromolecular structure may serve as potential targets for cancer therapy.

a. **Miyamoto, D.T.**, Perlman, Z.E., Burbank, K.S., Groen, A.C., and Mitchison, T.J. (2004). The kinesin Eg5 drives poleward microtubule flux in *Xenopus* egg extract spindles. ***The Journal of Cell Biology***, 167:813-8.
b. Haggarty, S.J., Mayer, T.U., **Miyamoto, D.T.**, Fathi, R., King, R.W., Mitchison, T.J., and Schreiber, S.L. (2000). Dissecting cellular processes using small molecules: identification of colchicine-, taxol-like, and other small molecules that perturb mitosis. ***Chemistry & Biology***, 7:275-86.
c. Groen, A.C., Cameron, L.A., Coughlin, M., **Miyamoto, D.T.**, Mitchison, T.J., and Ohi, R. (2004). XRHAMM functions in Ran-dependent microtubule nucleation and pole formation during anastral spindle assembly. ***Current Biology***, 14:1801-11.
d. **Miyamoto, D.T.**, Perlman, Z.E., Mitchison, T.J., and Shirasu-Hiza, M. (2003). Dynamics of the mitotic spindle – potential therapeutic targets. In: Meijer, L., Jezequel, A., and Roberge, M., editors. ***Progress in Cell Cycle Research***, Volume 5. New York: Plenum Press; p. 349-60.

2. ***Prognostic and predictive biomarkers in prostate cancer.*** There is an unmet clinical need for reliable prognostic and predictive biomarkers to guide prostate cancer therapy in a wide range of clinical settings, from localized to metastatic disease. We have developed a novel automated RNA in situ hybridization (RNA-ISH) platform capable of the sensitive and specific detection of AR-V7 transcripts in archival formalin-fixed, paraffin-embedded (FFPE) tissue, and have demonstrated its potential prognostic value in metastatic castration-sensitive prostate cancer. I have also developed a quantitative immunofluorescence assay to measure androgen receptor (AR) signaling activity status in CTCs from patients with prostate cancer, thus facilitating the rational application of second generation anti-androgen therapies. I have published several reviews on the potential value of circulating and tissue biomarkers in prostate cancer as tools for precision medicine.

a. **Miyamoto, D.T.,** Lee, R.J., Stott, S.L., Ting, D.T., Wittner, B.S., Ulman, M., Smas, M.E., Lord, J.B., Brannigan, B.W., Trautwein, J., Bander, N.H., Wu, C.L., Sequist, L.V., Smith, M.R., Ramaswamy, S., Toner, M., Maheswaran, S., Haber, D.A. (2012). Androgen receptor signaling in circulating tumor cells as a marker of hormonally responsive prostate cancer. ***Cancer Discovery***, 2:995-1003. PMCID:PMC3508523 *(featured as cover article)*
b. **Miyamoto, D.T.**, Sequist, L.V., Lee, R.J. (2014). Circulating tumour cells – monitoring treatment response in prostate cancer. ***Nature Reviews Clinical Oncology***, 11(7):401-12. PMID 24821215.
c. **Miyamoto, D.T.** and Lee, R.J. Cell-free and circulating tumor cell-based biomarkers in men with metastatic prostate cancer: Tools for real-time precision medicine? ***Urologic Oncology: Seminars and Original Investigations*** 2016; 34:490-501. PMID 27771279.
d. Saylor, P.J., Lee, R.J., Arora, K.S., Deshpande, V., Hu, R., Olivier, K., Meneely, E., Rivera, M.N., Ting, D.T., Wu, C.L., **Miyamoto, D.T.** (2017) Branched chain RNA in situ hybridization for androgen receptor splice variant AR-V7 as a prognostic biomarker for metastatic castration-sensitive prostate cancer. ***Clinical Cancer Research***, 23:363-369. PMID 27440270

3. ***Molecular characterization of circulating tumor cells.*** Circulating tumor cells (CTCs) are rare cancer cells shed from primary and metastatic tumors into the peripheral blood, and represent a “liquid biopsy” that may be used to sample tumor cells non-invasively. I have led key studies on the molecular characterization of CTCs isolated from men with localized and metastatic prostate cancer, yielding novel insights into mechanisms of treatment resistance and metastatic dissemination. I led the first large scale single cell RNA-seq analysis of CTCs from prostate cancer patients, and identified non-canonical Wnt signaling as a potential mechanism of resistance to antiandrogen therapy in prostate cancer, as well as ß-globin as a mechanism for CTCs to survive oxidative stress in the peripheral circulation.

a. **Miyamoto, D.T.**, Zheng, Y., Wittner, B.S., Lee, R.J., Zhu, H., Broderick, K.T., Desai, R., Fox, D.B., Brannigan, B.W., Trautwein, J., Arora, K.S., Desai, N., Dahl, D.M., Sequist, L.V., Smith, M.R., Kapur, R., Wu, C.L., Shioda, T., Ramaswamy, S., Ting, D.T., Toner, M., Maheswaran, S., Haber, D.A. (2015). RNA-Seq of single prostate CTCs implicates noncanonical Wnt signaling in antiandrogen resistance. ***Science***, 349:1351-1356.
b. Zheng, Y.*, **Miyamoto, D.T.*** (*equal contribution), Wittner, B.S., Sullivan, J.P., Aceto, N., Jordan, N.V., Yu, M., Karabacak, N.M., Comaills, V., Morris, R., Desai, R., Desai, N., Emmons, E., Lee, R.J., Wu., C.L., Sequist, L.V., Haas, W., Ting, D.T., Toner, M., Ramaswamy, S., Maheswaran, S., Haber, D.A. Expression of ß-globin by cancer cells promotes cell survival during dissemination. ***Nature Communications*** 2017; 8:14344. PMID 28181495
c. Stott, S.L., Lee, R.J., Nagrath, S., Yu, M., **Miyamoto, D.T.**, Ulkus, L., Inserra, E.J., Ulman, M., Springer, S., Nakamura, Z., Moore, A.L., Tsukrov, D.I., Kempner, M.E., Dahl, D.M., Wu, C., Iafrate, A.J., Smith, M.R., Tompkins, R.G., Sequist, L.V., Toner, M., Haber, D.A., Maheswaran, S. (2010). Microfluidic isolation and molecular characterization of circulating tumor cells from patients with localized and metastatic prostate cancer. ***Science Translational Medicine***, 2:25ra23:1-10. PMCID:PMC3141292.
d. **Miyamoto, D.T.**, Ting, D.T., Toner, M., Maheswaran, S., and Haber, D.A. Single-cell analysis of circulating tumor cells as a window into tumor heterogeneity. In: ***Cold Spring Harbor Symposia on Quantitative Biology***, Volume LXXXI. Cold Spring Harbor Laboratory Press; 2017. p. 1-6.

4. ***Novel technologies for the isolation and characterization of circulating tumor cells.*** CTCs may serve as useful biomarkers and a means to study of tumor evolution, but given their rarity and fragility, they are extremely difficult to isolate. I played an integral role in the development of novel microfluidic technologies to efficiently isolate single CTCs and CTC clusters from the peripheral blood of patients. I established methods for the isolation and molecular characterization of single CTCs, and used these methods to accomplish microfluidic qRT-PCR of single CTCs, single cell RNA-seq of CTCs from a mouse model of pancreatic cancer, and RNA-seq of single CTCs and CTC clusters from patients with breast cancer.

a. Aceto, N., Bardia, A., **Miyamoto, D.T.**, Donaldson, M.C., Wittner, B.S., Spencer, J.A., Yu, M., Pely, A., Engstrom, A., Zhu, H., Brannigan, B.W., Kapur, R., Stott, S.L., Shioda, T., Ramaswamy, S., Ting, D.T., Lin, C.P., Toner, M., Haber, D.A., Maheswaran, S. (2014). Circulating tumor cell clusters are oligoclonal precursors of breast cancer metastasis. ***Cell***, 158:1110-1122. PMCID:PMC4149753.
b. Ting, D.T., Wittner, B.S., Ligorio, M., Vincent Jordan, N., Shah, A.M., **Miyamoto, D.T.**, Aceto, N., Bersani, F., Brannigan, B.W., Xega, K., Ciciliano, J.C., Zhu, H., MacKenzie, O.C., Trautwein, J., Arora, K.S., Shahid, M., Ellis, H.L., Qu, N., Bardeesy, N., Rivera, M.N., Deshpande, V., Ferrone, C.R., Kapur, R., Ramaswamy, S., Shioda, T., Toner, M., Maheswaran, S., Haber, D.A. Single-cell RNA sequencing identifies extracellular matrix gene expression by pancreatic circulating tumor cells. ***Cell Reports*** 2014; 8:1905-18. PMCID:PMC4230325.
c. Ozkumur, E., Shah, A.M., Ciciliano, J.C., Emmink, B.L., **Miyamoto, D.T.**, Brachtel, E., Yu, M., Chen, P., Morgan, B., Trautwein, J., Kimura, A., Sengupta, S., Stott, S.L., Karabacak, N.M., Barber, T.A., Walsh, J.R., Smith, K., Spuhler, P., Sullivan, J., Lee, R., Ting, D.T., Luo, X., Shaw, A.T., Bardia, A., Sequist, L.V., Louis, D.N., Maheswaran, S., Kapur, R., Haber, D.A., Toner, M. (2013). Inertial Focusing for Positive and Negative Sorting of Rare Circulating Tumor Cells. ***Science Translational Medicine***, 5:179ra47. PMCID:PMC3760275.
d. Sarioglu, A.F., Aceto, N., Kojic, N., Donaldson, M.C., Zeinali, M., Hamza, B., Engstrom, A., Zhu, H., Sundarasen, T.K., **Miyamoto, D.T.**, Luo, X., Bardia, A., Wittner, B., Ramaswamy, S., Shioda, T., Ting, D.T., Stott, S.L., Kapur, R., Maheswaran, S., Haber, D., Toner, M. (2015). A microfluidic device for label-free, physical capture of circulating tumor cell-clusters. ***Nature Methods***, 12:685-91. PMCID:PMC4490017.

Complete List of Published Work in MyBibliography:
http://www.ncbi.nlm.nih.gov/sites/myncbi/1vG7CpGOY8jQt/bibliograpahy/45002366/public/?sort=date&direction=descending

D. Research Support

Ongoing Research Support

Prostate Cancer Foundation — Miyamoto (PI) — 06/01/2016-05/31/2019
Young Investigator Award
Molecular Analysis of CTCs to Study Mechanisms of Treatment resistance in Prostate Cancer
The main goals of this project are: 1) Evaluation of AR alterations in CTCs from metastatic prostate cancer patients. 2) Evaluation of ncWnt and GR pathways in CTCs from patients with treatment-resistant CRPC patients. 3) Identification of alternative resistance mechanisms using single CTC RNA-seq, and establishment of patient-derived CTC cultures to test the relevance of these pathways.

C06 CA059267 — Hong/Efstathiou (Co-PIs) — 10/1/2004 – 12/31/2019
NCI Federal Share of the Proton Beam Program
Proton Biospecimen & Biomarker Program
The major goal of this project is to establishment a Proton Biomarker Program (PBP) at MGH, which will provide necessary research tissue banking resources and consolidate biomarker research efforts for more effective incorporation of biomarker exploration in clinical trials at MGH and beyond. Role: Co-Investigator

C06 CA059267 — Efstathiou (PI) — 01/01/12-12/31/19
NCI Federal Share of the Proton Beam Program
Phase III Randomized Clinical Trial of Proton Therapy vs. IMRT for Low or Intermediate Risk Prostate Cancer
The main goals of this project are to assess the clinical and cost effectiveness of PBT versus IMRT for men with low or intermediate risk prostate cancer. Role: Co-Investigator

2U01EB012493 — Haber/Toner (PI) — 09/30/10-06/30/19
NIH/NIBIB
Point of Care Microfluidics for Early Detection of Cancer
Proposed technological innovations to allow sensitive and robust CTC detection strategies, with use of enhanced microfluidic isolation for screening in prostate and lung cancer. Role: Co-Investigator

Completed Research Support (last 5 years)

C06 CA059267, NCI/MGH — Miyamoto (PI) — 04/15/2014 – 10/14/2016
Federal Share of the Proton Beam Program, Spiro Award
Discovery of Genomic Classifiers for Prediction of Response to Bladder Sparing Therapy for Muscle-Invasive Bladder Cancer

Department of Defense — Miyamoto (PI) — 07/01/2012 – 06/30/2017
Physician Research Training Award, Prostate Cancer Research Program
Probing androgen receptor signaling in circulating tumor cells in prostate cancer.

Dana Farber/Harvard Cancer Center — Miyamoto (PI) — 08/01/2011-08/31/2013
A. David Mazzone Career Development Award
Probing androgen receptor signaling in circulating tumor cells in prostate cancer.

C06 CA059267, NCI/MGH — Miyamoto (PI) — 04/15/2012 – 10/14/2014
Federal Share of the Proton Beam Program, Spiro Award
Evaluation of Multigene Expression Signatures as Predictors of Outcome After Radiation Therapy for Prostate Cancer

CANCER DISCOVERY

Androgen Receptor Signaling in Circulating Tumor Cells as a Marker of Hormonally Responsive Prostate Cancer

David T. Miyamoto, Richard J. Lee, Shannon L. Stott, et al.

Cancer Discovery 2012;2:995-1003. Published OnlineFirst October 23, 2012.

Published OnlineFirst October 23, 2012; DOI: 10.1158/2159-8290.CD-12-0222

RESEARCH BRIEF

Androgen Receptor Signaling in Circulating Tumor Cells as a Marker of Hormonally Responsive Prostate Cancer

David T. Miyamoto[1,3], Richard J. Lee[1,4], Shannon L. Stott[2,5], David T. Ting[1,4], Ben S. Wittner[1], Matthew Ulman[1], Malgorzata E. Smas[1], Jenna B. Lord[1], Brian W. Brannigan[1], Julie Trautwein[1], Neil H. Bander[7], Chin-Lee Wu[6], Lecia V. Sequist[1,4], Matthew R. Smith[1,4], Sridhar Ramaswamy[1,4], Mehmet Toner[2,5], Shyamala Maheswaran[1,5], and Daniel A. Haber[1,4,8]

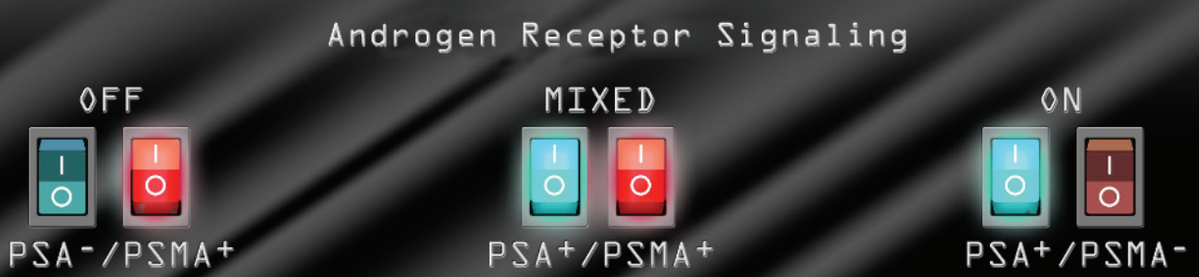

ABSTRACT

Androgen deprivation therapy (ADT) is initially effective in treating metastatic prostate cancer, and secondary hormonal therapies are being tested to suppress androgen receptor (AR) reactivation in castration-resistant prostate cancer (CRPC). Despite variable responses to AR pathway inhibitors in CRPC, there are no reliable biomarkers to guide their application. Here, we used microfluidic capture of circulating tumor cells (CTC) to measure AR signaling readouts before and after therapeutic interventions. Single-cell immunofluorescence analysis revealed predominantly "AR-on" CTC signatures in untreated patients, compared with heterogeneous ("AR-on, AR-off, and AR-mixed") CTC populations in patients with CRPC. Initiation of first-line ADT induced a profound switch from "AR-on" to "AR-off" CTCs, whereas secondary hormonal therapy in CRPC resulted in variable responses. Presence of "AR-mixed" CTCs and increasing "AR-on" cells despite treatment with abiraterone acetate were associated with an adverse treatment outcome. Measuring treatment-induced signaling responses within CTCs may help guide therapy in prostate cancer.

SIGNIFICANCE: Acquired resistance to first-line hormonal therapy in prostate cancer is heterogeneous in the extent of AR pathway reactivation. Measurement of pre- and posttreatment AR signaling within CTCs may help target such treatments to patients most likely to respond to second-line therapies. *Cancer Discov; 2(11); 995–1003. ©2012 AACR.*

Authors' Affiliations: [1]Massachusetts General Hospital Cancer Center, [2]Center for Bioengineering in Medicine and Departments of [3]Radiation Oncology, [4]Medicine, [5]Surgery and [6]Pathology, Harvard Medical School, Charlestown, Massachusetts; [7]Weill Cornell Medical College, New York Presbyterian Hospital, New York, New York; and [8]Howard Hughes Medical Institute, Chevy Chase, Maryland

Note: Supplementary data for this article are available at Cancer Discovery Online (http://cancerdiscovery.aacrjournals.org/).

D.T. Miyamoto, R.J. Lee, and S.L. Stott contributed equally to this work.

Corresponding Authors: Daniel Haber, Cancer Center, Massachusetts General Hospital, Building 149, 13th Street, Charlestown, MA 02129. Phone: 617-726-7805; Fax: 617-724-6919; E-mail: Haber@helix.mgh.harvard.edu; and Shyamala Maheswaran, E-mail: maheswaran@helix.mgh.harvard.edu.

doi: 10.1158/2159-8290.CD-12-0222

Published OnlineFirst October 23, 2012; DOI: 10.1158/2159-8290.CD-12-0222

INTRODUCTION

Prostate cancer is highly dependent upon androgen receptor (AR) signaling for cell proliferation and survival. Androgen deprivation therapy (ADT) results in high rates of initial response in most patients with metastatic prostate cancer. However, disease progression is invariably observed with tumor cells resuming proliferation despite continued treatment (termed castration-resistant prostate cancer or CRPC; ref. 1). The propensity of metastatic prostate cancer to spread to bone has limited repeated sampling of tumor deposits that have acquired castration resistance, but insights into resistance mechanisms have emerged through bone marrow biopsy and autopsy studies, as well as mouse modeling experiments (2). The concept that CRPC results from reactivation of AR signaling despite low levels of serum testosterone is consistent with a frequently observed rise in serum prostate-specific antigen (PSA), an androgen-responsive gene product secreted into blood by prostate cancer cells (1, 2). Potential mechanisms by which AR reactivation occurs in CRPC include variable levels of *AR* gene amplification (~30% of cases), activating *AR* mutations, alternative mRNA splicing (~10%), increased expression or activation of AR transcriptional coactivators, activation of modulatory kinase pathways [e.g., Ras, phosphoinositide-3 kinase (PI3K)], tyrosine phosphorylation of AR, and increased intratumoral androgen synthesis; (see ref. 2 for review). The functional significance of reactivated AR signaling in CRPC has been inferred from mouse xenograft models of prostate cancer, in which even modest increases in *AR* gene expression cause tumors to become resistant to castration (3).

The concept of AR reactivation in CRPC has become therapeutically relevant with the development of potent novel inhibitors of AR signaling (4, 5). The demonstration that abiraterone acetate, a CYP17A1 inhibitor that potently suppresses adrenal and intratumoral steroid biosynthesis, increases overall survival in men with metastatic CRPC who have previously received chemotherapy lends support to the rationale of suppressing AR reactivation in CRPC (5). Notably, there is a wide variation in patient response to abiraterone acetate as measured by serum PSA (5), and there is an unmet need for reliable biomarkers that can predict treatment response to abiraterone acetate and other potent inhibitors of AR signaling under development. Taking advantage of recent technological advances in the capture, imaging, and molecular characterization of rare circulating tumor cells (CTC) shed into blood from otherwise poorly accessible metastatic tumor deposits (6, 7), we established a noninvasive "real time" measure of intratumoral AR signaling before and after initial- or second-line hormonal therapy in patients with metastatic prostate cancer.

RESULTS

Single-Cell Measurement of AR Signaling Parameters in Prostate CTCs

To measure the status of AR signaling within individual cells, we established a quantitative immunofluorescence assay based on the expression of AR-regulated genes. We reasoned that such a readout would be independent of mechanisms of AR reactivation in CRPC (e.g., *AR* amplification or mutation, ligand overexpression, or AR cofactor misregulation) and would therefore provide a clear measure of whether the AR pathway has been reactivated during the acquisition of resistance to ADT. To identify optimal downstream readouts of AR signaling, we subjected a prostate cancer cell line (LNCaP) to androgen deprivation or stimulation, and used digital gene expression profiling to identify transcripts that are differentially regulated in response to changes in AR signaling (Supplementary Fig. S1). Among candidate gene products that are prostate cancer–specific and for which reliable antibodies are available, we selected PSA (*KLK3*) and prostate-specific membrane antigen (PSMA; *FOLH1*) as most consistently upregulated following AR activation and AR suppression, respectively (Fig. 1A and B; Supplementary Fig. S1A and S1B). Selection of PSMA as a marker of AR suppression was also recently described by Evans and colleagues while this work was in progress (8).

Our assay for quantitative measurement of signal intensity profiles for cells stained with antibodies against PSA and PSMA was developed using a model cell system (LNCaP). Treatment of androgen-starved LNCaP cells with the androgen R1881 and measurement of immunofluorescence signals using an automated fluorescence microscopy scanning platform revealed time-dependent progression from an initial "AR-off" ($PSA^-/PSMA^+$) to an intermediate "AR-mixed" ($PSA^+/PSMA^+$) phenotype, and finally to an "AR-on" ($PSA^+/PSMA^-$) pattern (Fig. 1C; Supplementary Fig. S2A). The reverse progression was observed upon treatment with the AR inhibitor bicalutamide (Fig. 1D; Supplementary Fig. S2B). Similar results were observed using VCaP cells, another androgen-responsive prostate cancer cell line (Supplementary Fig. S3).

For isolation of CTCs, we made use of our recently developed "second-generation" microfluidic chip, in which herringbone (HB) grooves in the ceiling of the channel create anisotropic flow conditions, generating microvortices that direct cells toward the anti–epithelial cell adhesion molecule (EpCAM) antibody–coated walls of the device (^{HB}CTC-Chip; ref. 7). ^{HB}CTC-Chip parameters for single-cell AR signaling analysis were first established by modeling LNCaP cells treated with R1881 or bicalutamide, spiked into control blood specimens, captured on the ^{HB}CTC-Chip, and stained with antibodies against PSA and PSMA (AR signaling) along with anti-CD45 (to exclude contaminating leukocytes) and 4′, 6-diamidino-2-phenylindole (DAPI; for nuclear morphology; Supplementary Fig. S4A and S4B). To achieve multiparameter single-cell analysis of AR activity, an automated fluorescence microscopy scanning platform was adapted to distinctly and specifically measure 4 fluorescent emission spectra simultaneously. We carefully selected the choice of secondary fluorophores and optical band pass filters to avoid "cross-talk" between the multiple fluorescent signals that are closely located on the electromagnetic spectrum while maximizing signal intensity (see Methods). The 4-color immunofluorescence imaging parameters established using LNCaP cells were then applied to accurately enumerate patient-derived CTCs (Fig. 2a). To minimize the risk of counting false-positive events as CTCs, we adopted a previously reported strategy (6), calibrating threshold signal intensity and setting a cut-off value for detection of CTCs based on the number of positive events detected in healthy donor samples. Using the newly optimized 4-color

Published OnlineFirst October 23, 2012; DOI: 10.1158/2159-8290.CD-12-0222

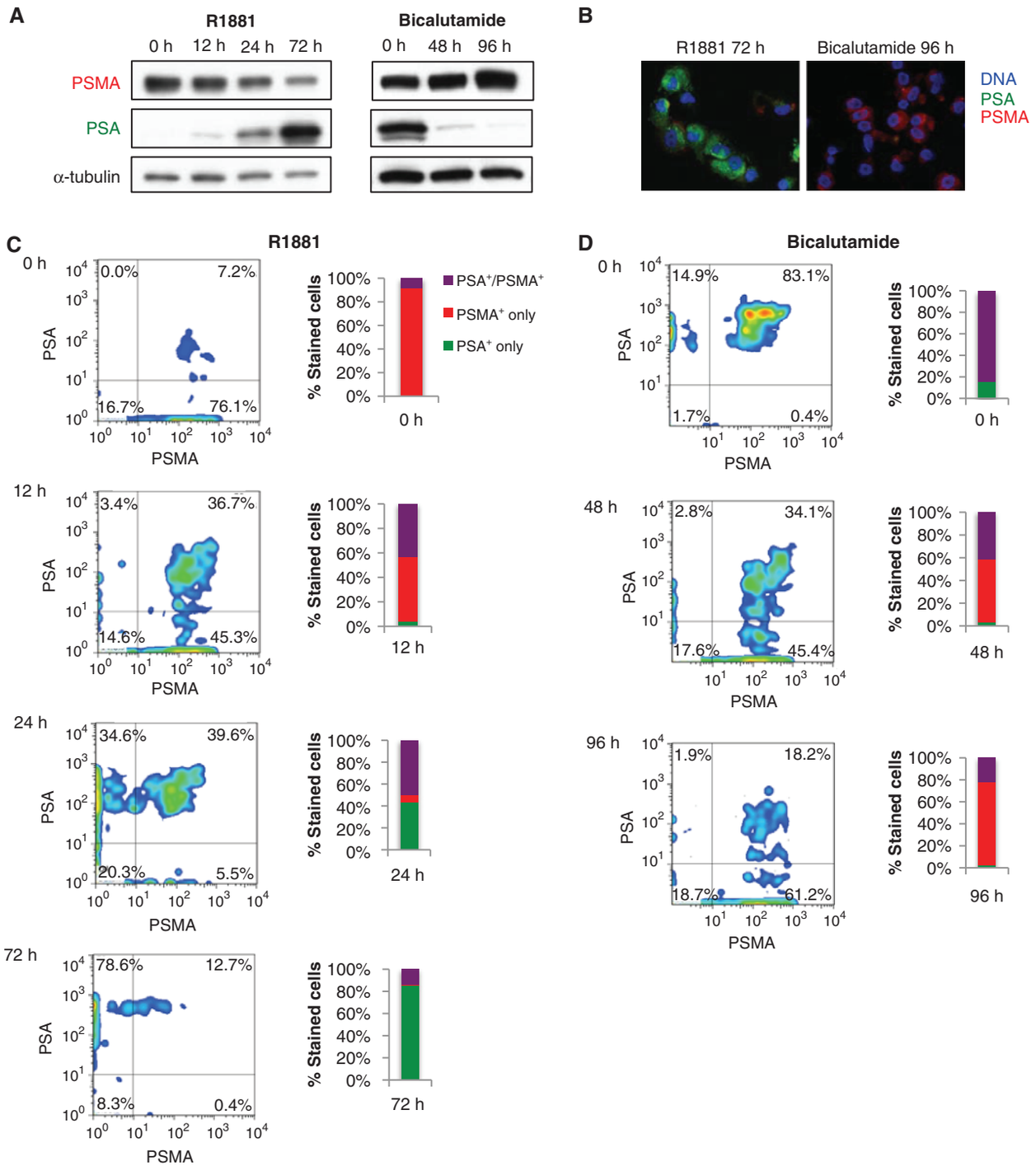

Figure 1. Multiparameter single-cell immunofluorescence assay to measure changes in AR activity in cultured prostate cancer cells. **A,** Western blot analysis for PSA, PSMA, and α-tubulin in LNCaP cells treated with 1 nmol/L R1881 after being cultured under androgen-deprived conditions (left), or treated with 10 μmol/L bicalutamide after being cultured under standard conditions (right). **B,** merged immunofluorescence images of LNCaP cells dual stained with antibodies against PSA (green) and PSMA (red) after treatment with 1 nmol/L R1881 or 10 μmol/L bicalutamide. **C,** pseudocolor density plots of multiparameter immunofluorescence profiles of LNCaP cells treated with 1 nmol/L R1881, imaged using an automated fluorescence microscopy scanning system. *x*- and *y*-axes represent "area-pixel" single-cell signal intensity measurements for PSMA and PSA, respectively. The total fraction of $PSA^+/PSMA^-$ (AR-on), $PSA^-/PSMA^+$ (AR-off), and $PSA^+/PSMA^+$ (AR-mixed) cells is shown in the bar graph. **D,** comparable analysis for LNCaP cells treated with 10 μmol/L bicalutamide after being cultured under standard conditions.

Published OnlineFirst October 23, 2012; DOI: 10.1158/2159-8290.CD-12-0222

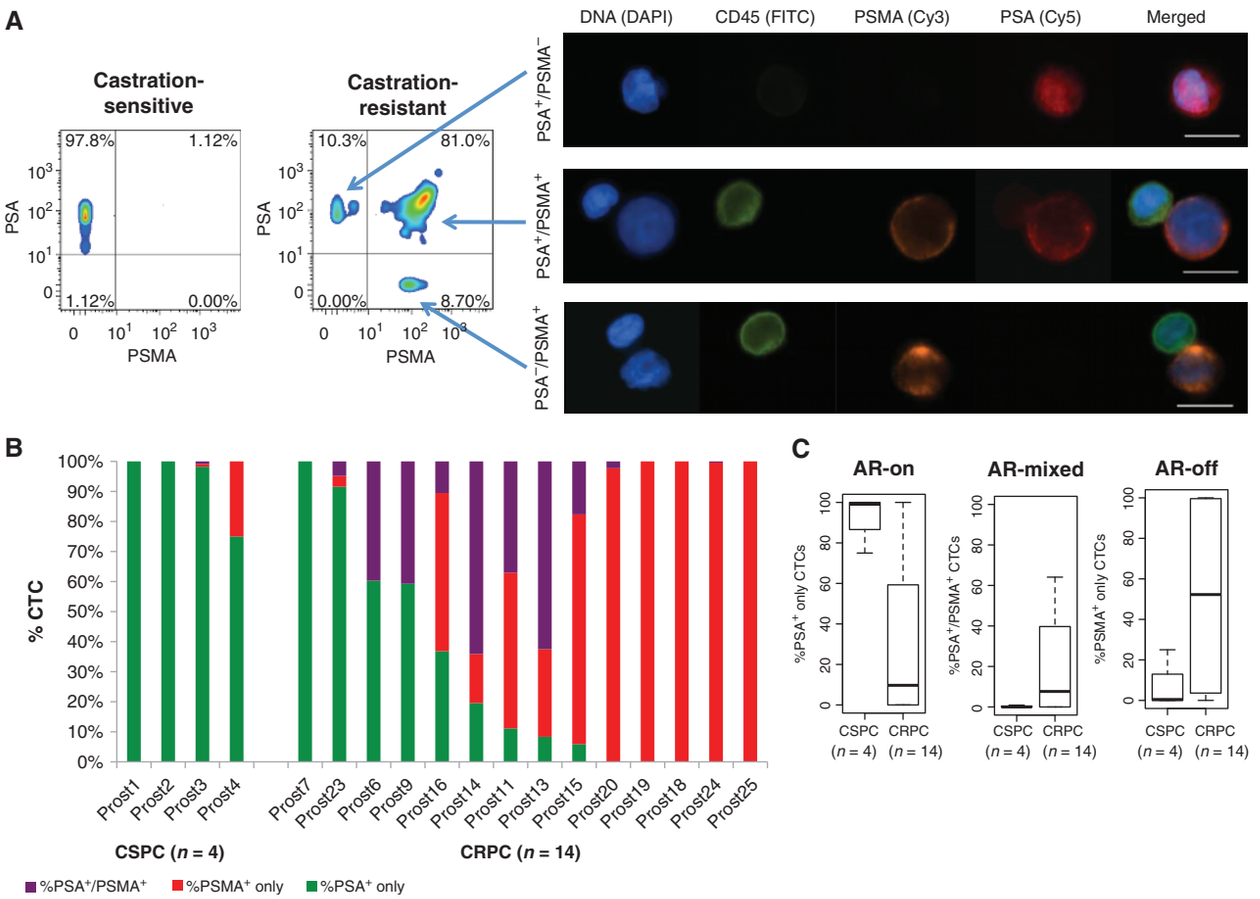

Figure 2. Single-cell measurements of AR signaling identify predominantly "AR-on" CTCs in castration-sensitive prostate cancer (CSPC) versus heterogeneous signatures in CRPC. **A,** pseudocolor density plots of multiparameter immunofluorescence profiles of CTCs from patient with CSPC (left) and CRPC (right). *x*- and *y*-axes represent "area-pixel" single-cell signal intensity measurements for PSMA and PSA, respectively. Representative images are depicted of an "AR-on" ($PSA^+/PSMA^-$) CTC (top row on right), an "AR-mixed" ($PSA^+/PSMA^+$) CTC (middle row), and an "AR-off" ($PSA^-/PSMA^+$) CTC (bottom row), with CD45 (FITC), PSMA (Cy3), and PSA (Cy5). Contaminating $CD45^+$ leukocytes are depicted for comparison in the middle and bottom rows. Scale bars, 10 μm. **B,** bar graphs showing proportional distribution of AR signaling phenotypes in CTCs from patients with CSPC or CRPC before initiation of therapy. Patient samples are ordered according to relative percentage of "AR-on" PSA^+ only CTCs. **C,** box plots showing the relative proportions of AR signaling phenotypes in CTCs from patients with CSPC compared with CRPC before initiation of therapy ($P = 0.012$ for $PSA^+/PSMA^-$; $P = 0.071$ for $PSA^+/PSMA^+$; $P = 0.076$ for $PSA^-/PSMA^+$).

immunofluorescence imaging parameters, we established a threshold value for positive CTC detection of more than 4 PSA^+ or $PSMA^+/CD45^-$ cells/mL, which was higher than any count noted in any healthy donor sample (Supplementary Fig. S5). The expansion of our CTC characterization to include 4-color staining in a high-throughput manner required the use of new organic fluorophores, narrow band fluorescent filter cubes, and a new automated imaging platform (see Methods). The result was a more specific assay with less background signal in our healthy donors compared with our previous papers (6, 7). We tested the validity of this threshold cut-off value in a separate cohort of age-matched male patients with no known diagnosis of cancer. Using this threshold, CTCs were not detectable in any patients without a diagnosis of prostate cancer ($n = 0/21$; Supplementary Fig. S5). In contrast, subsequent analysis of pretreatment blood samples from patients with metastatic prostate cancer revealed detectable CTCs above the predetermined threshold cut-off in 72% of patients ($n = 18/25$; Supplementary Fig. S5 and Supplementary Table S1).

Active AR Signaling in CTCs from Untreated Patients with Metastatic Prostate Cancer

Having standardized CTC detection using 4-color imaging criteria, we applied the PSA/PSMA dual immunophenotyping assay to patients with newly diagnosed metastatic prostate cancer. CTCs were detectable in 4 of 5 (80%) patients with newly diagnosed metastatic prostate cancer before the initiation of ADT. AR activity was predominantly positive among the patients with detectable CTCs, with the vast majority (median 99.1%; range, 75%–100%) of isolated CTCs from each patient showing the "AR-on" ($PSA^+/PSMA^-$) phenotype (Figs. 2B and C; Supplementary Table S2). The initiation of ADT in treatment-naïve patients with metastatic prostate cancer with detectable CTCs resulted in transformation of the majority of CTCs from the "AR-on" to the "AR-off" phenotype within 1 month, followed by the complete disappearance of CTCs by 3 months after initiation of therapy (Fig. 3A–C; Supplementary Table S2).

Published OnlineFirst October 23, 2012; DOI: 10.1158/2159-8290.CD-12-0222

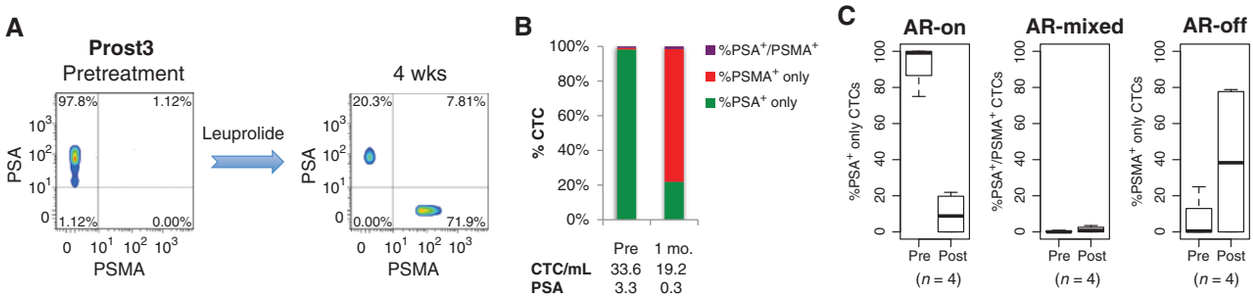

Figure 3. ADT-induced AR signaling changes in CTCs from patients with castration-sensitive metastatic prostate cancer. **A,** pseudocolor density plots of multiparameter immunofluorescence AR signaling profiles of CTCs in a patient (Prost3) with CSPC before and after ADT with leuprolide showing transformation of CTCs from the "AR-on" ($PSA^+/PSMA^-$) phenotype to the "AR-off" ($PSA^-/PSMA^+$) phenotype. **B,** bar graphs showing proportional distribution of AR signaling phenotypes in CTCs from this patient before and after ADT. Corresponding CTC numbers and serum PSA levels are shown for pretreatment (pre) and after therapy. **C,** box plots showing composite data for relative proportions of AR signaling phenotypes in CTCs from patients with CSPC ($n = 4$) pretreatment and after 4 weeks of ADT ($P = 0.028$ for $PSA^+/PSMA^-$; $P = 0.41$ for $PSA^+/PSMA^+$; $P = 0.64$ for $PSA^-/PSMA^+$).

Heterogeneous AR Signaling in CTCs from Patients with CRPC

In marked contrast, patients with CRPC with detectable CTCs pretreatment (n = 14/20; 70%) displayed both intrapatient and interpatient heterogeneity in CTC AR activity (Fig. 2; Supplementary Table S2). Most remarkable was the abundance within each patient of CTCs with the "AR-off" ($PSA^-/PSMA^+$) signature (median 51.9%), as well as CTCs with an "AR-mixed" ($PSA^+/PSMA^+$) phenotype (median 17.6%). Despite the expected reactivation of AR signaling in CRPC, only a relatively small fraction of CTCs in these patients had the "AR-on" ($PSA^+/PSMA^-$) phenotype (median 11.1%). In contrast to the consistent treatment-induced changes in AR signaling patterns seen within CTCs of patients with castration-sensitive prostate cancer (CSPC), second-line hormonal treatment in patients with CRPC had varying effects on CTC numbers and AR phenotypes (Fig. 4; Supplementary Tables S1 and S2). This included patients treated with the relatively weak hormonal agents ketoconazole ($n = 1$) and bicalutamide (n = 2), as well as the potent CYP17A1 inhibitor abiraterone acetate (n = 17; Supplemental Table S2). Four of 17 (24%) patients with CRPC treated with abiraterone acetate had a 50% or more decline in the percentage of "AR-on" CTCs within 2 to 5 weeks of therapy, suggesting that the reduction in systemic androgen levels may have suppressed a subset of metastatic tumor cells with reactivated AR signaling (Fig. 4A–C; Supplementary Tables S1 and S2). In contrast, 2 of 17 (12%) patients with CRPC had a 2-fold or more increase in the percentage of "AR-on" CTCs within the first 2 to 5 weeks of therapy with abiraterone acetate, suggesting increased AR signaling despite therapy (Fig. 4D–F; Supplementary Tables S1 and S2). Eleven of 17 (65%) patients with CRPC had a stable percentage of "AR-on" CTCs after therapy. Analysis of baseline CTC AR signaling before the initiation of abiraterone acetate therapy suggested that the presence of a more than 10% component of "AR-mixed" CTCs was associated with decreased overall survival (log-rank $P < 0.05$; Fig. 4G). In addition, an increase in the percentage of "AR-on" CTCs despite abiraterone acetate therapy was correlated with decreased overall survival (Supplementary Fig. S6).

DISCUSSION

Cancer cells circulating in the peripheral blood provide a uniquely accessible source of tumor-derived material for molecular analyses. In metastatic prostate cancer, which primarily spreads to bone, the inability to noninvasively sample metastatic lesions has limited the ability to individualize second-line therapies according to the mechanism of drug resistance. Thus, while potent new inhibitors of the AR pathway are under active development, their clinical deployment still remains empiric. Given the interpatient variation in outcome, there is an unmet clinical need for biomarkers that may enable prediction of treatment response for individual patients. Here, we show that the activity of the AR pathway may be monitored in CTCs. Although the trends we observe need confirmation in subsequent analysis with additional patients, our results support the relevance of CTCs as dynamic tumor-derived biomarkers, reflecting "real time" effects of cancer drugs on their therapeutic targets, and the potential of CTC signaling analysis to identify the early emergence of resistance to therapy.

Although CTC enumeration using immunomagnetic bead capture has previously been shown to be a potential prognostic biomarker in patients with metastatic prostate cancer (9), enumeration alone does not yield direct insight into the effects of drugs on their molecular targets and may simply reflect relative tumor burden or leakiness of tumor-associated vasculature. In contrast, interrogation of the activity of specific signaling pathways within CTCs may reveal whether targeted therapies are effectively hitting their target *in vivo*, thus providing information that may be useful in guiding therapeutic decisions. Reverse transcription–PCR of transcripts from CTC-enriched cell populations may provide an alternative method for detecting CTCs (10), with the potential for measuring changes in relevant transcriptional output in CTCs. However, the need for quantitative analysis of signal within the heterogeneous cell populations, as documented here, supports the importance of single-cell measurements based on CTC imaging.

Because PSMA is a cell surface protein, it has been used as an alternative to EpCAM for capture of CTCs from patients with prostate cancer (11). Although more specific to prostate

Published OnlineFirst October 23, 2012; DOI: 10.1158/2159-8290.CD-12-0222

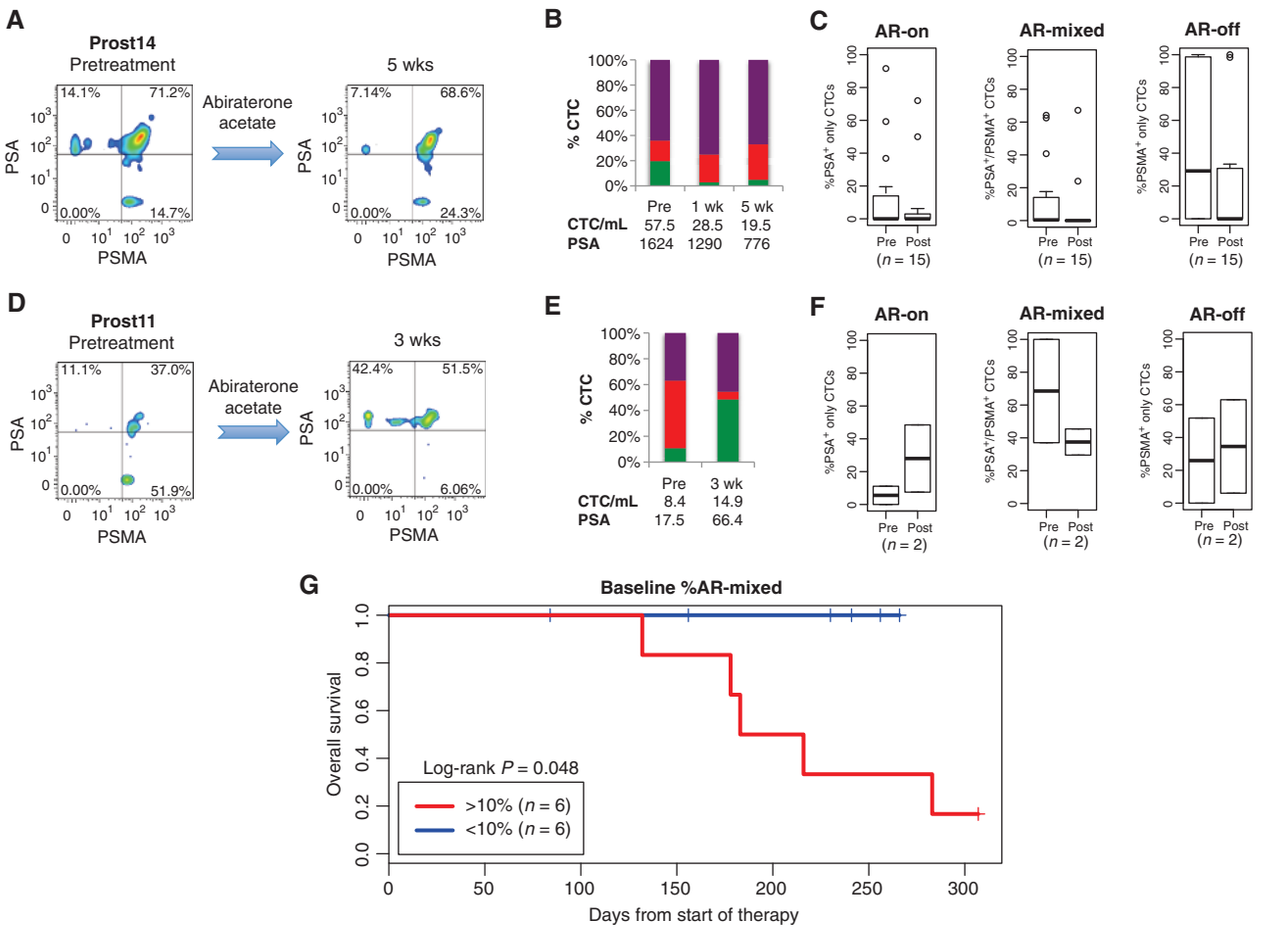

Figure 4. AR signaling in CTCs from CRPC patients treated with abiraterone acetate. **A,** pseudocolor density plots of multiparameter immunofluorescence AR signaling profiles of CTCs in a patient (Prost14) with CRPC, showing a decrease in the proportion of $PSA^+/PSMA^-$ "AR-on" CTCs after the initiation of abiraterone acetate. **B,** Bar graphs depicting the results for this patient at serial time points following treatment. Corresponding CTC numbers and serum PSA levels are shown for pretreatment (pre) and at weeks following therapy. **C,** box plots showing composite data for relative proportions of AR signaling phenotypes in CTCs from patients that exhibit stable or declining proportion of "AR-on" CTCs after initiation of therapy ($P = 0.56$ for PSA^+ only; $P = 0.12$ for $PSA^+/PSMA^+$; $P = 0.14$ for $PSMA^+$ only). **D,** increase in the proportion of $PSA^+/PSMA^-$ "AR-on" CTCs observed in a patient (Prost11) with CRPC after treatment with abiraterone acetate. **E,** bar graphs depicting the results for this patient. **F,** box plots showing composite data for relative proportions of AR signaling phenotypes in CTCs from patients that exhibit an increasing proportion of "AR-on" CTCs after initiation of therapy ($P = 0.67$ for PSA^+ only; $P = 0.67$ for $PSA^+/PSMA^+$; $P = 0.67$ for $PSMA^+$ only). **G,** Kaplan–Meier curves for overall survival in patients with CRPC treated with abiraterone acetate, according to baseline percentage of more than 10% "AR-mixed" CTCs (red) versus less than 10% "AR-mixed" CTCs [(blue) log-rank $P = 0.048$].

cancer, PSMA-based capture may miss the "AR-on" subsets of CTCs, whose phenotype is primarily $PSA^+/PSMA^-$, and which may be important in defining response to hormonal therapies. As such, anti-EpCAM antibody-mediated capture followed by immunophenotyping for PSA versus PSMA expression allows for broad capture of CTCs, followed by characterization of their AR signaling status. Critical for this approach is the optimization of 4-color immunofluorescence staining and imaging parameters, maximizing immunofluorescence signals, while minimizing cross-talk between channels for detection of PSA, PSMA, CD45, and nuclear signals, using a standardized semi-automated microscopy platform. Full automation of this assay will be required for its broad application in the context of clinical trials of novel hormonal agents in CRPC.

Although our study was designed as a "proof-of-concept" for a diagnostic approach, it also provides significant insight into the evolution of initially responsive prostate cancer into castration-resistant disease. We found that profound differences underlie the dramatic response of previously untreated, castration-sensitive disease to ADT, compared with the relatively limited effectiveness of even potent second-line hormonal agents in castration-resistant disease. CSPC is marked by the presence of predominant and strong "AR-on" CTC signals, with rapid switching to "AR-off" upon androgen withdrawal, preceding the disappearance of CTCs from the circulation. In contrast, CRPC is marked by striking heterogeneity among tumor cells from individual patients as well as between different patients with similar clinical histories. Few "AR-on" cells are observed, and instead there is an abundance of both "AR-off" and "AR-mixed" CTCs. Together, these suggest that pathways other than AR signaling contribute to disease progression in CRPC, and that the AR reactivation that

Published OnlineFirst October 23, 2012; DOI: 10.1158/2159-8290.CD-12-0222

does occur may be qualitatively altered despite the known overexpression of AR itself. Indeed, reactivation of AR signaling in CRPC does not seem to be as complete as previously suspected, and even potent AR suppression in this setting may be insufficient by itself to mediate dramatic tumor responses. Rising serum PSA levels in patients with CRPC have been taken as evidence of strong AR reactivation and potentially renewed susceptibility to hormonal manipulation. However, these serum measurements reflect total tumor burden, which may be considerable, whereas single-cell CTC analysis suggests that within individual tumor cells, AR signaling is not fully reactivated.

Although AR reactivation is the dominant model to explain acquisition of resistance to androgen withdrawal, the limited human data available are consistent with our observations of an attenuated AR phenotype in CRPC. For instance, gene expression studies of bone metastases have shown increased AR mRNA levels in CRPC (12), and bone marrow biopsy studies (13) as well as CTC analyses (14) have shown nuclear AR localization in resistant disease. However, expression levels of androgen-activated genes seem to be reduced by 2- to 3-fold in CRPC, compared with primary untreated prostate cancer (12, 15). The most common acquired genetic alteration affecting *AR*, a median 1.6- to 5-fold gene amplification seen in approximately 30% of cases (16, 17), may not be sufficient to fully overcome the effects of ligand withdrawal and reestablish full AR-driven tumor cell proliferation. Indeed, a recent analysis of gene promoters targeted by AR in cells that are sensitive to androgen withdrawal versus cells with acquired resistance showed a qualitatively distinct subset of AR-activated genes (18, 19). In our study, the complexity of AR signaling pathways in CRPC may be reflected by the presence of "AR-mixed" CTCs having simultaneous expression of androgen-induced and androgen-suppressed markers that was associated with decreased overall survival. Thus, expression analysis of AR target genes within CTCs may provide functionally relevant measures of aberrant AR activity.

In addition to altered AR signaling, AR-independent pathways, including PIK3CA-dependent signaling, have also been implicated in CRPC and may cooperate with partial AR reactivation in mediating disease progression in prostate cancer (20). Recent studies in mouse models of CRPC have suggested improved responses to combined AR and mTOR pathway inhibition (20). Given the potentially complex and heterogeneous mechanisms underlying CRPC, it is not surprising that treatment with the potent CYP-17A1 inhibitor abiraterone acetate alone has a varied effect on the number and composition of CTCs. Some patients with CRPC who did have measureable "AR-on" CTCs showed more than 50% decline in the percentage of this CTC subset within 2 to 5 weeks of abiraterone acetate therapy (4 of 17 patients; 24%). Given the mechanism of drug action, these cases may be enriched for patients in whom intratumoral or adrenal gland synthesis of androgens plays a major role in the development of castration resistance. In contrast, tumors driven by ligand-independent *AR* gene activation would not be expected to show any suppression in "AR-on" CTC numbers. Indeed, a rising fraction of "AR-on" CTCs despite continued abiraterone acetate therapy was associated with a poor outcome, defined as decreased overall survival. In these patients, ligand-independent AR activity may become a driver of tumor cell proliferation, leading to therapeutic failure. Potential mechanisms for the development of resistance to abiraterone acetate in CRPC are the subject of intense investigation (21). Further studies linking such mechanistic insights with the application of novel therapies targeting the relevant pathways may provide critical guidance in molecularly targeted therapy for CRPC.

In summary, in this exploratory study, we show that PSA/PSMA-based AR signaling assay in CTCs may enable real-time quantitative monitoring of intratumoral AR signaling and its potential contribution to disease progression within an individual patient. Although this assay has potential as a promising biomarker, it requires validation in larger prospective studies of patients with prostate cancer undergoing second-line hormonal therapy. While this work was in progress, positron emission tomography imaging using radiolabeled antibodies against PSMA and PSA were reported as biomarkers of AR signaling in prostate cancer mouse xenografts treated with the investigational AR inhibitor MDV 3100 (8, 22). If successful in human tumor imaging, radioisotope scanning for AR activity may complement single-cell CTC assays in providing ongoing monitoring for second-line hormonal agents in CRPC. Such individualization of second-line treatments in metastatic prostate cancer will be essential for therapeutic success, given the evident tumor cell heterogeneity that accompanies the emergence of resistance to initial androgen deprivation.

METHODS

Patients and Clinical Specimens

Patients with metastatic prostate cancer receiving treatment at the Massachusetts General Hospital (Boston, MA) were recruited according to an institutional review board (IRB)–approved protocol. Eligibility criteria included a histologic diagnosis of prostate adenocarcinoma and radiographic evidence of metastatic disease. For the CSPC cohort, recipients of prior hormonal therapy were excluded. Patients in the CRPC cohort required disease progression on ADT according to Prostate Cancer Working Group criteria (23), and may have received other therapies. A total of 25 patients donated 10 to 20 mL of blood on one or more occasions for CTC analysis. In addition, 21 male patients with no known diagnosis of cancer were recruited as controls using a separate IRB-approved protocol.

Cell Lines

LNCaP and VCaP cells were obtained from American Type Culture Collection after authentication by short tandem repeat profiling, and maintained as recommended. For generation of the AR signature, cells were cultured for 3 days in medium containing 10% charcoal-stripped FBS (Invitrogen) and treated with R1881 (Perkin-Elmer), bicalutamide (Sigma), or dimethyl sulfoxide (DMSO) as a vehicle control.

Immunofluorescence Staining and Automated Fluorescence Microscopy

Cells were captured on the ^{HB}CTC-chip as described (7), fixed and permeabilized as described (7), and stained with antibodies against PSA (rabbit polyclonal; DAKO), PSMA (J591 mouse monoclonal IgG1; N.H. Bander), and CD45 (mouse monoclonal IgG2a; Abcam), followed by appropriately matched secondary antibodies conjugated with DyLight 649 (Jackson ImmunoResearch), Alexa Fluor 555 (Invitrogen), and Alexa Fluor 488 (Invitrogen). Nuclei were stained with DAPI. An automated fluorescence microscopy scanning system (BioView)

Published OnlineFirst October 23, 2012; DOI: 10.1158/2159-8290.CD-12-0222

comprehensively imaged ^{HB}CTC-chips under ×10 magnification in seven *z*-planes in 4 colors at predetermined optimized exposure times, using modified Magnetron sputter-coated filter sets for the Cy3 and Cy5 spectra (Chroma; see Supplementary Methods for details). Potential CTCs were automatically classified using a previously described algorithm (6), followed by manual validation by a blinded human reviewer. High-resolution immunofluorescence images were obtained using an upright fluorescence microscope (Eclipse 90i, Nikon) under ×60 magnification.

Quantitative Single-Cell Immunofluorescence Analysis

Quantitative fluorescence intensity data for emission spectra (DAPI, FITC, Cy3, and Cy5) were obtained for each single cell as "Area pixels" measurements using image analysis software (Bioview). Data files were converted to CSV format and to FCS format (TextToFCS version 1.2.1; ref. 24) and analyzed using FlowJo version 7.6. Pseudocolor density plots were gated to display events that are CD45$^-$. Bar graphs were generated using Microsoft Excel reflecting proportions of PSA$^+$/PSMA$^-$/CD45$^-$, PSA$^+$/PSMA$^+$/CD45$^-$, and PSA$^-$/PSMA$^+$/CD45$^-$ CTCs tabulated after manual validation. Normalized counts (CTC/mL) were calculated by dividing the total CTC count by the total blood volume processed. A signal intensity threshold of detection based on healthy donors was determined to be 4 CTC/mL (Supplementary Fig. S5). Normalized counts below this threshold were considered as false-positive events and not included in the final analyses. In cases where normalized CTC counts were below the limit of reliable detection, percentage distributions of AR signaling phenotypes were not calculated (Supplementary Table S1).

Statistical Analysis

AR activity and the proportion of CTC phenotypes between samples were compared using the Wilcoxon rank-sum test. Overall survival was defined as the interval between the start of therapy and the date of death or censor. Serum PSA response was defined as a maximal decline of 50% or more in serum PSA (23). Survival curves were generated using the Kaplan–Meier method and compared using the log-rank test. Two-sided P values <0.05 were considered statistically significant. Statistical analyses were conducted using R, version 2.12.0.

Disclosure of Potential Conflicts of Interest

N.H. Bander has ownership interest (including patents) and is a consultant/advisory board member in BZL Biologics, Inc. No potential conflicts of interest were disclosed by the other authors.

Authors' Contributions

Conception and design: D.T. Miyamoto, R.J. Lee, S.L. Stott, M.R. Smith, M. Toner, S. Maheswaran, D.A. Haber

Development of methodology: D.T. Miyamoto, R.J. Lee, S.L. Stott, C.-L. Wu, M. Toner, S. Maheswaran, D.A. Haber

Acquisition of data (provided animals, acquired and managed patients, provided facilities, etc.): D.T. Miyamoto, R.J. Lee, D.T. Ting, M. Ulman, M.E. Smas, J.B. Lord, B.W. Brannigan, J. Trautwein, C.-L. Wu, L.V. Sequist, M.R. Smith

Analysis and interpretation of data (e.g., statistical analysis, biostatistics, computational analysis): D.T. Miyamoto, R.J. Lee, S.L. Stott, B.S. Wittner, M. Ulman, M.E. Smas, J.B. Lord, B.W. Brannigan, S. Ramaswamy, S. Maheswaran, D.A. Haber

Writing, review, and/or revision of the manuscript: D.T. Miyamoto, R.J. Lee, S.L. Stott, N.H. Bander, C.-L. Wu, L.V. Sequist, M.R. Smith, M. Toner, S. Maheswaran, D.A. Haber

Administrative, technical, or material support (i.e., reporting or organizing data, constructing databases): D.T. Miyamoto, S.L. Stott, D.T. Ting, N.H. Bander

Study supervision: R.J. Lee, L.V. Sequist, S. Ramaswamy, M. Toner, S. Maheswaran, D.A. Haber

Acknowledgments

The authors thank J. Walsh, F. Floyd, G. Korir, C. Koris, and L. Libby for technical support.

In memory of Charles Evans and in recognition of philanthropic support for prostate cancer research from the Evans Foundation, we propose that this CTC-based test be called the Evans Assay.

Grant Support

This work was supported by a Challenge Grant from the Evans Foundation and the Prostate Cancer Foundation (PCF); a Stand Up To Cancer Dream Team Translational Cancer Research Grant, a Program of the Entertainment Industry Foundation (SU2C-AACR-DT0309, to D.A. Haber, M. Toner, and S. Maheswaran); T.J. Martell Foundation (to D.A. Haber); Starr Cancer Consortium (to D.A. Haber); the Susan G. Komen for the Cure KG090412 (S. Maheswaran); NIH-NIBIB-5R01EB008047 (to M. Toner and D.A. Haber); NCI-CA129933 (to D.A. Haber); the NCI-MGH Federal Share Program (to S. Maheswaran); NCI-C06-CA-059267 (to D.T. Miyamoto); NIH-5K12CA87723-09 (to D.T. Ting); Department of Defense Physician Research Training Awards (to D.T. Miyamoto and R.J. Lee); Mazzone-DF/HCC Career Development Award (to D.T. Miyamoto); Conquer Cancer Foundation Career Development Award and PCF Young Investigator Award (to R.J. Lee); American Cancer Society (to S.L. Stott); and Howard Hughes Medical Institute (to D.A. Haber).

Received May 15, 2012; revised August 22, 2012; accepted August 22, 2012; published OnlineFirst October 23, 2012.

REFERENCES

1. Scher HI, Sawyers CL. Biology of progressive, castration-resistant prostate cancer: directed therapies targeting the androgen-receptor signaling axis. J Clin Oncol 2005;23:8253–61.
2. Yuan X, Balk SP. Mechanisms mediating androgen receptor reactivation after castration. Urol Oncol 2009;27:36–41.
3. Chen CD, Welsbie DS, Tran C, Baek SH, Chen R, Vessella R, et al. Molecular determinants of resistance to antiandrogen therapy. Nat Med 2004;10:33–9.
4. Tran C, Ouk S, Clegg NJ, Chen Y, Watson PA, Arora V, et al. Development of a second-generation antiandrogen for treatment of advanced prostate cancer. Science 2009;324:787–90.
5. de Bono JS, Logothetis CJ, Molina A, Fizazi K, North S, Chu L, et al. Abiraterone and increased survival in metastatic prostate cancer. N Engl J Med 2011;364:1995–2005.
6. Stott SL, Lee RJ, Nagrath S, Yu M, Miyamoto DT, Ulkus L, et al. Isolation and characterization of circulating tumor cells from patients with localized and metastatic prostate cancer. Sci Transl Med 2010;2: 25ra3.
7. Stott SL, Hsu CH, Tsukrov DI, Yu M, Miyamoto DT, Waltman BA, et al. Isolation of circulating tumor cells using a microvortex-generating herringbone-chip. Proc Natl Acad Sci U S A 2010;107:18392–7.
8. Evans MJ, Smith-Jones PM, Wongvipat J, Navarro V, Kim S, Bander NH, et al. Noninvasive measurement of androgen receptor signaling with a positron-emitting radiopharmaceutical that targets prostate-specific membrane antigen. Proc Natl Acad Sci U S A 2011;108:9578–82.
9. Danila DC, Heller G, Gignac GA, Gonzalez-Espinoza R, Anand A, Tanaka E, et al. Circulating tumor cell number and prognosis in progressive castration-resistant prostate cancer. Clin Cancer Res 2007;13:7053–8.
10. Helo P, Cronin AM, Danila DC, Wenske S, Gonzalez-Espinoza R, Anand A, et al. Circulating prostate tumor cells detected by reverse transcription-PCR in men with localized or castration-refractory prostate cancer: concordance with CellSearch assay and association with bone metastases and with survival. Clin Chem 2009;55:765–73.

Published OnlineFirst October 23, 2012; DOI: 10.1158/2159-8290.CD-12-0222

11. Kirby BJ, Jodari M, Loftus MS, Gakhar G, Pratt ED, Chanel-Vos C, et al. Functional characterization of circulating tumor cells with a prostate-cancer-specific microfluidic device. PLoS ONE 2012;7:e35976.
12. Stanbrough M, Bubley GJ, Ross K, Golub TR, Rubin MA, Penning TM, et al. Increased expression of genes converting adrenal androgens to testosterone in androgen-independent prostate cancer. Cancer Res 2006;66:2815–25.
13. Efstathiou E, Titus M, Tsavachidou D, Tzelepi V, Wen S, Hoang A, et al. Effects of abiraterone acetate on androgen signaling in castrate-resistant prostate cancer in bone. J Clin Oncol 2012;30:637–43.
14. Darshan MS, Loftus MS, Thadani-Mulero M, Levy BP, Escuin D, Zhou XK, et al. Taxane-induced blockade to nuclear accumulation of the androgen receptor predicts clinical responses in metastatic prostate cancer. Cancer Res 2011;71:6019–29.
15. Mendiratta P, Mostaghel E, Guinney J, Tewari AK, Porrello A, Barry WT, et al. Genomic strategy for targeting therapy in castration-resistant prostate cancer. J Clin Oncol 2009;27:2022–9.
16. Visakorpi T, Hyytinen E, Koivisto P, Tanner M, Keinanen R, Palmberg C, et al. *In vivo* amplification of the androgen receptor gene and progression of human prostate cancer. Nat Genet 1995;9:401–6.
17. Brown RS, Edwards J, Dogan A, Payne H, Harland SJ, Bartlett JM, et al. Amplification of the androgen receptor gene in bone metastases from hormone-refractory prostate cancer. J Pathol 2002; 198:237–44.
18. Wang Q, Li W, Zhang Y, Yuan X, Xu K, Yu J, et al. Androgen receptor regulates a distinct transcription program in androgen-independent prostate cancer. Cell 2009;138:245–56.
19. Cai C, He HH, Chen S, Coleman I, Wang H, Fang Z, et al. Androgen receptor gene expression in prostate cancer is directly suppressed by the androgen receptor through recruitment of lysine-specific demethylase 1. Cancer Cell 2011;20:457–71.
20. Carver BS, Chapinski C, Wongvipat J, Hieronymus H, Chen Y, Chandarlapaty S, et al. Reciprocal feedback regulation of PI3K and androgen receptor signaling in PTEN-deficient prostate cancer. Cancer Cell 2011;19:575–86.
21. Cai C, Chen S, Ng P, Bubley GJ, Nelson PS, Mostaghel EA, et al. Intratumoral *de novo* steroid synthesis activates androgen receptor in castration-resistant prostate cancer and is upregulated by treatment with CYP17A1 inhibitors. Cancer Res 2011;71:6503–13.
22. Ulmert D, Evans MJ, Holland JP, Rice SL, Wongvipat J, Pettersson K, et al. Imaging androgen receptor signaling with a radiotracer targeting free prostate-specific antigen. Cancer Discov 2012;2: 320–7.
23. Scher HI, Halabi S, Tannock I, Morris M, Sternberg CN, Carducci MA, et al. Design and end points of clinical trials for patients with progressive prostate cancer and castrate levels of testosterone: recommendations of the Prostate Cancer Clinical Trials Working Group. J Clin Oncol 2008;26:1148–59.
24. Text-ToFCS version 1.2.1. Available from: http://offsite.treestar.com/downloads/utilities/TextToFCS_documentation.

Science Translational Medicine
AAAS

Inertial Focusing for Tumor Antigen–Dependent and –Independent Sorting of Rare Circulating Tumor Cells

Emre Ozkumur *et al.*

Sci Transl Med **5**, 179ra47 (2013);
DOI: 10.1126/scitranslmed.3005616

Editor's Summary

Positive and Negative Outcomes

Usually people want the good news first, to help cope with the bad news that inevitably follows. However, patients will soon desire both the positive and the negative outcomes together, according to the latest study by Ozkumur and colleagues. These authors have developed a multistage microfluidic device that is capable of sorting rare circulating tumor cells (CTCs) that are either positive or negative for the surface antigen epithelial cell adhesion molecule (EpCAM).

$EpCAM^+$ cells found in the bloodstream have long defined the typical CTC. Many sorting technologies have been developed to enumerate $EpCAM^+$ CTCs in cancer patient's blood; however, these cells are not always detectable in cancers with low EpCAM expression, like triple-negative breast cancer or melanoma. Ozkumur *et al.* engineered an automated platform, called the "CTC-iChip," that captured both $EpCAM^+$ and $EpCAM^-$ cancer cells in clinical samples using a series of debulking, inertial focusing, and magnetic separation steps. The sorted CTCs could then be interrogated using standard clinical protocols, such as immunocytochemistry. The authors tested the "positive mode" of their device using whole blood from patients with prostate, lung, breast, pancreatic, and colorectal cancers. After successfully separating out the $EpCAM^+$ CTCs, they confirmed that the cells were viable and had high-quality RNA for molecular analysis, in one example, detecting the *EML4-ALK* gene fusion in lung cancer. Using the "negative mode" of their device, the authors were able to capture $EpCAM^-$ CTCs from patients with metastatic breast cancer, pancreatic cancer, and melanoma. The isolated CTCs showed similar morphology when compared with primary tumor tissue from these patients, suggesting that the microfluidic device can be used for clinical diagnoses—delivering both positive and negative news at once.

Ozkumur *et al.* also demonstrated that CTCs isolated using the iChip could be analyzed on the single-cell level. One such demonstration with 15 CTCs from a prostate cancer patient reveals marked heterogeneity in the expression of mesenchymal and stem cell markers as well as typical prostate cancer –related antigens. The CTC-iChip can therefore process large volumes of patient blood to obtain not just $EpCAM^+$ CTCs but also the $EpCAM^-$ ones, thus giving a broader picture of an individual's cancer status and also allowing the device to be used for more cancer types. With the ability to further analyze the molecular characteristics of CTCs, this CTC-iChip could be a promising addition to current diagnostic tools used in the clinic.

Science Translational Medicine (print ISSN 1946-6234; online ISSN 1946-6242) is published weekly, except the last week in December, by the American Association for the Advancement of Science, 1200 New York Avenue NW, Washington, DC 20005.

Science Translational Medicine (print ISSN 1946-6234; online ISSN 1946-6242) is published weekly, except the last week in December, by the American Association for the Advancement of Science, 1200 New York Avenue NW, Washington, DC 20005.

CANCER DIAGNOSTICS

Inertial Focusing for Tumor Antigen–Dependent and –Independent Sorting of Rare Circulating Tumor Cells

Emre Ozkumur,[1]* Ajay M. Shah,[1]* Jordan C. Ciciliano,[2] Benjamin L. Emmink,[1] David T. Miyamoto,[2,3] Elena Brachtel,[4] Min Yu,[2,5] Pin-i Chen,[1] Bailey Morgan,[1] Julie Trautwein,[2] Anya Kimura,[2] Sudarshana Sengupta,[2] Shannon L. Stott,[1,2] Nezihi Murat Karabacak,[1] Thomas A. Barber,[1] John R. Walsh,[1] Kyle Smith,[1] Philipp S. Spuhler,[1] James P. Sullivan,[2,6] Richard J. Lee,[2,6] David T. Ting,[2,6] Xi Luo,[2,5] Alice T. Shaw,[2,6] Aditya Bardia,[2,6] Lecia V. Sequist,[2,6] David N. Louis,[4] Shyamala Maheswaran,[2,7] Ravi Kapur,[1] Daniel A. Haber,[2,5,6] Mehmet Toner[1,7†]

Circulating tumor cells (CTCs) are shed into the bloodstream from primary and metastatic tumor deposits. Their isolation and analysis hold great promise for the early detection of invasive cancer and the management of advanced disease, but technological hurdles have limited their broad clinical utility. We describe an inertial focusing–enhanced microfluidic CTC capture platform, termed "CTC-iChip," that is capable of sorting rare CTCs from whole blood at 10^7 cells/s. Most importantly, the iChip is capable of isolating CTCs using strategies that are either dependent or independent of tumor membrane epitopes, and thus applicable to virtually all cancers. We specifically demonstrate the use of the iChip in an expanded set of both epithelial and nonepithelial cancers including lung, prostate, pancreas, breast, and melanoma. The sorting of CTCs as unfixed cells in solution allows for the application of high-quality clinically standardized morphological and immunohistochemical analyses, as well as RNA-based single-cell molecular characterization. The combination of an unbiased, broadly applicable, high-throughput, and automatable rare cell sorting technology with generally accepted molecular assays and cytology standards will enable the integration of CTC-based diagnostics into the clinical management of cancer.

INTRODUCTION

The rarity of circulating tumor cells (CTCs) in the blood of cancer patients has required development of highly specialized technologies for their isolation (*1, 2*). Once detected, enumeration and molecular characterization of CTCs have been applied to prognostic classifications of breast, prostate, and colon cancers (*3*), and to predictive markers of targeted drug therapy in lung cancer (*4*). However, the limited sensitivity of commercially available approaches combined with the complexity and heterogeneity of the disease has restricted the broad acceptance and dissemination of CTC-based diagnostics (*5*).

Several strategies have been used to process blood for analysis of CTCs, including platforms for rapid scanning of unpurified cell populations (*6–8*). The most common enrichment approaches have used antibodies against the cell surface protein epithelial cell adhesion molecule (EpCAM). Labeling CTCs with anti-EpCAM–coated beads, followed by bulk magnetic enrichment methods (*9–11*), has been tested. The U.S. Food and Drug Administration (FDA)–approved Veridex system, CellSearch, immunomagnetically labels CTCs and then enriches the cells by bulk purification across a magnetic field. Conceptually, EpCAM-based CTC capture may have limited ability to identify tumor cells with reduced expression of this epithelial marker as a result of the epithelial-mesenchymal transition (EMT) (*12*). However, tumor antigen–independent CTC enrichment, such as bulk depletion of hematopoietic cells, suffers from poor yields and low purity (*13, 14*). Together, CTC isolation approaches have traditionally involved multiple batch processing steps, resulting in substantial loss of CTCs (*14*).

Recently, we introduced microfluidic methods to improve the sensitivity of CTC isolation (*15*), a strategy that is particularly attractive because it can lead to efficient purification of viable CTCs from unprocessed whole blood (*16–21*). The micropost CTC-Chip ($^{\mu P}$CTC-Chip) relies on laminar flow of blood cells through anti-EpCAM antibody-coated microposts (*15*), whereas the herringbone CTC-Chip (^{Hb}CTC-Chip) uses microvortices generated by herringbone-shaped grooves to direct cells toward antibody-coated surfaces (*16*). Although promising, these methods require surface functionalization to bind to tumor antigens on CTCs and thus yield CTCs that are immobilized within a microfluidic chamber and are not readily subjected to either standard clinical cytopathological imaging or single-cell molecular characterization.

To address the shortcomings of the current approaches, we developed a strategy that combines the strengths of microfluidics for rare cell handling while incorporating the benefits of magnetic-based cell sorting. After the magnetic labeling of cells in whole blood, this capture platform integrates three sequential microfluidic technologies within a single automated system: (i) debulking by separation of nucleated cells, including CTCs and white blood cells (WBCs), from red blood cells (RBCs) and platelets using deterministic lateral displacement (*22*); (ii) alignment of nucleated cells within a microfluidic channel using inertial focusing (*23*); and (iii) deflection of magnetically tagged cells into a collection

[1]Massachusetts General Hospital Center for Engineering in Medicine, Harvard Medical School, Boston, MA 02114, USA. [2]Massachusetts General Hospital Cancer Center, Harvard Medical School, Boston, MA 02114, USA. [3]Department of Radiation Oncology, Massachusetts General Hospital, Harvard Medical School, Boston, MA 02114, USA. [4]Department of Pathology, Massachusetts General Hospital, Harvard Medical School, Boston, MA 02114, USA. [5]Howard Hughes Medical Institute, Chevy Chase, MD 20815, USA. [6]Department of Medicine, Massachusetts General Hospital, Harvard Medical School, Boston, MA 02114, USA. [7]Department of Surgery, Massachusetts General Hospital, Harvard Medical School, Boston, MA 02114, USA.
*These authors contributed equally to this work.
†Corresponding author. E-mail: mtoner@hms.harvard.edu

channel. In essence, these three integrated microfluidic functions replace bulk RBC lysis and/or centrifugation, hydrodynamic sheath flow in flow cytometry, and magnetic-activated cell sorting (MACS). We call this integrated microfluidic system the CTC-iChip, based on the inertial focusing strategy, which allows positioning of cells in a near-single file line, such that they can be precisely deflected using minimal magnetic force. This integrated microfluidic platform, with its ability to isolate CTCs in suspension using both tumor antigen–dependent and tumor antigen–independent modes, is compatible with high-definition imaging and single-cell molecular analyses, as well as standard clinical cytopathology. We demonstrate its capabilities for diverse cancer diagnostic applications in both epithelial and nonepithelial cancers.

RESULTS

CTC-iChip design and function

The overall CTC-iChip isolation strategy is depicted in Fig. 1 and fig. S1. We explored two modes of immunomagnetic sorting to isolate CTCs: a positive selection mode (^{pos}CTC-iChip), whereby CTCs are identified and sorted on the basis of their expression of EpCAM, and a negative selection mode (^{neg}CTC-iChip), in which the blood sample is depleted of leukocytes by immunomagnetically targeting both the common leukocyte antigen CD45 and the granulocyte marker CD15.

Target cell labeling was developed and characterized for both operational modes (fig. S2). After labeling, the first stage within the CTC-iChip used hydrodynamic size–based sorting to achieve low shear microfluidic debulking of whole blood (*22*, *24*). RBCs, platelets, plasma proteins, and free magnetic beads were discarded, whereas nucleated cells (WBCs and CTCs) were retained and presented to the second stage for inertial focusing. The efficient removal of free beads is critical because these may accumulate in the magnetophoresis channel and significantly reduce the sensitivity and specificity of the approach. The operational principle of microfluidic debulking is based on hydrodynamic size–dependent deterministic lateral displacement (*22*, *24*), in which coincident flow of cell-containing and cell-free solutions through an array of microposts leads to rapid size-based separation (Fig. 1C and fig. S3). We tested two different array configurations with gaps between

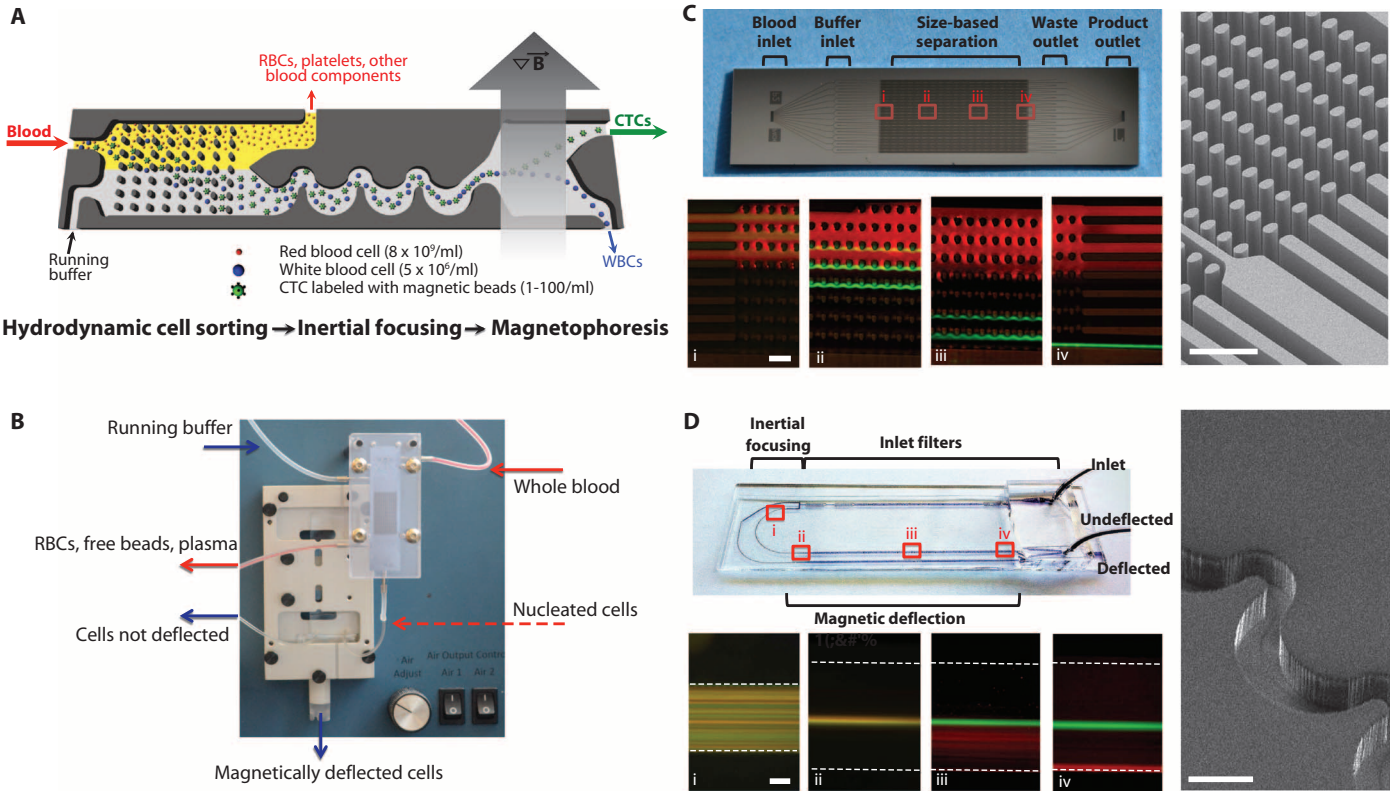

Fig. 1. The CTC-iChip system. (**A**) Three microfluidic components of the CTC-iChip are shown schematically. Whole blood premixed with immunomagnetic beads and buffer comprises the inputs. The figure demonstrates the positive isolation method; however, the system can be operated in negative depletion mode. (**B**) Integrated microfluidic system. The debulking array sits in a custom polycarbonate manifold that enables fluidic connections to the inputs, waste line, and second-stage microfluidic channels. The inertial focusing and magnetophoresis chip is placed in an aluminum manifold that houses the quadrupole magnetic circuit. Magnetically deflected cells are collected in a vial. (**C**) Hydrodynamic size–based sorting. A mixture of 2-μm (red) and 10-μm (green) beads enters the channel (i). Whereas the 2-μm beads remain in laminar flow and follow the fluid streamlines, the 10-μm spheres interact with the post-array (ii and iii) as shown in the scanning electron microscope (SEM) image (right panel). Larger beads are fully deflected into the coincident running buffer stream by the end of the array (iv). Scale bars, 100 μm. (**D**) Cell focusing and magnetophoretic sorting. Magnetically labeled SKBR3 (red) and unlabeled PC3-9 (green) cell populations are mixed and enter the channel in random distribution (i). After passing through 60 asymmetric focusing units (pictured in the SEM, right panel), the cells align in a single central stream (ii). Magnetically tagged cells are then deflected (iii) using an external magnetic field, and separation is achieved by the end of the channel (iv). Scale bars, 100 μm.

microposts of 20 or 32 μm. An array with 20-μm gaps retains virtually all nucleated cells with minimal contaminating RBCs but has a cutoff for cells larger than 21 μm and may therefore lose large CTCs or CTC clusters. In contrast, an array with 32-μm gaps has an extended operating range for cells between 8 and 30 μm but retains only 60% of WBCs. Because the cells lost in the 32-μm gap array are granulocytes and lymphocytes that are smaller than the reported CTC sizes (*16*), we selected this array for the CTC-iChip.

The second CTC-iChip component orders nucleated cells within the microfluidic channel, both laterally and longitudinally, so they can be precisely deflected into a collection channel with minimal magnetic moment. The rationale underlying the inertial focusing of cells in microchannels is based on the principles of pipe flow (*23*, *25*); essentially, a cellular fluid entering asymmetric, curved channels emerges as a tight row of individual cells traveling within a defined streamline position (Fig. 1D). We tested variable cell suspensions for focusing performance; WBCs as well as cancer cell lines were well focused within the operational parameters (hematocrit less than 0.4%; flow rate between 50 and 150 μl/min; nucleated cell concentration less than 3×10^6/ml) (fig. S4). Inertial focusing operational parameters were matched to output of the preceding debulking array, and the in-line integration of these complex microfluidic structures within the CTC-iChip thus avoided cell losses associated with commonly used batch processing strategies.

In the final CTC-iChip component, magnetically labeled cells are separated from unlabeled cells within a deflection channel. The precise control over cell position provided by inertial focusing prevents cellular collisions during magnetophoresis; therefore, cell displacement occurs as a predictable function of magnetic load. We modeled the forces exerted on cells labeled with 1-μm beads using a quadrupole magnetic circuit (fig. S5) and predicted deflection patterns under different flow and magnetic load conditions (Fig. 2A). This model was tested using magnetically labeled PC3-9 human prostate cancer cells. The measured deflection distance, plotted as a function of magnetic load, matched the prediction (Fig. 2B).

To demonstrate the dependence of sensitivity on flow speed, we processed labeled cells at various flow rates and quantified the number of beads per cell for deflected and nondeflected outputs (Fig. 2C and fig. S6). The improvement in sensitivity with increasing magnetic residence time (by reducing flow speed) correlated with the predictive model (Fig. 2D), indicating high magnetic sensitivity for the overall system (5 to 20 beads per cell, depending on cell size). The process parameters characterized for the ^{pos}CTC-iChip applied similarly to the ^{neg}CTC-iChip.

Evaluating the CTC-iChip using cells spiked into whole blood

To evaluate the efficiency of the CTC-iChip, we spiked five cell lines spanning a broad range of EpCAM expression into healthy whole blood and isolated using ^{pos}CTC-iChip or ^{neg}CTC-iChip modes. The EpCAM expression of each cell line was quantified by comparing the anti-EpCAM signal to that of a matched irrelevant antibody (Fig. 3A). Recovery of SKBR3 human breast cancer cells [24-fold EpCAM signal over control immunoglobulin G (IgG)] was 98.6 ± 4.3% (mean ± SD), and capture of human prostate PC3-9 cancer cells (3.7-fold EpCAM signal) was 89.7 ± 4.5% (Fig. 3B). Even cells with minimal EpCAM expression, such as MDA-MB-231 (*26*), a "triple-negative" mesenchymal breast

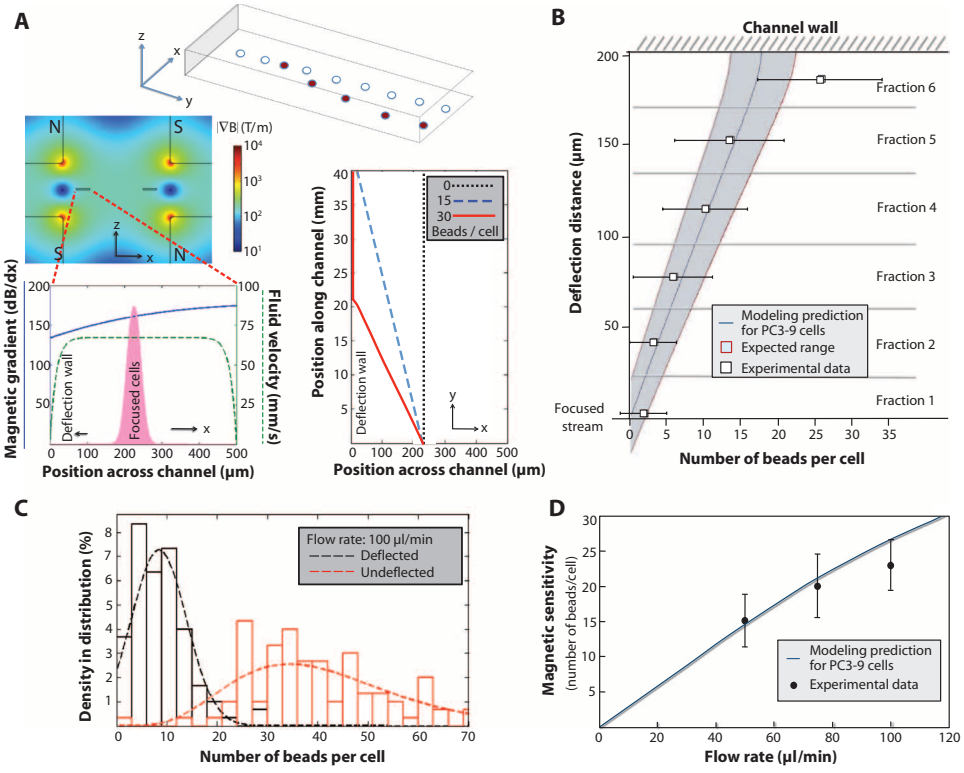

Fig. 2. Modeling and magnetic sensitivity of the system. (**A**) A mathematical model describes the deflection of labeled cells (red) from a focused stream (white). Finite element method analysis of the quadrupole magnetic circuit and fluid flow in the channel provided estimates of the magnetic gradient (blue) and flow rate (green) across the deflection channel (left panel). This information, in conjunction with our experimental understanding of cell position in the focused stream (pink), was used to construct an overall model to predict the trajectories of focused cells with varying magnetic loads (right panel). (**B**) High sensitivity of inertial focusing enhanced magnetophoresis. Human PC3-9 cells were labeled with varying numbers of magnetic beads and collected in separate exit streams after traveling in the 4-cm-long magnetic deflection channel, fractionating the cells based on magnetic deflection distance. The beads on a representative population of cells were counted in each fraction. The deflection distance was measured from focused stream position to the channel wall. Fraction 6 included cells that deflected all the way and traveled at the wall; therefore, this data point did not match the simulation. The expected variations in cell sizes and the initial distribution of cells in the focused stream contribute to a variation in the deflection pattern that is reflected by shading the expected range around the model prediction. (**C**) The experimental "magnetic sensitivity" was determined by plotting histograms of bead loading density for deflected and undeflected cells for a given flow rate. The intersection of curve fits of these data represents the minimum number of beads required to deflect a cell. (**D**) The minimum required magnetic load increases with higher flow rates, as expected, and is accurately predicted by the model.

cancer cell line (only 2.5-fold EpCAM signal over control), were recovered with 77.8 ± 7.8% capture efficiency by ^{pos}CTC-iChip. Virtually complete abrogation of EpCAM expression, achieved by ectopic expression of the EMT master regulator LBX1 in MCF10A human breast cancer cells (MCF10A-LBX1) (*27*), resulted in 10.9 ± 3.0% capture efficiency.

Switching to the ^{neg}CTC-iChip, both the epithelial parental MCF10A cells and their highly mesenchymal MCF10A-LBX1 derivatives were captured at equal efficiency (96.7 ± 1.9% for MCF10As and 97.0 ± 1.7% for the MCF10A-LBX1 derivatives) (Fig. 3B). Together, these two modes demonstrate the flexibility of the CTC-iChip to isolate a broad spectrum of rare cells with high efficiency in both tumor antigen–dependent and tumor antigen–independent modes.

Sample purity was analyzed for both operating modes. Using EpCAM-based positive selection, we achieved an average >3.5-log purification (mean, 1500 WBCs/ml of whole blood; range, 67 to 2537 WBCs/ml). In the leukocyte depletion mode, purification was 2.5 log (mean, 32,000 WBCs/ml; range, 17,264 to 39,172 WBCs/ml) (Fig. 3C). In the ^{pos}CTC-iChip, the vast majority of contaminating WBCs carried magnetic beads, suggesting that nonspecific interactions between WBCs and either the anti-EpCAM antibody or the beads themselves caused the contamination. In the ^{neg}CTC-iChip, contaminating WBCs were free of beads, suggesting that they comprise a population of leukocytes with reduced CD45 or CD15 expression, as confirmed by flow cytometry (table S1).

^{pos}CTC-iChip isolation of CTCs

We tested the ^{pos}CTC-iChip in patients with prostate cancer, a disease in which metastatic lesions primarily affect bone, and hence, CTC analysis is key to analyzing recurrences after resection of the primary tumor. On average, 10 ml (range, 6 to 12 ml) of whole blood was analyzed from these patients. Using triple staining for cytokeratins (CKs) (epithelial marker), CD45 (leukocytes), and 4′,6-diamidino-2-phenylindole (DAPI) (nuclear marker), we identified ≥0.5 CTC/ml in 37 of 41 (90%) prostate patients with recurrent (castration-resistant) disease (mean, 50.3/ml; range, 0.5 to 610/ml; median, 3.2/ml) (Fig. 4A). The detection cutoff of 0.5 CTC/ml was more than 2 SDs above the mean number of CK$^+$ cells detected in 13 healthy donors (excluding an outlier with 0.7/ml; mean ± SD, 0.17 ± 0.12/ml; median, 0.19/ml; range, 0 to 0.33/ml). WBC contamination in the ^{pos}CTC-iChip product was low (mean, 1188/ml; median, 352/ml; range, 58 to 9249/ml), resulting in high sample purities (mean, 7.8%; median, 0.8%; range for samples with ≥0.5 CTC/ml, 0.02 to 43%) (fig. S7).

We performed a detailed comparison of the ^{pos}CTC-iChip with the FDA-approved CellSearch system (Fig. 4B). To minimize reagent variability between platforms, we used anti-EpCAM capture as well as CK and CD45 staining antibodies from the same source, and consistent criteria were used to evaluate putative CTCs. CTCs were defined as DAPI$^+$/CD45$^-$/CK$^+$, and WBCs were defined as DAPI$^+$ or DAPI$^+$/CD45$^+$ events. Specimens from prostate (n = 19) and other cancers (breast, n = 12; pancreas, n = 6; colorectal, n = 2; lung, n = 2) were compared. Although both assays performed well with high CTC loads (>30 CTCs per 7.5 ml), at lower CTC numbers, there was a marked differential in capture efficiency. Among the 86% (36 of 42) of metastatic cancer patients with fewer than 30 CTCs/7.5 ml, the number of CK$^+$ CTCs isolated with the ^{pos}CTC-iChip was significantly higher in 22 cases (P < 0.001, paired t test analysis). The remaining 14 cases had CTCs below detection limits for both systems (Fig. 4B and table S2). Thus, the sensitivity of the CTC-iChip is particularly critical in patients with a lower CTC burden.

In addition to capturing more CTCs in patients with lower CTC burdens, the iChip isolates these cells in suspension, which in turn enables their immobilization on a standard glass slide for high-resolution imaging and standard clinical cytopathological examination (fig. S8), as well as simultaneous staining for multiple biomarkers (Fig. 4, C and D). Beyond imaging, molecular genetic tools are increasingly applied to the characterization of CTCs. Nowhere is this more evident than in non–small cell lung cancer (NSCLC), where targeted therapies can provide marked clinical benefit (*28*). Among the most challenging assays is detection of the *EML4-ALK* translocation in about 3% of cases, which marks those responsive to the selective

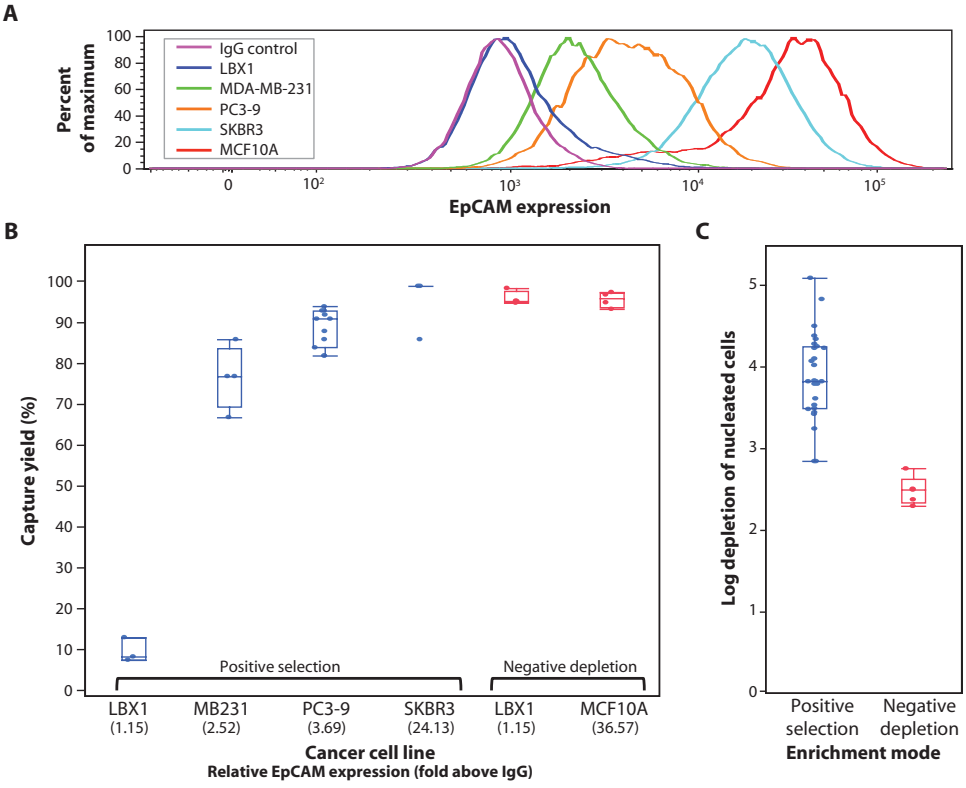

Fig. 3. Evaluation of overall system performance using cancer cell lines spiked into whole blood. (**A**) Quantitation of variable EpCAM expression in five cell lines using flow cytometry. (**B**) Capture yield of positive selection and negative depletion modes using various cell lines expressing different levels of EpCAM. (**C**) Background in ^{pos}CTC-iChip product is measured, achieving >3.5-log depletion of WBCs. In contrast, ^{neg}CTC-iChip has an order of magnitude lower purification. In both (B) and (C), each data point is an experimental result. Upper and lower bounds of the boxes signify the 75th and 25th quantiles, respectively. Perpendicular line in the box represents median value, and data points left above or below the error bars are outliers.

targeted inhibitor crizotinib. Detection of this intrachromosomal translocation by fluorescence in situ hybridization (FISH) is difficult, and, at the molecular level, the variability of chromosomal breakpoints necessitates RNA-based detection of the fusion transcript, which cannot be readily achieved using either fixed CTCs or free plasma nucleic acids.

We established a reverse transcription polymerase chain reaction (RT-PCR) assay capable of detecting the *EML4-ALK* translocation in H3122 lung cancer cells spiked into WBCs at a purity of 0.1% or introduced into whole blood (10 cells/10 ml) and processed through the ^{pos}CTC-iChip (Fig. 4E). In patient specimens, the *EML4-ALK* transcript was detected in CTCs from four cases known to have this chromosome rearrangement by FISH analysis of the primary tumor. It was absent in CTCs from two NSCLC patients and one patient with prostate cancer whose tumors were all known to lack this abnormality. In cases where CTC-based RNA analysis identified the expected product, nucleotide sequencing confirmed the breakpoint in the fusion transcript (Fig. 4F). Thus, the ^{pos}CTC-iChip allowed purification of CTCs for RNA-based molecular genotyping.

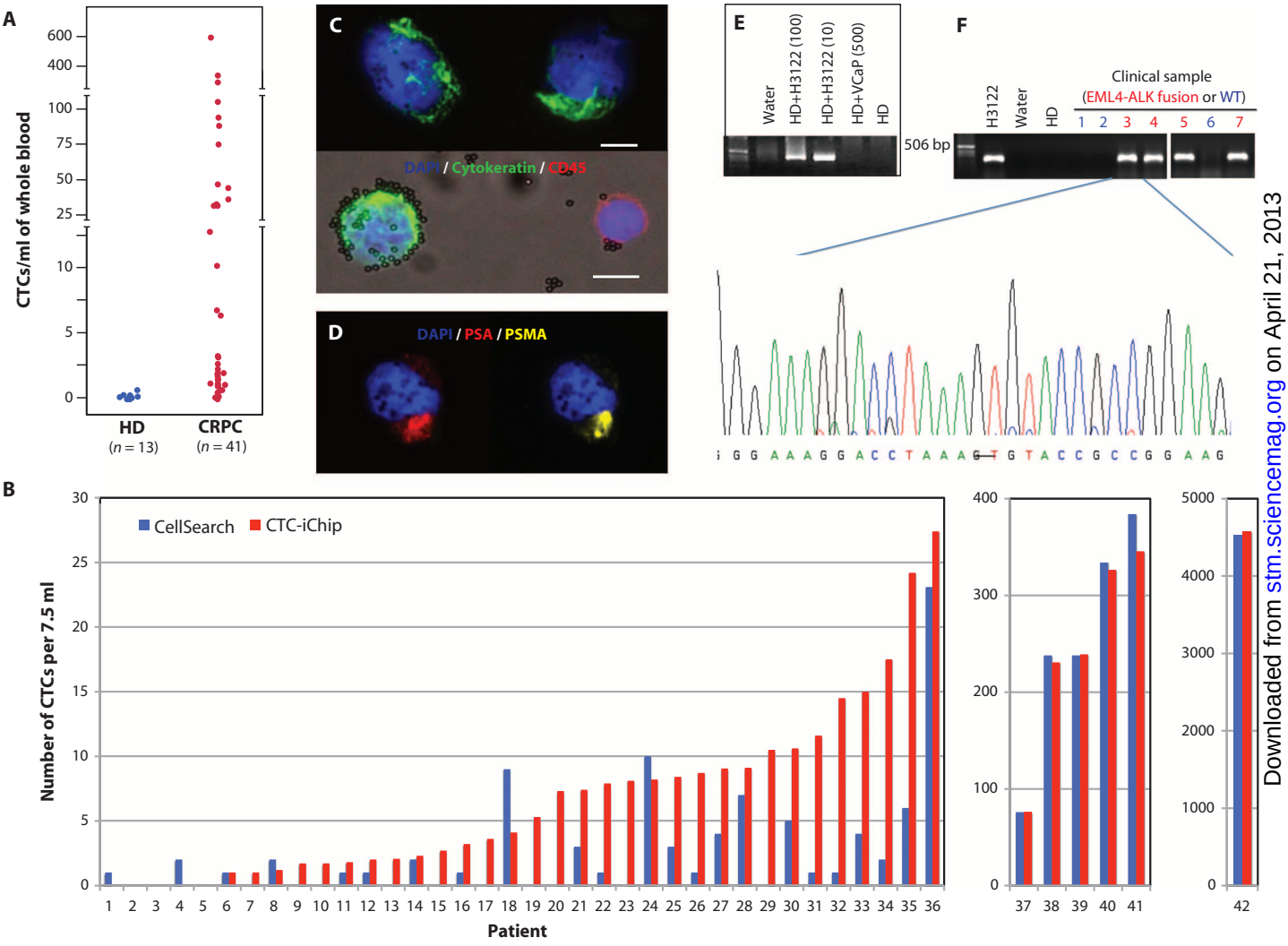

Fig. 4. CTC isolation by ^{pos}CTC-iChip in cancer patients. (**A**) CTCs isolated from castrate-resistant prostate cancer (CRPC) patients were enumerated and compared with blood specimens processed from healthy donors. (**B**) EpCAM-based isolation using ^{pos}CTC-iChip was compared with the CellSearch system. Clinical samples were metastatic cancer patients of prostate (n = 19), breast (n = 12), pancreas (n = 6), colorectal (n = 2), and lung (n = 2). All counts were normalized to 7.5 ml. (**C**) For enumeration of CTCs from CRPC patients, CK8/18/19 staining was used (green). CD45 antigen (red) was used to identify contaminating leukocytes. Scale bars, 10 μm. (**D**) A CTC from a CRPC patient was stained for prostate-specific antigen (PSA) (red), prostate-specific membrane antigen (PSMA) (yellow), and DAPI (blue) to demonstrate dual immunofluorescence staining for PSAs. (**E**) Validation of *EML4-ALK* RT-PCR assay was completed with cell lines. ^{pos}CTC-iChip products of whole blood from a healthy donor (HD) spiked with 0, 10, and 100 H3122 cells (expressing *EML4-ALK* variant 1) per 10 ml were subjected to RT-PCR for detection of the *EML4-ALK* fusion. Product isolated from healthy donor blood spiked with 500 VCaP cells/ml was processed as a negative control. (**F**) ^{pos}CTC-iChip products from patient samples known to harbor the *EML4-ALK* translocation by FISH were similarly processed as in (E), and the bands were sequenced to confirm the presence of the fusion transcript. A representative sequence trace from patient 3 shows the translocation breakpoint between exon 13 of *EML4* and exon 20 of *ALK*. CTC analysis of three patients whose cancer lacks the translocation was used to establish specificity: a prostate cancer patient (lane 1), an *EGFR* mutant lung cancer patient (lane 2), and a *HER2*-amplified lung cancer patient (lane 6).

^{neg}CTC-iChip to isolate CTCs

Given the heterogeneity of circulating cancer cells, including the subset thought to undergo EMT, depletion of normal blood cells from clinical specimens should allow characterization of unlabeled nonhematopoietic cells. We analyzed CTCs from 10 patients with metastatic breast cancer, including luminal (ER^+/PR^+, $n = 6$), triple-negative ($ER^-/PR^-/HER2^-$, $n = 2$), and $HER2^+$ ($n = 2$) subtypes. Triple-negative breast cancers are noteworthy in that they express primarily mesenchymal markers and are unlikely to be captured efficiently using positive selection for $EpCAM^+$ cells (*20*).

We stained the enriched CTC specimens using the Papanicolaou (Pap) stain, which is used for cytopathology analysis in clinical laboratories. In selected cases, the hematoxylin and eosin (H&E)–stained primary tumor tissue was compared with Pap-stained fine needle aspirates (FNAs) of the tumor or pleural effusions from the same patient. A remarkably similar morphological appearance was evident between cancer cells in the primary breast tumors and the isolated CTCs, as shown for three different patients in Fig. 5A. An ER^+ breast cancer patient revealed small and regularly shaped cells in H&E, cytology, and CTC samples. Similarly, larger and more irregular tumor cells were found in a $HER2^+$ primary breast cancer by H&E cytology and CTC analysis. In another example from a triple-negative high-grade breast cancer patient, pleomorphic CTCs similar to the patient's previously sampled cytology specimen were seen.

We extended these morphological analyses to pancreatic cancer and melanoma with similar findings (Fig. 5A). For these, pancreatic adenocarcinoma showed CTCs of comparable size to the primary tumor by both histology and Pap cytology. Conversely, melanoma consisted of dyshesive tumor cells. The spindled cytoplasm in melanoma was also

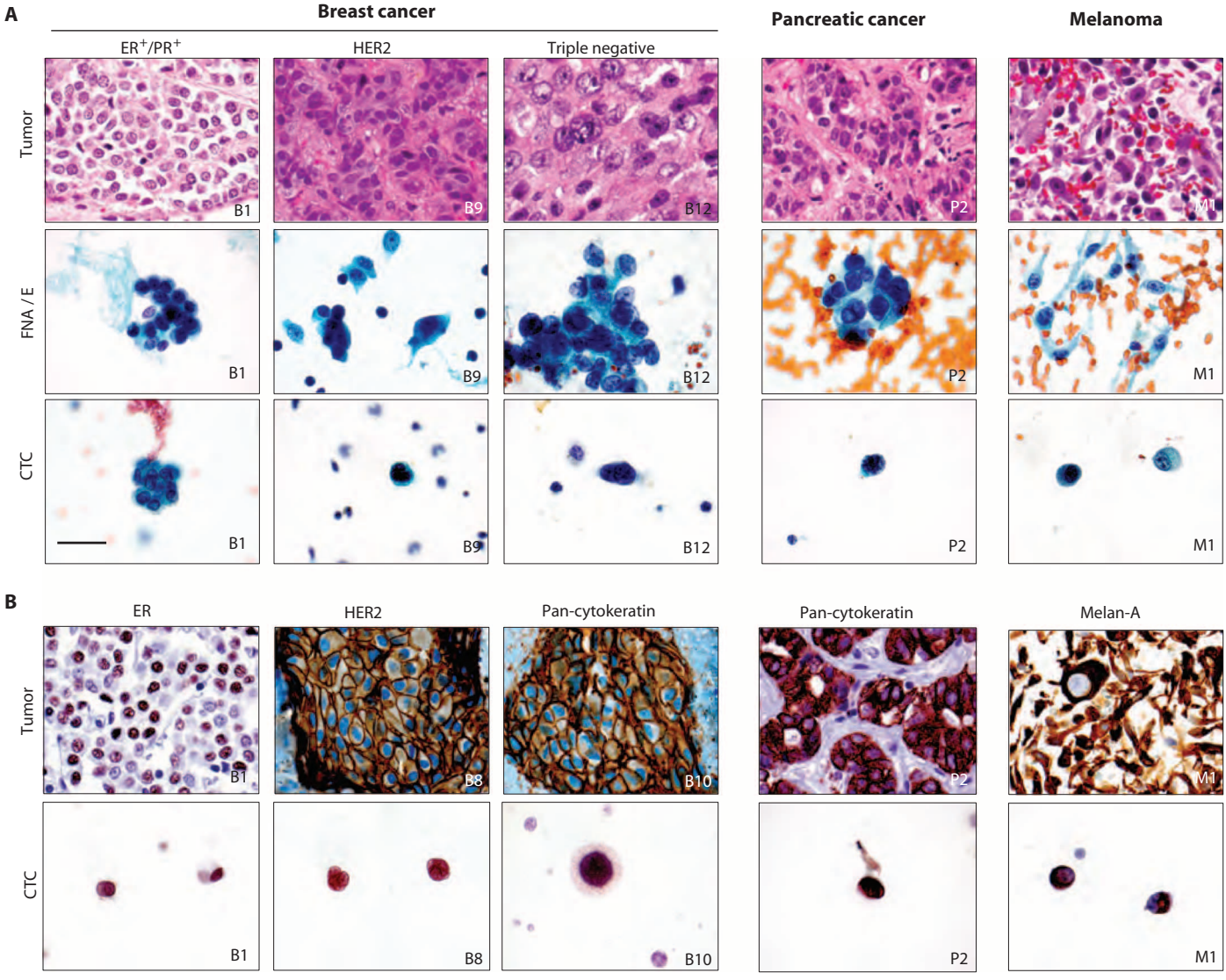

Fig. 5. Classification of CTCs with cytopathology and ICC. (**A**) Specimens from H&E-stained primary and metastatic tumors (upper row) are compared with matched Pap-stained cytology samples from FNAs or pleural effusions (FNA/E) (middle row) and Pap-stained CTCs enriched from blood samples of the same patient using ^{neg}CTC-iChip (lower row). Marked morphological similarity is seen between isolated CTCs and main tumors or cytology samples. (**B**) ICC profiles of primary and metastatic tumors (upper panel) matched to CTCs from the same patient (lower panel). All images: ×1000 original magnification. Scale bar is 30 μm and valid for all images.

seen on the cytology preparation, but the CTCs appeared round. As a neural crest–derived malignancy, melanoma cells do not express EpCAM, and hence, their detection requires the ^{neg}CTC-iChip isolation mode. Nevertheless, on the basis of established cellular and nuclear morphology criteria, our CTC analyses were considered to be of sufficient quality to enable a clinical diagnosis of suspicious for malignancy.

Pap-stained CTC slides were destained and then subjected to immunocytochemistry (ICC), which was first validated through cell lines (fig. S9). ICC of CTCs identified estrogen receptor (ER) protein in luminal breast cancer cells, keratin in triple-negative cells, and strong HER2 staining in cells from HER2$^+$ breast cancers (Fig. 5B and fig. S10). Similarly, CTCs from patients with pancreatic cancer stained positive by ICC for CK, and CTCs from melanoma patients stained positive for the melanocytic marker Melan-A (Fig. 5B and fig. S10). The combination of Pap staining followed by ICC enabled enumeration of CTCs isolated by ^{neg}CTC-iChip despite the presence of surrounding leukocytes.

Not all cytologically suspicious cells (for example, large cells with large, irregular nuclei as identified on the Pap-stained CTC slide) could be confirmed as tumor cells by ICC staining. Conversely, cells that were not scored as CTCs on initial cytological evaluation were subsequently identified as tumor cells by ICC, reflecting substantial heterogeneity in CTC size and morphology (fig. S11). Thus, by not relying exclusively on immunofluorescence-based scoring of CK$^+$ cells, we were able to apply to CTCs the same rigorous morphological and immunohistochemical criteria used by clinical cytopathologists in the diagnosis of malignancy.

We observed large variation in CTC size among different cancer types. Although some CTCs were larger than leukocytes, there was considerable overlap between the two cell populations (Fig. 6). The variation in CTC size was not restricted to different cancer histologies. In one patient with ER$^+$/PR$^+$ breast cancer whose CTCs were isolated using the ^{neg}CTC-iChip and analyzed using a combination of Pap stain and ICC, we identified CTCs ranging from 9 to 19 μm in diameter.

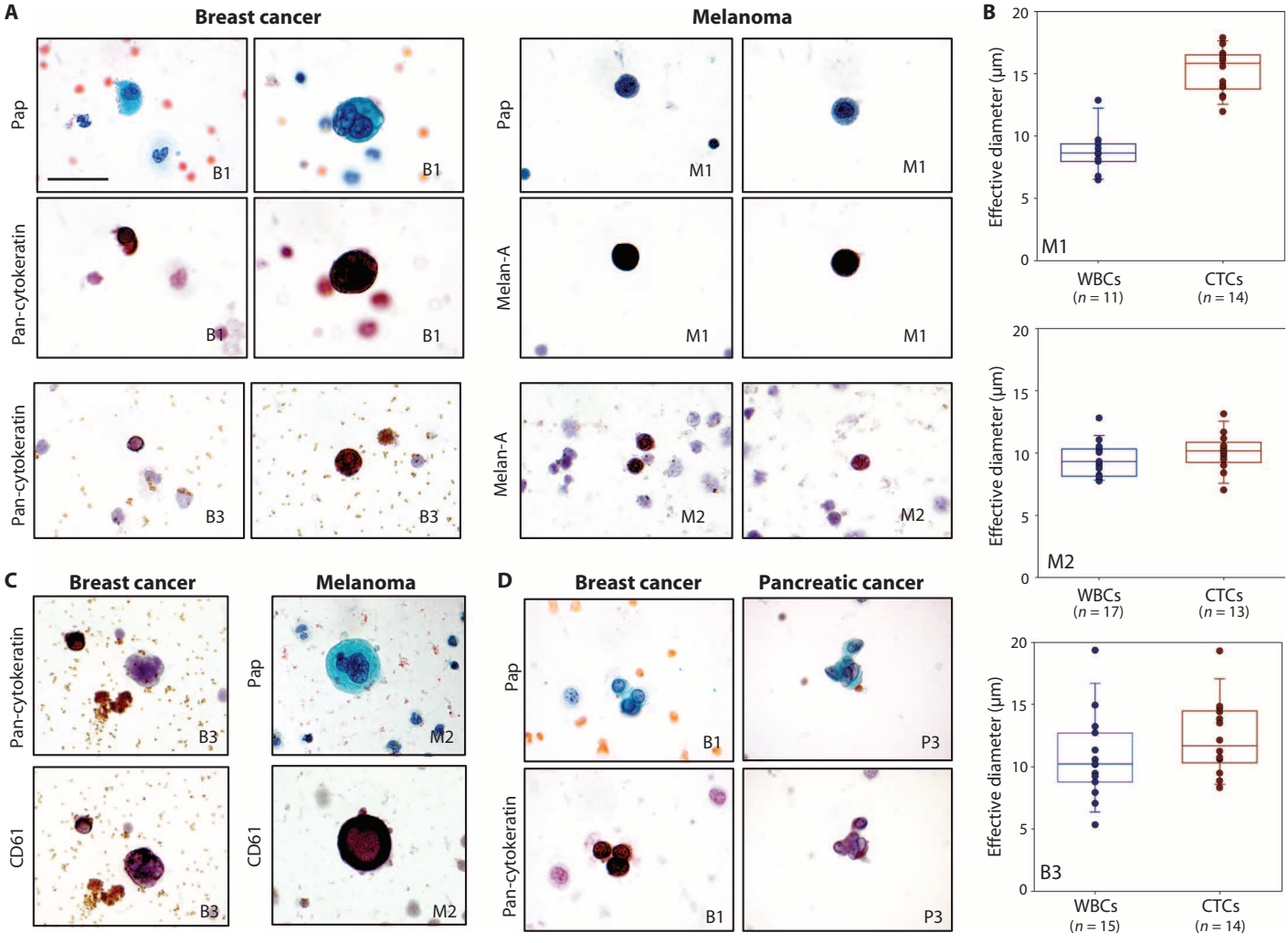

Fig. 6. Variation of CTC sizes and morphologies. (**A**) CTCs from breast cancer and melanoma patients consecutively stained with Pap and either anti-CK (breast) or anti–Melan-A (melanoma) antibodies. (**B**) Quantitative analysis of the effective diameter (maximum feret diameter) for individual cells isolated in three cases. The top two panels are from different melanoma patients (M1 and M2). The bottom panel is from a breast cancer patient (B3). (**C**) Occasional very large cells with ample cytoplasm and multilobed nuclei were initially considered suspicious but were CK$^-$. The same cells were subsequently restained for the platelet marker CD61, which supports their identification as circulating megakaryocytes. (**D**) CTCs were occasionally observed as clusters and confirmed by positive CK staining. All images: ×1000 original magnification. Scale bar, 30 μm.

Although most melanoma CTCs were large in size (>12 μm), one patient with metastatic melanoma had numerous CTCs less than 10 μm in diameter, detected using Pap and ICC for Melan-A (Fig. 6, A and B). In breast cancer and melanoma patients, some very large atypical cells (>30 μm) identified by Pap staining as having multilobed nuclei were at first assumed to be CTCs. However, ICC staining for the platelet marker CD61 confirmed their identity as megakaryocytes (Fig. 6C). Finally, application of the ^{neg}CTC-iChip platform identified clusters of two to six CK$^+$ CTCs in breast and pancreatic cancers, consistent with our previous detection of CTC clusters using the ^{Hb}CTC-Chip (*16*) (Fig. 6D). The negative selection mode of the CTC-iChip thus provided a comprehensive and unbiased view of nonhematological cells in the bloodstream of cancer patients.

Single-cell RNA expression in CTCs

Global CTC expression analyses may identify major pathways involved in metastasis (*20*), but the inherent heterogeneity of CTCs necessitates the identification of expression patterns and signaling pathways within individual cells. We therefore applied a series of single-cell micromanipulation approaches to interrogate individual CTCs isolated from a patient with prostate cancer using the ^{neg}CTC-iChip. Although micromanipulation approaches require expertise and can be time-consuming, the fact that the CTCs are unadulterated allows for more accurate RNA-based expression profiling than isolated fixed cells. EpCAM$^+$ CTCs were distinguished from contaminating CD45$^+$ leukocytes within the ^{neg}CTC-iChip product by immunostaining (Fig. 7, A and B). CTCs identified as EpCAM$^+$/CD45$^-$ were individually isolated and subjected to RNA analysis by multigene microfluidic quantitative RT-PCR (qRT-PCR), profiling for a panel of transcripts implicated in androgen receptor (AR) signaling, cellular proliferation, stem cell, epithelial and mesenchymal cell fates, and leukocyte-specific lineage (Fig. 7C). Single cells from the human prostate cancer cell line LNCaP were used to optimize assay conditions (fig. S12).

A marked heterogeneity was apparent among 15 CTCs isolated from a single patient with metastatic CRPC who had progressed through multiple lines of therapy, including androgen deprivation therapy with leuprolide, the chemotherapeutic drug docetaxel, and the second-line androgen biosynthesis inhibitor abiraterone acetate. Consistent with EpCAM$^+$ immunostaining, 13 of the 15 CTCs were positive for epithelial gene expression, of which 2 CTCs were dual positive for epithelial as well as mesenchymal markers vimentin and N-cadherin (Fig. 7D). Thus, a subset of CTCs appears to have undergone partial EMT. CTC heterogeneity was also evident with expression of stem cell markers [Nanog, Oct-4 (POU5F1), and c-Myc] in 10 of the 15 CTCs, which overlapped primarily with epithelial markers within individual CTCs (Fig. 7C). Proliferation markers cyclin B, cyclin D, Aurora A kinase, and MYBL2 were detected in another subset of seven CTCs.

AR activity, previously defined in CTCs as the ratio of androgen-driven PSA to androgen-repressed PSMA expression (*21*), was heterogeneous among CTCs. The "AR on" phenotype (PSA expression only) was only seen in 2 of the 15 CTCs, whereas the "AR-off" state (PSMA only) was evident in 2 CTCs, and the "mixed AR" state (PSA$^+$/PSMA$^+$) in 10 CTCs (Fig. 7D). This distribution is concordant with single-cell immunofluorescence analysis of AR signaling status in CTCs from patients with CRPC (*21*).

DISCUSSION

The CTC-iChip described here has the ability to process large volumes of whole blood (8 ml/hour), with high throughput (10^7 cells/s) and

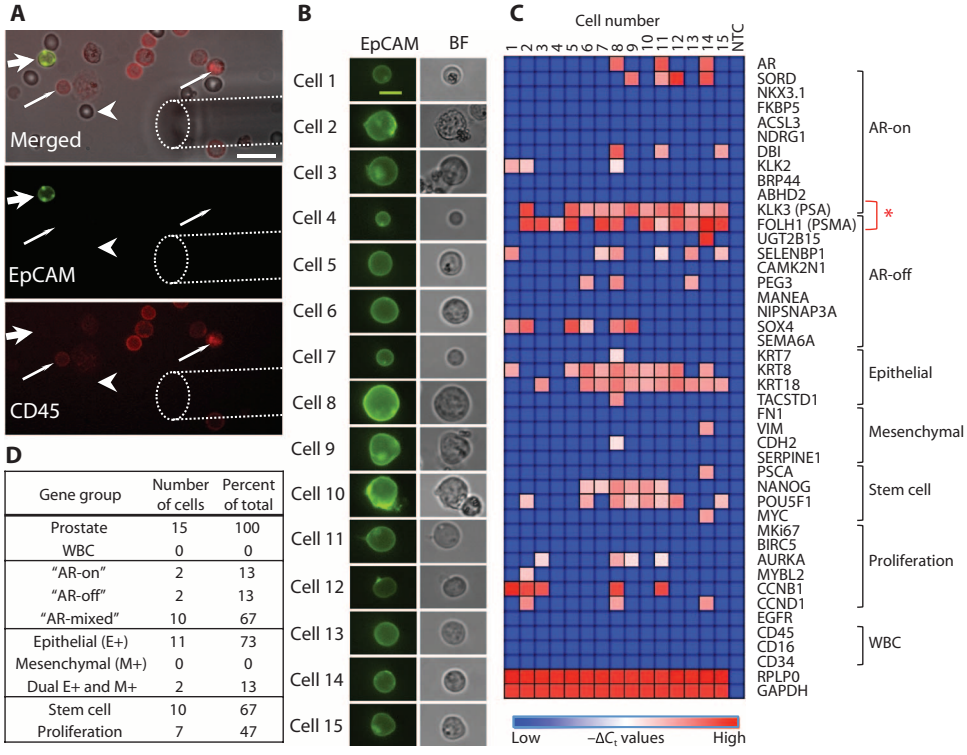

D

Gene group	Number of cells	Percent of total
Prostate	15	100
WBC	0	0
"AR-on"	2	13
"AR-off"	2	13
"AR-mixed"	10	67
Epithelial (E+)	11	73
Mesenchymal (M+)	0	0
Dual E+ and M+	2	13
Stem cell	10	67
Proliferation	7	47

Fig. 7. Heterogeneity of RNA expression between CTCs isolated from a prostate cancer patient. (**A**) Micromanipulation of single CTCs isolated from a blood specimen of a patient with prostate cancer using the ^{neg}CTC-iChip and stained in solution with anti-EpCAM (green) and anti-CD45 (red) antibodies. Top panel shows a bright-field image merged. Wide arrow points to an EpCAM$^+$/CD45$^-$ CTC. Thin arrow points to EpCAM$^-$/CD45$^+$ leukocytes. Arrowhead denotes an erythrocyte. Dashed line outlines the micromanipulator needle tip. Bottom two panels show distinct imaging channels. Scale bar, 20 μm. (**B**) EpCAM and bright-field images of 15 single prostate cancer CTCs from a single patient selected for transcriptional profiling. Scale bar, 10 μm. (**C**) Heat map of normalized gene expression ($-\Delta C_t$) of 43 genes in each of the single CTCs measured by microfluidic qRT-PCR. Columns list each individual prostate CTC, and rows show the panel of genes assayed, grouped thematically. The red asterisk highlights the gene expression patterns of PSA and PSMA, which provide a measure of AR signaling activity. NTC, no-template control. (**D**) Table listing the proportional distribution of various gene groups expressed in single CTCs isolated from the prostate cancer patient.

at high efficiency, in positive selection (tumor antigen–dependent) and negative depletion (tumor antigen–independent) modes, thus enabling cytopathological and molecular characterization of both epithelial and nonepithelial cancers. Traditional magnetophoresis requires the attachment of either hundreds of beads per cell or very large beads to provide sufficient magnetic moment for cell isolation (*11, 29*). In contrast, by virtue of its ability to precisely position cells within the channel using inertial focusing, the fluidic design of the CTC-iChip allows for efficient fractionation of cells with only a few 1-μm beads, resulting in high yields and purity of CTC isolation.

We have tested initial "proof-of-principle" clinical applications of both the positive and negative selection modes of the CTC-iChip. The ^{pos}CTC-iChip isolated CTCs at a purity of >0.1%, which is sufficient for molecular analyses, including detection of the *EML4-ALK* fusion transcript in NSCLC. Total CTC capture yield is critical to both genotyping and other applications, including enumeration for either prognostic or drug response measurements. The median number of CTCs detected by CK staining of ^{pos}CTC-iChip product was 3.2 CTCs/ml, with 90% of clinical samples having CK^+ cells above the threshold set using healthy donors. In a similar cohort using the CellSearch system, a median of 1.7 CTCs/ml was detected, with 57% of samples above the threshold (*30*). In our direct comparison between the ^{pos}CTC-iChip and the CellSearch system, the microfluidic device was significantly more sensitive at low CTC numbers (<30 CTC/7.5 ml). These results suggest that a subpopulation of $EpCAM^{low}$ cells was missed by the CellSearch bulk processing approach. Thus, whereas current commercially available approaches may be effective in patients with $EpCAM^{hi}$ CTCs, the CTC-iChip displayed increased sensitivity for patients with low numbers of circulating cancer cells, which may also have $EpCAM^{low}$ expression.

Previously, we demonstrated the efficacy of two microfluidic systems to isolate CTCs from whole blood. CK^+ CTCs were detected in 99% of patients with high purity (18 to 70%) in the first-generation micropost chip (*15*), and application of disease-specific markers for staining (PSA) and computer-assisted enumeration methods were later found to improve system reliability and specificity (*19*). Building on the improved heuristics and staining, CTCs were subsequently detected in 64% of prostate patients using the first-generation micropost chip (*19*), and in 93% of patients using the second-generation herringbone chip (*16*). Yet, these systems remain limited by low throughput (~1 to 2 ml of blood/hour), the inability to conduct single-cell or slide-based analyses, the requirement for three-dimensional image scanning platforms, and the availability of only a positive selection mode. The CTC-iChip system presented here thus encompasses major advances over our previous methods. Whole blood is now processed through a microscale system at speeds comparable to bulk systems (8 ml/hour) while preserving the high sensitivity afforded by microfluidic isolation techniques. Furthermore, rapid and gentle isolation of CTCs, as well as their collection in suspension, increases the integrity of these cells and their RNA quality, which are crucial for downstream analyses, such as cytopathology and single-cell expression profiling.

Moreover, the system can be run in either a positive selection or a negative depletion mode, thus broadening its potential application in the clinic and in basic research studies. The ^{neg}CTC-iChip allows for depletion of normal blood cells, uncovering an unselected population of nonhematopoietic cells for analysis. The robustness of this platform was demonstrated by staining CTCs per clinical pathology protocols, which yielded high-quality diagnostic images. The ^{neg}CTC-iChip allowed for isolation of CTCs from a nonepithelial cancer (melanoma) and from cancer that has undergone EMT and lost virtually all detectable EpCAM expression (triple-negative breast cancer). Hence, the ^{neg}CTC-iChip will be broadly applicable to all cancers that demonstrate vascular invasion, a major limitation of current technologies.

However, several additional optimizations should be considered before the CTC-iChip technology can be deployed for large-scale clinical applications. These include further improvements in CTC purity to facilitate routine molecular analyses of CTCs and in total blood volume processed to enable early cancer detection. From a manufacturing standpoint, we envision the CTC-iChip being integrated into a single monolithic device made of plastic and incorporating all three components of the CTC-iChip within a single footprint. Integration of such an economical chip into a fully automated device would potentially enable broad dissemination of this technology.

The emerging field of CTC biology brings with it unprecedented insight into the mechanisms underlying the blood-borne metastasis of cancer, as well as powerful new clinical applications to help diagnose and manage disease. As the technology matures, these are likely to include the initial genotyping and molecular characterization of cancer, as well as repeated noninvasive sampling of tumors during treatment. Because targeted therapies increasingly shape the clinical paradigm of cancer therapeutics, such serial "real-time" monitoring of cancer for indicators of drug response and emerging resistance is likely to become a mainstay of clinical oncology. The integrated microfluidic technology platform presented here provides a major step in this direction by enabling processing of large blood volumes with high throughput and efficiency, isolating CTCs regardless of tumor surface epitopes, and providing an end product that is compatible with both standardized clinical diagnostics and advanced molecular analyses. Because rare cell detection technologies continue to improve in sensitivity, they may ultimately provide novel approaches for early detection of invasive cancer before the establishment of metastatic disease.

MATERIALS AND METHODS

Samples

MDA-MB-231, SKBR3, and MCF10A cell lines were obtained from the American Type Culture Collection. PC3-9 cells were obtained from Veridex, LLC, and LBX1-expressing MCF10A cells were derived from a stable cell line previously published by our laboratory (*27*). Device performance was evaluated by prelabeling the cell lines with a fluorescent marker and spiking them into whole blood at ~200 to 1000/ml of whole blood (Supplementary Materials and Methods).

Fresh whole blood was collected from healthy volunteers under an Institutional Review Board (IRB)–approved protocol or commercially sourced from Research Blood Components. Samples from metastatic breast, colorectal, pancreas, lung, melanoma, and prostate cancer patients were collected under a separate IRB-approved protocol.

Chip design and fabrication

Hydrodynamic sorting chips were designed at Massachusetts General Hospital (MGH) and fabricated by Silex with deep reactive ion etching on silicon wafers. The chip was sealed with anodically bonded glass cover to form the microfluidic chamber. A custom polycarbonate manifold was used to form the fluidic connections to the microchip (fig. S3). The

inertial focusing and magnetophoresis chips were designed and fabricated at MGH with soft lithography and polydimethylsiloxane (fig. S4). The chip was placed within a custom stainless steel manifold that held four magnets in a quadrupole configuration to create a magnetic circuit enabling cell deflection (fig. S5) (Supplementary Materials and Methods).

Magnetic bead labeling of target cells in whole blood

Before processing the whole blood, samples were incubated with functionalized magnetic beads 1 μm in diameter (Dynal MyOne 656-01, Life Technologies) (fig. S2). For ^{pos}CTC-iChip, beads were functionalized with a biotinylated anti-EpCAM antibody, and active magnetic mixing was applied to achieve good labeling of EpCAM^{low} cell lines. For negative depletion, anti-CD45 and anti-CD15 functionalized beads were used (Supplementary Materials and Methods).

Immunofluorescence staining of CTCs

For enumeration analysis, isolated cells were incubated with saponin, DAPI, and anti-CK [phycoerythrin (PE)] and anti-CD45 [allophycocyanin (APC)] antibodies, acquired from Veridex, still in suspension. Cells were plated on a poly-L-lysine–functionalized glass slide with a closed chamber (fig. S8), and glass slide was scanned with the BioView imaging system while the chamber was still intact. Cells that were CK$^+$/DAPI$^+$/CD45$^-$ were scored as CTCs. Samples evaluated for PSA/PSMA expression were stained with a primary/secondary approach. All antibodies are catalogued in table S3.

Comparison to CellSearch

For the CellSearch and ^{pos}CTC-iChip comparison, two blood tubes were drawn: one CellSave tube for CellSearch run and one EDTA tube for ^{pos}CTC-iChip run. Samples in CellSave tubes were processed within 3 days after the draw as optimized and recommended for CellSearch approach, and EDTA samples were processed with the ^{pos}CTC-iChip within 4 hours of draw. CellSearch product was scanned in Magnest cartridges with CellTracks system. ^{pos}CTC-iChip product was plated and scanned with the BioView system.

RT-PCR analysis

RNA isolation was done with RNeasy Micro Kit (Qiagen). After RNA isolation, reverse transcription of RNA to complementary DNA (cDNA) using oligo(dT) was performed with SuperScript III First-Strand Synthesis System for RT-PCR (Invitrogen). For detection of *EML4-ALK* fusion cDNAs, partial nested PCR analysis was done with FideliTaq PCR Master Mix (Affymetrix). PCR amplification was performed in a thermocycler (Peltier Thermal Cycler, MJ Research). Gel electrophoresis was done with an aliquot of RT-PCR products. The amplified *EML4-ALK* products were sequenced, and results were analyzed with the ABI PRISM DNA sequence analysis software (Applied Biosystems) (Supplementary Materials and Methods).

Cytology and ICC

CTCs were enriched via ^{neg}CTC-iChip from the whole blood of cancer patients and plated on a poly-L-lysine surface (fig. S8). Plating chamber was removed after cell adhesion to facilitate standard cytopathology processing. Pap stain was done with hematoxylin, eosin-azure, and orange G and initially reviewed for suspicious cells by a certified cytotechnologist (N. Hartford, MGH) and then formally reviewed by a staff cytopathologist (E.B.). Slides were then destained and exposed to ICC process (Supplementary Materials and Methods).

Single-cell micromanipulation and qRT-PCR

Blood samples from a patient with metastatic prostate cancer were processed through the ^{neg}CTC-iChip, and unfixed CTCs and contaminating leukocytes were stained in solution with fluorophore-conjugated antibodies against EpCAM and CD45. Single CTCs were identified based on an EpCAM$^+$/CD45$^-$ phenotype and transferred under direct microscopic visualization to individual PCR tubes with a TransferMan NK2 micromanipulator (Eppendorf AG). Single-cell cDNA was prepared and amplified for single-cell transcriptome analysis, followed by specific target preamplification (Fluidigm Corp.). Microfluidic qRT-PCR was performed with the BioMark Real-Time PCR system (Fluidigm Corp.). The normalized gene expression in each cell ($-\Delta C_t$) was calculated as the negative of the difference between the C_t value for each gene and the *GAPDH* C_t value for the cell. Heat maps of normalized gene expression ($-\Delta C_t$) were generated with the Heat Map image module of GenePattern, with global color normalization.

SUPPLEMENTARY MATERIALS

www.sciencetranslationalmedicine.org/cgi/content/full/5/179/179ra47/DC1
Materials and Methods
Fig. S1. CTC-iChip system details.
Fig. S2. Optimization of labeling in whole blood.
Fig. S3. Hydrodynamic size–based separation.
Fig. S4. Inertial focusing and magnetophoresis channels.
Fig. S5. Magnetic configuration.
Fig. S6. Beads per cell distribution in deflected and undeflected outputs.
Fig. S7. WBC contamination in ^{pos}CTC-iChip.
Fig. S8. Cell plating chamber.
Fig. S9. ICC stain validation through cell lines.
Fig. S10. Additional images of ICC-stained cells.
Fig. S11. Comparison of cell identification through Pap and ICC.
Fig. S12. Single-cell qRT-PCR optimization using cell lines.
Table S1. Contaminating cells in the ^{neg}CTC-iChip product are leukocytes.
Table S2. CellSearch versus ^{pos}CTC-iChip comparison.
Table S3. Antibodies used throughout the study.

REFERENCES AND NOTES

1. K. Pantel, R. H. Brakenhoff, B. Brandt, Detection, clinical relevance and specific biological properties of disseminating tumour cells. *Nat. Rev. Cancer* **8**, 329–340 (2008).
2. M. Yu, S. Stott, M. Toner, S. Maheswaran, D. A. Haber, Circulating tumor cells: Approaches to isolation and characterization. *J. Cell Biol.* **192**, 373–382 (2011).
3. M. C. Miller, G. V. Doyle, L. W. Terstappen, Significance of circulating tumor cells detected by the cellsearch system in patients with metastatic breast colorectal and prostate cancer. *J. Oncol.* **2010**, 617421 (2010).
4. S. Maheswaran, L. V. Sequist, S. Nagrath, L. Ulkus, B. Brannigan, C. V. Collura, E. Inserra, S. Diederichs, A. J. Iafrate, D. W. Bell, S. Digumarthy, A. Muzikansky, D. Irimia, J. Settleman, R. G. Tompkins, T. J. Lynch, M. Toner, D. A. Haber, Detection of mutations in *EGFR* in circulating lung-cancer cells. *N. Engl. J. Med.* **359**, 366–377 (2008).
5. J. M. Lang, B. P. Casavant, D. J. Beebe, Circulating tumor cells: Getting more from less. *Sci. Transl. Med.* **4**, 141ps13 (2012).
6. R. T. Krivacic, A. Ladanyi, D. N. Curry, H. B. Hsieh, P. Kuhn, D. E. Bergsrud, J. F. Kepros, T. Barbera, M. Y. Ho, L. B. Chen, R. A. Lerner, R. H. Bruce, A rare-cell detector for cancer. *Proc. Natl. Acad. Sci. U.S.A.* **101**, 10501–10504 (2004).
7. D. Marrinucci, K. Bethel, A. Kolatkar, M. S. Luttgen, M. Malchiodi, F. Baehring, K. Voigt, D. Lazar, J. Nieva, L. Bazhenova, A. H. Ko, W. M. Korn, E. Schram, M. Coward, X. Yang, T. Metzner, R. Lamy, M. Honnatti, C. Yoshioka, J. Kunken, Y. Petrova, D. Sok, D. Nelson, P. Kuhn, Fluid biopsy in patients with metastatic prostate, pancreatic and breast cancers. *Phys. Biol.* **9**, 016003 (2012).
8. D. Issadore, J. Chung, H. Shao, M. Liong, A. A. Ghazani, C. M. Castro, R. Weissleder, H. Lee, Ultrasensitive clinical enumeration of rare cells ex vivo using a micro-Hall detector. *Sci. Transl. Med.* **4**, 141ra92 (2012).
9. S. Miltenyi, W. Müller, W. Weichel, A. Radbruch, High gradient magnetic cell separation with MACS. *Cytometry* **11**, 231–238 (1990).

10. G. Deng, M. Herrler, D. Burgess, E. Manna, D. Krag, J. F. Burke, Enrichment with anti-cytokeratin alone or combined with anti-EpCAM antibodies significantly increases the sensitivity for circulating tumor cell detection in metastatic breast cancer patients. *Breast Cancer Res.* **10**, R69 (2008).
11. A. H. Talasaz, A. A. Powell, D. E. Huber, J. G. Berbee, K. H. Roh, W. Yu, W. Xiao, M. M. Davis, R. F. Pease, M. N. Mindrinos, S. S. Jeffrey, R. W. Davis, Isolating highly enriched populations of circulating epithelial cells and other rare cells from blood using a magnetic sweeper device. *Proc. Natl. Acad. Sci. U.S.A.* **106**, 3970–3975 (2009).
12. R. Kalluri, R. A. Weinberg, The basics of epithelial-mesenchymal transition. *J. Clin. Invest.* **119**, 1420–1428 (2009).
13. O. Lara, X. Tong, M. Zborowski, J. J. Chalmers, Enrichment of rare cancer cells through depletion of normal cells using density and flow-through, immunomagnetic cell separation. *Exp. Hematol.* **32**, 891–904 (2004).
14. L. Yang, J. C. Lang, P. Balasubramanian, K. R. Jatana, D. Schuller, A. Agrawal, M. Zborowski, J. J. Chalmers, Optimization of an enrichment process for circulating tumor cells from the blood of head and neck cancer patients through depletion of normal cells. *Biotechnol. Bioeng.* **102**, 521–534 (2009).
15. S. Nagrath, L. V. Sequist, S. Maheswaran, D. W. Bell, D. Irimia, L. Ulkus, M. R. Smith, E. L. Kwak, S. Digumarthy, A. Muzikansky, P. Ryan, U. J. Balis, R. G. Tompkins, D. A. Haber, M. Toner, Isolation of rare circulating tumour cells in cancer patients by microchip technology. *Nature* **450**, 1235–1239 (2007).
16. S. L. Stott, C. H. Hsu, D. I. Tsukrov, M. Yu, D. T. Miyamoto, B. A. Waltman, S. M. Rothenberg, A. M. Shah, M. E. Smas, G. K. Korir, F. P. Floyd Jr., A. J. Gilman, J. B. Lord, D. Winokur, S. Springer, D. Irimia, S. Nagrath, L. V. Sequist, R. J. Lee, K. J. Isselbacher, S. Maheswaran, D. A. Haber, M. Toner, Isolation of circulating tumor cells using a microvortex-generating herringbone-chip. *Proc. Natl. Acad. Sci. U.S.A.* **107**, 18392–18397 (2010).
17. S. Wang, K. Liu, J. Liu, Z. T. F. Yu, X. Xu, L. Zhao, T. Lee, E. K. Lee, J. Reiss, Y.-K. Lee, L. W. K. Chung, J. Huang, M. Rettig, D. Seligson, K. N. Duraiswamy, C. K. Shen, H. R. Tseng, Highly efficient capture of circulating tumor cells by using nanostructured silicon substrates with integrated chaotic micromixers. *Angew. Chem. Int. Ed. Engl.* **50**, 3084–3088 (2011).
18. U. Dharmasiri, S. K. Njoroge, M. A. Witek, M. G. Adebiyi, J. W. Kamande, M. L. Hupert, F. Barany, S. A. Soper, High-throughput selection, enumeration, electrokinetic manipulation, and molecular profiling of low-abundance circulating tumor cells using a microfluidic system. *Anal. Chem.* **83**, 2301–2309 (2011).
19. S. L. Stott, R. J. Lee, S. Nagrath, M. Yu, D. T. Miyamoto, L. Ulkus, E. J. Inserra, M. Ulman, S. Springer, Z. Nakamura, A. L. Moore, D. I. Tsukrov, M. E. Kempner, D. M. Dahl, C. L. Wu, A. J. Iafrate, M. R. Smith, R. G. Tompkins, L. V. Sequist, M. Toner, D. A. Haber, S. Maheswaran, Isolation and characterization of circulating tumor cells from patients with localized and metastatic prostate cancer. *Sci. Transl. Med.* **2**, 25ra23 (2010).
20. M. Yu, A. Bardia, B. S. Wittner, S. L. Stott, M. E. Smas, D. T. Ting, S. J. Isakoff, J. C. Ciciliano, M. N. Wells, A. M. Shah, K. F. Concannon, M. C. Donaldson, L. V. Sequist, E. Brachtel, D. Sgroi, J. Baselga, S. Ramaswamy, M. Toner, D. A. Haber, S. Maheswaran, Circulating breast tumor cells exhibit dynamic changes in epithelial and mesenchymal composition. *Science* **339**, 580–584 (2013).
21. D. T. Miyamoto, R. J. Lee, S. L. Stott, D. T. Ting, B. S. Wittner, M. Ulman, M. E. Smas, J. B. Lord, B. W. Brannigan, J. Trautwein, N. H. Bander, C. L. Wu, L. V. Sequist, M. R. Smith, S. Ramaswamy, M. Toner, S. Maheswaran, D. A. Haber, Androgen receptor signaling in circulating tumor cells as a marker of hormonally responsive prostate cancer. *Cancer Discov.* **2**, 995–1003 (2012).
22. L. R. Huang, E. C. Cox, R. H. Austin, J. C. Sturm, Continuous particle separation through deterministic lateral displacement. *Science* **304**, 987–990 (2004).
23. D. Di Carlo, D. Irimia, R. G. Tompkins, M. Toner, Continuous inertial focusing, ordering, and separation of particles in microchannels. *Proc. Natl. Acad. Sci. U.S.A.* **104**, 18892–18897 (2007).
24. R. Huang, T. A. Barber, M. A. Schmidt, R. G. Tompkins, M. Toner, D. W. Bianchi, R. Kapur, W. L. Flejter, A microfluidics approach for the isolation of nucleated red blood cells (NRBCs) from the peripheral blood of pregnant women. *Prenat. Diagn.* **28**, 892–899 (2008).
25. G. Segré, A. Silberberg, Radial particle displacements in Poiseuille flow of suspensions. *Nature* **189**, 209–210 (1961).
26. A. M. Sieuwerts, J. Kraan, J. Bolt, P. van der Spoel, F. Elstrodt, M. Schutte, J. W. M. Martens, J. W. Gratama, S. Sleijfer, J. A. Foekens, Anti-epithelial cell adhesion molecule antibodies and the detection of circulating normal-like breast tumor cells. *J. Natl. Cancer Inst.* **101**, 61–66 (2009).
27. M. Yu, G. A. Smolen, J. Zhang, B. Wittner, B. J. Schott, E. Brachtel, S. Ramaswamy, S. Maheswaran, D. A. Haber, A developmentally regulated inducer of EMT, LBX1, contributes to breast cancer progression. *Genes Dev.* **23**, 1737–1742 (2009).
28. D. A. Haber, N. S. Gray, J. Baselga, The evolving war on cancer. *Cell* **145**, 19–24 (2011).
29. B. D. Plouffe, L. H. Lewis, S. K. Murthy, Computational design optimization for microfluidic magnetophoresis. *Biomicrofluidics* **5**, 13413 (2011).
30. W. J. Allard, J. Matera, M. C. Miller, M. Repollet, M. C. Connelly, C. Rao, A. G. Tibbe, J. W. Uhr, L. W. Terstappen, Tumor cells circulate in the peripheral blood of all major carcinomas but not in healthy subjects or patients with nonmalignant diseases. *Clin. Cancer Res.* **10**, 6897–6904 (2004).

Acknowledgments: We express our gratitude to all patients who participated in this study and healthy volunteers who contributed blood samples. We thank C. Koris and the MGH clinical research coordinators for help with clinical studies; B. Brannigan and H. Zhu for support of molecular analyses; E. Lim, J. Martel, J. Oakey, and F. Fachin for assistance in microfluidic device development; H. Cho for contributions to illustrations; L. Libby, O. Hurtado, and A. J. Aranyosi for coordination of the research labs; B. Hamza for expertise in device fabrication; D. Chianese and T. Bendele from Johnson & Johnson for supplying reagents and materials; and N. Bander from Weill Cornell Medical College for supplying anti-PSMA antibody, clone J591. **Funding:** This work was partially supported by NIH P41 Biotechnology Resource Center (M.T.), NIH National Institute of Biomedical Imaging and Bioengineering (M.T. and D.A.H.), Stand Up to Cancer (D.A.H., M.T., and S.M.), Howard Hughes Medical Institute (D.A.H.), Prostate Cancer Foundation and Charles Evans Foundation (D.A.H. and M.T.), Department of Defense Prostate Cancer Research Program (D.T.M. and R.J.L.), Mazzone-DF/HCC (Dana-Farber/Harvard Cancer Center) (D.T.M.), Conquer Cancer Foundation (R.J.L.), Prostate Cancer Foundation (R.J.L.), and Johnson & Johnson (M.T. and S.M.). **Author contributions:** E.O., A.M.S., B.L.E., D.T.M., E.B., M.Y., S.L.S., N.M.K., T.A.B., J.R.W., K.S., P.S.S., J.P.S., R.J.L., D.T.T., X.L., A.T.S., A.B., L.V.S., D.N.L., S.M., R.K., D.A.H., and M.T. designed the research. E.O., A.M.S., and J.C.C. were responsible for overall system design and characterization. B.L.E., A.K., and M.Y. optimized and performed cytology and ICC staining on slides. D.T.M. and J.T. executed single-cell micromanipulation and RNA analysis. S.S. conducted molecular detection of NSCLC patients. P.C., B.M., J.T., S.S., and J.C.C. executed chip operation and blood processing. N.M.K. completed characterization of cell plating chamber. E.O., P.C., and B.M. completed immunofluorescence staining, scanning, and enumeration. E.O., A.M.S., B.L.E., D.T.M., E.B., M.Y., S.L.S., N.M.K., L.V.S., S.M., R.K., D.A.H., and M.T. analyzed the research. E.O., A.M.S., B.L.E., D.T.M., S.M., R.K., D.A.H., and M.T. wrote the paper. **Competing interests:** MGH filed for patent protection for the CTC-iChip technology. The authors declare that they have no competing interests. **Data and materials availability:** Biotinylated anti-EpCAM mouse monoclonal IgG1 (clone VU-1D9), PE-conjugated anti-CK8/18 mouse monoclonal IgG1 (clone C11), PE-conjugated anti-CK19 mouse monoclonal IgG2a (clone A53-B/A2), APC-conjugated anti-CD45 mouse monoclonal IgG1 (clone HI30), nuclear staining reagent DAPI, and cell membrane permeabilization reagent saponin were obtained under a Materials Transfer Agreement from Johnson & Johnson (contact: David Chianese). Anti-PSMA monoclonal mouse IgG1 antibody (clone J591) was obtained under Materials Transfer Agreement from Weill Medical College (contact: Neil Bander).

Submitted 27 August 2012
Accepted 22 March 2013
Published 3 April 2013
10.1126/scitranslmed.3005616

Citation: E. Ozkumur, A. M. Shah, J. C. Ciciliano, B. L. Emmink, D. T. Miyamoto, E. Brachtel, M. Yu, P. Chen, B. Morgan, J. Trautwein, A. Kimura, S. Sengupta, S. L. Stott, N. M. Karabacak, T. A. Barber, J. R. Walsh, K. Smith, P. S. Spuhler, J. P. Sullivan, R. J. Lee, D. T. Ting, X. Luo, A. T. Shaw, A. Bardia, L. V. Sequist, D. N. Louis, S. Maheswaran, R. Kapur, D. A. Haber, M. Toner, Inertial focusing for tumor antigen–dependent and –independent sorting of rare circulating tumor cells. *Sci. Transl. Med.* **5**, 179ra47 (2013).

Circulating tumour cells—monitoring treatment response in prostate cancer

David T. Miyamoto, Lecia V. Sequist and Richard J. Lee

Abstract | The availability of new therapeutic options for the treatment of metastatic castration-resistant prostate cancer (mCRPC) has heightened the importance of monitoring and assessing treatment response. Accordingly, there is an unmet clinical need for reliable biomarkers that can be used to guide therapy. Circulating tumour cells (CTCs) are rare cells that are shed from primary and metastatic tumour deposits into the peripheral circulation, and represent a means of performing noninvasive tumour sampling. Indeed, enumeration of CTCs before and after therapy has shown that CTC burden correlates with prognosis in patients with mCRPC. Moreover, studies have demonstrated the potential of molecular analysis of CTCs in monitoring and predicting response to therapy in patients. This Review describes the challenges associated with monitoring treatment response in mCRPC, and the advancements in CTC-analysis technologies applied to such assessments and, ultimately, guiding prostate cancer treatment.

Miyamoto, D. T. *et al. Nat. Rev. Clin. Oncol*. advance online publication 13 May 2014; doi:10.1038/nrclinonc.2014.82

Introduction

In the USA, prostate cancer is the most common cancer in men and second most common cause of cancer-related death, with an estimated 29,480 deaths likely to be attributed to this disease in 2014.[1] In the past 3 years, the therapeutic landscape in metastatic castration-resistant prostate cancer (mCRPC) has changed substantially, with the FDA approval of five therapies associated with improved overall survival.[2–7] Monitoring the effectiveness of individual therapies in patients with mCRPC is a complex problem because of the high prevalence of bone metastases, which are difficult to quantitate. Furthermore, the currently available biomarkers and imaging assessments of clinical response do not enable optimal management of individual patients, owing to insufficient specificity for clinically relevant outcomes.[8] Additionally, the increasing number of treatment options available in mCRPC has created new challenges with regard to the design of clinical trials investigating novel therapies: whereas overall survival was a reasonable clinical trial end point in an earlier era, the availability of effective therapies that patients might receive after an experimental treatment confounds the ability to measure any survival benefit attributable to the new therapy. Although serum prostate-specific antigen (PSA) serves as a useful biomarker of treatment response and disease progression in the earlier stages of prostate cancer, this protein has been shown to be an unreliable biomarker in the setting of mCRPC and fails to meet the strict definitions of surrogacy for overall survival.[9] Thus, for both the clinical management of an individual patient and the assessment of novel therapies in development, new biomarkers in the metastatic setting represent an unmet clinical need.[8]

Circulating tumour cells (CTCs) are rare cancer cells that have been shed from primary or metastatic tumour deposits and have entered into the peripheral blood.[10,11] Studies have demonstrated that CTCs are genetically representative of the main tumour deposit and, therefore, might serve as a readily accessible source of tumour cells for various analyses.[12,13] In other types of cancers, tumour biopsies performed before and after initiation of therapy can enable molecular evaluation of the cancer during treatment and provide the opportunity to tailor the use of molecularly targeted therapies. However, as prostate cancer frequently metastasizes to the bone and bone tumour biopsies are relatively challenging to reliably obtain, this approach is not always feasible in patients with mCRPC. Thus, CTCs could serve as a 'liquid biopsy' that might provide the opportunity to noninvasively and repeatedly sample representative tumour cells before and during therapy, and thus provide information concerning not only tumour burden, but also the molecular characteristics of tumour cells as they evolve during treatment.[14,15] However, CTCs are rare, with an estimated abundance of one cell per billion normal blood cells, and reliable isolation and detection of these cells from peripheral blood has proven extremely challenging. This Review provides an overview of the challenges associated with monitoring therapeutic responses in prostate cancer and summarizes developments in technologies that enable the detection and analysis of CTCs associated with prostate cancer. In addition, the available data supporting the potential for CTC analysis to provide prognostic information that could be used to guide therapy in mCRPC are examined.

Department of Radiation Oncology (**D.T.M.**), Department of Medicine (**L.V.S.**, **R.J.L.**), MGH Cancer Center, Massachusetts General Hospital, 55 Fruit Street, Boston, MA 02114, USA.

Correspondence to: D.T.M. dmiyamoto@partners.org

Competing interests
R.J.L. has received research funding from Exelixis and Janssen, and has acted as a consultant for Medivation. D.T.M. and L.V.S. declare no competing interests.

Key points

- Reliable biomarkers that can guide the treatment of metastatic prostate cancer in the clinic remain an unmet need
- Circulating tumour cells (CTCs) are rare cells shed by tumours into the peripheral circulation, and might represent a means of noninvasive tumour sampling
- Technological advances have improved the isolation and analysis of rare CTCs from patients with cancer
- CTC enumeration has been shown to be predictive of prognosis in patients with metastatic castration-resistant prostate cancer
- Molecular analyses of CTCs have the potential to enable real-time monitoring and predictions of response to therapy in patients with metastatic prostate cancer

Methods of evaluating prostate cancer

The most common sites of prostate cancer metastasis are bone and lymph nodes. Bone metastases are present in 90% of men with terminal prostate cancer and represent the major cause of morbidity and mortality associated with this disease. Skeletal-related events, including pathological fractures and spinal cord compression in particular, have substantial effects on health and quality of life, and contribute to mCRPC mortality.[16] Standard imaging modalities for assessment of prostate cancer and associated metastases include CT of the abdomen and pelvis, largely to evaluate lymph nodes, and bone scan using ^{99m}Tc-methylene diphosphonate (^{99m}Tc-MDP) as the imaging agent. Although lymph nodes or other visceral metastases constitute measurable disease using the modified Response Evaluation Criteria in Solid Tumours (mRECIST) criteria,[17] bone lesions change slowly over time and are considered unmeasurable sites of disease according to these criteria. The Prostate Cancer Working Group 2 (PCWG2) guidelines defined progression of metastatic disease as the identification of at least two new bone lesions on two consecutive bone scans;[18] however, improvement in disease according to information from bone scans is often not defined. PET scans were not recommended for the assessment of bone metastases by the PCWG2.[18] More recently, however, the use of ^{18}F-fluorodeoxyglucose (^{18}F-FDG), ^{18}F sodium fluoride (^{18}F-NaF), and ^{11}C-based tracers (such as choline and acetate) has shown promise in PET-based monitoring of prostate cancer in small studies,[19–22] but, to date, these investigations have not resulted in a widely available, clinically useful PET tracer. Hence, PET remains an investigational imaging modality in patients with prostate cancer at present.

Owing to the high prevalence of bone metastases in patients with mCRPC, improved assessment of tumour burden on bone scans might provide a clinically relevant tool for both individual patient management and imaging end points for clinical trials. An automated computer-aided detection (CAD) assessment system has been described that could provide objective, reproducible, and quantifiable measurements of ^{99m}Tc-MDP uptake in bone.[23] The CAD system integrates image intensity normalization, lesion identification and segmentation according to anatomical-region-specific intensity thresholds, and quantitation of disease burden, as well as independent review by a nuclear-medicine physician.[23] Using this assessment system, 'Bone Scan Lesion Area' (BSLA) was found to be the most informative metric in differentiating between patients with mCRPC who were treated with cabozantinib, an investigational drug that inhibits c-Met and VEGFR, and those patients who did not receive this agent.[23] BSLA might, therefore, represent a promising new indicator of disease response in mCRPC. At present, validation of BSLA as an objective measure of post-treatment response in comparison with other clinically relevant outcome measures is required; the results of small studies have indicated the potential utility of this approach.[24]

Assays of serum PSA levels are widely available, and this biomarker is generally considered to reflect tumour burden in patients with prostate cancer; however, post-treatment changes in serum PSA levels have not been proven as a surrogate measure of clinical benefit.[9,25] Indeed, no therapy for prostate cancer has been approved solely based on an observed post-treatment decline in serum PSA levels. Furthermore, several FDA-approved and experimental therapies have demonstrated beneficial therapeutic effects that were not concordant with decreased serum PSA levels.[26] Thus, there is a critical unmet need for improved biomarkers of therapeutic response in patients with prostate cancer.

Cell-free circulating tumour DNA and RNA have been detected in plasma and serum from patients with prostate cancer, and studies have observed a correlation between circulating tumour nucleic acid burden and prognosis in men with metastatic prostate cancer.[27,28] These cell-free nucleic acids might originate from necrotic tumour tissues, exosomes, oncosomes, or dead tumour cells that enter the circulation.[28,29] A principle advantage of assessments based on the detection of circulating nucleic acids is the high sensitivity potentially obtainable using PCR-based amplification techniques; a chief disadvantage is that separation of tumour-derived nucleic acids from other circulating nucleic acids is not possible and, therefore, only the detection of tumour-specific gene mutations can prove the presence of DNA or RNA released from tumour cells. In addition, as individual tumour cells themselves are not identified using this approach, potentially useful information on intercellular heterogeneity and intracellular signalling pathway activity is lost. Thus, assays for circulating tumour-derived nucleic acid and CTC might have complementary uses, with the former providing information regarding gene mutations and genetic translocations, and the latter providing specific information regarding CTC numbers, cell morphology, and intracellular signalling events in response to therapy.

Technologies for the detection of CTCs

The presence of CTCs in a patient with metastatic cancer was first reported in 1869,[30] but these cells have been extremely difficult to isolate and study because of their rarity (abundance of approximately one CTC per billion normal blood cells). Although considerable challenges remain in the development of robust technologies that enable detection of CTC with high accuracy, sensitivity, and specificity, owing to the rarity, fragility, and biological heterogeneity of CTCs, improved methods for CTC detection have been developed over the past

Table 1 | Selected CTC-detection technologies that have been tested in patients with prostate cancer

CTC-detection technology or process	Basis of CTC enrichment and detection	Assay examples (manufacturer)
Positive selection using cell-surface antigen(s)		
Immunomagnetic beads	EpCAM-based immunomagnetic selection; immunofluorescence for $CK^+/CD45^-$ cells or RT-PCR for a panel of genes (*MUC1, HER2, EPCAM*)	CellSearch® (Veridex, USA),[37] AdnaTest (AdnaGen, Germany)[46]
Microfluidic microposts chip	EpCAM-based or PSMA-based selection; immunofluorescence for $CK^+/CD45^-$, $PSA^+/CD45^-$, or $PSMA^+/CD45^-$ cells, or RT-PCR for selected genes	$^{\mu p}$CTC-Chip (MGH, USA),[51] GEDI (Cornell University, USA)[54]
Microfluidic mixing chip	Selection based on EpCAM or other tumour-specific markers; immunofluorescence for selected tumour markers (such as CK, PSA, and PMSA), or RT-PCR for selected genes	^{HB}CTC-Chip (MGH, USA)[52]
Microfluidic inertial focusing chip	EpCAM-based selection; immunofluorescence for selected tumour markers (CK, PSA, and PSMA)	^{pos}CTC-iChip (MGH, USA)[36]
Patterned silicon nanowire microfluidic chip	EpCAM-based selection; immunofluorescence for $CK^+/CD45^-$ cells	NanoVelcro (UCLA, USA)[53]
Immunomagnetic sweeper	EpCAM-based immunomagnetic selection; immunofluorescence for $CK^+/CD45^-$ cells, or RT-PCR for selected genes	MagSweeper (Stanford University, USA)[47]
Immiscible phase filtration	EpCAM-based immunomagnetic selection; immunofluorescence for $CK^+/CD45^-$ cells	VerIFAST (University of Wisconsin, USA)[50]
Negative selection using cell-surface antigen(s)		
Microfluidic inertial focusing chip	Depletion of $CD45^+$ cells; immunofluorescence for selected tumour markers (CK, PSA, and PSMA); RT-PCR for selected genes	^{neg}CTC-iChip (MGH, USA)[36]
Microfluidic negative selection	Bulk haematopoietic-cell removal, followed by depletion of $CD45^+$ cells; immunofluorescence for $CK^+/CD45^-$ cells	Microfluidic Cell Concentrator[55]
Other biological approaches		
Detection of proteins shed from viable CTCs	Short-term cell culture after $CD45^+$-cell depletion; immunofluorescence for MUC1, PSA, or CK-19	EPISPOT (CHU, France & UKE, Germany)[56]
CAM ingestion	Density-gradient centrifugation, short-term culture; immunofluorescence for cell-surface markers	CAM Vita-Assay™ (Vitatex, USA)[57]
RT-PCR in whole-blood nucleated cells	RT-PCR for gene panels (such as *KLK3, KLK2, HOXB13, GRHL2,* and *FOXA1*)	PAXgene Blood RNA tube and RT-PCR[69]
Physical selection methods		
Size-based separation	Filtration based on cell size; immunofluorescence or FISH	ISET® (RARECELLS, France),[61] CTC Membrane Microfilter (University of Miami, USA)[63]
Dielectric field flow fractionation (DFFF)	Application of electric field to isolate cells; immunofluorescence for tumour-specific markers	ApoStream® (ApoCell, USA)[60]
Other approaches		
Fibre-optic array scanning technology (FAST) cytometry	RBC lysis and density-gradient centrifugation; immunofluorescence for CK, PSMA, or other tumour-cell markers	Epic HD-CTC Assay (Epic Sciences, USA)[71]
Laser-scanning cytometry	RBC lysis; immunofluorescence for $EpCAM^+/CD45^-$ cells	Maintrac® (Simfo, Germany)[72]
Functionalized nanodetector inserted into patient's vein	EpCAM-based selection; immunofluorescence for EpCAM or CK	CellCollector™ (GILUPI, Germany)[73]

Abbreviations: $^{\mu p}$CTC-Chip, micropost CTC-Chip; CAM, cell-adhesion molecule; CHU, Centre Hospitaliers Universitaires; CK, cytokeratin; CTC, circulating tumour cell; EpCAM, epithelial cell-adhesion molecule; EPISPOT, epithelial immunospot; FAST, fibre-optic array scanning technology; FISH, fluorescence *in situ* hybridization; GEDI, geometrically enhanced differential immunocapture; ^{HB}CTC-Chip, herringbone CTC-chip; HD-CTC, high-definition-CTC (assay); ISET, isolation by size of epithelial tumour cells; MGH, Massachusetts General Hospital; ^{neg}CTC-iChip, negative selection CTC-inertial-focusing-chip; ^{pos}CTC-iChip, positive selection CTC-inertial-focusing-chip; PSA, prostate-specific antigen; PSMA, prostate-specific membrane antigen; RBC, red blood cell; RT-PCR, reverse transcription polymerase chain reaction; UCLA, University College of Los Angeles; UKE, Universitätsklinikum Hamburg–Eppendorf.

two decades.[11,14,31] A number of these technologies have been applied to the detection and analysis of CTCs in patients with prostate cancer in pilot studies. However, translation of any of these technologies into routine clinical practice will require extensive analytical and clinical validation in prospective trials. We provide an overview of currently available CTC-detection technologies, with a particular emphasis on technologies that have shown promise in the study of CTCs in patients with prostate cancer. These technologies can be stratified into methods that rely on either biological or physical cellular characteristics for detection of CTCs (Table 1; Figure 1).

Surface-antigen-based enrichment of CTCs

Two general approaches to surface-antigen-based enrichment of CTCs have been developed: positive selection, in which CTC-specific cell-surface markers are used to purify CTCs away from normal blood cells; and negative selection, which uses leukocyte-specific cell-surface markers to remove immune cells from blood, thus leaving behind other cells, including CTCs. Epithelial cell-adhesion molecule (EpCAM) has been widely used for positive selection of CTCs (Table 1), as this transmembrane glycoprotein is consistently expressed by epithelial-derived tumour cells, but is not found on

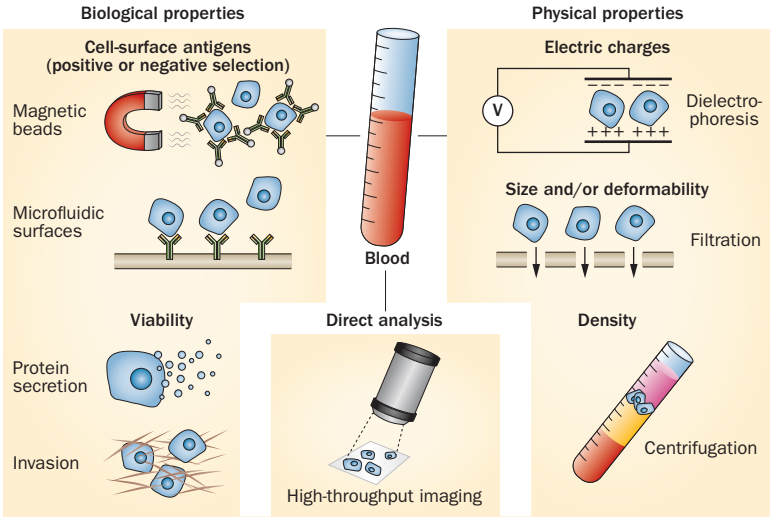

Figure 1 | Approaches to detection of CTC. CTCs can be enriched from whole-blood samples based on biological or physical properties, or can be detected directly after lysis of red blood cells through high-throughput imaging approaches. Enrichment of CTCs based on biological properties can be achieved through positive or negative selection for tumour-specific cell-surface antigens, and assays for cell viability and phenotype. Approaches to enrichment of these cells based on physical properties exploit tumour-specific differences in density, size, deformability, and electric charges. Abbreviation: CTCs, circulating tumour cells.

normal leukocytes. Indeed, EpCAM is expressed highly in a variety of carcinomas, including prostate cancers, and has an important role in cell adhesion, signalling, migration, proliferation, and differentiation.[32] Although EpCAM-based positive selection has been successfully used as a strategy to isolate CTCs in a variety of cancer types, EpCAM expression might decrease in cells undergoing epithelial–mesenchymal transition (EMT), a potential key process in tumour metastasis (Figure 2).[33,34] Thus, interest in positive selection using alternate tumour-cell markers that enable capture of CTCs with low EpCAM expression is increasing.[34,35] Alternatively, CTCs expressing low levels of EpCAM have been identified using negative selection strategies that deplete blood samples of normal haematopoietic cells and, therefore, leave behind enriched populations of all CTCs.[36] The two broad categories of technologies that have been used for surface-antigen-based enrichment of CTCs are methods based on immunomagnetic beads and approaches using microfluidic devices.

Immunomagnetic-bead-based enrichment of CTCs

The CellSearch® assay (Veridex, USA), the only FDA-cleared CTC-detection technology,[37] relies on anti-EpCAM-antibody-coated magnetic beads for capture of CTCs, which are subsequently identified as cells positive for cytokeratin (CK)-8, CK-18, and CK-19 expression, and negative for common leucocyte antigen (CD45) expression by immunofluorescence staining (Table 1).[38–40] As the CellSearch® platform has undergone extensive analytical validation and clinical qualification,[38–40] leading to its FDA clearance,[37] this CTC-detection assay is used widely among the prostate cancer research community. Several clinical studies have demonstrated a relationship between patient prognosis and CellSearch®-determined CTC abundance before and after treatment of prostate cancer.[38–41] However, several limitations of the CellSearch® system have stimulated the development of new technologies for CTC enrichment and detection. For example, performing informative molecular analyses in CTCs isolated using the CellSearch® technology is relatively difficult because of the low purity of the cell populations obtained, the requirement for fixation of cells in preparation for immunofluorescence-based detection, and the nature of the processing conditions. Nevertheless, studies have demonstrated the feasibility of molecular characterization of CellSearch®-derived CTCs.[13,42] The requirement for operator review and interpretation of the CellSearch® data has been shown to contribute to variability in CTC counts;[43] therefore, an automated algorithm has been developed to provide unbiased counts of CTCs in the recorded CellSearch® images.[44] This automated algorithm has also been used to extract data on the morphological features of CTCs, including cell size, roundness, and apoptotic features, which were found to be closely correlated with overall survival in univariate analysis, although not in multivariate analysis.[45]

To address the problem of capturing cells that are undergoing EMT (Figure 2), a cadherin-11-based capture method has been developed by investigators at Duke University, NC, USA, to complement the EpCAM-based CellSearch® platform.[35] Cadherin-11 (also known as osteoblast cadherin) is a cell-adhesion molecule expressed in osteoblasts and prostate cancer cells.[35] Mesenchymal cells are immunomagnetically enriched using anti-cadherin-11-antibody-conjugated magnetic particles, and potential CTCs are identified by immunofluorescence analysis according to expression of β-catenin, after exclusion of contaminating CD45-positive leukocytes.[35] A pilot study using this method detected potential mesenchymal CTCs in a subset of patients with mCRPC at an increased frequency compared with healthy volunteers,[35] although further studies will be required to define the clinical relevance of these findings.

Other immunomagnetic-bead-based systems, such as the AdnaTest (AdnaGen, Germany; Table 1), enable molecular characterization of CTCs, including reverse transcription-PCR (RT-PCR) analysis of prostate-specific gene transcripts.[46] The MagSweeper device, developed by researchers at Stanford University, CA, USA, is an immunomagnetic cell separator that uses magnetic rods to collect CTCs that are bound to anti-EpCAM-antibody-coated magnetic beads from diluted blood samples (Table 1);[47] nonspecifically bound blood cells are released through a controlled shear force produced by movement of the magnetic rods in wash buffer.[47] The isolated cells have been demonstrated to contain RNA of sufficient quality to perform multiplex quantitative RT-PCR and RNA sequencing of single CTCs, although the RNA from many of the CTCs showed signs of degradation consistent with apoptosis.[48,49] Another promising

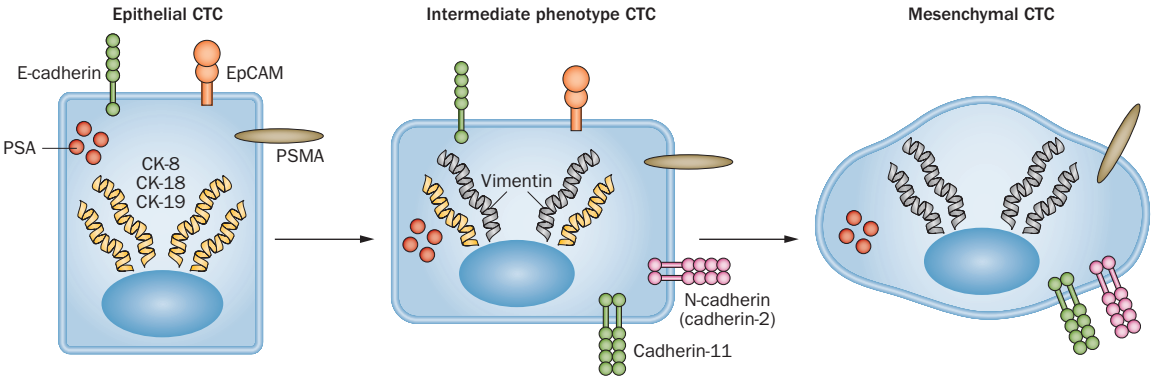

Figure 2 | Molecular markers used to detect prostate CTCs undergoing epithelial–mesenchymal transition. Epithelial–mesenchymal transition is characterized by the gain and loss of specific molecular markers, and the exclusive use of epithelial markers for the isolation and detection of CTCs could result in lack of detection of the mesenchymal subpopulation of these cells. For example, since EpCAM is often downregulated in mesenchymal cells, the use of EpCAM as a selection marker is probably not sufficient to detect mesenchymal CTCs. Abbreviations: CK, cytokeratin; CTC, circulating tumour cell; EpCAM, epithelial cell-adhesion molecule; PSA, prostate-specific antigen; PSMA, prostate-specific membrane antigen.

immunomagnetic approach to isolation of CTC from blood samples is the immiscible phase filtration platform VerIFAST, developed by a team at the University of Wisconsin, WI, USA.[50] The VerIFAST technique uses magnets to selectively move the desired cells between immiscible liquids, relying upon the high interfacial energy between the immiscible liquids to ensure that only the cells bound to immunomagnetic beads can cross between phases (Table 1), and enables rapid isolation and processing of CTCs.[50]

Microfluidic devices for enrichment of CTCs

Improvements in microfluidic engineering over the past decade have enabled the development of innovative microfluidic devices for efficient and gentle isolation of CTCs from whole-blood samples. Our group at the Massachusetts General Hospital (MGH), MA, USA, has developed a series of microfluidic devices that enrich CTCs from whole blood using cell-surface antigens. The first generation $^{\mu P}$CTC-Chip consisted of 78,000 microposts coated with anti-EpCAM antibodies, which capture EpCAM-expressing CTCs that come into contact with the microposts as blood flows through the microfluidic chip (Table 1).[51] A second generation version of the CTC-Chip, the ^{HB}CTC-Chip, consists of microfluidic channels etched with herringbone patterns, inducing the formation of microvortices as blood flows through the chip, thus increasing the contact time between cells and the walls of the channel coated with anti-EpCAM antibodies (Figure 3).[52] The capture antibodies used to functionalize the microfluidic channels can be tailored based on the biological characteristics of the cells of interest, such as in the use of antibodies against nonepithelial tumour antigens to capture CTCs undergoing EMT.[34]

Other microfluidic technologies have also been developed based on the concept of positive selection. Developed by researchers at the University of California Los Angeles (UCLA), CA, USA, the NanoVelcro microfluidic device incorporates anti-EpCAM-antibody-coated silicon nanowires integrated with an overlaid polydimethylsiloxane (PDMS) chaotic mixer, which generates vertical flows and enhances contacts between CTCs and the capture substrate (Table 1).[53] This technology has been piloted in patients with CRPC, and produced data that suggested a correlation exists between changes in CTC numbers and response to therapy.[53] To specifically capture prostate-cancer-associated CTCs, a platform with microposts coated with antibodies targeting prostate-specific membrane antigen (PSMA), the 'geometrically enhanced differential immunocapture' (GEDI) device, has been developed by a team at Cornell University, NY, USA.[54] A pilot study of the GEDI device showed that PSMA-expressing CTCs were more abundant in samples from patients with CRPC compared with blood from healthy donors, and that on-chip monitoring of effective drug-target engagement to predict treatment response might be feasible.[54]

In addition to the positive selection strategy used by earlier microfluidic technologies, a third generation CTC-Chip technology developed at the MGH, the CTC-iChip, also enables a negative selection strategy that purifies CTCs independent of antigens present on the tumour-cell surface (Table 1).[36] The CTC-iChip consists of three integrated components: a hydrodynamic sorting step that results in size-based removal of red blood cells and platelets; an inertial focusing step that aligns the remaining cells in a single file in the flow channel; and a subsequent magnetophoresis step that removes cells that have been labelled with antibody-coated magnetic beads, which are CTCs in the case of positive selection or leukocytes in the case of negative selection.[36] The negative selection mode (^{neg}CTC-iChip) yields a gently isolated population of CTCs that have not been labelled with antibodies or magnetic beads, thus enabling subsequent molecular analyses, including single-cell transcriptional profiling.[36] Moreover, the CTC population obtained using the ^{neg}CTC-iChip is unselected and, therefore, CTCs with a range of phenotypes, including epithelial and mesenchymal cells, can potentially be detected and analysed for molecular

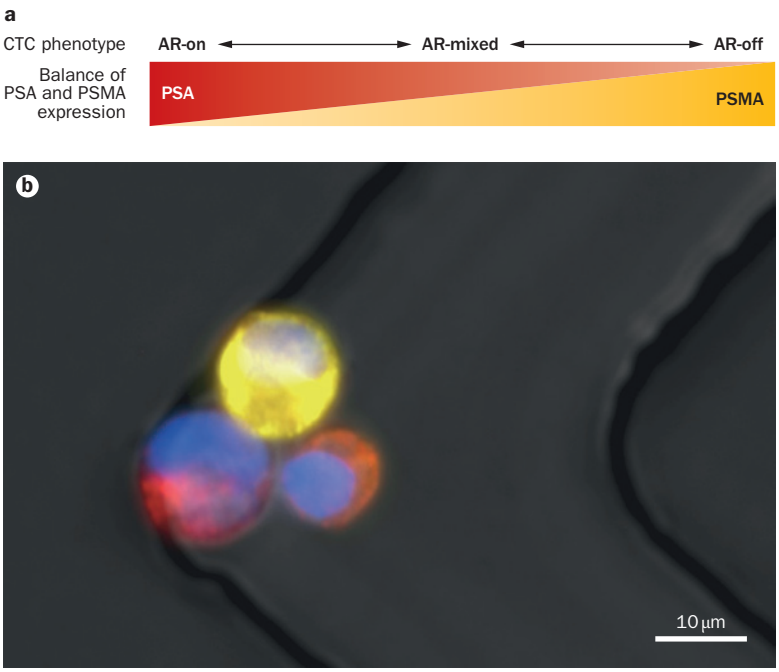

Figure 3 | Assay for measuring signalling activity of the AR in prostate CTCs.[70] **a** | Schematic shows the relative expression levels of PSA and PSMA in 'AR-on', 'AR-off', and 'AR-mixed' signalling states. **b** | CTCs from a patient with mCRPC captured on the ^{HB}CTC-Chip, a microfluidics-based assay that enables anti-EpCAM-antibody-mediated capture of CTCs from whole-blood samples. The image is a composite of fluorescence micrographs that visualize immunostaining of PSA (red) and PSMA (yellow) expression, and DAPI staining of DNA (cell nuclei; blue), merged with a phase contrast microscopy image. Heterogeneity in AR signalling activity between mCRPC-associated CTCs is evident, as demonstrated by the presence of a red cell (AR-on), a yellow cell (AR-off), and an orange cell (AR-mixed). Herringbone grooves on the ^{HB}CTC-Chip, which generate microvortices within the microfluidics channels that direct the cells towards the antibody-coated surfaces to increase the efficiency of CTC capture, are visible (dark angled lines). Abbreviations: AR, androgen receptor; CTC, circulating tumour cell; DAPI, 4',6-diamidino-2-phenylindole; EpCAM, epithelial cell-adhesion molecule; ^{HB}CTC-Chip, herringbone CTC-Chip; mCRPC, metastatic castration-resistant prostate cancer; PSA, prostate-specific antigen; PSMA, prostate-specific membrane antigen.

variation. Other groups have also developed methodologies based on negative selection that have been applied to the isolation of CTCs associated with prostate cancer, including a microfluidic device called the Microfluidic Cell Concentrator (MCC), which performs gentle negative selection of CTCs after bulk erythrocyte and haematopoietic-cell removal.[55]

CTC isolation using other biological properties

Alternative approaches to the isolation of CTCs rely on biological characteristics of viable CTCs, such as invasiveness and secretion of specific proteins. These approaches are not based on assumptions regarding the physical properties of CTCs or differential expression of cell-surface antigens, and thus have the potential advantage of capturing subsets of CTCs that would not be otherwise identified. However, such methods necessitate the assumption that CTCs will remain viable under the *in vitro* cell-culture conditions used, and that these specific culture conditions are sufficient to recapitulate the *in vivo* biological behaviour of CTCs.

A functional enzyme-linked immunosorbent spot (EPISPOT) assay, for example, can detect the presence of viable CTCs based on proteins released during short-term cell culture (24–48 h), such as PSA secreted by CTCs associated with prostate cancer (Table 1).[56] Similarly, the cell-adhesion matrix (CAM)-based Vita-Assay™ platform (Vitatex, USA) enables viable invasive CTCs to be isolated by virtue of the propensity of tumour cells to invade into collagenous matrices (Figure 1).[57] Thus, the Vita-Assay™ can be used for identification of CTCs independent of EpCAM status, and enables CTC enumeration and analysis of CTC DNA.[57] These approaches have been used in several pilot analyses of CTCs from patients with mCRPC, including immunocytochemistry for PSMA, and markers of EMT and stemness, array comparative genomic hybridisation (CGH), and whole-genome methylation array analysis.[58] Follow-up studies are required to clarify the potential utility of these methodologies in the isolation and assessment of CTCs.

Physical-property-based enrichment of CTCs

Several physical properties seem to distinguish CTCs from most normal peripheral blood cells, and many of these have been exploited to isolate CTCs from blood (Figure 1). The characteristics that can differ between CTCs and other blood-borne cells include density, size, deformability, and electrical properties.[14,59,60] After enrichment based on these physical properties, CTCs can be detected using immunohistochemistry, immunofluorescence, or molecular techniques such as PCR. In patients with prostate cancer, microfiltration methods have been used according to the assumption that CTCs are larger than leukocytes, and thus pores of varying geometries can retain CTCs while allowing leukocytes to pass through.[61–65] For example, the ISET® (Isolation by Size of Epithelial Tumour cells) system (RARECELLS, France) enriches for CTCs by filtering blood through membranes with pores 8 μm in diameter, followed by staining of cells retained on the filter for cytomorphological examination or immunocytochemistry (Table 1).[61] Although most prostate CTCs do seem to be larger than leukocytes, they exhibit wide variation in size, and a subset of these cells might be smaller than leukocytes.[36,66] A direct comparison between the CellSearch® assay and the ISET® microfiltration assay demonstrated only 60% concordance in the results obtained using samples from patients with prostate cancer, suggesting that these two cell-isolation techniques can identify different subpopulations of CTCs;[67] however, different criteria were used to validate and characterize CTCs isolated using each of these two platforms, which might account for some of the discordance observed. Specifically, CTCs detected using the ISET® assay were identified by a cytopathologist according to morphological criteria, whereas CTCs detected according to the CellSearch® methodology were identified based on the intensity of cytokeratin immunofluorescence signals and location of the 4',6-diamidino-2-phenylindole (DAPI) nuclear stain in the cell.[67] Thus, the ISET® protocol might have identified a subset of CTCs that do not stain for epithelial markers and,

therefore, were not detected using the CellSearch® assay, whereas the CellSearch® could potentially have identified smaller CTCs that were lost during the ISET® procedure.

Enrichment of CTCs using methods based on other biophysical properties include dielectrophoresis to separate CTCs from peripheral blood cells based on intrinsic differences in the polarizability (that is, the electrical properties) of these cell types (Table 1), thus avoiding the necessity for antibody labelling and enabling the isolation of minimally modified CTCs for subsequent analysis.[59,60] Application of a nonuniform electric field generated by electrodes causes the attraction of tumour cells by positive dielectrophoretic forces while other cells flow past, and subsequent removal of the electric field enables the captured tumour cells to be collected.[59,60] Nevertheless, evidence indicates that dielectrophoresis and microfluidic immunocapture using the J591 anti-PSMA antibody can be used synergistically to improve the performance of CTC capture modalities.[68] These physical-property-based CTC enrichment technologies require further evaluation and clinical validation in patients with prostate cancer.

Other innovative approaches to CTC detection

Other approaches to CTC detection have been developed that avoid enrichment biases that might arise from the assumptions made regarding the physical or biological differences between CTCs and normal blood cells that often form the basis of cell selection. One method relies on RT-PCR-based detection of transcripts specific to prostate cancer cells in whole-blood nucleated-cell populations, and was shown to enable prediction of overall survival in patients with mCRPC in a pilot study.[69] However, this bulk RNA-assessment technique does not provide morphological data for the cells from which the prostate-cancer-related RNA transcripts are derived.

A technique that provides extensive morphological data is the high-throughput fibre-optic array scanning technology (FAST), which involves imaging every nucleated cell contained in a whole-blood sample spun onto a microscope slide (Table 1; Figure 1), thus avoiding the biases that might occur when CTC enrichment technologies are used.[66,70,71] However, the FAST approach remains limited by the choice of antibodies used for the immunofluorescence-based detection of CTC, as only cells expressing cytokeratin or other selected markers can be detected at present, which re-introduces a source of potential bias that is also encountered using other isolation methodologies. Another technology based on laser-scanning cytometry, a technique that combines flow cytometry with microscopy-based imaging, similarly avoids an enrichment step to maximize the detection of CTCs, but also relies on anti-EpCAM antibodies for visualization of these cells.[72] An additional comprehensive approach has been developed that enables the detection of CTCs directly in the blood *in vivo* using a medical wire functionalized with EpCAM antibodies that is placed into the patient's peripheral arm vein;[73] however, this unique method is again restricted by the limited number of available markers that are known to distinguish CTCs.

Standardization and validation of technologies

The development of innovative CTC-detection technologies has been driven largely by a desired ability to perform more sensitive and comprehensive analyses of CTCs, and many of the novel modalities have shown increased sensitivity of CTC detection in single-arm pilot studies. However, comparisons of sensitivity of cell detection across different platforms and validation of results have been hampered by a lack of standardization in the definition of CTCs, as well as differences in the clinical characteristics of the patient cohorts studied. At present, considerable disagreement regarding the classification of CTCs remains, depending on the isolation technique used, ranging from cytomorphological criteria, to the presence of specific protein markers (epithelial and/or mesenchymal), to measures of cell viability or invasiveness. Of note, in a comparison between the CellSearch® and ISET® systems, certain cells isolated by ISET® and identified as CTCs by an expert cytopathologist would not be identified using the CellSearch® assay, owing to the absence of immunostaining of these cells by specific antibodies.[67] In the development of our own microfluidic devices, definitions of CTCs have evolved with the use of different detection antibodies and increasingly sophisticated semi-automated image analysis technologies, necessitating recalibration of scoring parameters based on frequencies and intensities of the signals measured in healthy donor controls and cell-spiking experiments.[52,74] Thus, standardized comparisons of sensitivity of CTC detection between platforms and clinical validation are difficult to achieve, as a result of the wide-ranging, varied, and rapidly evolving definitions and criteria used for CTC classification and enumeration.

Standardization of the criteria that define CTCs will require coordination and consensus among pathologists, biologists, clinical investigators, and bioengineers from different institutions. Key issues that need to be addressed include the development of clear guidelines for the biological markers and cytomorphological characteristics that define CTCs, and whether different sets of criteria will be necessary to define specific subsets of CTCs (for example, epithelial versus mesenchymal). Standardized classification criteria for CTCs will be necessary not only for meaningful comparisons of sensitivity and specificity across CTC-detection platforms, but also as a prerequisite for analytical validation of CTC-related biomarkers before routine clinical use.

CTC enumeration in prostate cancer

CTC enumeration and prognosis

Although numerous pilot studies have been conducted assessing CTCs in patients with prostate cancer using a variety of cell-detection platforms, limited data from large clinical trials have been reported. The largest datasets relating to CTCs in prostate cancer were obtained using the CellSearch® system. Indeed, the FDA has cleared CellSearch®-based assessment of CTCs as a prognostic indicator in patients with metastatic breast, colon, and prostate cancers.[8,37] The prospective study

that led to FDA clearance of the prognostic use of the CellSearch® assay in prostate cancer, IMMC38,[39] enrolled 276 patients with progressive mCRPC who were starting a new chemotherapy regimen, 231 of whom were evaluable. Similar to prior studies in breast cancer,[75,76] CTC numbers were evaluated in blood samples taken before treatment and monthly after initiation of therapy using the CellSearch® assay, and patients were categorized as having 'unfavourable' (five or more CTCs in 7.5 ml blood) or 'favourable' (fewer than five CTCs in 7.5 ml of blood) CTC counts.[39] The primary outcome of the IMMC38 trial[39] was that median overall survival in patients with unfavourable CTC counts at 2–5 weeks after initiation of the new chemotherapy regimen was >50% shorter than in the individuals with favourable CTC counts at this time point (9.5 months versus 20.7 months; HR 4.5; P <0.0001). Pretreatment CTC enumeration was also shown to have prognostic value, as patients with unfavourable numbers of CTCs before induction of the new therapy had shorter median overall survival compared with individuals with favourable CTC counts (11.5 months versus 21.7 months, respectively; HR 3.3; P <0.0001).[39] Unfavourable post-treatment CTC numbers were also significantly associated with shorter median overall survival regardless of the time point at which CTCs were assessed (6.7–9.5 months versus 19.6–20.7 months; HR 3.6–6.5; P <0.0001).[39] Furthermore, patients who converted from unfavourable CTC numbers at baseline to favourable CTC counts after treatment had a corresponding improvement in median overall survival (from 6.8 months to 21.3 months);[39] conversely, those who converted from favourable to unfavourable CTC levels had reduced median overall survival (from >26 months to 9.3 months).[39] Importantly, CTC count was a better predictor of overall survival than post-treatment changes in serum PSA levels at all time points.[39] Together, these findings indicated that CTC count was a useful biomarker of treatment response and overall survival in patients with mCRPC, with better performance than assessment of serum PSA.

A re-analysis of the IMMC38 trial data was performed,[40] focusing on the patients included who were receiving first-line chemotherapy, and evaluating CTC count as a continuous variable (rather than according to favourable versus unfavourable risk categories), as well as other pretreatment and post-treatment variables. Patients with bone metastases had higher CTC counts in general than individuals with visceral metastases, although this difference was not statistically significant.[40] Higher lactate dehydrogenase (LDH) concentrations (HR 6.44, 95% CI 4.24–9.79; P <0.0001), CTC counts (HR 1.58, 95% CI 1.41–1.77; P <0.0001), and serum PSA (HR 1.26, 95% CI 1.10–1.45; P = 0.0008) in baseline samples were associated with increased risk of death.[40] CTCs were also evaluated as an intermediate end point, by examining the relationship between changes in CTC numbers and survival. An increase in CTC count was moderately associated with decreased survival, whereas increased serum PSA levels were weakly or not associated with risk of death, suggesting that change in CTC counts could be a more accurate intermediate end point for clinical trials than variation in post-treatment PSA titres.[40]

Other studies have confirmed the prognostic value of CTC enumeration in mCRPC using the CellSearch® assay. A study in 120 patients with progressive mCRPC initiating treatment with a variety of hormonal or cytotoxic therapies found that baseline CTC count was strongly associated with overall survival, without a threshold 'unfavourable' effect.[38] The optimal cutoff point designation for favourable and unfavourable CTC counts has been evaluated in a single-institution study involving 100 patients with CRPC, with or without metastatic disease;[41] threshold analysis identified four CTCs in 7.5 ml of blood as the optimal cutoff point for correlation of CTC numbers with overall survival, and this threshold was 100% specific for the presence of radiographically evident metastatic disease.[41] Multivariate analysis also identified serum LDH concentration and CTC counts as independent prognostic factors.[41]

CTC enumeration as an intermediate end point

COU-AA-301[4] was a phase III, double-blind, randomized placebo-controlled trial that evaluated abiraterone acetate in 1,195 men with mCRPC who had previously received chemotherapy with docetaxel. Patients were randomized 2:1 to receive 1,000 mg of abiraterone acetate daily or placebo, together with 5 mg of prednisone twice daily.[4] At a median follow-up period of 12.8 months, this study met its primary end point of significantly improved overall survival in the abiraterone cohort versus the placebo cohort (14.8 months versus 10.9 months; P <0.001).[4] Of note, this trial was the first phase III trial to prospectively define a secondary end point evaluating whether CTC enumeration could be used as a surrogate efficacy-response biomarker of overall survival. In the planned final analysis of COU-AA-301 at a median follow-up duration of 20.2 months,[77] abiraterone treatment (HR 0.70, 95% CI 0.59–0.828; P <0.0001), baseline LDH concentration (HR 2.98, 95% CI 2.496–3.565; P <0.0001), and CTC count (HR 1.19, 95% CI 1.137–1.245 ; P <0.0001) were prognostic for survival, although PSA was not (HR 1.04, 95% CI 0.983–1.093; P = 0.1797). Interestingly, a change in CTC numbers from unfavourable (five or more CTCs in 7.5 ml of blood) to favourable (fewer than five CTC in the 7.5 ml of blood), or vice versa, was predictive of overall survival at the earliest post-treatment time point assessed (4 weeks), and conversion to an unfavourable CTC count substantially reduced the abiraterone-related treatment effect at all post-treatment time points.[77] A combined biomarker panel including CTC number conversion (from unfavourable to favourable) and baseline LDH level was developed using the trial data, and the treatment effect on survival was found to be correlated with this biomarker panel.[77] Further development of CTC assessments, possibly in the context of a biomarker panel including baseline LDH concentrations, are needed to clarify the potential role of CTC enumeration as an intermediate end-point surrogate for overall survival.

Molecular analysis of prostate CTCs

Genetic alterations in CTCs

Several studies have demonstrated the feasibility of molecular characterization of prostate-cancer-related CTCs, which might provide prognostic information beyond CTC enumeration alone. Several groups have detected chromosomal translocations resulting in *TMPRSS2–ERG* gene fusion in CTCs isolated from patients with prostate cancer using RT-PCR and fluorescence *in situ* hybridization (FISH), with around 70% concordance between the presence of this genetic aberration in CTCs and the primary tumour.[74,78] The predictive value of *TMPRSS2–ERG* fusion status in CTCs was evaluated in patients with mCRPC who were treated with abiraterone acetate, but the presence of this gene fusion was not predictive of treatment response.[79] Other genetic alterations have been identified in CTCs, including loss of *PTEN* and *MYC* amplification,[78,80] as well as both amplification[78,80] and point mutation of the *AR* gene,[81] which encodes the androgen receptor. Other studies have extended the scope of molecular analyses to genome-wide copy number analysis in prostate CTCs.[82] The potential clinical relevance of these molecular analyses, however, remains limited at this time, given the paucity of effective molecularly targeted therapies targeting factors relating to specific genetic mutations in prostate cancer.

Predictive protein markers in CTCs

Several protein markers have been evaluated for their potential prognostic value when measured in CTCs. In a pilot study assessing the marker of proliferation Ki-67, CTCs isolated from different patients with prostate cancer exhibited wide variability in Ki-67 positivity (1–81%), and an increased Ki-67 proliferative index in CTCs was associated with resistance to castration therapy.[74] The AR protein has also been investigated in CTCs derived from patients with prostate cancer, with nuclear versus cytoplasmic localization demonstrated to correlate with clinical response to docetaxel chemotherapy.[83] Other studies have suggested that visualization and measurement of microtubule bundling in CTCs can be used to monitor the drug–target engagement of docetaxel chemotherapy and, therefore, might be useful in predicting the effectiveness of this treatment in individual patients.[54] Further refinement of these CTC-based assays of protein markers and incorporation of such assessments into clinical trials will be required for analytical validation and clinical qualification.

Androgen receptor signalling in CTCs

AR signalling is central to prostate cancer biology, and reactivation of AR signalling despite androgen deprivation therapy represents a fundamental mechanism underlying the emergence of castration-resistant disease.[84] Several effective therapies for mCRPC that target the AR signalling axis, such as abiraterone acetate and enzalutamide, have now been approved by the FDA,[4,5,7] creating an urgent need for biomarkers that can guide the application of these agents in the clinic. Several mechanisms of AR reactivation in mCRPC have been proposed, including *AR* gene amplification and activating mutations in *AR*.[84] *AR* copy number has been studied in prostate-cancer-associated CTCs through the use of FISH, and one study identified amplification of this gene in CTCs from 38% of the men with mCRPC evaluated,[80] similar to the proportion of patients in which *AR* amplification has been observed in bone metastasis biopsy studies.[85] Another study of genomic profiling of CTCs showed high-level copy number gains at the *AR* locus in seven of nine cases (78%), although interestingly these gains in *AR* copy number were not observed in matched archival primary tumour tissues, suggesting the occurrence of genomic evolution during cancer progression.[82] A separate study also demonstrated that mutations in the *AR* gene could be detected in CTCs from patients with prostate cancer using PCR amplification and direct sequencing.[81] Although these approaches can provide a snapshot of *AR* gene status in CTCs, they might have a limited ability to provide a dynamic readout of changes in *AR* signalling in response to therapy, as treatment-induced changes at the genomic level typically take longer to manifest than changes at the protein signalling or transcriptomic levels.

Using the ^{HB}CTC-Chip, our group has developed a single-cell immunophenotyping approach to dynamically measure AR signalling in CTCs.[86] The relative activity of AR signalling in a given cell can be estimated based on the levels of the proteins PSA and PSMA, which are encoded by genes that have been identified as consistently upregulated and downregulated, respectively, following AR activation in prostate cancer cells (Figure 3a); *KLK3* (encoding PSA) is a classic androgen-upregulated gene, whereas *FOLH1* (encoding PSMA) has been demonstrated to be androgen-downregulated in an AR-dependent manner.[87–89] In developing our two-colour immunofluorescence assay using androgen-responsive prostate cancer cell lines, we identified $PSA^+/PSMA^-$ cells as androgen-induced ('AR-on'), $PSA^-/PSMA^+$ cells as androgen-suppressed ('AR-off'), and $PSA^+/PSMA^+$ ('AR-mixed') cells as cells transitioning between AR-off and AR-on states.[86] Applying this assay to CTCs isolated from patients with untreated metastatic prostate cancer, the majority of CTCs initially had an AR-on phenotype, but switched to AR-off phenotype within 1 month of initiation of androgen-deprivation therapy.[86] By contrast, a striking heterogeneity was evident in CTCs derived from patients with mCRPC, with only AR-on or AR-off cells isolated from some patients, whereas AR-mixed cells or CTCs demonstrating all three AR-activity phenotypes were observed in samples from other individuals (Figure 3b).[86] These results suggest that AR reactivation in CRPC could, in some cases, be more modest than expected, pointing to important contributions from other signalling pathways leading to androgen resistance. On the basis of blood samples from patients with mCRPC treated with abiraterone acetate, an increase in the proportion of AR-on CTCs (despite this hormonal therapy) was predictive of decreased overall survival, as was the presence of an AR-mixed population of CTCs at

baseline.[86] These findings highlight the potential utility of assessing dynamic AR signalling in CTCs in monitoring and predicting treatment responses to AR-targeting therapies, although further evaluation of this approach is required in prospective clinical trials.

Other approaches have also been taken to evaluate the status of AR and its signalling axis in CTCs associated with prostate cancer. The results of one study suggest that AR activity can be inferred based on the subcellular localization of the AR protein in CTCs, with nuclear localization indicative of transcriptionally active AR and cytoplasmic localization reflecting AR inactivity.[83] As introduced earlier, analysis of CTCs isolated from a series of patients with mCRPC revealed a correlation between cytoplasmic sequestration of AR protein and clinical response to docetaxel, leading the authors to postulate that this agent acts in part through inhibition of microtubule trafficking and, therefore, nuclear translocation of the AR.[83] This approach to determining the subcellular localization of AR protein currently requires the use of confocal microscopy and is time intensive; however, advances in semi-automated high-resolution imaging technologies in combination with multispectral imaging might enable the future integration of this assay into a comprehensive panel of biomarker analyses, including assessment of PSA and PSMA expression, that provide data on AR signalling in CTCs.

Conclusions

For both the clinical management of individual patients with prostate cancer and the assessment of therapies in clinical trials, the clinical need for highly informative biomarkers remains unmet. Conventional imaging modalities, serum PSA assays, and biopsy of bone metastases each have important limitations that restrict their utility in the assessment of prostate cancer. New CTC-detection technologies that enable highly sensitive CTC isolation and subsequent detailed molecular analyses of these cell types offer the potential for noninvasive real-time monitoring of disease, although large validation studies are required to clarify the clinical relevance of such approaches. Key advances in CTC isolation made in recent years include: improved sensitivity of CTC detection; increased purity of isolated cell populations, which is important for performing molecular analyses; the development of methodologies for isolating CTCs using cell-surface proteins other than EpCAM, which might enable for capture of cells undergoing EMT; and the use of negative selection to isolate CTCs with minimal manipulation. The ultimate clinical application of CTCs could involve a 'point-of-care' device that provides CTC counts rapidly and reliably, performs molecular characterization of these cells, and assists with therapeutic decision-making. Indeed, the marriage of bioengineering, biology, and medicine that has given rise to CTC isolation technologies promises to propel patient care forward by facilitating the use of rationally targeted therapies based on real-time molecular information obtained from CTC-based liquid biopsies.

Review criteria

We searched PubMed for English-language full-text manuscripts and abstracts published up to November 2013. The search terms used, alone and in various combinations, were "circulating tumour cell", "circulating tumour cells", "circulating tumor cell", "prostate cancer", and "single-cell DNA/RNA". The reference lists of the articles identified were also searched for additional relevant publications.

1. Siegel, R., Ma, J., Zou, Z. & Jemal, A. Cancer statistics, 2014. *CA Cancer J. Clin.* **64**, 9–29 (2014).
2. Kantoff, P. W. *et al.* Sipuleucel-T immunotherapy for castration-resistant prostate cancer. *N. Engl. J. Med.* **363**, 411–422 (2010).
3. de Bono, J. S. *et al.* Prednisone plus cabazitaxel or mitoxantrone for metastatic castration-resistant prostate cancer progressing after docetaxel treatment: a randomised open-label trial. *Lancet* **376**, 1147–1154 (2010).
4. de Bono, J. S. *et al.* Abiraterone and increased survival in metastatic prostate cancer. *N. Engl. J. Med.* **364**, 1995–2005 (2011).
5. Scher, H. I. *et al.* Increased survival with enzalutamide in prostate cancer after chemotherapy. *N. Engl. J. Med.* **367**, 1187–1197 (2012).
6. Parker, C. *et al.* Alpha emitter radium-223 and survival in metastatic prostate cancer. *N. Engl. J. Med.* **369**, 213–223 (2013).
7. Ryan, C. J. *et al.* Abiraterone in metastatic prostate cancer without previous chemotherapy. *N. Engl. J. Med.* **368**, 138–148 (2013).
8. Scher, H. I., Morris, M. J., Larson, S. & Heller, G. Validation and clinical utility of prostate cancer biomarkers. *Nat. Rev. Clin. Oncol.* **10**, 225–234 (2013).
9. Halabi, S. *et al.* Prostate-specific antigen changes as surrogate for overall survival in men with metastatic castration-resistant prostate cancer treated with second-line chemotherapy. *J. Clin. Oncol.* **31**, 3944–3950 (2013).
10. Pantel, K., Alix-Panabieres, C. & Riethdorf, S. Cancer micrometastases. *Nat. Rev. Clin. Oncol.* **6**, 339–351 (2009).
11. Yu, M., Stott, S., Toner, M., Maheswaran, S. & Haber, D. A. Circulating tumor cells: approaches to isolation and characterization. *J. Cell. Biol.* **192**, 373–382 (2011).
12. Fehm, T. *et al.* Cytogenetic evidence that circulating epithelial cells in patients with carcinoma are malignant. *Clin. Cancer Res.* **8**, 2073–2084 (2002).
13. Heitzer, E. *et al.* Complex tumor genomes inferred from single circulating tumor cells by array-CGH and next-generation sequencing. *Cancer Res.* **73**, 2965–2975 (2013).
14. Alix-Panabieres, C. & Pantel, K. Circulating tumor cells: liquid biopsy of cancer. *Clin. Chem.* **59**, 110–118 (2013).
15. Heitzer, E., Auer, M., Ulz, P., Geigl, J. B. & Speicher, M. R. Circulating tumor cells and DNA as liquid biopsies. *Genome Med.* **5**, 73 (2013).
16. Saylor, P. J., Lee, R. J. & Smith, M. R. Emerging therapies to prevent skeletal morbidity in men with prostate cancer. *J. Clin. Oncol.* **29**, 3705–3714 (2011).
17. Scher, H. I., Morris, M. J., Kelly, W. K., Schwartz, L. H. & Heller, G. Prostate cancer clinical trial end points: "RECIST"ing a step backwards. *Clin. Cancer Res.* **11**, 5223–5232 (2005).
18. Scher, H. I. *et al.* Design and end points of clinical trials for patients with progressive prostate cancer and castrate levels of testosterone: recommendations of the Prostate Cancer Clinical Trials Working Group. *J. Clin. Oncol.* **26**, 1148–1159 (2008).
19. Jadvar, H. *et al.* Baseline ^{18}F-FDG PET/CT parameters as imaging biomarkers of overall survival in castrate-resistant metastatic prostate cancer. *J. Nucl. Med.* **54**, 1195–1201 (2013).
20. Jadvar, H. *et al.* Prospective evaluation of ^{18}F-NaF and ^{18}F-FDG PET/CT in detection of occult metastatic disease in biochemical recurrence of prostate cancer. *Clin. Nucl. Med.* **37**, 637–643 (2012).
21. Mosavi, F. *et al.* Whole-body diffusion-weighted MRI compared with ^{18}F-NaF PET/CT for detection of bone metastases in patients with high-risk prostate carcinoma. *AJR Am. J. Roentgenol.* **199**, 1114–1120 (2012).
22. Yu, E. Y. *et al.* C11-acetate and F-18 FDG PET for men with prostate cancer bone metastases: relative findings and response to therapy. *Clin. Nucl. Med.* **36**, 192–198 (2011).
23. Brown, M. S. *et al.* Computer-aided quantitative bone scan assessment of prostate cancer treatment response. *Nucl. Med. Commun.* **33**, 384–394 (2012).

24. Lee, R. J. *et al.* A dose-ranging study of cabozantinib in men with castration-resistant prostate cancer and bone metastases. *Clin. Cancer Res.* **19**, 3088–3094 (2013).
25. Fleming, M. T., Morris, M. J., Heller, G. & Scher, H. I. Post-therapy changes in PSA as an outcome measure in prostate cancer clinical trials. *Nat. Clin. Pract. Oncol.* **3**, 658–667 (2006).
26. Smith, D. C. *et al.* Cabozantinib in patients with advanced prostate cancer: results of a phase II randomized discontinuation trial. *J. Clin. Oncol.* **31**, 412–419 (2013).
27. Ellinger, J. *et al.* The role of cell-free circulating DNA in the diagnosis and prognosis of prostate cancer. *Urol. Oncol.* **29**, 124–129 (2011).
28. Schwarzenbach, H. *et al.* Cell-free tumor DNA in blood plasma as a marker for circulating tumor cells in prostate cancer. *Clin. Cancer Res.* **15**, 1032–1038 (2009).
29. Dawson, S. J. *et al.* Analysis of circulating tumor DNA to monitor metastatic breast cancer. *N. Engl. J. Med.* **368**, 1199–1209 (2013).
30. Ashworth, T. R. A case of cancer in which cells similar to those in the tumors were seen in the blood after death. *Aust. Med. J.* **14**, 146–149 (1869).
31. Parkinson, D. R. *et al.* Considerations in the development of circulating tumor cell technology for clinical use. *J. Transl. Med.* **10**, 138 (2012).
32. Ni, J. *et al.* Role of the EpCAM (CD326) in prostate cancer metastasis and progression. *Cancer Metastasis Rev.* **31**, 779–791 (2012).
33. Gorges, T. M. *et al.* Circulating tumour cells escape from EpCAM-based detection due to epithelial-to-mesenchymal transition. *BMC Cancer* **12**, 178 (2012).
34. Yu, M. *et al.* Circulating breast tumor cells exhibit dynamic changes in epithelial and mesenchymal composition. *Science* **339**, 580–584 (2013).
35. Bitting, R. L. *et al.* Development of a method to isolate circulating tumor cells using mesenchymal-based capture. *Methods* **64**, 129–136 (2013).
36. Ozkumur, E. *et al.* Inertial focusing for tumor antigen-dependent and -independent sorting of rare circulating tumor cells. *Sci. Transl. Med.* **5**, 179ra47 (2013).
37. Veridex, LLC CellSearch™ Circulating Tumor Cell Kit. *Premarket notification—expanded indications for use—metastatic prostate cancer* [online], http://www.accessdata.fda.gov/cdrh_docs/pdf7/K073338.pdf (2008).
38. Danila, D. C. *et al.* Circulating tumor cell number and prognosis in progressive castration-resistant prostate cancer. *Clin. Cancer Res.* **13**, 7053–7058 (2007).
39. de Bono, J. S. *et al.* Circulating tumor cells predict survival benefit from treatment in metastatic castration-resistant prostate cancer. *Clin. Cancer Res.* **14**, 6302–6309 (2008).
40. Scher, H. I. *et al.* Circulating tumour cells as prognostic markers in progressive, castration-resistant prostate cancer: a reanalysis of IMMC38 trial data. *Lancet Oncol.* **10**, 233–239 (2009).
41. Goodman, O. B. Jr *et al.* Circulating tumor cells in patients with castration-resistant prostate cancer baseline values and correlation with prognostic factors. *Cancer Epidemiol. Biomarkers Prev.* **18**, 1904–1913 (2009).
42. Gasch, C. *et al.* Heterogeneity of epidermal growth factor receptor status and mutations of *KRAS*/*PIK3CA* in circulating tumor cells of patients with colorectal cancer. *Clin. Chem.* **59**, 252–260 (2013).
43. Kraan, J. *et al.* External quality assurance of circulating tumor cell enumeration using the CellSearch® system: a feasibility study. *Cytometry B Clin. Cytom.* **80**, 112–118 (2011).
44. Ligthart, S. T. *et al.* Unbiased and automated identification of a circulating tumour cell definition that associates with overall survival. *PLoS ONE* **6**, e27419 (2011).
45. Ligthart, S. T. *et al.* Circulating tumor cells count and morphological features in breast, colorectal and prostate cancer. *PLoS ONE* **8**, e67148 (2013).
46. Todenhofer, T. *et al.* Preliminary experience on the use of the Adnatest® system for detection of circulating tumor cells in prostate cancer patients. *Anticancer Res.* **32**, 3507–3513 (2012).
47. Talasaz, A. H. *et al.* Isolating highly enriched populations of circulating epithelial cells and other rare cells from blood using a magnetic sweeper device. *Proc. Natl Acad. Sci. USA* **106**, 3970–3975 (2009).
48. Cann, G. M. *et al.* mRNA-Seq of single prostate cancer circulating tumor cells reveals recapitulation of gene expression and pathways found in prostate cancer. *PLoS ONE* **7**, e49144 (2012).
49. Powell, A. A. *et al.* Single cell profiling of circulating tumor cells: transcriptional heterogeneity and diversity from breast cancer cell lines. *PLoS ONE* **7**, e33788 (2012).
50. Casavant, B. P. *et al.* The VerIFAST: an integrated method for cell isolation and extracellular/intracellular staining. *Lab Chip* **13**, 391–396 (2013).
51. Nagrath, S. *et al.* Isolation of rare circulating tumour cells in cancer patients by microchip technology. *Nature* **450**, 1235–1239 (2007).
52. Stott, S. L. *et al.* Isolation of circulating tumor cells using a microvortex-generating herringbone-chip. *Proc. Natl Acad. Sci. USA* **107**, 18392–18397 (2010).
53. Lu, Y. T. *et al.* NanoVelcro Chip for CTC enumeration in prostate cancer patients. *Methods* **64**, 144–152 (2013).
54. Kirby, B. J. *et al.* Functional characterization of circulating tumor cells with a prostate-cancer-specific microfluidic device. *PLoS ONE* **7**, e35976 (2012).
55. Casavant, B. P. *et al.* A negative selection methodology using a microfluidic platform for the isolation and enumeration of circulating tumor cells. *Methods* **64**, 137–143 (2013).
56. Alix-Panabieres, C. *et al.* Detection of circulating prostate-specific antigen-secreting cells in prostate cancer patients. *Clin. Chem.* **51**, 1538–1541 (2005).
57. Paris, P. L. *et al.* Functional phenotyping and genotyping of circulating tumor cells from patients with castration resistant prostate cancer. *Cancer Lett.* **277**, 164–173 (2009).
58. Friedlander, T. W. *et al.* Detection and characterization of invasive circulating tumor cells derived from men with metastatic castration-resistant prostate cancer. *Int. J. Cancer* **134**, 2284–2293 (2014).
59. Gascoyne, P. R., Noshari, J., Anderson, T. J. & Becker, F. F. Isolation of rare cells from cell mixtures by dielectrophoresis. *Electrophoresis* **30**, 1388–1398 (2009).
60. Gupta, V. *et al.* ApoStream™, a new dielectrophoretic device for antibody independent isolation and recovery of viable cancer cells from blood. *Biomicrofluidics* **6**, 24133 (2012).
61. Vona, G. *et al.* Isolation by size of epithelial tumor cells: a new method for the immunomorphological and molecular characterization of circulating tumor cells. *Am. J. Pathol.* **156**, 57–63 (2000).
62. Xu, T., Lu, B., Tai, Y. C. & Goldkorn, A. A cancer detection platform which measures telomerase activity from live circulating tumor cells captured on a microfilter. *Cancer Res.* **70**, 6420–6426 (2010).
63. Lin, H. K. *et al.* Portable filter-based microdevice for detection and characterization of circulating tumor cells. *Clin. Cancer Res.* **16**, 5011–5018 (2010).
64. Chen, C. L. *et al.* Single-cell analysis of circulating tumor cells identifies cumulative expression patterns of EMT-related genes in metastatic prostate cancer. *Prostate* **73**, 813–826 (2013).
65. Coumans, F. A., van Dalum, G., Beck, M. & Terstappen, L. W. Filter characteristics influencing circulating tumor cell enrichment from whole blood. *PLoS ONE* **8**, e61770 (2013).
66. Lazar, D. C. *et al.* Cytometric comparisons between circulating tumor cells from prostate cancer patients and the prostate-tumor-derived LNCaP cell line. *Phys. Biol.* **9**, 016002 (2012).
67. Farace, F. *et al.* A direct comparison of CellSearch and ISET for circulating tumour-cell detection in patients with metastatic carcinomas. *Br. J. Cancer* **105**, 847–853 (2011).
68. Huang, C., Liu, H., Bander, N. H. & Kirby, B. J. Enrichment of prostate cancer cells from blood cells with a hybrid dielectrophoresis and immunocapture microfluidic system. *Biomed. Microdevices* **15**, 941–948 (2013).
69. Danila, D. C. *et al.* Analytic and clinical validation of a prostate cancer-enhanced messenger RNA detection assay in whole blood as a prognostic biomarker for survival. *Eur. Urol.* **65**, 1191–1197 (2014).
70. Cho, E. H. *et al.* Characterization of circulating tumor cell aggregates identified in patients with epithelial tumors. *Phys. Biol.* **9**, 016001 (2012).
71. Marrinucci, D. *et al.* Fluid biopsy in patients with metastatic prostate, pancreatic and breast cancers. *Phys. Biol.* **9**, 016003 (2012).
72. Pachmann, K. *et al.* Standardized quantification of circulating peripheral tumor cells from lung and breast cancer. *Clin. Chem. Lab. Med.* **43**, 617–627 (2005).
73. Saucedo-Zeni, N. *et al.* A novel method for the *in vivo* isolation of circulating tumor cells from peripheral blood of cancer patients using a functionalized and structured medical wire. *Int. J. Oncol.* **41**, 1241–1250 (2012).
74. Stott, S. L. *et al.* Isolation and characterization of circulating tumor cells from patients with localized and metastatic prostate cancer. *Sci. Transl. Med.* **2**, 25ra23 (2010).
75. Allard, W. J. *et al.* Tumor cells circulate in the peripheral blood of all major carcinomas but not in healthy subjects or patients with nonmalignant diseases. *Clin. Cancer Res.* **10**, 6897–6904 (2004).
76. Cristofanilli, M. *et al.* Circulating tumor cells, disease progression, and survival in metastatic breast cancer. *N. Engl. J. Med.* **351**, 781–791 (2004).
77. Scher, H. I. *et al.* Evaluation of circulating tumor cell (CTC) enumeration as an efficacy response biomarker of overall survival (OS) in metastatic castration-resistant prostate cancer (mCRPC): planned final analysis (FA) of COU-AA-301, a randomized, double-blind, placebo-controlled, phase III study of abiraterone acetate (AA) plus low-dose prednisone (P) post docetaxel [abstract]. *J. Clin. Oncol.* **29** (Suppl.), LBA4517 (2011).
78. Attard, G. *et al.* Characterization of *ERG*, *AR* and *PTEN* gene status in circulating tumor cells from patients with castration-resistant prostate cancer. *Cancer Res.* **69**, 2912–2918 (2009).

79. Danila, D. C. *et al. TMPRSS2–ERG* status in circulating tumor cells as a predictive biomarker of sensitivity in castration-resistant prostate cancer patients treated with abiraterone acetate. *Eur. Urol.* **60**, 897–904 (2011).
80. Leversha, M. A. *et al.* Fluorescence *in situ* hybridization analysis of circulating tumor cells in metastatic prostate cancer. *Clin. Cancer Res.* **15**, 2091–2097 (2009).
81. Jiang, Y., Palma, J. F., Agus, D. B., Wang, Y. & Gross, M. E. Detection of androgen receptor mutations in circulating tumor cells in castration-resistant prostate cancer. *Clin. Chem.* **56**, 1492–1495 (2010).
82. Magbanua, M. J. *et al.* Isolation and genomic analysis of circulating tumor cells from castration resistant metastatic prostate cancer. *BMC Cancer* **12**, 78 (2012).
83. Darshan, M. S. *et al.* Taxane-induced blockade to nuclear accumulation of the androgen receptor predicts clinical responses in metastatic prostate cancer. *Cancer Res.* **71**, 6019–6029 (2011).
84. Scher, H. I. & Sawyers, C. L. Biology of progressive, castration-resistant prostate cancer: directed therapies targeting the androgen-receptor signaling axis. *J. Clin. Oncol.* **23**, 8253–8261 (2005).
85. Brown, R. S. *et al.* Amplification of the androgen receptor gene in bone metastases from hormone-refractory prostate cancer. *J. Pathol.* **198**, 237–244 (2002).
86. Miyamoto, D. T. *et al.* Androgen receptor signaling in circulating tumor cells as a marker of hormonally responsive prostate cancer. *Cancer Discov.* **2**, 995–1003 (2012).
87. Evans, M. J. *et al.* Noninvasive measurement of androgen receptor signaling with a positron-emitting radiopharmaceutical that targets prostate-specific membrane antigen. *Proc. Natl Acad. Sci. USA* **108**, 9578–9582 (2011).
88. Noss, K. R., Wolfe, S. A. & Grimes, S. R. Upregulation of prostate specific membrane antigen/folate hydrolase transcription by an enhancer. *Gene* **285**, 247–256 (2002).
89. Wright, G. L. Jr *et al.* Upregulation of prostate-specific membrane antigen after androgen-deprivation therapy. *Urology* **48**, 326–334 (1996).

Acknowledgements
The authors thank S. Maheswaran and D. Haber for reading the manuscript and for helpful discussions before submission. The authors acknowledge research support from the Department of Defence Prostate Cancer Research Program (award W81XWH-09-1-0471 to R.J.L.; award W81XWH-12-1-0153 to D.T.M.), the Conquer Cancer Foundation (Career Development Award to R.J.L.), the Prostate Cancer Foundation (Young Investigator Award to R.J.L.), the Mazzone Program/Dana-Farber Harvard Cancer Center (Career Development Award to D.T.M.), and Stand Up To Cancer (L.V.S.).

Author contributions
All authors made substantial contributions to all stages of the preparation of the manuscript for submission.

Article

Cell Reports

Single-Cell RNA Sequencing Identifies Extracellular Matrix Gene Expression by Pancreatic Circulating Tumor Cells

Graphical Abstract

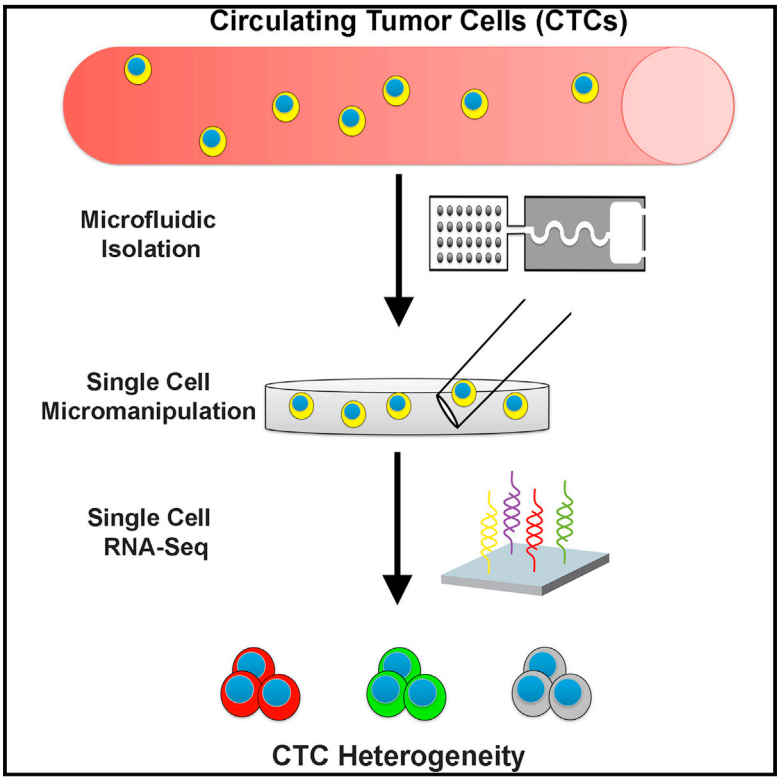

Highlights

Pancreatic CTCs can be enriched with antigen-agnostic microfluidic technology

Single-cell RNA sequencing of pancreatic CTCs reveals three distinct CTC populations

Extracellular matrix genes are highly expressed in mouse and human CTCs

The extracellular matrix protein SPARC contributes to pancreatic tumor metastasis

Authors

David T. Ting, Ben S. Wittner, ..., Shyamala Maheswaran, Daniel A. Haber

Correspondence

maheswaran@helix.mgh.harvard.edu (S.M.),
haber@helix.mgh.harvard.edu (D.A.H.)

In Brief

Circulating tumor cells (CTCs) are enriched for the precursors of metastasis, but their composition has not been fully defined. Ting et al. have utilized a microfluidic device to perform single-cell RNA sequencing of pancreatic CTCs, identifying three distinct populations that suggest multiple paths in the metastatic cascade. Extracellular matrix gene expression in particular was highly enriched in CTCs, pointing to a contribution to distal spread of cancer.

Accession Numbers

GSE51372
GSE60407
GSE51827

Ting et al., 2014, Cell Reports 8, 1905–1918
September 25, 2014 ©2014 The Authors
http://dx.doi.org/10.1016/j.celrep.2014.08.029

Cell Reports
Article

Single-Cell RNA Sequencing Identifies Extracellular Matrix Gene Expression by Pancreatic Circulating Tumor Cells

David T. Ting,[1,3] Ben S. Wittner,[1,3] Matteo Ligorio,[1,4,7] Nicole Vincent Jordan,[1,3] Ajay M. Shah,[2,4] David T. Miyamoto,[1,5] Nicola Aceto,[1,3] Francesca Bersani,[1,3] Brian W. Brannigan,[1,3] Kristina Xega,[1,3] Jordan C. Ciciliano,[1,3] Huili Zhu,[1,3] Olivia C. MacKenzie,[1,3] Julie Trautwein,[1,3] Kshitij S. Arora,[1,4,6] Mohammad Shahid,[1,4,6] Haley L. Ellis,[1,3] Na Qu,[1,3] Nabeel Bardeesy,[1,3] Miguel N. Rivera,[1,6] Vikram Deshpande,[1,6] Cristina R. Ferrone,[1,4] Ravi Kapur,[2] Sridhar Ramaswamy,[1,3] Toshi Shioda,[1,3] Mehmet Toner,[2,4] Shyamala Maheswaran,[1,4,*] and Daniel A. Haber[1,3,8,*]
[1]Massachusetts General Hospital Cancer Center, Harvard Medical School, Boston, MA 02114, USA
[2]Center for Engineering in Medicine, Harvard Medical School, Boston, MA 02114, USA
[3]Department of Medicine, Harvard Medical School, Boston, MA 02114, USA
[4]Department of Surgery, Harvard Medical School, Boston, MA 02114, USA
[5]Department of Radiation Oncology, Harvard Medical School, Boston, MA 02114, USA
[6]Department of Pathology, Harvard Medical School, Boston, MA 02114, USA
[7]Department of Health Sciences, University of Genoa, 16126 Genoa, Italy
[8]Howard Hughes Medical Institute, Chevy Chase, MD 20815, USA
*Correspondence: maheswaran@helix.mgh.harvard.edu (S.M.), haber@helix.mgh.harvard.edu (D.A.H.)
http://dx.doi.org/10.1016/j.celrep.2014.08.029

SUMMARY

Circulating tumor cells (CTCs) are shed from primary tumors into the bloodstream, mediating the hematogenous spread of cancer to distant organs. To define their composition, we compared genome-wide expression profiles of CTCs with matched primary tumors in a mouse model of pancreatic cancer, isolating individual CTCs using epitope-independent microfluidic capture, followed by single-cell RNA sequencing. CTCs clustered separately from primary tumors and tumor-derived cell lines, showing low-proliferative signatures, enrichment for the stem-cell-associated gene *Aldh1a2*, biphenotypic expression of epithelial and mesenchymal markers, and expression of *Igfbp5*, a gene transcript enriched at the epithelial-stromal interface. Mouse as well as human pancreatic CTCs exhibit a very high expression of stromal-derived extracellular matrix (ECM) proteins, including *SPARC*, whose knockdown in cancer cells suppresses cell migration and invasiveness. The aberrant expression by CTCs of stromal ECM genes points to their contribution of microenvironmental signals for the spread of cancer to distant organs.

INTRODUCTION

Pancreatic ductal adenocarcinoma (PDAC) is a highly lethal cancer, which stems from the rapid dissemination of tumor cells leading to widespread metastasis. While local tissue and lymphatic invasion are evident even in early PDAC, the presence of circulating tumor cells (CTCs) in the bloodstream ultimately leads to spread of cancer to distant organs. CTCs are rare, estimated at one to ten tumor cells among ten billion normal blood cells in a milliliter of blood. As such, their isolation and molecular analysis has posed a significant technological challenge (Pantel et al., 2008; Yu et al., 2011). Given their role in blood-borne metastasis, CTC populations are likely to be enriched for metastatic precursors, and their analysis may identify potential therapeutic targets as well as provide opportunities for early detection of pancreatic cancer.

Genetically engineered mouse pancreatic cancer models have provided important insight into the progression of this disease. Specifically, the genetically engineered *LSL-Kras*^{G12D}, *Trp53*$^{flox/flox\ or\ +}$, *Pdx1-Cre* (KPC) mouse model recapitulates the histological progression from preneoplastic pancreatic intraepithelial neoplasia to invasive carcinoma (Bardeesy et al., 2006). Recent studies have suggested that epithelial-to-mesenchymal transition (EMT) occurs early in this model, potentially enhancing tumor invasiveness (Rhim et al., 2012). In an initial molecular characterization of mouse pancreatic CTCs, we undertook RNA sequencing (RNA-seq) of CTC-enriched populations, identifying activation of noncanonical WNT signaling as a recurrent event, potentially contributing to the anoikis resistance of circulating epithelial cells (Yu et al., 2012). In that study, analysis of pooled CTCs, enriched from the blood but still contaminated with leukocytes, was accomplished using single-molecule RNA sequencing, combined with digital subtraction of matched leukocyte RNA reads, so as to derive a CTC-specific expression signature. However, transcriptome analysis of such partially purified cell populations is limited by depth of coverage to the most highly differentially expressed genes, and such studies of bulk CTC populations cannot resolve the degree of heterogeneity across these poorly understood cell populations.

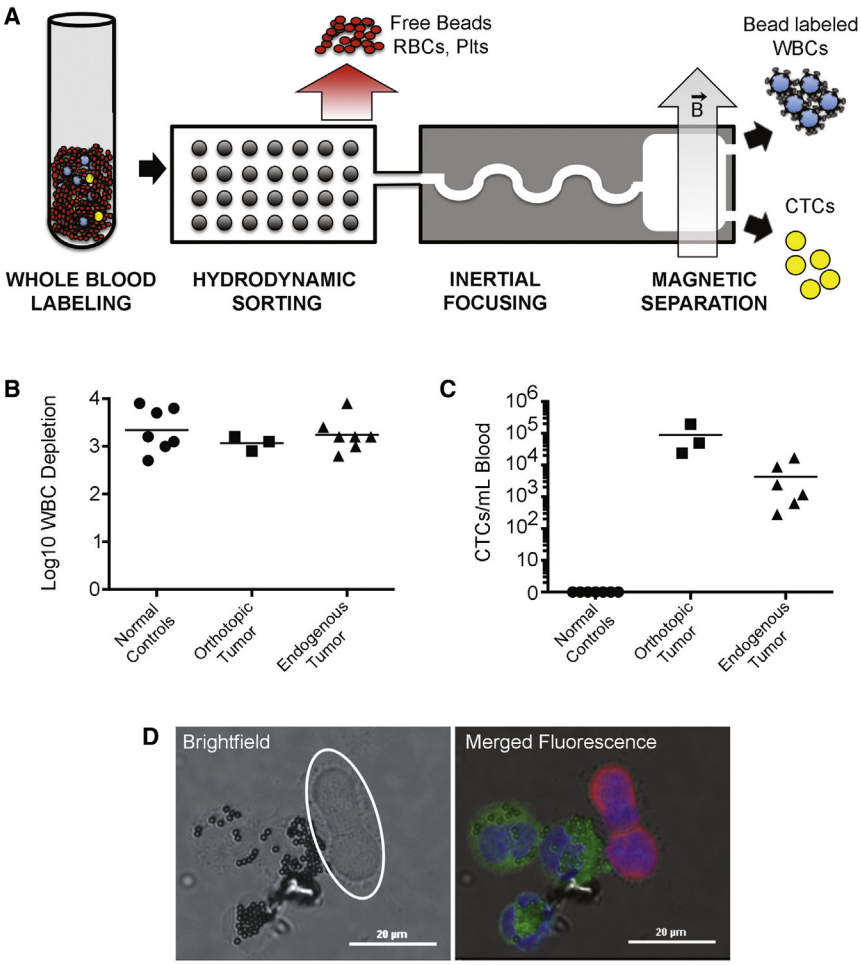

Figure 1. CTC Single-Cell Isolation

(A) Schematic of the CTC-iChip-negative inertial focusing device system.

(B) Mouse WBC depletion consistency between normal and cancer mouse models. WBC depletion is shown in log10.

(C) CTC enumeration by immunofluorescent staining (CK+/CD45-/DAPI+) from normal and cancer mice. Bar represents mean.

(D) Representative image of CK-positive CTCs. DAPI (blue), CK (red), and CD45 (green). Scale bar, 20 μm. Bright-field image highlighting lack of immunomagnetic anti-CD45 beads on CK+ CTCs (white circle).

To achieve deep RNA-sequencing profiles of CTCs at the single-cell level, we applied an inertial focusing-enhanced microfluidic device, the CTC-iChip, which allows high-efficiency negative depletion of normal blood cells, leaving CTCs in solution where they can be individually selected and analyzed as single cells (Ozkumur et al., 2013). This antigen-agnostic isolation of CTCs enables the characterization of CTCs with both epithelial and mesenchymal characteristics. Further, the high quality of RNA purified from viable, untagged CTCs is particularly well suited for detailed transcriptome analysis. We applied the CTC-iChip to the pancreatic cancer mouse model that allows for simultaneous analysis of primary tumor and CTCs, with the shared driver mutations across different animals facilitating the identification of CTC-specific heterogeneity. Here, we present a comprehensive transcriptome analysis of CTCs at the single-cell level, pointing to distinct cell subsets within CTC populations. Notably, we have identified the unexpected abundant expression of extracellular matrix (ECM) genes in mouse pancreatic CTCs and across human CTCs of pancreatic, breast, and prostate origin. Consistent with the importance of tumor stroma-derived ECM signaling in targeting cancer cell metastasis (Zhang et al., 2013), the cell-autonomous expression of ECM genes by CTCs may contribute to the dissemination of cancer to distal organs.

RESULTS

Isolation of Mouse Pancreatic CTCs

The CTC-iChip combines initial hydrodynamic size-based separation of all nucleated cells (leukocytes [WBCs] and CTCs) away from red blood cells, platelets, and plasma, with subsequent inertial focusing of the nucleated cells into a single streamline to achieve high-efficiency in-line magnetic sorting. While tumor epitopes are highly variable, WBC cell-surface markers are well established; applying magnetic-conjugated anti-WBC to this very high-throughput microfluidic cell-separation device can thus exclude the vast majority of WBCs to reveal a small number of untagged CTCs (Figure 1A). Whole-blood labeling using 100 anti-CD45 beads per WBC achieved >10^3 depletion in normal mice, mice bearing orthotopic tumors, and the KPC mice (Figure 1B).

We first tested the efficacy of the CTC-iChip using a GFP-tagged mouse PDAC cell line (NB508). CTC recovery through the CTC-iChip was measured to be 95% (mean ± 3% SD), using GFP-tagged NB508 cells spiked into whole mouse blood. Applying the CTC-iChip to orthotopic tumors derived from pancreatic inoculation of GFP-tagged NB508 cells generated >1,000 CTCs/ml in all three mice tested (Figure 1C). Finally, CTC analysis of blood specimens from KPC mice bearing endogenous tumors, using dual immunofluorescent staining of cells with the epithelial marker pan-cytokeratin (CK) and the leukocyte marker CD45, revealed a median 118 CTCs/ml (mean 429 CTCs/ml; range, 0–1,694) (Figures 1C and 1D). No CK-positive cells were detected in seven healthy control mice. The majority of CD45-positive cells that remained in the product after blood processing through the microfluidic device retained immunomagnetic beads on their surface. Thus, the untagged cells constituting CTCs were readily distinguished from WBCs in the final CTC-iChip product (Figure 1D),

enabling single-cell manipulation without additional surface epitope staining.

Single-CTC RNA-Seq

Five tumor-bearing KPC mice generated a total of 168 single CTCs (Figure S1) that were subjected to a modified single-cell amplification and library protocol (Tang et al., 2010), followed by a screen for RNA quality (*Gapdh*, *Actb*). Of these, 75 (45%) were of sufficient quality to proceed to further amplification and library construction for next-generation sequencing. It is noteworthy that a majority of candidate CTCs (55%) appeared morphologically intact but had degraded RNA. These cells likely represent tumor cells that have lost viability in the bloodstream. Given the rapid processing of blood samples from mouse models, the minimal shear condition in the microfluidic device, and the preserved RNA quality of control cells processed identically, it is unlikely that cells underwent such damage during in vitro purification. For comparison, single-cell RNA-seq was also performed on 12 WBCs from a control mouse, 12 mouse embryonic fibroblasts (MEFs), and 16 single cells from the mouse NB508 pancreatic cancer cell line. Over 90% of single cells from NB508 and MEF cultures met criteria for sequencing quality, highlighting the high frequency of CTCs with compromised RNA templates under the same conditions. To compare CTC profiles to that of matched parental tumors harvested at the time of CTC isolation, bulk RNA from each primary tumor was diluted to 1 or 10 cell equivalents (10 or 100 pg RNA) and subjected to the same amplification and RNA-seq protocol (n = 34; minimum of eight replicates from four matched tumors).

Single-cell RNA-seq performance was comparable for all samples analyzed, with a mean 4.4–8.5 million reads, of which a mean 46%–61% uniquely aligned to the mouse genome (Figure S1). Genome-aligned reads were annotated and counted using UCSC Known Gene transcriptome reference and normalized in reads per million (rpm). Normalized reads were then analyzed by unsupervised hierarchical clustering (Figure 2A). Single-cell transcriptomes from MEFs, the NB508 pancreatic cancer cell line, and normal WBCs clustered tightly, supporting the analytic reliability of the RNA-seq strategy. Three distinct clustering patterns of candidate CTCs were identified, all of which were distinct from matched primary tumor sequences and cancer cell lines. Principal component analysis shows the clustering and interrelationships of these different groups (Figure 2B).

The uniform genetic drivers in the KPC mouse model made it possible to quantify the degree of cellular heterogeneity in CTCs derived from individual mice and across different mice. Single-cell heterogeneity within each CTC cluster was assessed by intracluster correlation coefficients, where lower correlation coefficients reflect higher heterogeneity (Figure S1). As expected, CTC clusters showed considerably more heterogeneity (mean 0.42, 95% confidence interval [CI] 0.36–0.47) than single cells derived from the NB508 cancer cell line (mean 0.86, 95% CI 0.80-0.91, p value 1.2×10^{-15}). To assess heterogeneity of cells within a primary PDAC, a conditional Tomato/enhanced EGFP (EGFP) (mT/mG) expression marker (Muzumdar et al., 2007) was crossed with the KPC mouse to generate a lineage-tagged mouse tumor (KPC-mT/mG) and was used to isolate individual EGFP-positive primary tumor cells away from contaminating stromal cells. A primary tumor (TuGMP3) was disaggregated into single-cell suspension, and 20 EGFP-positive cells were subjected to RNA-seq. The single primary tumor cells clustered with the previously analyzed bulk tumor material (Figure S2), with a heterogeneity score (mean 0.38, 95% CI 0.28–0.47) similar to that of CTCs (p value 0.49).

In summary, we achieved single-cell RNA-seq of mouse pancreatic CTCs isolated without positive selection bias, along with parental tumors, an established genotype-matched cancer cell line, MEFs, and WBCs. CTCs clustered separately from the primary tumor (both bulk tumor and isolated single cells) and from the tumor-derived cell line, with comparable degrees of intercellular heterogeneity between CTCs and primary tumor cells.

Defining Subsets of Pancreatic CTCs

To identify and classify candidate CTCs, we initially applied gene sets for known epithelial, hematopoietic, and endothelial markers across all clustered samples. As expected, epithelial markers (*Krt7*, *Krt8*, *Krt18*, *Krt19*, *Epcam*, *Egfr*, *Cdh1*) were highly expressed in primary pancreatic tumors and in the cancer cell line NB508 and nearly absent in the nonepithelial MEFs and in normal WBCs (Figure S3). In contrast, hematopoietic markers (*Ptprc/Cd45*, *Csf3r/Cd114*, *Cd14*, *Fcgr3/Cd16*, *Itga2b/Cd41*, *Itgb3/Cd61*) were present in normal WBCs and absent in NB508 and MEFs. Some expression of hematopoietic markers was detectable in the bulk primary tumor samples, consistent with varying degrees of leukocytic infiltrates. No specific cluster of endothelial cells was identified, based on expression of characteristic markers (*Cdh5/Cd144*, *Vwf*, *Thbd/Cd141*, *Pecam1/Cd31*, *Mcam/Cd146*, *Sele/E-selectin*, *Cd34*) and absence of epithelial and hematopoietic markers.

Interrogation of single cells isolated by CD45 depletion from tumor-bearing mice, using the epithelial, hematopoietic, and endothelial markers, revealed notable differences among the three major candidate CTC groupings (clusters 1, 3, and 7; Figures 3A and S3). Cluster 3 showed strong expression of epithelial markers, consistent with a ''classical'' CTC phenotype (denoted CTC-c). A subset of these cells expressed *Cd34*, an endothelial progenitor marker that is also found in mesenchymal cells including MEFs (Figures 3A and S3) and stromal cells (Krause et al., 1994), but other characteristic endothelial lineage markers were absent. Clusters 1 and 7 were more complex, with the former noteworthy for enrichment of platelet markers CD41 (*Itga2b*) and CD61 (*Itgb3*) (hence denoted CTC-plt) and the latter having a prominent cellular proliferation signature (CTC-pro).

To better define the characteristics of each candidate CTC cluster, we used a nonparametric differential gene expression analysis including a rank product (RP) methodology adapted to variations in absolute transcript levels and differences in transcriptome representation from cell to cell (Breitling et al., 2004). Setting highly stringent parameters (false discovery rate ≤ 0.01), the control comparison of primary tumors versus WBCs identified 927 genes relatively overexpressed in tumors and 293 genes high in WBCs, including the expected differential expression of epithelial tumor markers keratin 7, 8, 18, and 19, versus the leukocyte-specific CD45 (Table S1). Comparing the classical

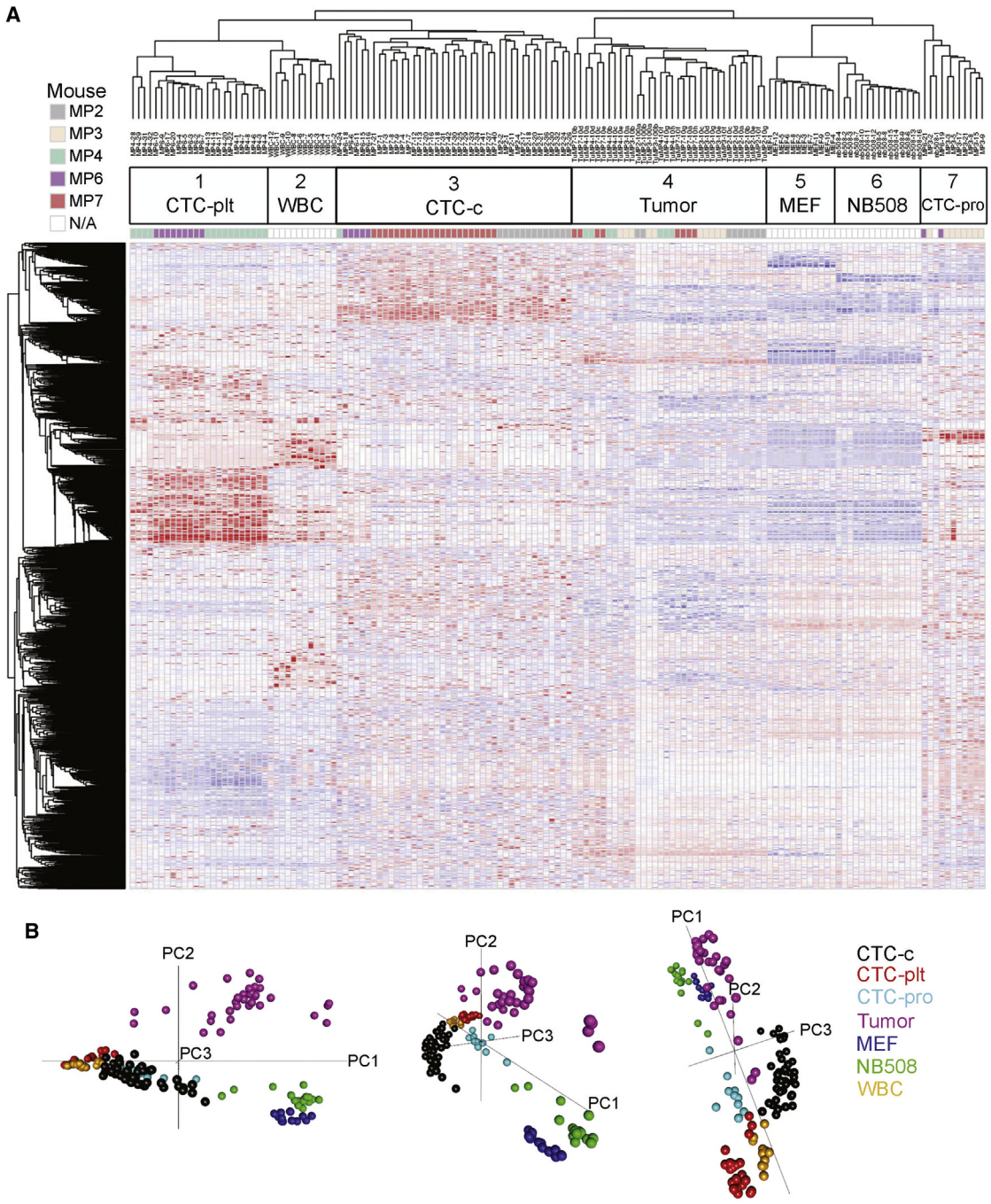

Figure 2. Single-Cell RNA-Seq Global Analysis

(A) Unsupervised hierarchical clustering of candidate single CTCs (1, 3, and 7), single WBCs (2), single MEFs (5), single NB508 cancer cell line (6), and bulk primary tumors diluted to 10 or 100 pg of RNA (4). CTC-c, classical CTCs; CTC-plt, platelet-adhered CTCs; CTC-pro, proliferative CTCs. Data shown log transformed and median polished.

(B) Principal component analysis of single-cell samples.

CTC cluster to WBCs also showed enrichment for cytokeratin 18 and 19 in CTC-c versus CD45 in WBCs, validating the RP methodology to identify relevant differentially expressed genes between single-cell populations.

The most abundant CTC cluster, CTC-c, comprised 41 of 75 cells (55%) meeting established criteria for epithelial tumor cells (versus CTC-plt: 32%; CTC-pro: 13%). Compared with matched primary tumors, CTCs had 878 transcripts increased in

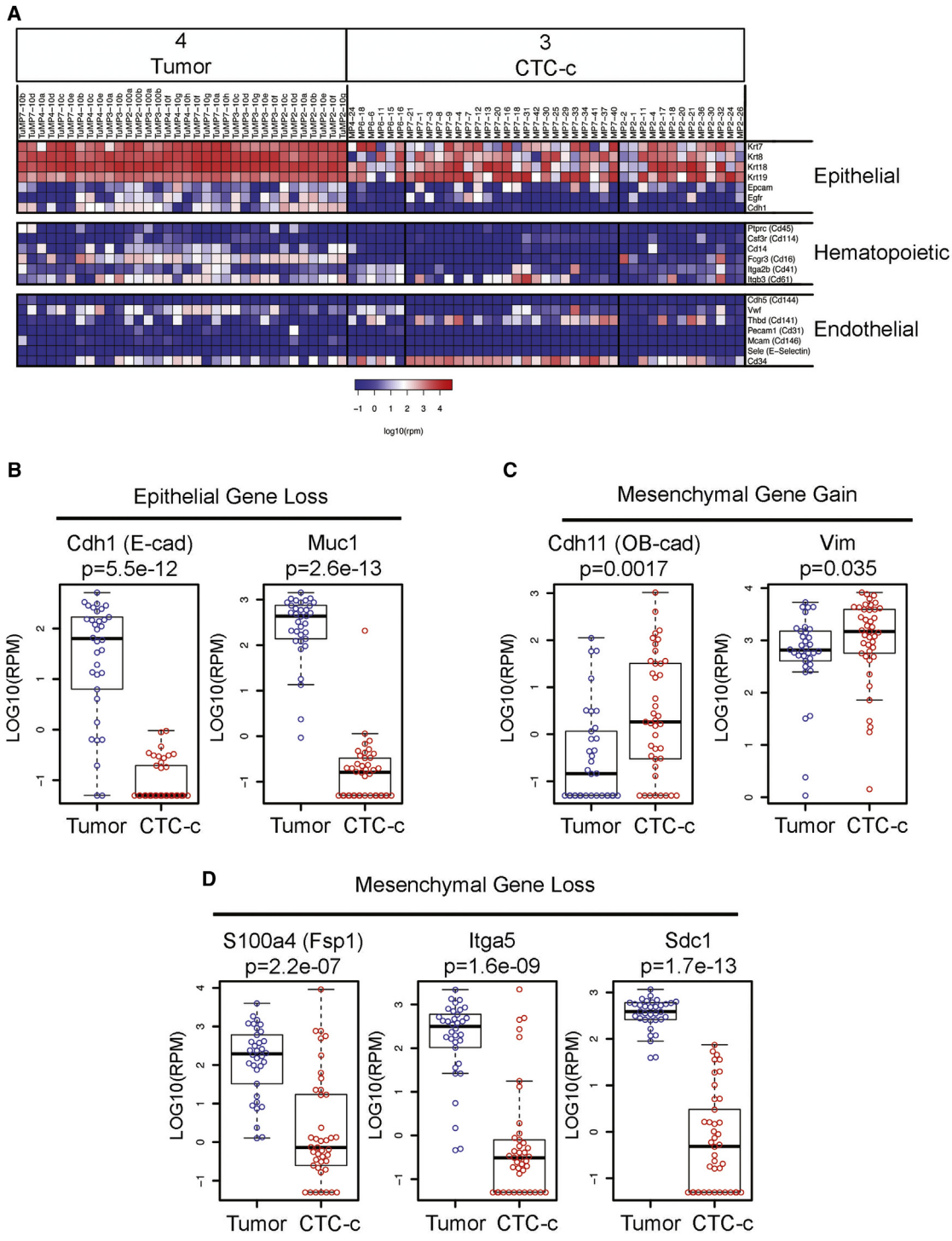

Figure 3. Targeted Analysis of Single-Cell RNA-Seq Data

(A) Expression heatmap of epithelial, hematopoietic, and endothelial markers in primary tumors and classical epithelial CTCs (CTC-c). Scale in log10(rpm).

(B–D) Epithelial and mesenchymal genes differentially expressed in CTCs versus tumors.

Boxplot of epithelial genes that are (B) downregulated or mesenchymal genes that are (C) upregulated or (D) downregulated in CTCs (red) versus tumors (blue). Bar represents median, and boxplot represents quartiles; scale in log10(rpm).

expression and 774 genes with reduced expression (Table S1). Gene Ontology (GO) analysis of CTC-enriched genes (Table S2) indicated enrichment for signatures associated with cellular interactions with environmental signals (GO:0045785, positive regulation of cell adhesion), cell shape and structure (GO:0030036, actin cytoskeleton organization), and transcriptional states (GO:0045449, regulation of transcription). Kyoto Encyclopedia of Genes and Genomes (KEGG) pathway analysis (Table S3) similarly showed enrichment for focal adhesion (odds ratio [OR] 2.7, q-value 6.7×10^{-4}) and regulation of actin cytoskeleton (OR 2.4, q-value 0.005). Notably, of the KEGG signaling pathways annotated, the mitogen-activated protein kinase (MAPK) pathway was most highly enriched (OR 2.2, q-value 0.006); MAPK signaling is already activated in the $Kras^{G12D}$-driven primary tumor. However, while MSigDB Kras dependency signatures were enriched in primary tumors compared with CTCs, the latter had increased expression of *Braf*, *Mras*, and *Rras2*, pointing to alternative paths to further activate MAPK in CTCs. This finding is consistent with another study that identified the MAPK pathway as being the most highly enriched in pancreatic CTCs with microarray-based methodologies (Carvalho et al., 2013).

While single cells within the CTC cluster exhibited the characteristic features of tumor cells, defining the identity of the nonclassical CTC clusters, CTC-plt and CTC-pro, required additional analyses. Compared with CTC-c, single cells within the CTC-plt cluster were highly enriched for wound healing as well as platelet and megakaryocyte expression profiles (Table S4). While this suggests that these cells are either circulating megakaryocytes/giant platelets or CTCs covered with adherent platelets, tumor cell-specific lineage tagging supports the identification of CTC-plt cells as being of tumor origin. Eighteen EGFP lineage-tagged single CTCs from two KPC-mT/mG mice were subjected to single-cell RNA-seq: a total of nine CTCs from the two mice (seven out of seven CTCs from GMP1 and 2 out of 11 from GMP2) were included within CTC-plt using unsupervised hierarchical clustering (Figure S2). Thus, the CTC-plt cluster includes CTCs that exhibit strong platelet markers, most likely derived from transcripts encoded by adherent platelets. Interestingly, CTC-plt cells maintained their distinct segregation from CTC-c, even after digital removal of all annotated platelet transcripts (Figure S4). Thus, the adherence of abundant platelets may modulate the intrinsic CTC expression profile, as recently suggested by in vitro modeling experiments (Labelle et al., 2011).

The CTC-pro cluster was most similar to both the NB508 pancreatic cancer cell line and MEFs, and it was enriched for the cellular proliferation marker *Mki67* when compared to CTC-c. Multiple lineages are likely to have contributed to this complex grouping; nine CTCs from the two KPC-mT/mG mice described above clustered with CTC-pro (Figure S2), characterized by abundant expression of *Mki67* and an annotated cell-cycle signature (Whitfield et al., 2002) (Figure S5). One single cell within the CTC-pro cluster was derived from the pancreatic cancer cell line NB508, while another (MP3-2) had high keratin/high E-cadherin expression characteristic of classical CTCs (Figure S3). Another subcluster contained immune and dendritic cells, identified by their expression of antigen processing and presentation genes (Table S5). Taken together, the CTC-pro cluster appears to represent a grouping of highly proliferative cells, of which a subset is tumor-derived CTCs.

Together, unbiased isolation and RNA-seq evaluation of single pancreatic CTCs indicate that over half of these are nonviable with RNA at various stages of degradation. Among the remaining viable CTCs, three major classes are distinguishable by unsupervised clustering: the classical subset (CTC-c) accounts for 55%, with a second platelet-adherent group (CTC-plt; 32%) and a third heterogeneous cluster marked by proliferative signatures (CTC-pro; 13%). Given their most clearly defined tumor-derived characteristics, we selected the CTC-c cluster for detailed analysis of metastasis-associated pathways.

Pancreatic CTCs Coexpress Epithelial, Mesenchymal, and Stem Cell Markers

The relevance of EMT to early metastasis in pancreatic cancer has been supported by lineage tracing studies in the KPC mouse (Rhim et al., 2012). We recently reported a distribution of epithelial and mesenchymal markers within individual CTCs in human breast cancer, reflecting both tumor histology and response or resistance to diverse therapies (Yu et al., 2013). To directly test for EMT in the mouse pancreatic classical CTCs, we used established epithelial (E) and mesenchymal (M) markers (Kalluri and Weinberg, 2009) to evaluate each cell within the CTC cluster (Figure S6). Compared with the primary tumor, CTC-c cells demonstrated clear loss of the epithelial markers E-cadherin (*Cdh1*) and *Muc1* (Figure 3B), whereas mesenchymal transcripts were mixed, with some showing increased expression (*Cdh11*, *Vim*) and others with reduced levels (*S100a4*, *Itga5*, *Sdc1*) (Figures 3C and 3D). Notably, even the mesenchymal genes that were upregulated in CTCs showed a high degree of heterogeneous expression across single cells (Figure S6). In contrast, loss of E-cadherin (*Cdh1*) was nearly universal across all classical CTCs, suggesting that pancreatic CTCs indeed lose some of their epithelial characteristics.

CTCs are also likely to be enriched for metastatic precursors capable of initiating metastatic tumor deposits. The relationship between such precursor cells and cancer stem cells is uncertain, as is the relevance of established stem cell markers in identifying these cells. We evaluated putative pancreatic cancer stem cell genes (Rasheed and Matsui, 2012; Rasheed et al., 2010) in the single-cell RNA-seq reads (Figures 4A and S6). Among all candidate markers tested (*Aldh1a1*, *Aldh1a2*, *Prom1/Cd133*, *Cd44*, *Met*, *EpCAM*), only *Aldh1a1* and *Aldh1a2* were enriched in CTCs. Classical CTCs expressed predominantly the *Aldh1a2* isoform, while *Aldh1a1* was expressed in a variety of cell types (Figure S6). Within single CTCs, there was no correlation between expression of Aldh1 isoforms and either enrichment for the mesenchymal genes (*Cdh11*, *Vim*) or loss of epithelial genes (*Cdh1*, *Muc1*), suggesting that stem cell and EMT markers are not intrinsically linked in CTCs. Analysis of primary pancreatic tumors for *Aldh1a2* using RNA in situ hybridization (RNA-ISH) identified rare epithelial tumor cells expressing this stem cell marker, but the majority of expression was present within the cancer associated stromal cells (Figure 4B), consistent with immunohistochemistry for ALDH protein in human PDAC (Rasheed et al., 2010).

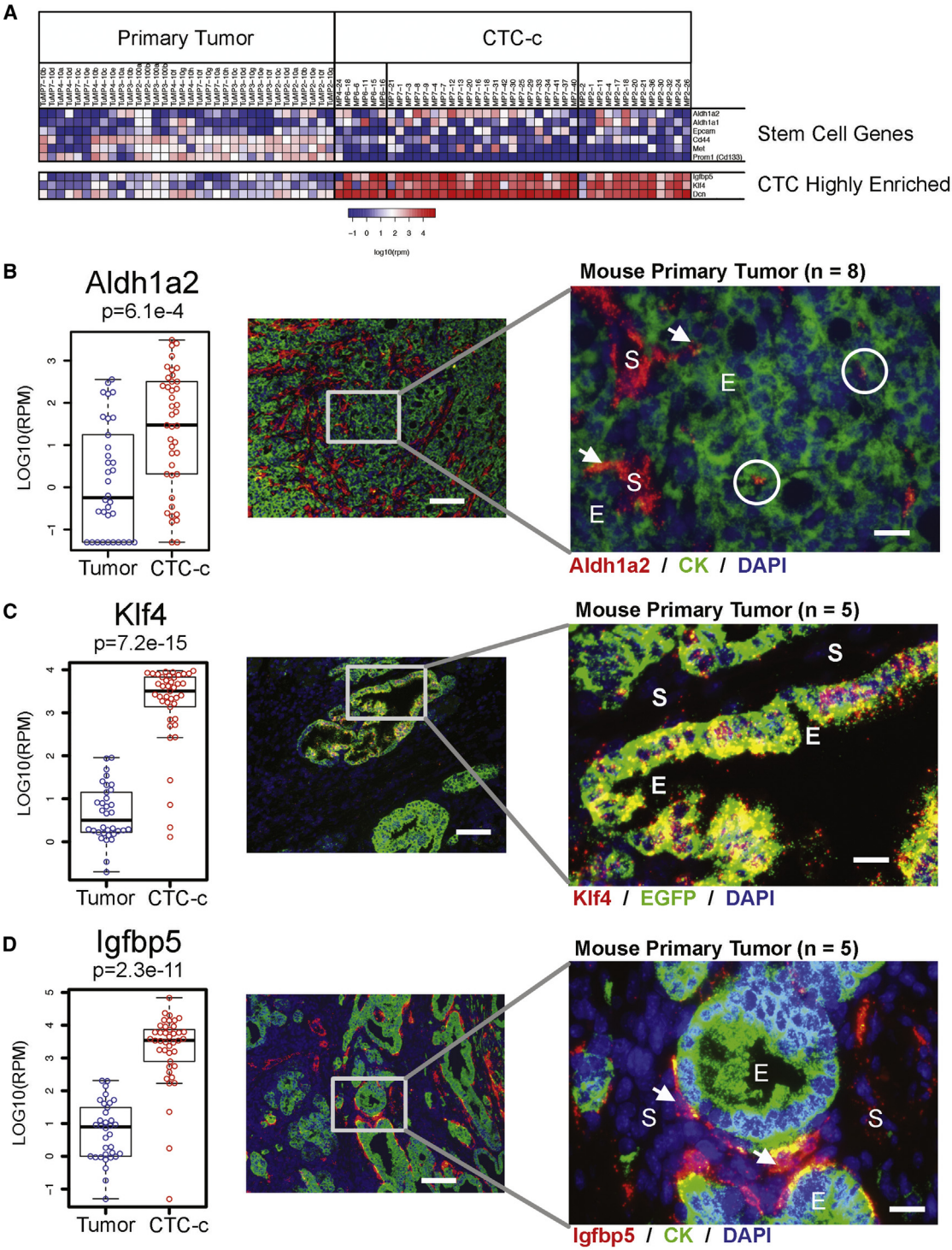

Figure 4. CTC-Enriched Genes Found in Epithelial and Stromal Components of Primary Tumors

(A) Expression heatmap of stem cell genes and highly enriched CTC genes in primary tumors and CTC-c cells. Scale in log10(rpm).

(B–D) Expression boxplot (left) analysis of (B) *Aldh1a2* stem cell and CTC highly enriched genes (C) *Klf4* and (D) *Igfbp5* genes with RNA-ISH of primary tumors (right). Bar = median, box plot = quartiles, scale in log10(rpm). RNA-ISH color key shown (CK = *Krt8+18*). Circles indicate a subpopulation of keratin-positive tumor cells with *Aldh1a2* marker, and arrowheads identify dual-positive cells at the epithelial-stromal interface (E, epithelial; S, stromal) with DAPI nuclear stain (blue). Low-magnification fluorescent images taken at 100× magnification (scale bar represents 100 μm) and high magnification at 400× (scale bar represents 20 μm).

Classical CTCs Share Expression of Stromal Enriched Genes

Besides the evident diversity of CTCs, we searched for shared transcripts that might provide further insight into their cell of origin within the primary tumor and the mechanisms by which they invade and survive within the bloodstream and ultimately identify potential CTC-specific therapeutic targets. We selected rigorous criteria to identify the most highly enriched CTC-c transcripts (RP score < 300), expressed at very high levels (>100 rpm) in ≥90% of all classical CTCs. Three genes met these criteria: Kruppel-like factor 4 (*Klf4*), one of the key stem cell (iPS) reprogramming factors (Takahashi and Yamanaka, 2006), which has been implicated in pancreatic cancer development (Brembeck and Rustgi, 2000; Prasad et al., 2005; Wei et al., 2010); insulin-like growth factor binding protein 5 (*Igfbp5*), an extracellular growth factor binding protein expressed in human PDAC reported to have both pro- and antiproliferative properties (Johnson et al., 2006; Johnson and Haun, 2009); and decorin (*Dcn*), a extracellular matrix proteoglycan expressed in tumor stroma across a variety of different cancers (Adany et al., 1990; Boström et al., 2013; Henke et al., 2012; Hunzelmann et al., 1995; Iozzo and Cohen, 1994; Mu et al., 2013; Nash et al., 2002). We utilized RNA-ISH in primary tumor specimens to identify the potential colocalization of these three highly enriched CTC genes. In contrast to *Aldh1a2*, *Klf4* is expressed in epithelial components of the primary tumor (Figure 4C). *Igfbp5* is of particular interest, in that it is expressed focally at the tumor epithelial-stromal interface (Figure 4D). This geographic area may be enriched for cancer cells undergoing EMT, contributing to the mixed epithelial/stromal transcriptional programs evident by RNA-seq of single CTCs.

In addition to highly expressing *Dcn*, CTCs consistently had high levels of multiple ECM gene transcripts. GO analysis of all CTC-enriched genes (Table S2) identified 32 proteinaceous ECM genes (GO:0005578, OR 2.4, q-value 4.8×10^{-3}). These genes are normally expressed in reactive stromal cells, rather than in epithelial cancer cells, and while recent studies have highlighted the importance of the stroma in supporting pancreatic cancer pathogenesis and metastasis (Feig et al., 2012; Neesse et al., 2011, 2013; Olive et al., 2009; Provenzano et al., 2012), the expression of these stroma-associated ECM genes within tumor cells in circulation was unexpected. Using RP differential expression analysis, we compared CTCs with purified EGFP-tagged primary tumor single cells (TuGMP3) and bulk tumor samples (tumor cells admixed with reactive stromal cells). Six proteinaceous ECM genes were highly expressed by CTCs and by stromal component, but not by epithelial cells within primary tumors: *Dcn*, *Sparc*, *Ccdc80, Col1a2, Col3a1*, and *Timp2* (Figure 5A). RNA-ISH analysis of both *Dcn* and *Sparc* confirmed diffuse expression in stromal elements of mouse primary tumors, with rare areas where these transcripts are colocalized with keratin-expressing cells at the epithelial-stromal border (Figure 5B). *SPARC* is a well-known ECM protein gene found in stroma of human primary PDAC (Infante et al., 2007; Neuzillet et al., 2013; Sato et al., 2003). Indeed, RNA-ISH analysis of 198 primary human PDACs demonstrates abundant stromal cell expression of *SPARC* transcripts in 99% of cases, with up to a third of tumors with rare epithelial cells expressing this ECM gene product (Figure 5C). Consistent with these observations, RNA-seq of EGFP-tagged single primary tumor cells (Figure 5A) identified only 1 of 20 cells (5%) with coexpression of high levels (>100 rpm) of *Sparc* and *Krt19*. In summary, abundant expression of ECM genes is a common feature of all keratin-rich classical CTCs. This is in marked contrast to the primary tumor, where these gene products are secreted by supporting stromal cells and not by the epithelial cancer cells. However, rare cells at the epithelial-stromal interface of primary tumors do appear to express both keratins and ECM genes, consistent with the pattern observed in CTCs themselves.

Human CTCs Express Diverse Proteinaceous ECM Genes

To confirm the expression of proteinaceous ECM genes by human cancer cells circulating in the bloodstream, we isolated single CTCs from patients with pancreatic (n = 7), breast (n = 29), and prostate (n = 77) cancers and subjected these to single-cell RNA-seq. Six ECM protein genes were highly expressed in human CTCs (>100 rpm in >15% of all CTC samples) (Figure 5D; Table S6). Notably, three genes (*SPARC*, *MGP*, *SPON2*) are ECM glycoproteins, defined as part of the core matrisome (Naba et al., 2012). The core matrisome protein *SPARC* was particularly enriched in pancreatic CTCs being expressed at high levels (>100 rpm) in 100% of pancreatic CTCs compared to 31% of breast and 9% of prostate CTCs. The notable differences in ECM protein gene expression across human epithelial CTCs suggest microenvironment tissue specificity as well as probable redundancies in ECM protein signaling. Together, the consistent expression of ECM gene family members in human CTCs suggests that their upregulation may contribute either to the generation of CTCs from primary tumors or to the survival of cancer cells deprived of microenvironmental signals as they circulate in the bloodstream.

ECM Protein Gene SPARC Enhances Pancreatic Cancer Metastatic Potential

In order to define the functional consequences of *SPARC* expression in pancreatic cancer cells, we screened a panel of patient-derived, low-passage PDAC cell lines for expression. Two human PDAC cell lines with relatively high *SPARC* expression were identified (PDAC2 and PDAC3), making it possible to test the consequences of small hairpin RNA (shRNA)-mediated knockdown (Figures 6A, 6B, and S7). Suppression of endogenous *SPARC* expression in both PDAC2 and PDAC3 cell lines using two independent shRNA constructs did not affect proliferation in 2D cultures or anchorage-independent tumor sphere formation (Figures 6C, 6D, and S7). However, *SPARC* knockdown by both shRNAs significantly reduced pancreatic cancer cell migration in wound scratch assays and their invasive properties, as measured by in vitro Boyden assays (Figures 6E–6G and S7). Tail vein injection of *SPARC*-suppressed PDAC3 cells using both shRNA constructs generated significantly fewer lung metastases than cells expressing nontargeting hairpin (shNT) controls (Figure 6H). Metastases generated from orthotopic pancreatic xenografts were also significantly reduced for *SPARC*-suppressed PDAC3 cells, as measured by luciferase imaging and normalized for primary tumor size (Figure 6I). Thus, *SPARC* expression by

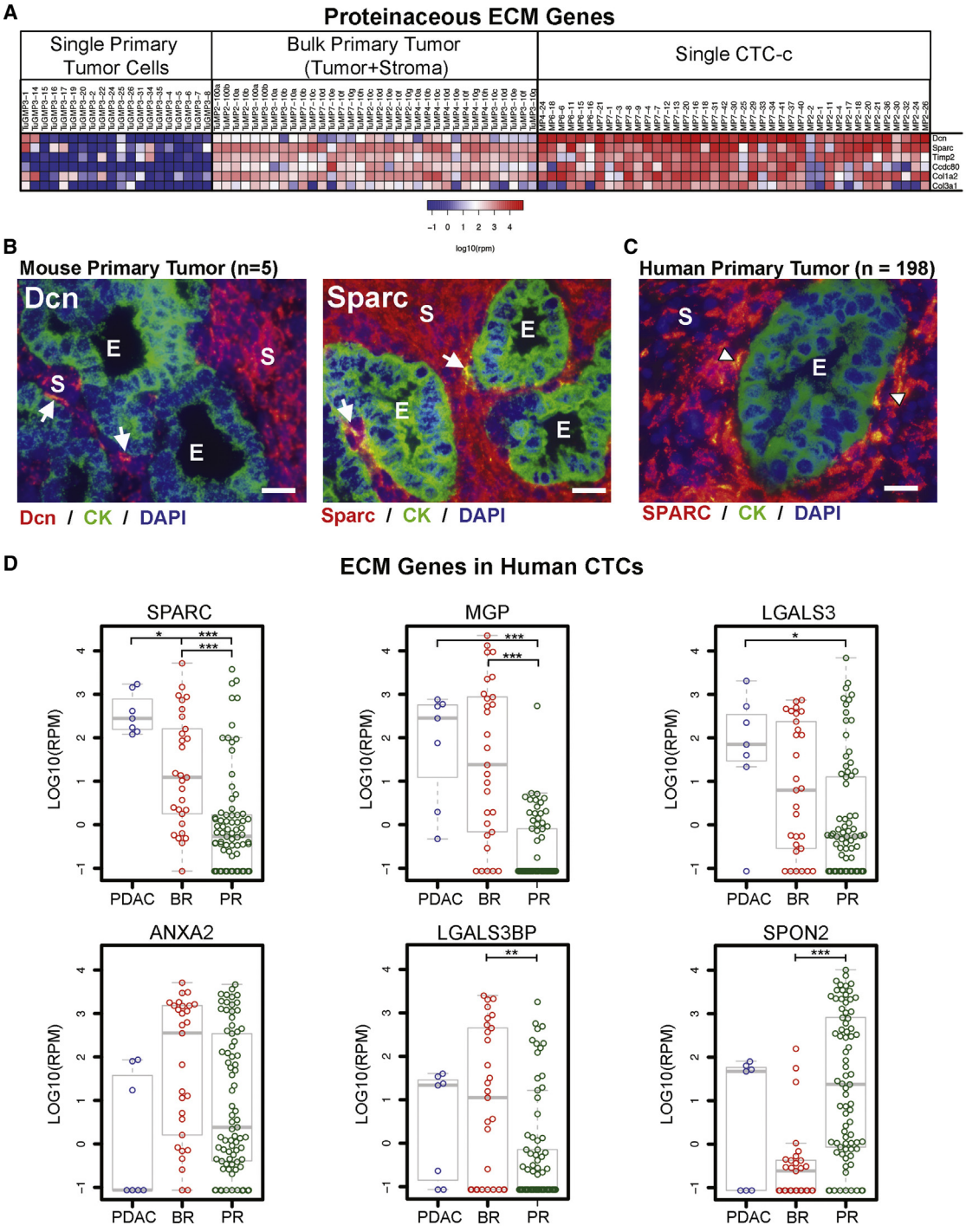

Figure 5. Human and Mouse CTCs across Different Epithelial Cancer Express High Levels of ECM Protein Genes

(A) Expression heatmap of mouse single primary tumor cells, bulk tumor, and CTCs for ECM protein genes. Scale in log10(rpm).

(B) RNA-ISH of ECM protein genes *Dcn* and *Sparc* with CK (*Krt8+18*) in mouse primary PDAC tumors.

(C) RNA-ISH of *SPARC* with CK (*KRT7,8,18,+19*) in human primary PDAC tumors. Arrowheads identify dual-positive cells at the epithelial-stromal interface (E, epithelial; S, stromal) with DAPI nuclear stain (blue). Images taken at 400× magnification (scale bar represents 20 μm).

(D) Expression boxplot of highly expressed ECM genes in human PDAC, breast (BR), and prostate (PR) CTCs. Bar, median; boxplot, quartiles; scale in log10(rpm). Holm-adjusted p value < 0.05 (*), 0.01 (**), 0.001 (***).

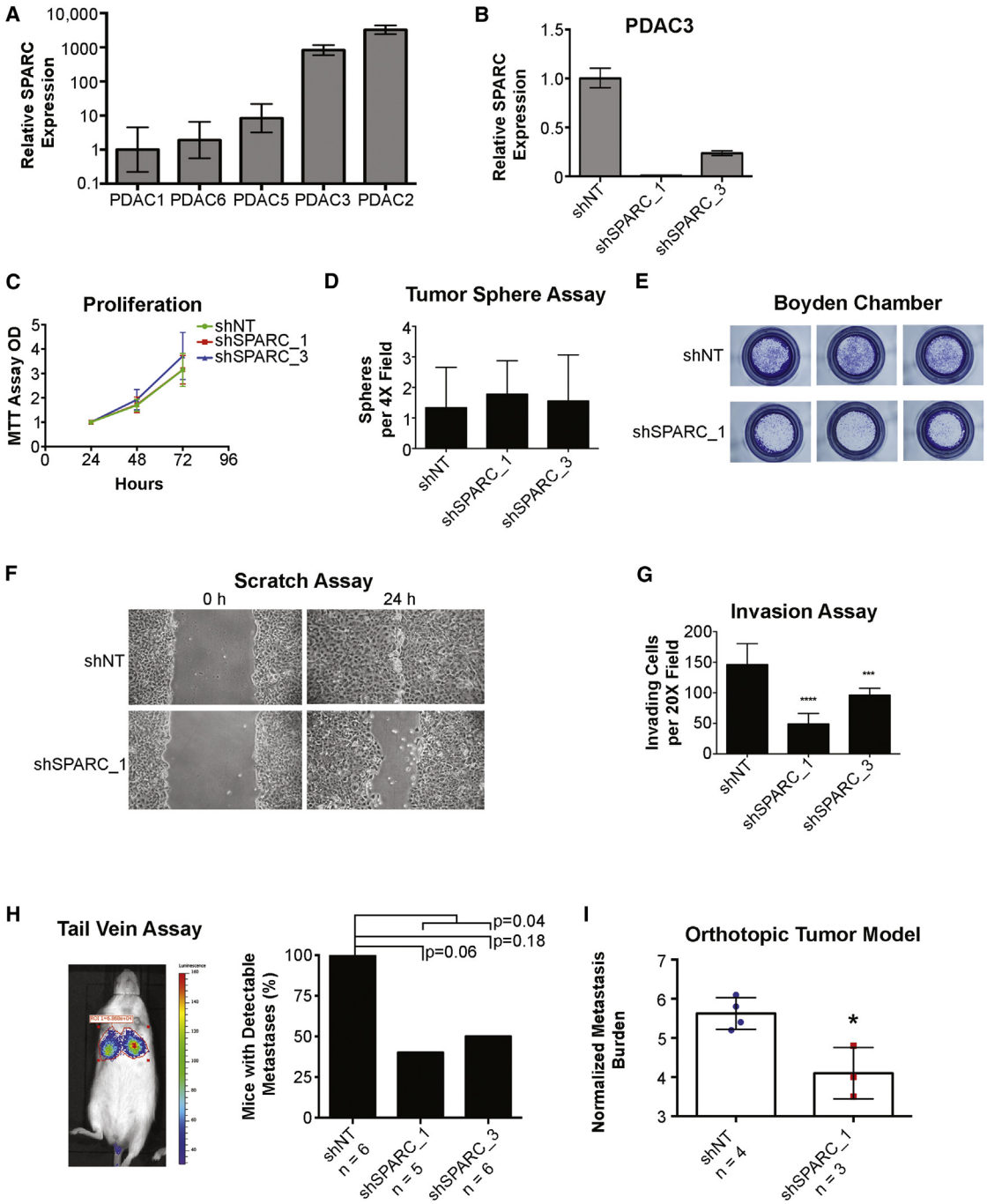

Figure 6. *SPARC* Expression in Human PDAC Enhances Invasion and Metastasis

(A–C) Relative *SPARC* expression in (A) patient-derived human PDAC cell lines and in (B) PDAC3 cell line with shRNA against *SPARC* and nontarget (NT). Error bars represent range. (C) Proliferation of PDAC3 cell lines determined by MTT.

(D) Tumor spheres in PDAC3 shNT versus shSPARC counted per 4× field (error bars represent SD).

(E) Boyden migration chamber assay stained with crystal violet and imaged.

(F) Scratch assay of shSPARC and shNT cell lines at 24 hr.

(G) Invasion of shSPARC and shNT cell lines quantitated by number of nuclei/20× field. p value < 0.01 (**), 0.001 (***), 0.0001 (****). Error bars represent SD.

(H) Percentage of detectable lung metastases by in vivo luciferase imaging after 3 weeks after tail vein inoculation of PDAC3 cell lines. Fisher's exact test p value is shown.

(I) Normalized metastasis burden in mice with orthotopic pancreatic tumors from PDAC3 cell lines. Error bars represent SD (*p < 0.05).

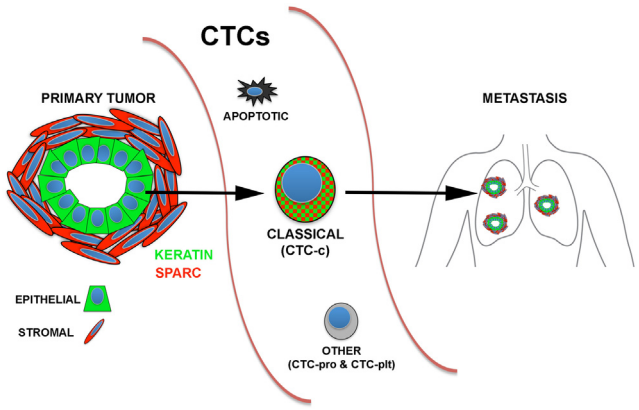

Figure 7. Summary Model of the Role of Pancreatic CTCs in the Metastatic Cascade

Shown are the heterogeneous subsets of pancreatic CTCs with a focus on the most prominent classical CTC group, which are enriched for coexpression of epithelial (keratin) and stromal (*Sparc*) genes.

pancreatic cancer cells appears to selectively enhance their invasive and migratory properties to augment metastatic virulence. The high levels of *SPARC* expression evident in virtually all pancreatic CTCs thus raises the possibility that it contributes significantly to the metastatic spread of pancreatic cancer.

DISCUSSION

We present a detailed analysis of CTC composition and diversity in pancreatic cancer, using single-cell RNA-seq. We achieved high-quality transcriptomes in 93 single mouse pancreatic CTCs, which were compared with bulk and single-cell preparations from matched primary tumors and from an immortalized cell line established from the same mouse pancreatic tumor model. The use of the KPC mouse model made it possible to compare simultaneously isolated primary tumor specimens and CTCs, and it allowed measurements of CTC heterogeneity across multiple mice sharing the same *Kras*/*Trp53* genetic drivers. The large number of isolated CTCs and the high quality of the isolated RNA from these cells reflect the application of the CTC-iChip technology, which effectively depletes normal blood components, enriching for CTCs that are untagged and accessible for single-cell manipulation. Finally, the purification of CTCs irrespective of their cell-surface epitopes avoids any bias associated with their purification based on expression of common epithelial markers such as EpCAM.

Together, our observations include the following. (1) CTC expression profiles cluster into three classes, including a major "classical CTC" group, and others that are defined by platelet-derived markers or proliferative signatures. (2) Common features shared by virtually all classical CTCs include expression of both epithelial and mesenchymal markers, the stem cell-associated gene *Aldh1a2*, and three highly expressed transcripts, *Klf4*, *Igfbp5*, and *Dcn*. The specific localization of *Igfbp5*-expressing cells at the epithelial-stromal boundary within primary tumors may point to a region that contributes significantly to CTC generation. (3) The most highly enriched CTC-specific transcripts shared by almost all classical CTCs encode extracellular matrix proteins, such as *Sparc*. (4) Aberrant expression in CTCs of this ECM gene product, which is normally abundant in the tumor stromal compartment, is observed in both mouse and human pancreatic CTCs, and its knockdown attenuates cancer cell migration and invasion in reconstituted systems. (Figure 7)

Compared with our previous RNA-seq of partially purified, bulk CTC populations, which required digital subtraction of leukocyte-derived reads (Yu et al., 2012, 2013), the single-cell analysis reported here provides considerably more depth of tumor cell-specific transcript reads, and it allows measurements of CTC heterogeneity. The feasibility of single-cell RNA-seq applied to CTCs has been reported for small numbers of immunoselected melanoma and prostate CTCs (Cann et al., 2012; Ramsköld et al., 2012), and our work extends these studies by providing a comprehensive landscape of mouse pancreatic CTCs, whose gene expression profile is directly compared to matched primary tumor cells. Since KPC mice primarily produce disseminated micrometastatic foci, we were unable to directly compare the expression profile of CTCs with that of metastatic lesions. The shared genetic drivers in the KPC mouse model enabled the collection and analysis of sufficient numbers of single CTCs across different animals, yet we note significant animal-specific clustering in RNA-seq data. Thus, in addition to the initiating mutations, somatically acquired genetic and epigenetic changes may distinguish CTCs derived from different tumors. Multiple mouse tumors contributed to each of the three distinct clusters of CTCs. Despite their atypical expression pattern, the identification of platelet-associated and proliferative CTC subsets as being tumor-derived is established by their inclusion of lineage-tagged tumor cells. The more characteristic expression pattern exhibited by the classical CTC cluster enabled detailed comparison with primary tumor cells, thereby providing further insight into the origin and properties of CTCs.

Mouse pancreatic classical CTCs uniformly lose expression of the epithelial marker E-cadherin (*Cdh1*), a key feature of epithelial-to-mesenchymal transition. However, the cells do not lose expression of other epithelial markers, such as cytokeratins, nor is there a consistent increase in classical mesenchymal markers such as vimentin. As such, most classical CTCs appear arrested in a biphenotypic state. Despite their expression of cytokeratins, which are present in the epithelial components of the primary tumor, most other highly expressed markers in CTCs are shared with the stromal component of the primary tumor. Among these stromal genes is *Aldh1a2*, a putative pancreatic cancer stem cell marker (Rasheed and Matsui, 2012; Rasheed et al., 2010). A provocative observation relating to the shared epithelial and mesenchymal state of classical CTCs is their virtually universal (93%) expression of *Igfbp5,* which is uniquely expressed in a small subpopulation of cells at the epithelial/stromal interface within primary tumors. This raises the possibility that this critical location within the primary tumor generates a disproportionate fraction of viable CTCs. The postulated role of human *IGFBP5* in metastasis (Hao et al., 2004) as well as in pancreatic malignancy (Johnson et al., 2006; Johnson and Haun, 2009) makes its unique expression pattern in both tumors and CTCs particularly noteworthy.

The most unexpected observation from our single-CTC RNA-seq study is the high abundance of ECM transcripts in the vast majority of classical CTCs. The coexpression of pancreatic cancer-enriched cytokeratins (*Krt7* and *Krt19*) in single cells expressing these ECM gene products excludes the possibility that these represent circulating tumor-derived fibroblasts. Interestingly, prior evaluation of matched primary and metastatic breast tumors identified the most prevalent gene expression difference as enrichment for ECM molecules in the metastases, comprising some 18% of differentially expressed genes (Weigelt et al., 2005). While this has been interpreted as reflecting differences in the local environment of the metastatic site, our data suggest that ECM proteins are highly expressed by CTCs themselves. By analogy with the classical "seed versus soil" debate (Fidler, 2003), CTCs may in fact be seeds carrying some of their own soil. These findings are also consistent with recent work highlighting the importance of tumor stromal signaling in priming cancer cells to metastasize (Zhang et al., 2013).

Consistent with the aberrant expression of *SPARC* in some pancreatic cancer cells, a subset of patient-derived tumor cell lines also coexpress it along with epithelial cytokeratins. The reduction in cell migration and metastatic potential exhibited by these pancreatic cell lines following *SPARC* knockdown suggests that it may contribute to CTC-mediated metastasis, consistent with prior work in breast cancer models (Minn et al., 2005). However, *Sparc* null pancreatic mouse tumors demonstrate some effects on collagen maturation but do not show suppressed metastasis (Neesse et al., 2014). Similar findings have been reported in prostate and breast *Sparc* null mouse cancer models (Wong et al., 2008). Thus, *Sparc* expression may contribute to metastasis, but inherent redundancies in ECM protein expression may mitigate this effect. Nonetheless, considerable effort has been directed to targeting the pancreatic cancer stroma as a means of improving delivery of chemotherapeutics as well as stripping tumor cells of their supportive microenvironment (Neesse et al., 2011; Olive et al., 2009; Provenzano et al., 2012; Rasheed et al., 2012). Our finding that these gene products are also expressed by CTCs themselves suggests a remarkable level of cellular plasticity. To the extent that invasive properties of CTCs are mediated in part by expression of such ECM proteins, it also raises the possibility of targeting cancer cells in the blood.

The ability to dissect critical components of the metastatic process at the single-cell level depends upon critical technological developments that have only recently become available, namely the efficient isolation of extraordinarily rare CTCs in solution without the bias of tumor antigen selection combined with the ability to perform high-fidelity single-cell RNA-seq. These approaches now allow CTC analyses to extend from matching them to known tumor-defining markers to interrogating them for unique properties that in fact distinguish them from primary tumor cells. Identifying such CTC-specific gene expression patterns may provide additional insight into mechanisms that underlie their ability to survive in the bloodstream and generate distant metastases, which are critical to the ultimate goal of preventing the spread of cancer to distant organs.

EXPERIMENTAL PROCEDURES

Mice and Cell Lines

Mice with pancreatic cancer used in these experiments express Cre driven by *Pdx1*, *LSL-Kras^{G12D}*, and *Trp53$^{lox/+}$* or *Trp53$^{lox/lox}$* as previously described (Bardeesy et al., 2006). EGFP pancreatic lineage-tagged KPC mice were generated by breeding the mT/mG mouse [Jackson Laboratory; Gt(ROSA)26Sortm4(ACTB-tdTomato,-EGFP)Luo/J] into the breeder pairs used for KPC mouse generation. Normal FVB mice were purchased from Jackson Laboratory. All mice care and procedures were done under Massachusetts General Hospital (MGH) Subcommittee on Research Animal Care-approved protocols.

Human CTCs and Cell Lines

Human blood for CTC analysis was obtained after consent was obtained on an existing Dana-Farber/Harvard Cancer Center institutional review board (IRB)-approved protocol (05-300) at the Massachusetts General Hospital. A maximum of 20 ml of blood was obtained from patients at any given blood draw in two 10 ml EDTA tubes, and approximately 8–10 ml of blood was processed per patient. Newly derived pancreatic cancer cell lines were generated from metastatic ascites fluid from patients receiving diagnostic or therapeutic paracentesis under MGH IRB protocol 2011P001236. Cell lines were subcultured until a pure cell line was obtained. All cell lines studied had KRAS mutation genotyping to confirm cancer origins, and both PDAC2 and PDAC3 were both found to have KRAS G12V point mutations. Cell lines were grown in standard culture conditions using Dulbecco's modified Eagle's medium, high glucose + 10% fetal bovine serum + 1% penicillin/streptomycin (Gibco/Life Technologies).

CTC Enrichment Technology

Given the desire for an unbiased enrichment system, the previously presented negative depletion technology was selected for this application. Before running blood, mouse and human blood were analyzed by a cell blood count machine to determine total WBC count. For mouse CTC samples, a rat anti-mouse CD45 antibody (BAM114, R&D Systems) was preconjugated to Dynabeads MyOne Strepavidin T1 (Life Technologies, 65602). Beads were added at a ratio of 125 beads/WBC, mixed, and incubated for 40 min at room temperature. Human CTC samples utilized a primary and secondary immunolabeling approach. Biotinylated primary antibodies against anti-human CD45 antibody (clone 2D1, R&D Systems, BAM1430) and anti-human CD66b antibody (Abd Serotec, 80H3) were spiked into whole blood at 100 fg/WBC and 37.5 fg/WBC, respectively, and incubated rocking at room temperature for 20 min. Dynabeads MyOne Strepavidin T1 (Life Technologies, 65602) were then added and incubated rocking at room temperature for an additional 20 min.

Single-Cell Micromanipulation, Amplification, and Sequencing

After whole-blood CTC-iChip processing, the product containing enriched cells was collected in a 35 mm petri dish and viewed using a Nikon Eclipse Ti inverted microscope. Cells of interest were identified based on intact cellular morphology and lack of labeling with anti-CD45 magnetic beads. These target cells were individually micromanipulated with a 10 μm transfer tip on an Eppendorf TransferMan NK 2 micromanipulator and ejected into PCR tubes containing RNA protective lysis buffer and immediately flash frozen in liquid nitrogen. Single cells were amplified with a modified protocol (Tang et al., 2010) and sequenced on the ABI 5500XL system.

RNA In Situ Hybridization

RNA-ISH was performed according to the Affymetrix ViewRNA ISH Tissue-2 Plex Assay. Fluorescent images were taken in using a Nikon 90i microscope. See Supplemental Experimental Procedures for details.

ACCESSION NUMBERS

Pancreatic and breast sequencing data have been deposited to the NCBI Gene Expression Omnibus with the accession numbers GSE51372, GSE60407, and GSE51827.

SUPPLEMENTAL INFORMATION

Supplemental Information includes Supplemental Experimental Procedures, seven figures, and six tables and can be found with this article online at http://dx.doi.org/10.1016/j.celrep.2014.08.029.

ACKNOWLEDGMENTS

We are grateful to Laura Libby for mouse colony care, Lev Silberstein for providing technical assistance in single-cell RNA sequencing, Linda Nieman for microscopy expertise, and engineering techs for their help in running samples on the CTC-iChip. This work was supported by Stand Up to Cancer (D.A.H., M.T., and S.M.), Howard Hughes Medical Institute (D.A.H. and M.N.R.), NIBIB Quantum grant 5R01EB008047 (M.T.), NCI 2R01CA129933 (D.A.H.), National Foundation for Cancer Research (D.A.H.), the Burroughs Wellcome Fund (D.T.T. and M.N.R.), K12CA087723-11A1 (D.T.T.), Department of Defense (D.T.M. and D.T.T.), Affymetrix, Inc. (D.T.T., M.N.R., and V.D.), the Warshaw Institute for Pancreatic Cancer Research (D.T.T.), and the Verville Family Pancreatic Cancer Research Fund (D.T.T.).

Received: April 8, 2014
Revised: July 16, 2014
Accepted: August 13, 2014
Published: September 18, 2014

REFERENCES

Adany, R., Heimer, R., Caterson, B., Sorrell, J.M., and Iozzo, R.V. (1990). Altered expression of chondroitin sulfate proteoglycan in the stroma of human colon carcinoma. Hypomethylation of PG-40 gene correlates with increased PG-40 content and mRNA levels. J. Biol. Chem. *265*, 11389–11396.

Bardeesy, N., Aguirre, A.J., Chu, G.C., Cheng, K.H., Lopez, L.V., Hezel, A.F., Feng, B., Brennan, C., Weissleder, R., Mahmood, U., et al. (2006). Both p16(Ink4a) and the p19(Arf)-p53 pathway constrain progression of pancreatic adenocarcinoma in the mouse. Proc. Natl. Acad. Sci. USA *103*, 5947–5952.

Boström, P., Sainio, A., Kakko, T., Savontaus, M., Söderström, M., and Järveläinen, H. (2013). Localization of decorin gene expression in normal human breast tissue and in benign and malignant tumors of the human breast. Histochem. Cell Biol. *139*, 161–171.

Breitling, R., Armengaud, P., Amtmann, A., and Herzyk, P. (2004). Rank products: a simple, yet powerful, new method to detect differentially regulated genes in replicated microarray experiments. FEBS Lett. *573*, 83–92.

Brembeck, F.H., and Rustgi, A.K. (2000). The tissue-dependent keratin 19 gene transcription is regulated by GKLF/KLF4 and Sp1. J. Biol. Chem. *275*, 28230–28239.

Cann, G.M., Gulzar, Z.G., Cooper, S., Li, R., Luo, S., Tat, M., Stuart, S., Schroth, G., Srinivas, S., Ronaghi, M., et al. (2012). mRNA-Seq of single prostate cancer circulating tumor cells reveals recapitulation of gene expression and pathways found in prostate cancer. PLoS ONE *7*, e49144.

Carvalho, F.L., Simons, B.W., Antonarakis, E.S., Rasheed, Z., Douglas, N., Villegas, D., Matsui, W., and Berman, D.M. (2013). Tumorigenic potential of circulating prostate tumor cells. Oncotarget *4*, 413–421.

Feig, C., Gopinathan, A., Neesse, A., Chan, D.S., Cook, N., and Tuveson, D.A. (2012). The pancreas cancer microenvironment. Clin. Cancer Res. *18*, 4266–4276.

Fidler, I.J. (2003). The pathogenesis of cancer metastasis: the 'seed and soil' hypothesis revisited. Nat. Rev. Cancer *3*, 453–458.

Hao, X., Sun, B., Hu, L., Lähdesmäki, H., Dunmire, V., Feng, Y., Zhang, S.W., Wang, H., Wu, C., Wang, H., et al. (2004). Differential gene and protein expression in primary breast malignancies and their lymph node metastases as revealed by combined cDNA microarray and tissue microarray analysis. Cancer *100*, 1110–1122.

Henke, A., Grace, O.C., Ashley, G.R., Stewart, G.D., Riddick, A.C., Yeun, H., O'Donnell, M., Anderson, R.A., and Thomson, A.A. (2012). Stromal expression of decorin, Semaphorin6D, SPARC, Sprouty1 and Tsukushi in developing prostate and decreased levels of decorin in prostate cancer. PLoS ONE *7*, e42516.

Hunzelmann, N., Schönherr, E., Bonnekoh, B., Hartmann, C., Kresse, H., and Krieg, T. (1995). Altered immunohistochemical expression of small proteoglycans in the tumor tissue and stroma of basal cell carcinoma. J. Invest. Dermatol. *104*, 509–513.

Infante, J.R., Matsubayashi, H., Sato, N., Tonascia, J., Klein, A.P., Riall, T.A., Yeo, C., Iacobuzio-Donahue, C., and Goggins, M. (2007). Peritumoral fibroblast SPARC expression and patient outcome with resectable pancreatic adenocarcinoma. J. Clin. Oncol. *25*, 319–325.

Iozzo, R.V., and Cohen, I. (1994). Altered proteoglycan gene expression and the tumor stroma. EXS *70*, 199–214.

Johnson, S.K., and Haun, R.S. (2009). Insulin-like growth factor binding protein-5 influences pancreatic cancer cell growth. World J. Gastroenterol. *15*, 3355–3366.

Johnson, S.K., Dennis, R.A., Barone, G.W., Lamps, L.W., and Haun, R.S. (2006). Differential expression of insulin-like growth factor binding protein-5 in pancreatic adenocarcinomas: identification using DNA microarray. Mol. Carcinog. *45*, 814–827.

Kalluri, R., and Weinberg, R.A. (2009). The basics of epithelial-mesenchymal transition. J. Clin. Invest. *119*, 1420–1428.

Krause, D.S., Ito, T., Fackler, M.J., Smith, O.M., Collector, M.I., Sharkis, S.J., and May, W.S. (1994). Characterization of murine CD34, a marker for hematopoietic progenitor and stem cells. Blood *84*, 691–701.

Labelle, M., Begum, S., and Hynes, R.O. (2011). Direct signaling between platelets and cancer cells induces an epithelial-mesenchymal-like transition and promotes metastasis. Cancer Cell *20*, 576–590.

Minn, A.J., Gupta, G.P., Siegel, P.M., Bos, P.D., Shu, W., Giri, D.D., Viale, A., Olshen, A.B., Gerald, W.L., and Massagué, J. (2005). Genes that mediate breast cancer metastasis to lung. Nature *436*, 518–524.

Mu, Y., Chen, Y., Zhang, G., Zhan, X., Li, Y., Liu, T., Li, G., Li, M., Xiao, Z., Gong, X., and Chen, Z. (2013). Identification of stromal differentially expressed proteins in the colon carcinoma by quantitative proteomics. Electrophoresis *34*, 1679–1692.

Muzumdar, M.D., Tasic, B., Miyamichi, K., Li, L., and Luo, L. (2007). A global double-fluorescent Cre reporter mouse. Genesis *45*, 593–605.

Naba, A., Clauser, K.R., Hoersch, S., Liu, H., Carr, S.A., and Hynes, R.O. (2012). The matrisome: in silico definition and in vivo characterization by proteomics of normal and tumor extracellular matrices. Mol Cell Proteomics *11*, M111 014647.

Nash, M.A., Deavers, M.T., and Freedman, R.S. (2002). The expression of decorin in human ovarian tumors. Clin. Cancer Res. *8*, 1754–1760.

Neesse, A., Michl, P., Frese, K.K., Feig, C., Cook, N., Jacobetz, M.A., Lolkema, M.P., Buchholz, M., Olive, K.P., Gress, T.M., and Tuveson, D.A. (2011). Stromal biology and therapy in pancreatic cancer. Gut *60*, 861–868.

Neesse, A., Frese, K.K., Bapiro, T.E., Nakagawa, T., Sternlicht, M.D., Seeley, T.W., Pilarsky, C., Jodrell, D.I., Spong, S.M., and Tuveson, D.A. (2013). CTGF antagonism with mAb FG-3019 enhances chemotherapy response without increasing drug delivery in murine ductal pancreas cancer. Proc. Natl. Acad. Sci. USA *110*, 12325–12330.

Neesse, A., Frese, K.K., Chan, D.S., Bapiro, T.E., Howat, W.J., Richards, F.M., Ellenrieder, V., Jodrell, D.I., and Tuveson, D.A. (2014). SPARC independent drug delivery and antitumour effects of nab-paclitaxel in genetically engineered mice. Gut *63*, 974–983.

Neuzillet, C., Tijeras-Raballand, A., Cros, J., Faivre, S., Hammel, P., and Raymond, E. (2013). Stromal expression of SPARC in pancreatic adenocarcinoma. Cancer Metastasis Rev. *32*, 585–602.

Olive, K.P., Jacobetz, M.A., Davidson, C.J., Gopinathan, A., McIntyre, D., Honess, D., Madhu, B., Goldgraben, M.A., Caldwell, M.E., Allard, D., et al. (2009). Inhibition of Hedgehog signaling enhances delivery of chemotherapy in a mouse model of pancreatic cancer. Science *324*, 1457–1461.

Ozkumur, E., Shah, A.M., Ciciliano, J.C., Emmink, B.L., Miyamoto, D.T., Brachtel, E., Yu, M., Chen, P.I., Morgan, B., Trautwein, J., et al. (2013). Inertial

focusing for tumor antigen-dependent and -independent sorting of rare circulating tumor cells. Sci Transl Med *5*, 179ra147.

Pantel, K., Brakenhoff, R.H., and Brandt, B. (2008). Detection, clinical relevance and specific biological properties of disseminating tumour cells. Nat. Rev. Cancer *8*, 329–340.

Prasad, N.B., Biankin, A.V., Fukushima, N., Maitra, A., Dhara, S., Elkahloun, A.G., Hruban, R.H., Goggins, M., and Leach, S.D. (2005). Gene expression profiles in pancreatic intraepithelial neoplasia reflect the effects of Hedgehog signaling on pancreatic ductal epithelial cells. Cancer Res. *65*, 1619–1626.

Provenzano, P.P., Cuevas, C., Chang, A.E., Goel, V.K., Von Hoff, D.D., and Hingorani, S.R. (2012). Enzymatic targeting of the stroma ablates physical barriers to treatment of pancreatic ductal adenocarcinoma. Cancer Cell *21*, 418–429.

Ramsköld, D., Luo, S., Wang, Y.C., Li, R., Deng, Q., Faridani, O.R., Daniels, G.A., Khrebtukova, I., Loring, J.F., Laurent, L.C., et al. (2012). Full-length mRNA-Seq from single-cell levels of RNA and individual circulating tumor cells. Nat. Biotechnol. *30*, 777–782.

Rasheed, Z.A., and Matsui, W. (2012). Biological and clinical relevance of stem cells in pancreatic adenocarcinoma. J. Gastroenterol. Hepatol. *27* (*Suppl 2*), 15–18.

Rasheed, Z.A., Yang, J., Wang, Q., Kowalski, J., Freed, I., Murter, C., Hong, S.M., Koorstra, J.B., Rajeshkumar, N.V., He, X., et al. (2010). Prognostic significance of tumorigenic cells with mesenchymal features in pancreatic adenocarcinoma. J. Natl. Cancer Inst. *102*, 340–351.

Rasheed, Z.A., Matsui, W., and Maitra, A. (2012). Pathology of pancreatic stroma in PDAC. In Pancreatic Cancer and Tumor Microenvironment, P.J. Grippo and H.G. Munshi, eds. (India: Trivandrum).

Rhim, A.D., Mirek, E.T., Aiello, N.M., Maitra, A., Bailey, J.M., McAllister, F., Reichert, M., Beatty, G.L., Rustgi, A.K., Vonderheide, R.H., et al. (2012). EMT and dissemination precede pancreatic tumor formation. Cell *148*, 349–361.

Sato, N., Fukushima, N., Maehara, N., Matsubayashi, H., Koopmann, J., Su, G.H., Hruban, R.H., and Goggins, M. (2003). SPARC/osteonectin is a frequent target for aberrant methylation in pancreatic adenocarcinoma and a mediator of tumor-stromal interactions. Oncogene *22*, 5021–5030.

Takahashi, K., and Yamanaka, S. (2006). Induction of pluripotent stem cells from mouse embryonic and adult fibroblast cultures by defined factors. Cell *126*, 663–676.

Tang, F., Barbacioru, C., Nordman, E., Li, B., Xu, N., Bashkirov, V.I., Lao, K., and Surani, M.A. (2010). RNA-Seq analysis to capture the transcriptome landscape of a single cell. Nat. Protoc. *5*, 516–535.

Wei, D., Wang, L., Kanai, M., Jia, Z., Le, X., Li, Q., Wang, H., and Xie, K. (2010). KLF4α up-regulation promotes cell cycle progression and reduces survival time of patients with pancreatic cancer. Gastroenterology *139*, 2135–2145.

Weigelt, B., Wessels, L.F., Bosma, A.J., Glas, A.M., Nuyten, D.S., He, Y.D., Dai, H., Peterse, J.L., and van't Veer, L.J. (2005). No common denominator for breast cancer lymph node metastasis. Br. J. Cancer *93*, 924–932.

Whitfield, M.L., Sherlock, G., Saldanha, A.J., Murray, J.I., Ball, C.A., Alexander, K.E., Matese, J.C., Perou, C.M., Hurt, M.M., Brown, P.O., and Botstein, D. (2002). Identification of genes periodically expressed in the human cell cycle and their expression in tumors. Mol. Biol. Cell *13*, 1977–2000.

Wong, S.Y., Crowley, D., Bronson, R.T., and Hynes, R.O. (2008). Analyses of the role of endogenous SPARC in mouse models of prostate and breast cancer. Clin. Exp. Metastasis *25*, 109–118.

Yu, M., Stott, S., Toner, M., Maheswaran, S., and Haber, D.A. (2011). Circulating tumor cells: approaches to isolation and characterization. J. Cell Biol. *192*, 373–382.

Yu, M., Ting, D.T., Stott, S.L., Wittner, B.S., Ozsolak, F., Paul, S., Ciciliano, J.C., Smas, M.E., Winokur, D., Gilman, A.J., et al. (2012). RNA sequencing of pancreatic circulating tumour cells implicates WNT signalling in metastasis. Nature *487*, 510–513.

Yu, M., Bardia, A., Wittner, B.S., Stott, S.L., Smas, M.E., Ting, D.T., Isakoff, S.J., Ciciliano, J.C., Wells, M.N., Shah, A.M., et al. (2013). Circulating breast tumor cells exhibit dynamic changes in epithelial and mesenchymal composition. Science *339*, 580–584.

Zhang, X.H., Jin, X., Malladi, S., Zou, Y., Wen, Y.H., Brogi, E., Smid, M., Foekens, J.A., and Massagué, J. (2013). Selection of bone metastasis seeds by mesenchymal signals in the primary tumor stroma. Cell *154*, 1060–1073.

PROSTATE CANCER

RNA-Seq of single prostate CTCs implicates noncanonical Wnt signaling in antiandrogen resistance

David T. Miyamoto,[1,2*] Yu Zheng,[1,3*] Ben S. Wittner,[1,4] Richard J. Lee,[1,4] Huili Zhu,[1] Katherine T. Broderick,[1] Rushil Desai,[1] Douglas B. Fox,[1] Brian W. Brannigan,[1] Julie Trautwein,[1] Kshitij S. Arora,[1,5] Niyati Desai,[1,5] Douglas M. Dahl,[1,6] Lecia V. Sequist,[1,4] Matthew R. Smith,[1,4] Ravi Kapur,[7] Chin-Lee Wu,[1,5] Toshi Shioda,[1] Sridhar Ramaswamy,[1,4] David T. Ting,[1,4] Mehmet Toner,[7] Shyamala Maheswaran,[1,8]† Daniel A. Haber[1,3,4]†

Prostate cancer is initially responsive to androgen deprivation, but the effectiveness of androgen receptor (AR) inhibitors in recurrent disease is variable. Biopsy of bone metastases is challenging; hence, sampling circulating tumor cells (CTCs) may reveal drug-resistance mechanisms. We established single-cell RNA-sequencing (RNA-Seq) profiles of 77 intact CTCs isolated from 13 patients (mean six CTCs per patient), by using microfluidic enrichment. Single CTCs from each individual display considerable heterogeneity, including expression of *AR* gene mutations and splicing variants. Retrospective analysis of CTCs from patients progressing under treatment with an AR inhibitor, compared with untreated cases, indicates activation of noncanonical Wnt signaling ($P = 0.0064$). Ectopic expression of Wnt5a in prostate cancer cells attenuates the antiproliferative effect of AR inhibition, whereas its suppression in drug-resistant cells restores partial sensitivity, a correlation also evident in an established mouse model. Thus, single-cell analysis of prostate CTCs reveals heterogeneity in signaling pathways that could contribute to treatment failure.

After the initial response of metastatic prostate cancer to androgen deprivation therapy (ADT), it invariably recurs as castration-resistant disease (*1*). Second-line inhibitors of the androgen receptor (AR) have been shown to increase overall survival in castration-resistant prostate cancer (CRPC), consistent with the reactivation of AR signaling in the tumor, but responses are heterogeneous and often short-lived, and resistance to therapy is a pressing clinical problem (*1*). In other types of cancer, molecular analyses of serial biopsies have enabled the study of acquired drug-resistance mechanisms, intratumor heterogeneity, and tumor evolution in response to therapy (*2*)—an approach that is restricted by the predominance of bone metastases in prostate cancer (*3*, *4*). Thus, isolation of circulating tumor cells (CTCs) may enable noninvasive monitoring, as patients initially respond and subsequently become refractory to therapies targeting the AR pathway (*5*). Here, we established single-cell RNA-sequencing (RNA-Seq) profiles of CTCs, individually isolated after microfluidic enrichment from blood specimens of men with prostate cancer, to address their heterogeneity within and across different patients and their differences from primary tumor specimens. Retrospective analyses of clinical and molecular data were then performed to identify potentially clinically relevant mechanisms of acquired drug resistance.

Building on earlier approaches for capturing and scoring CTCs (*3*), highly efficient microfluidic technologies enable molecular analyses (*6*–*9*). We applied the CTC-iChip to magnetically deplete normal hematopoietic cells from whole-blood specimens (*10*). Untagged and unfixed CTCs were identified by cell surface staining for epithelial and mesenchymal markers [epithelial cell adhesion molecule (EpCAM) and cadherin-11 (CDH11), respectively], and absent staining for the common leukocyte marker CD45. These labeled CTCs were then individually micromanipulated (fig. S1, A and B). A total of 221 single-candidate prostate CTCs were isolated from 18 patients with metastatic prostate cancer and 4 patients with localized prostate cancer (fig. S1C and table S1). Of these, 133 cells (60%) had RNA of sufficient quality for amplification and next-generation RNA sequencing, and 122 (55%) had >100,000 uniquely aligned sequencing reads (*11*) (figs. S1C and S2A). Although many cancer cells in the circulation appear to undergo apoptosis, the presence of intact RNA identifies the subset enriched for viable cells. In addition to candidate CTCs, we also obtained comprehensive transcriptomes for bulk primary prostate cancers from a separate cohort of 12 patients (macrodissected for >70% tumor content) (table S2), 30 single cells derived from four different prostate cancer cell lines, and five patient-derived leukocyte controls (fig. S1C). The leukocytes were readily distinguished by their expression of hematopoietic lineage markers and served to exclude any CTCs with potentially contaminating signals. Strict expression thresholds were used to define lineage-confirmed CTCs, scored by prostate lineage-specific genes (*PSA*, *PSMA*, *AMACR*, and *AR*) and standard epithelial markers (*KRT7*, *KRT8*, *KRT18*, *KRT19*, and *EPCAM*) (*11*) (fig. S2B). Given the presence of leukocyte transcripts suggestive of cellular contamination or misidentification during selection, 28 cells were excluded, and, given low expression of both prostate lineage-specific genes and standard epithelial markers, 17 cells were excluded. The remaining 77 cells (from 13 patients; average of six CTCs per patient) were defined as categorical CTCs (fig. S1C and table S1).

Unsupervised hierarchical clustering analysis of single prostate CTCs, primary tumor samples, and cancer cell lines resulted in their organization into distinct clusters (Fig. 1A). Single CTCs from an individual patient showed considerably greater intercellular heterogeneity in their transcriptional profiles than single cells from prostate cancer cell lines (Fig. 1, B and C) (mean correlation coefficient 0.10 versus 0.44, $P < 1 \times 10^{-20}$), but they strongly clustered according to patient of origin, which indicated higher diversity in CTCs from different patients (Fig. 1C and fig. S2C) (mean correlation coefficient 0.10 for CTCs within patient versus 0.0014 for CTCs between patients, $P = 2.0 \times 10^{-11}$).

We examined gene markers of prostate lineage, epithelial, mesenchymal, and stem cell fates, and cellular proliferation (Fig. 2A). Epithelial markers were abundantly expressed [>10 reads per million (rpm)] by nearly all CTCs analyzed (92%), whereas mesenchymal genes were not up-regulated compared with primary tumors or prostate cancer–derived cell lines. Among robustly expressed transcripts were putative stem cell markers (*12*), including *ALDH7A1*, *CD44*, and *KLF4*, present in 60% of CTCs. In addition, 47% of CTCs expressed markers of cell proliferation. We performed differential gene expression analysis to identify genes that are up-regulated in prostate CTCs compared with primary tumor samples. A total of 711 genes were highly expressed in CTCs compared with primary tumors; the most enriched were (i) the molecular chaperone *HSP90AA1*, which regulates the activation and stability of AR, among other functions (*13*), and (ii) the non-coding RNA transcript *MALAT1*, which has been implicated in alternative mRNA splicing and transcriptional control of gene expression (*14*) (Fig. 2B, fig. S4A, and table S3) [false discovery rate (FDR) < 0.1, and fold change > 2]. We used the Pathway Interaction Database (PID) (*15*) to identify key molecular pathways up-regulated in

[1]Massachusetts General Cancer Center, Massachusetts General Hospital, Harvard Medical School, Charlestown, MA 02129, USA. [2]Department of Radiation Oncology, Massachusetts General Hospital, Harvard Medical School, Charlestown, MA 02129, USA. [3]Howard Hughes Medical Institute, Chevy Chase, MD 20815, USA. [4]Department of Medicine, Massachusetts General Hospital, Harvard Medical School, Charlestown, MA 02129, USA. [5]Department of Pathology, Massachusetts General Hospital, Harvard Medical School, Charlestown, MA 02129, USA. [6]Department of Urology, Massachusetts General Hospital, Harvard Medical School, Charlestown, MA 02129, USA. [7]Center for Bioengineering in Medicine, Massachusetts General Hospital, Harvard Medical School, Charlestown, MA 02129, USA. [8]Department of Surgery, Massachusetts General Hospital, Harvard Medical School, Charlestown, MA 02129, USA.
*These authors contributed equally to this work. †Corresponding author. E-mail: haber@helix.mgh.harvard.edu (D.H.); smaheswaran@mgh.harvard.edu (S.M.)

CTCs versus primary tumors, as well as those upregulated in metastatic versus primary prostate tumors, on the basis of analyses of previously published data sets (*11*) (Fig. 2C, fig. S5, and table S4). In total, 21 pathways were specifically enriched in prostate CTCs, with the majority implicated in growth factor, cell adhesion, and hormone signaling (Fig. 2D and fig. S5).

The AR pathway constitutes the primary therapeutic target in prostate cancer, with specific mutations in *AR* (*1*, *16*) and *AR* mRNA splice variants (*17*, *18*) implicated in acquired resistance. The *AR* transcript was expressed (>10 rpm) in 60 out of 77 (78%) CTCs (12 out of 13 patients with prostate cancer). The T877A mutation (Thr^{877} replaced by Ala) in AR, previously associated with ligand promiscuity and resistance to antiandrogens (*1*), was identified in five out of nine CTCs from a single (1 out of 13) patient with metastatic CRPC (Fig. 3A and table S5). The F876L mutation (Phe^{876} replaced by Leu) in the ligand-binding domain, which converts the AR antagonist enzalutamide to a potential AR agonist (*19*, *20*), was not detected in any of the CTCs (<1 out of 32 CTCs with sufficient sequencing reads for mutational analysis). Thus, in our study, point mutations in *AR* known to be associated with altered signaling were uncommon in patients with CRPC, consistent with other reports (*4*, *21*).

We then analyzed *AR* mRNA splice variants lacking a ligand-binding domain and encoding constitutively active proteins (*1*, *17*). These alternative transcripts are not attributable to discrete genetic mutations, but they are commonly expressed in CRPC (*4*), and detection in bulk CTC preparations of the single splice variant *AR-V7* has been correlated to clinical resistance to antiandrogens (*18*). Our single-cell analysis revealed far more complex and heterogeneous patterns of *AR* splice-variant expression among individual CTCs from patients with CRPC: 33 out of 73 (43%) expressed at least one type of *AR* splice variant (8 out of 11 CRPC patients). Among these CTCs, 26 out of 73 (36%) expressed *AR-V7* (8 out of 11 patients); 18 out of 73 (25%) had a distinct splice form *ARv567es* (*AR-V12*) (8 out of 11 patients); and 7 out of 73 (10%) had *AR-V1*, *AR-V3*, or *AR-V4* splice variants (5 out of 11 patients), all of which are known to result in altered signaling (Fig. 3A and table S6). Simultaneous expression of more than one type of *AR* splice variant was observed in 13 out of 73 (18%) single CTCs (7 out of 11 patients). In total, 7 out of 11 (64%) CRPC patients had CTCs with more than one type of *AR* alteration (including *AR* splice variants and point mutations). In contrast, no such alterations were evident in 12 primary prostate tumors, and only one out of four CTCs from two patients with castration-sensitive prostate cancer (CSPC) that was previously untreated had low-level expression of the *AR-V7* splice variant (Fig. 3A and table S6). Aberrant alternative splicing is a recognized feature of many cancers (*22*), and indeed, another prostate-specific transcript, *KLK3* (*PSA*) (*23*), showed many more alternative splice variants in CTCs from metastatic patients compared with primary tumors (P = 0.0088) (fig. S4B). Taken together, our observations indicate that intrapatient tumor heterogeneity is such that individual CTCs may have different or multiple mRNA splicing alterations.

Tumor heterogeneity is thought to increase further as second-line therapies exert additional selective pressure. We performed retrospective differential analyses in subsets of CTCs to identify mechanisms of resistance to enzalutamide, a potent AR inhibitor recently approved by the U.S. Food and Drug Administration for CRPC (*24*). From eight patients with metastatic prostate cancer who had not received enzalutamide (group A), 41 CTCs were compared with 36 CTCs from five patients whose cancer exhibited radiographic and/or prostate-specific antigen (PSA) progression during therapy (group B) (Fig. 3A and table S1). Gene set enrichment analysis (GSEA) of candidate PID cellular signaling pathways showed significant enrichment for noncanonical Wnt signaling in group B compared with group A CTCs

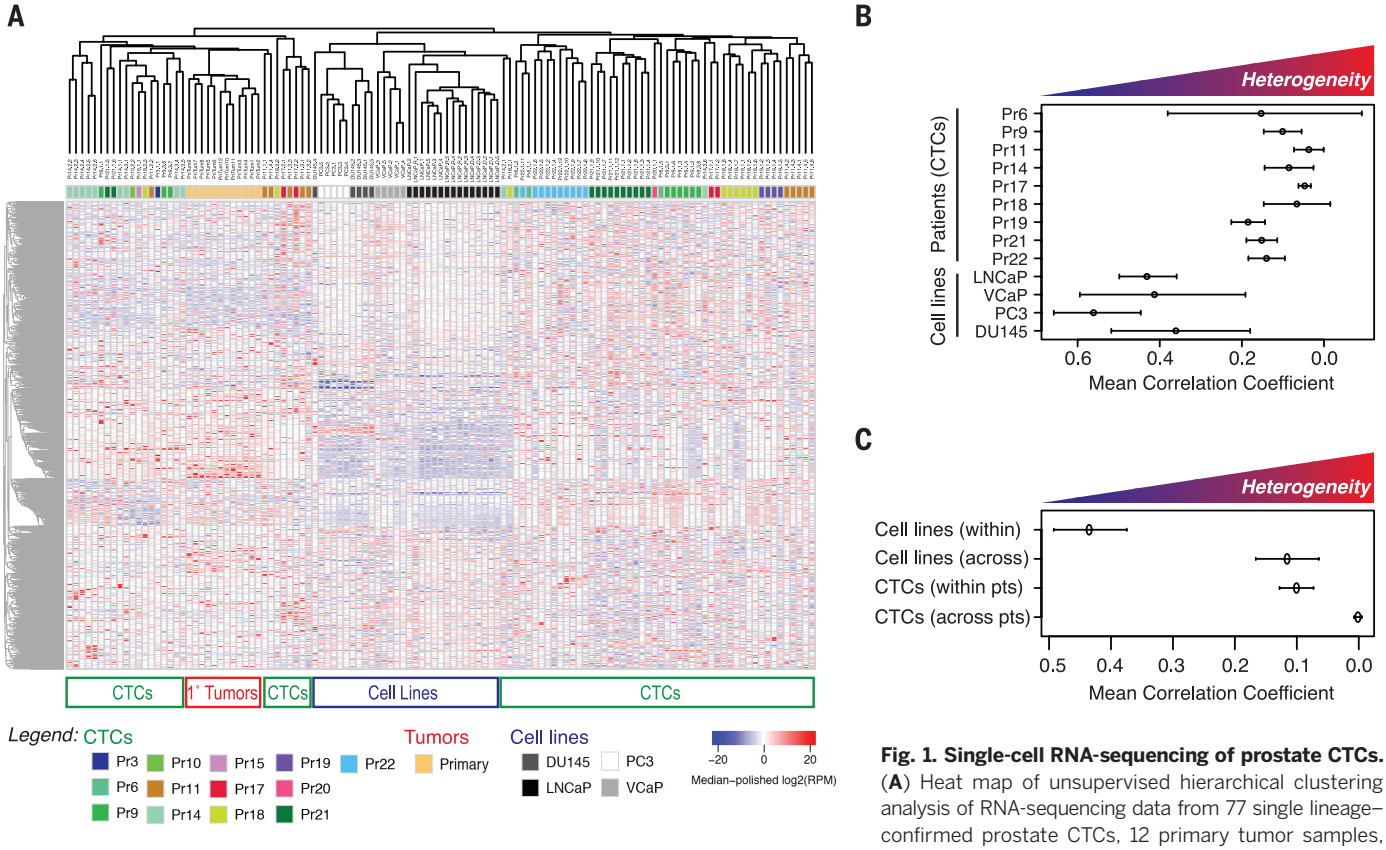

Fig. 1. Single-cell RNA-sequencing of prostate CTCs. (**A**) Heat map of unsupervised hierarchical clustering analysis of RNA-sequencing data from 77 single lineage–confirmed prostate CTCs, 12 primary tumor samples, and 30 single cells from four prostate cancer cell lines. (**B**) Heterogeneity, measured by mean correlation coefficient within individual samples with three or more cells available for analysis. (**C**) Heterogeneity analysis showing mean correlation coefficients from expression data for CTCs between and within patients (0.0013838 versus 0.10055; Holm corrected $P = 2.0 \times 10^{-11}$), and for prostate cancer cell lines between and within lines (0.11568 versus 0.43534; Holm corrected $P = 5.42 \times 10^{-14}$).

(Fig. 3B and fig. S6A) (P = 0.0064; FDR = 0.239). This signaling pathway, activated by a subset of Wnt ligands, mediates multiple downstream regulators of cell survival, proliferation, and motility (fig. S6B) (*25*–*28*). A separate analysis using a metagene for the PID noncanonical Wnt signature (*11*) (table S7) confirmed enrichment of the signature in group B compared with group A CTCs, at the level of both individual CTCs and individual patients (Fig. 3A) [P = 0.0041 (CTCs); P = 0.04 (patients)]. Among the downstream components of noncanonical Wnt, the most significantly enriched were *RAC1*, *RHOA*, and *CDC42*, signaling molecules involved in actin cytoskeleton remodeling and cell migration (Fig. 3A and fig. S6B) [$P = 1 \times 10^{-6}$ (*RAC1*), P = 0.0046 (*RHOA*), P = 0.0097 (*CDC42*)]. In contrast, *AR* abnormalities were not significantly increased among either individual CTCs or patients, when comparing enzalutamide-resistant versus enzalutamide-naïve cases, using a similar analysis (Fig. 3A).

Although most studies of CRPC have focused on acquired *AR* gene abnormalities, an alternative pathway, glucocorticoid receptor (GR) signaling, has recently been shown to contribute to antiandrogen resistance in a prostate cancer mouse xenograft model (*29*). Within our human prostate CTC data set, *GR* transcripts and a metagene signature of GR signaling (*11*) (table S7) did not reach statistical significance between patients in group A versus B [P = 0.35 (CTCs); P = 0.59 (patients)] (Fig. 3A), but an inverse relationship between *GR* expression and noncanonical Wnt signaling was evident. Among CTCs with low *GR* expression, GSEA analysis showed significant enrichment for noncanonical Wnt signaling in

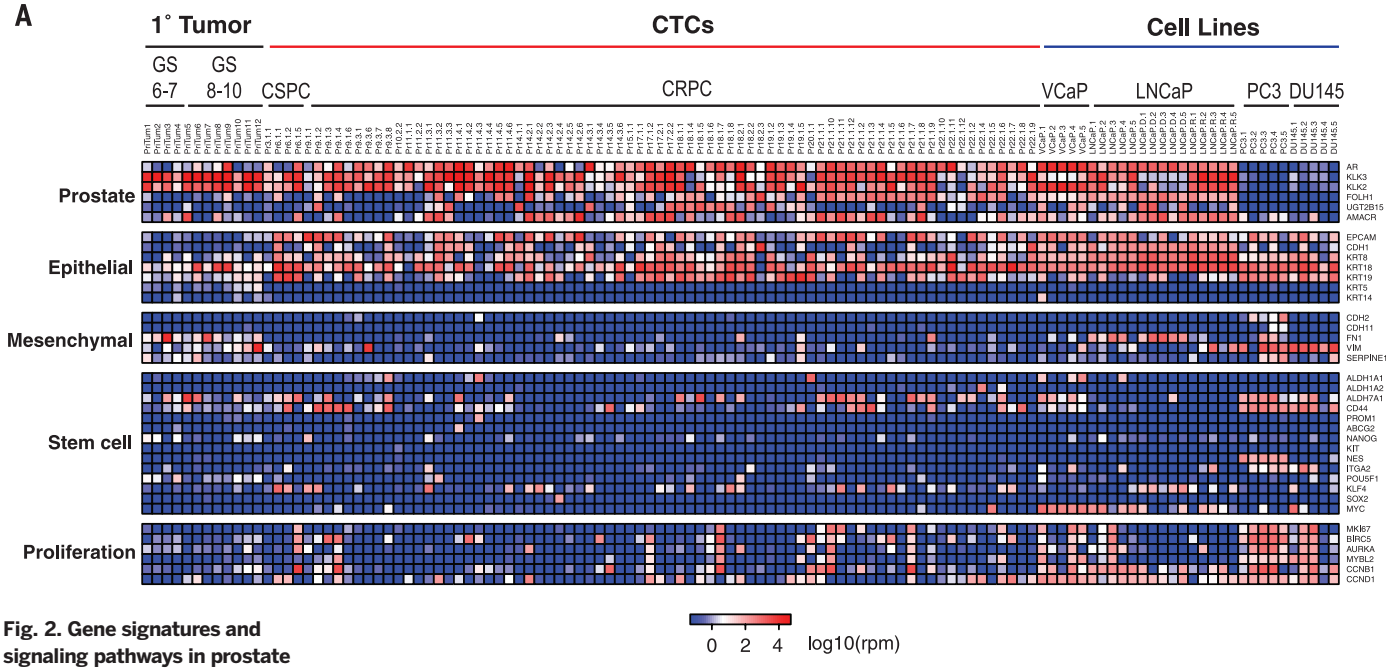

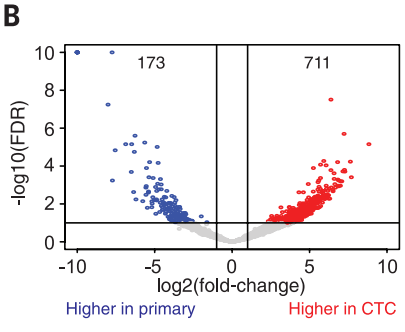

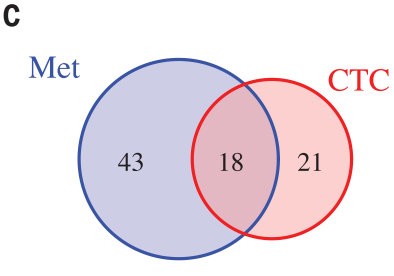

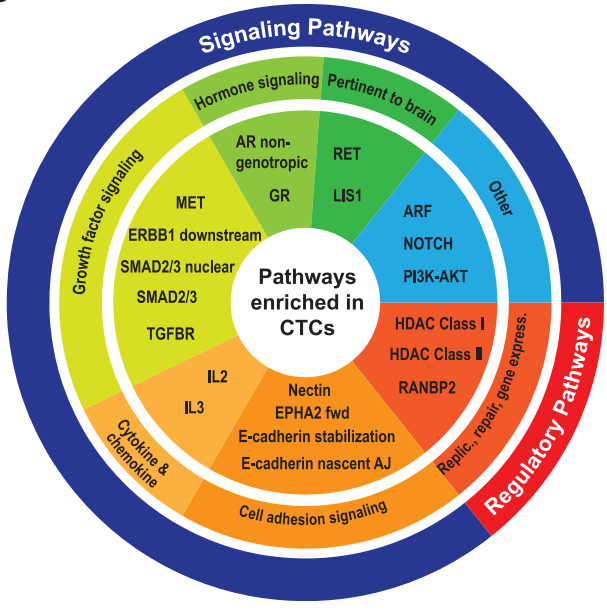

Fig. 2. Gene signatures and signaling pathways in prostate CTCs. (**A**) High-resolution heat map showing expression of selected gene panels in single prostate CTCs, primary tumor samples, and prostate cancer cell lines. GS, Gleason score; VCaP, a PSA-producing cell line; LNCaP.R, LNCaP cells treated with R1881; LNCaP.D, LNCaP cells treated with dimethyl sulfoxide as a vehicle control. (**B**) Genes differentially expressed by prostate CTCs and primary prostate tumors (FDR < 0.1, and fold change > 2). (**C**) PID molecular pathways (*15*) enriched in CTCs compared with primary tumors and in metastases compared with primary tumors (based on analysis of multiple data sets; see fig. S5 and table S4). (**D**) Signaling pathways enriched in prostate CTCs. Molecular pathways from the PID up-regulated in CTCs versus primary tumors (excluding those enriched in metastases compared with primary tumors), organized by PID categorization (*15*) (fig. S5). Abbreviations (other than proteins, clockwise from top): HDAC, histone deacetylase; AJ, adherens junction; IL2 and IL3, interleukins; ERBB1, epidermal growth factor receptor B1; TGFBR, transforming growth factor-β receptor.

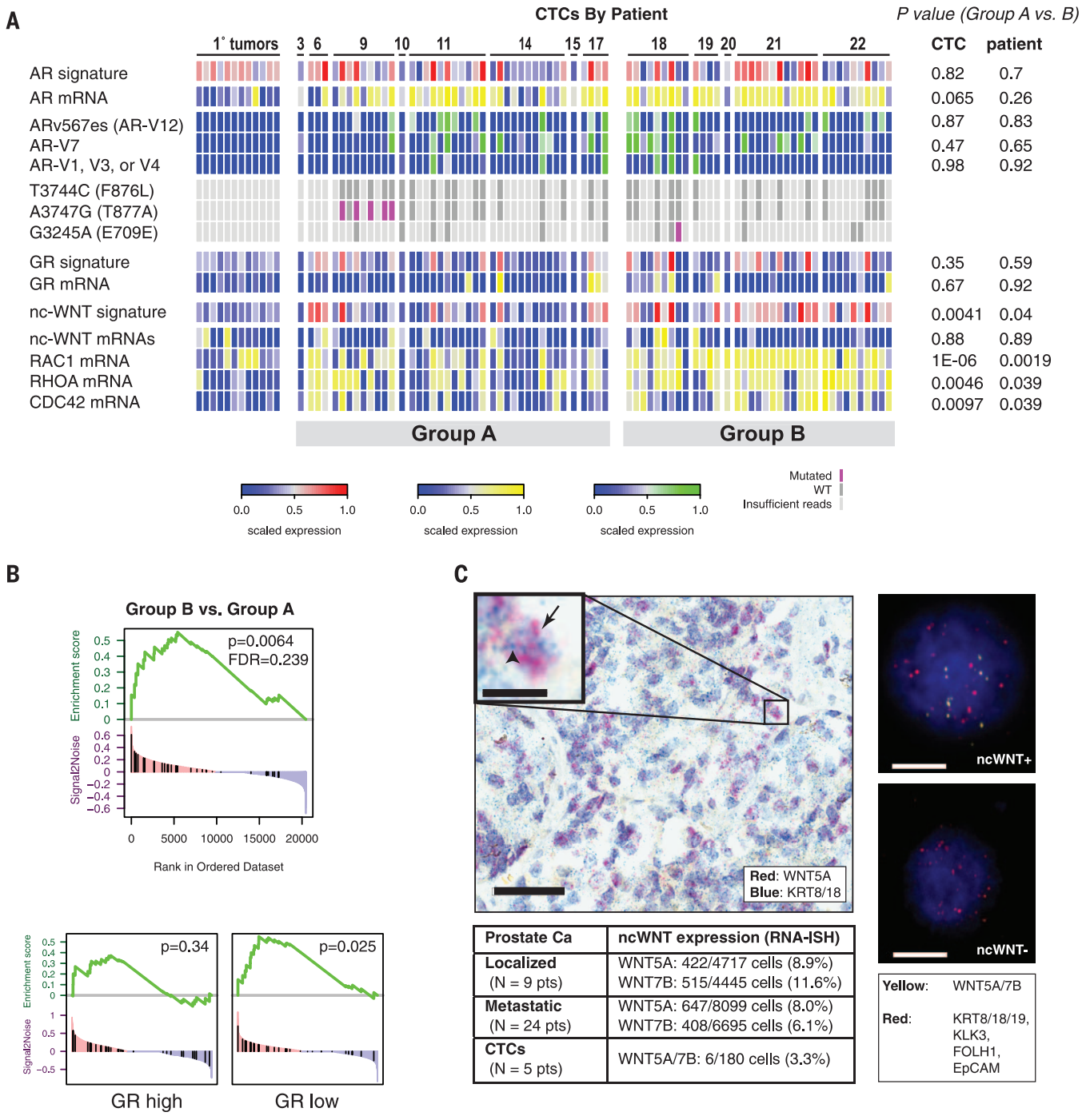

Prostate Ca	ncWNT expression (RNA-ISH)
Localized (N = 9 pts)	WNT5A: 422/4717 cells (8.9%) WNT7B: 515/4445 cells (11.6%)
Metastatic (N = 24 pts)	WNT5A: 647/8099 cells (8.0%) WNT7B: 408/6695 cells (6.1%)
CTCs (N = 5 pts)	WNT5A/7B: 6/180 cells (3.3%)

Fig. 3. Heterogeneity of treatment resistance mechanisms in prostate CTCs. (**A**) Heat map depicting androgen receptor (AR) abnormalities, selected signaling pathway signatures, and genes in radical prostatectomy specimens, prostate CTCs from enzalutamide-naïve patients (group A), and prostate CTCs from patients who had radiographic or biochemical progression of disease while receiving treatment with enzalutamide (group B). Noncanonical Wnt signature is from reference (*15*), glucocorticoid receptor (GR) signature is from reference (*29*), and AR signature is from reference (*32*) (table S7). Numbers at top of heat map represent ID numbers (Pr numbers) for patients from which each CTC is derived. (**B**) (Top) GSEA plots showing enrichment of noncanonical Wnt (nc-Wnt) pathway in CTCs from group B (patients with cancer progression on enzalutamide) compared with group A (enzalutamide-naïve patients). (Bottom) Enrichment of noncanonical Wnt pathway in CTCs from group B compared with group A, stratified by GR gene expression. (**C**) (Left) Representative micrograph (40×) of RNA-in situ hybridization assay in metastatic prostate tumors, probing for *WNT5A* and *KRT8/18*, scale bar, 50 μm. (Inset) High magnification, arrow points to *WNT5A* signal (red dot), arrowhead points to *KRT8/18* signal (blue dot), scale bar, 10 μm. Adjacent tissue sections were probed for *WNT7B*, and quantification of RNA-ISH data are displayed in the table. Of nine primary tumors examined, five had >1% WNT5A expression in KRT+ cells (range 0.3%-42%) and seven had >1% WNT7B expression (range 0.5%-33.6%). Of 24 metastatic tumors examined, 16 had >1% WNT5A expression (range 0 to 50.5%) and 15 had >1% WNT7B expression (range 0 to 26%). (Right) Representative fluorescence micrographs of RNA in situ hybridization in prostate CTCs, probing for *WNT5A/7B* (yellow dots), and prostate CTC-specific markers (*EPCAM*, *KLK3*, *FOLH1*, *KRT8/18/19*) (red dots). DNA is stained with 4′,6′-diamidino-2-phenylindole (blue). Scale bar, 10 μm.

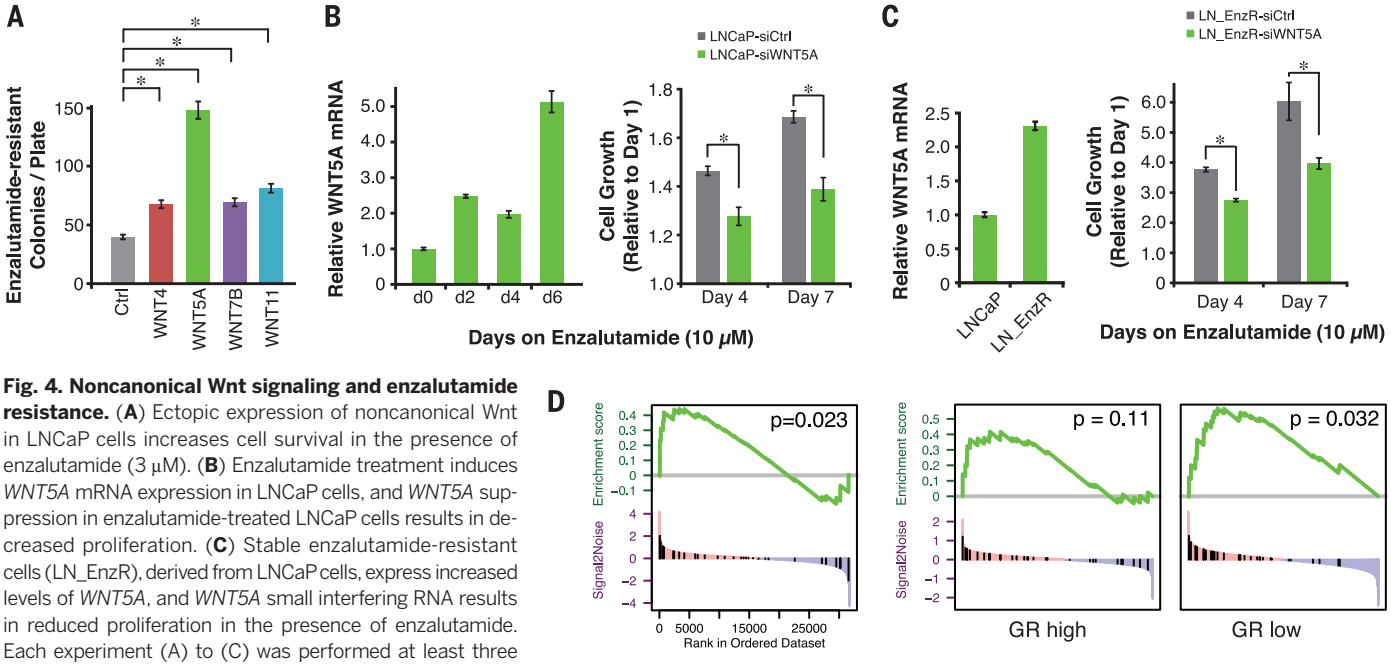

Fig. 4. Noncanonical Wnt signaling and enzalutamide resistance. (**A**) Ectopic expression of noncanonical Wnt in LNCaP cells increases cell survival in the presence of enzalutamide (3 μM). (**B**) Enzalutamide treatment induces *WNT5A* mRNA expression in LNCaP cells, and *WNT5A* suppression in enzalutamide-treated LNCaP cells results in decreased proliferation. (**C**) Stable enzalutamide-resistant cells (LN_EnzR), derived from LNCaP cells, express increased levels of *WNT5A*, and *WNT5A* small interfering RNA results in reduced proliferation in the presence of enzalutamide. Each experiment (A) to (C) was performed at least three times. Data are presented as means ± SD. (**D**) (Left) GSEA plot showing enrichment of noncanonical Wnt pathway in mouse xenografts derived from enzalutamide-resistant LREX′ cells (*29*) compared with control xenografts derived from LNCaP/AR cells (data from LREX′ and Con B entries, GEO GSE52169). (Right) GSEA plots showing noncanonical Wnt pathway enrichment in antiandrogen-resistant xenografts, when stratified by GR gene expression (data from Res and Con A entries, GEO GSE52169).

enzalutamide-progressing patients (group B) (P = 0.025), which was absent in CTCs with high *GR* expression (P = 0.34) (Fig. 3B and fig. S6D). Thus, these two AR-independent drug resistance pathways may predominate in different subsets of cancer cells.

Wnt proteins may be secreted by tumor cells as part of an autocrine loop, or they may be produced by surrounding stromal cells. We used RNA in situ hybridization (RNA-ISH) to identify the source of WNT production in tumor specimens and CTCs. Within primary untreated prostate cancers (n = 9), the noncanonical *WNT5A* and *WNT7B* mRNAs were present in a subset of tumor cells (8.9 and 11.6%, respectively), but both were rare in surrounding stromal cells (<0.2 and 0.5%, respectively) (Fig. 3C and fig. S6C). Metastatic tumor biopsies from patients with CRPC (n = 24) also had readily detectable *WNT5A* and *WNT7B* (8.0 and 6.1%, respectively) (Fig. 3C). Similarly, *WNT5A* or *WNT7B* mRNA was detected by RNA-ISH in a subset of CTCs from patients (n = 5) with CRPC (6 out of 180 CTCs; 3.3%) (Fig. 3C). Thus, a subset of prostate cancer cells express noncanonical Wnt ligands, which may provide survival signals in the context of AR inhibition.

To test whether activation of noncanonical Wnt signaling modulates enzalutamide sensitivity, we ectopically expressed the noncanonical ligands *WNT4*, *WNT5A*, *WNT7B*, or *WNT11* in LNCaP androgen-sensitive human prostate cancer cells, which express low endogenous levels (fig. S7, A and B). Survival of the AR-positive LNCaP cells in the presence of enzalutamide was enhanced by the noncanonical Wnt ligands, particularly *WNT5A* (Fig. 4A) ($P = 2.8 \times 10^{-5}$) (fig. S7C). Remarkably, endogenous *WNT5A* was acutely induced upon treatment with enzalutamide, suggestive of a feedback mechanism, and its depletion (knockdown) resulted in reduced cell proliferation (Fig. 4B and fig. S7D) ($P = 6.6 \times 10^{-4}$). We also generated stable enzalutamide-resistant LNCaP cells through prolonged in vitro selection (fig. S7E). These cells also exhibited increased expression of endogenous *WNT5A*, whose suppression reduced proliferation in enzalutamide-supplemented medium (Fig. 4C) (P = 0.005) (fig. S7F). Finally, we tested the contribution of noncanonical Wnt to antiandrogen resistance in an independent data set, interrogating the previously published mouse LNCaP xenograft model, in which aberrant activation of GR contributes to enzalutamide resistance (*29*). A significant association between enzalutamide resistance and noncanonical Wnt signaling was evident (P = 0.023), which again showed an inverse relation between *GR* expression and noncanonical Wnt signaling (P = 0.032 for *GR* low versus P = 0.11 for *GR* high) (Fig. 4D and fig. S8, A and B). This independent data set further validates the independent contributions of GR and noncanonical Wnt signaling to antiandrogen resistance.

In summary, by RNA profiling single prostate CTCs, we demonstrate their differences from primary tumors, as well as their heterogeneity within individual patients. The acquisition of AR-dependent and AR-independent alterations conferring resistance to antiandrogen therapies is also heterogeneous. Among *AR* alterations, more than half of all patients had multiple *AR* splice variants present within different CTCs and about 1 out of 6 of single cancer cells had simultaneous expression of several *AR* splice variants. Two AR-independent pathways, activation of GR and noncanonical Wnt signaling, coexist in different subsets of cells. Wnt signaling has been implicated in multiple cellular functions linked to prostate cancer progression (*4*, *25*–*28*), and noncanonical Wnt signaling may be targeted by suppression of its key downstream components, such as Rho kinase (*30*). Our study is limited by its retrospective nature and relatively small sample size (13 patients; average of six CTCs per patient), a consequence of the rarity of intact CTCs and inefficiencies inherent in manual single-cell micromanipulation techniques, obstacles that might be overcome with future improvements in CTC isolation and single-cell sequencing technologies. Nevertheless, the heterogeneity of CTCs in patients with CRPC stands in contrast to the striking homogeneity of AR signaling in single CTCs from untreated patients (*5*). Although these observations require validation in prospective trials, they point to complex and heterogeneous drug resistance mechanisms in advanced prostate cancer, which may affect therapeutic efficacy.

REFERENCES AND NOTES

1. A. Egan *et al.*, *Cancer Treat. Rev.* **40**, 426–433 (2014).
2. M. Gerlinger *et al.*, *N. Engl. J. Med.* **366**, 883–892 (2012).
3. H. I. Scher, M. J. Morris, S. Larson, G. Heller, *Nat. Rev. Clin. Oncol.* **10**, 225–234 (2013).
4. D. Robinson *et al.*, *Cell* **161**, 1215–1228 (2015).
5. D. T. Miyamoto *et al.*, *Cancer Discov* **2**, 995–1003 (2012).
6. D. Ramsköld *et al.*, *Nat. Biotechnol.* **30**, 777–782 (2012).
7. J. G. Lohr *et al.*, *Nat. Biotechnol.* **32**, 479–484 (2014).
8. N. Aceto *et al.*, *Cell* **158**, 1110–1122 (2014).
9. D. T. Ting *et al.*, *Cell Reports* **8**, 1905–1918 (2014).
10. E. Ozkumur *et al.*, *Sci. Transl. Med.* **5**, 179ra47 (2013).
11. Materials and methods are available as supporting material on *Science* Online.

12. B. Sharpe, M. Beresford, R. Bowen, J. Mitchard, A. D. Chalmers, *Stem Cell Rev.* **9**, 721–730 (2013).
13. J. Trepel, M. Mollapour, G. Giaccone, L. Neckers, *Nat. Rev. Cancer* **10**, 537–549 (2010).
14. T. Gutschner, M. Hämmerle, S. Diederichs, *J. Mol. Med. (Berlin)* **91**, 791–801 (2013).
15. C. F. Schaefer *et al.*, *Nucleic Acids Res.* **37** (Database), D674–D679 (2009).
16. B. Gottlieb, L. K. Beitel, A. Nadarajah, M. Paliouras, M. Trifiro, *Hum. Mutat.* **33**, 887–894 (2012).
17. C. Lu, J. Luo, *Transl. Androl. Urol.* **2**, 178–186 (2013).
18. E. S. Antonarakis *et al.*, *N. Engl. J. Med.* **371**, 1028–1038 (2014).
19. M. D. Balbas *et al.*, *eLife* **2**, e00499 (2013).
20. J. D. Joseph *et al.*, *Cancer Discov* **3**, 1020–1029 (2013).
21. S. Carreira *et al.*, *Sci. Transl. Med.* **6**, 254ra125 (2014).
22. J. Zhang, J. L. Manley, *Cancer Discov* **3**, 1228–1237 (2013).
23. L. Kurlender *et al.*, *Biochim. Biophys. Acta* **1755**, 1–14 (2005).
24. H. I. Scher *et al.*, *N. Engl. J. Med.* **367**, 1187–1197 (2012).
25. M. Katoh, M. Katoh, *Clin. Cancer Res.* **13**, 4042–4045 (2007).
26. S. Takahashi *et al.*, *Proc. Natl. Acad. Sci. U.S.A.* **108**, 4938–4943 (2011).
27. D. Zheng *et al.*, *Mol. Cancer Res.* **11**, 482–493 (2013).
28. T. S. Gujral *et al.*, *Cell* **159**, 844–856 (2014).
29. V. K. Arora *et al.*, *Cell* **155**, 1309–1322 (2013).
30. N. Rath, M. F. Olson, *EMBO Rep.* **13**, 900–908 (2012).
31. F. Tang *et al.*, *Nat. Methods* **6**, 377–382 (2009).
32. H. Hieronymus *et al.*, *Cancer Cell* **10**, 321–330 (2006).

ACKNOWLEDGMENTS

We thank C. Sawyers for helpful discussions; A. McGovern, E. Stadtmueller, and B. Abebe for clinical trial support; and L. Libby and L. Nieman for technical assistance. This work was supported by grants from the Prostate Cancer Foundation (D.A.H., S.M., M.T., M.R.S., and R.J.L.), Charles Evans Foundation (D.A.H.), Department of Defense (D.T.M., R.J.L., and D.T.T.), Stand Up to Cancer (D.A.H., M.T., S.M., and L.V.S.), Howard Hughes Medical Institute (D.A.H.), National Institute of Biomedical Imaging and Bioengineering (NIBIB), NIH, EB008047 (M.T.), NCI 2RO1CA129933 (D.A.H.), National Cancer Institute, NCI, Federal Share Program and Income (S.M. and D.T.M.), Affymetrix, Inc. (D.T.T., K.A., and N.D.), Mazzone Program–Dana-Farber Harvard Cancer Center (D.T.M.), Burroughs Wellcome Fund (D.T.T.), and the Massachusetts General Hospital–Johnson & Johnson Center for Excellence in CTC Technologies (D.A.H., M.T., and S.M.). D.T.T. is a paid consultant for Affymetrix, Inc.; R.J.L. is a paid consultant for Janssen LLC. The Massachusetts General Hospital has filed for patent protection for the CTC-iChip technology. RNA-sequencing data have been deposited in GEO under accession number GSE67980.

SUPPLEMENTARY MATERIALS

www.sciencemag.org/content/349/6254/1351/suppl/DC1
Materials and Methods
Figs. S1 to S8
Tables S1 to S7
References (*33*–*37*)

10 March 2015; accepted 3 August 2015
10.1126/science.aab0917

SMALL PEPTIDES

Pri sORF peptides induce selective proteasome-mediated protein processing

J. Zanet,[1,2]* E. Benrabah,[1,2]* T. Li,[3] A. Pélissier-Monier,[1,2] H. Chanut-Delalande,[1,2] B. Ronsin,[1,2] H. J. Bellen,[3,4] F. Payre,[1,2]† S. Plaza[1,2]†

A wide variety of RNAs encode small open-reading-frame (smORF/sORF) peptides, but their functions are largely unknown. Here, we show that *Drosophila polished-rice* (*pri*) sORF peptides trigger proteasome-mediated protein processing, converting the Shavenbaby (Svb) transcription repressor into a shorter activator. A genome-wide RNA interference screen identifies an E2-E3 ubiquitin-conjugating complex, UbcD6-Ubr3, which targets Svb to the proteasome in a *pri*-dependent manner. Upon interaction with Ubr3, Pri peptides promote the binding of Ubr3 to Svb. Ubr3 can then ubiquitinate the Svb N terminus, which is degraded by the proteasome. The C-terminal domains protect Svb from complete degradation and ensure appropriate processing. Our data show that Pri peptides control selectivity of Ubr3 binding, which suggests that the family of sORF peptides may contain an extended repertoire of protein regulators.

Eukaryotic genomes encode many noncoding RNAs (ncRNAs) that lack the classical hallmarks of protein-coding genes. However, both ncRNAs and mRNAs often contain small open reading frames (sORFs), and there is growing evidence that they can produce peptides, from yeast (*1*) to plants (*2*, *3*) or humans (*4*, *5*). The *polished rice* or *tarsal-less* (*pri*) RNA contains four sORFs that encode highly related 11– to 32–amino acid peptides, required for embryonic development across insect species (*6*–*8*). In flies, *pri* is essential for the differentiation of epidermal outgrowths called trichomes (*7*, *8*). Trichome development is governed by the Shavenbaby (Svb) transcription factor (*9*–*11*); however, only in the presence of *pri* can Svb turn on the program of trichome development, i.e., activate expression of cellular effectors (*12*, *13*). Indeed, the Svb protein is translated as a large repressor, *pri* then induces truncation of its N-terminal region, which leads to a shorter activator (*12*). Thereby, *pri* defines the developmental timing of epidermal differentiation, in a direct response to systemic ecdysone hormonal signaling (*14*). Although we now have a clear framework for the developmental functions of *pri*, how these small peptides can trigger Svb processing is unknown.

To identify factors required for Svb processing in response to *pri*, we performed a genome-wide RNA interference (RNAi) screen in a cell line co-expressing green fluorescent protein (GFP)–tagged Svb and *pri* (Fig. 1A). We set up an automated assay quantifying Svb processing for each of the *Drosophila* genes, with an inhibitory score reflecting the proportion of cells unable to cleave off the Svb N terminus (see the supplementary materials). *pri* RNAi displayed the highest score, which validated our approach to identifying molecular players in Svb processing. Methods used to evaluate results from genome-wide screening all converged on a key role for the proteasome. For instance, COMPLEAT, a bioinformatic frame-

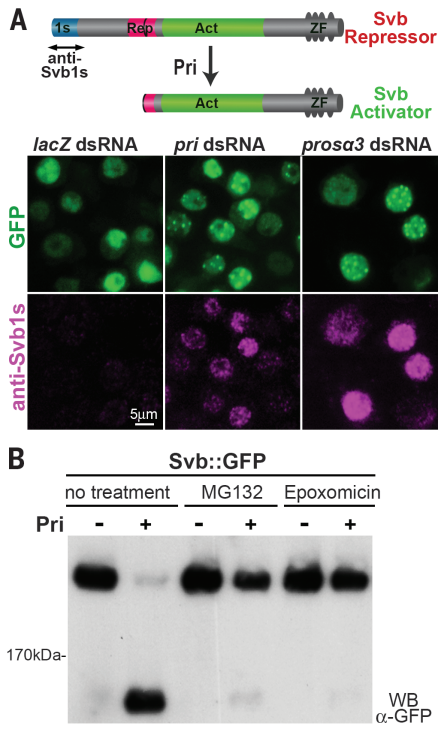

Fig. 1. Pri-dependent processing of Svb requires proteasome activity. (**A**) Drawing of Svb processing (antibody against Svb1s recognizes the repressor-specific N-terminal region) and snapshots from the screen illustrating the effect of double-stranded RNA against *lacZ* (negative control), *pri*, and *proteasomeα3* subunit (*prosα3*) on Svb::GFP processing. Cells were stained for Svb1s (purple) and GFP (green). (**B**) Western blot analysis of cells that express Svb::GFP, with or without *pri* and proteasome inhibitors (MG132, epoxomicin).

[1]Centre de Biologie du Développement, Université de Toulouse III—Paul Sabatier, Bâtiment 4R3, 118 route de Narbonne, F-31062 Toulouse, France. [2]CNRS, UMR5547, Centre de Biologie du Développement, F-31062 Toulouse, France. [3]Program in Developmental Biology, Baylor College of Medicine, Houston, TX 77030, USA. [4]Department of Molecular and Human Genetics, Howard Hughes Medical Institute, Neurological Research Institute, Baylor College of Medicine, Houston, TX 77030, USA.
*These authors contributed equally to this work. **†Corresponding author. E-mail: francois.payre@univ-tlse3.fr (F.P.); serge.plaza@univ-tlse3.f (S.P.)**

Originally posted 17 September 2015; revised 25 September 2015

www.sciencemag.org/content/349/6254/1351/suppl/DC1

Supplementary Materials for

RNA-Seq of single prostate CTCs implicates noncanonical Wnt signaling in antiandrogen resistance

David T. Miyamoto, Yu Zheng, Ben S. Wittner, Richard J. Lee, Huili Zhu, Katherine T. Broderick, Rushil Desai, Douglas B. Fox, Brian W. Brannigan, Julie Trautwein, Kshitij S. Arora, Niyati Desai, Douglas M. Dahl, Lecia V. Sequist, Matthew R. Smith, Ravi Kapur, Chin-Lee Wu, Toshi Shioda, Sridhar Ramaswamy, David T. Ting, Mehmet Toner, Shyamala Maheswaran,* Daniel A. Haber*

*Corresponding author. E-mail: haber@helix.mgh.harvard.edu (D.H.); smaheswaran@mgh.harvard.edu (S.M.)

Published 18 September 2015, *Science* **349**, 1351 (2015)
DOI: 10.1126/science.aab0917

This PDF file includes

Other Supplementary Material for this manuscript includes the following:
(available at www.sciencemag.org/content/349/6254/1351/suppl/DC1)

Correction (25 September 2015): References were renumbered after the file was posted. The renumbering affected the supplementary reference citations, the list of references, and Table S7. The originally posted version can be seen here.

Materials and Methods

Patients and clinical specimens

Patients with a diagnosis of prostate cancer provided informed consent to one of two Institutional Review Board approved protocols (metastatic disease, (DF/HCC 05-300), or localized prostate cancer, (DF/HCC 08-207)). A total of 38 patients donated 20 mL of blood for CTC analysis, of which 18 patients with metastatic prostate cancer and 4 patients with localized untreated prostate cancer had identifiable CTCs (see below and Fig. S1C). Disease status and therapy at the time of CTC collection for each patient are provided in Table S1. Patients were retrospectively categorized as Group A if they had not received enzalutamide at the time of CTC collection (enzalutamide-naïve), and Group B if they were treated with enzalutamide at the time of CTC collection and their cancer exhibited radiographic and/or PSA progression during enzalutamide therapy. Frozen primary tumor tissues from an additional 12 patients with localized prostate cancer were sectioned, macrodissected for >70% tumor content, and subjected to RNA extraction, prior to diluting to single cell levels and processing for RNA sequencing (see below). Detailed patient characteristics are provided in Table S2. Additional frozen primary prostate tumors from 9 patients and metastatic tumors from 24 patients were obtained, sectioned, and processed for RNA-ISH (see below).

Circulating tumor cell isolation

Single CTCs were isolated from fresh whole blood following leukocyte depletion using the microfluidic CTC-iChip as previously described (*10*). To maximize recovery of intact CTCs with high quality RNA, blood samples were processed within 4 hours of being collected from the patient. The total time for single CTC isolation after receipt of fresh blood samples in the lab was approximately 2.5 hours. Briefly, whole blood samples were spiked with biotinylated antibodies against CD45 (R&D Systems, clone 2D1) and CD66 (AbD Serotec, clone 80H3), followed by incubation with Dynabeads MyOne Streptavidin T1 (Invitrogen) to achieve magnetic labeling and depletion of white blood cells. After processing of whole blood with the CTC-iChip, the CTC-enriched product was stained in solution with Alexa 488-conjugated antibodies against EpCAM (Cell Signaling Technology, clone VU1D9) and Cadherin 11 (CDH11) (R&D Systems, clone 667039) to identify CTCs, and PE-CF594-conjugated antibody against CD45 (BD Biosciences, clone HI30) to counterstain contaminating leukocytes. Patient blood samples were screened by microscopic visualization for stained CTCs. Single cells were individually micromanipulated using a 10 μm transfer tip on an Eppendorf TransferMan NK 2 micromanipulator, transferred into PCR tubes containing RNA protective lysis buffer, and flash frozen in liquid nitrogen. A total of 221 putative single CTCs were successfully isolated by micromanipulation (see Fig. S1C).

Single cell RNA sequencing

Complementary DNA (cDNA) was prepared from single cells, amplified and subjected to

library construction for transcriptome analysis using the ABI SOLiD platform, following published protocols (*31*), with slight modifications as previously described (*9*). Only cells passing quality control qPCR for GAPDH and beta-actin were subjected to library construction, followed by sequencing on the ABI 5500XL. RNA sequencing and digital gene expression profiling yielded an average of 4 to 5 million uniquely aligned reads per sample (Fig. S2A). Of the 133 single prostate CTCs that were successfully subjected to next generation RNA sequencing, 122 (92%) had greater than 100,000 aligned reads (Fig. S2A).

Bioinformatic analyses

RNA sequences from single cells, patient-derived leukocytes, and primary tumor samples were aligned to the known human transcriptome (hg19) using TopHat (*33*). Determination of Reads-Per-Million (RPM) and log10(RPM) were performed as previously described (*8*). The reads from dbGaP dataset phs000443.v1.p1 (*34*) were processed the same way with the exception that, since these samples were run on an Illumina GAII rather than a SOLiD sequencer, we first subjected the reads to the program trimmomatic's ILLUMINACLIP TruSeq2-SE.fa function to remove the adapter and other Illumina-specific sequences from the read. Unsupervised clustering analysis was performed using agglomerative hierarchical clustering with average linkage (Fig. 1A).

For independent validation of the quality of our single cell RNA-seq data, we confirmed the expression of a panel of genes in a subset of isolated single prostate CTCs using an independent methodology, single cell multiplex qRT-PCR (Fluidigm Biomark), as previously described (*10*) (Fig. S2D). In addition, we compared a list of genes that were highly upregulated in primary tumors in our RNA-seq data set with the expression profiles of these same genes in a previously published RNA-seq data set that included primary and metastatic prostate tumors (dbGaP dataset phs000443.v1.p1) (*34*) (Fig. S3). This analysis showed that genes that were highly expressed in primary tumors compared to CTCs in our data set were also highly expressed in primary tumors compared to metastases in the previously published data set.

Thresholding to select lineage-confirmed CTCs

Stringent expression thresholds were used to define lineage-confirmed CTCs, in order to exclude specimens containing contaminating leukocytes and ensure analysis of bonafide prostate CTCs (Fig. S2B). For each specimen we let its y-value be the maximum of its log10(RPM) for CD45 and CD16 (leukocyte markers) and let its x-value be the maximum of its log10(RPM) for KRT7, KRT8, KRT18, KRT19, EPCAM, AR, KLK3 (PSA), FOLH1 (PSMA) and AMACR (prostate-specific and epithelial markers). We defined an x-threshold as the midpoint between the maximum x-value of the white blood cells and the minimum x-value of the prostate cell lines. We defined a y-threshold as the midpoint between the minimum y-value of the white blood cells and the maximum y-value of the prostate cancer cell lines. We designated a candidate CTC as lineage-confirmed if its x-value was greater than the x-threshold and its y-value was less than the y-threshold.

Heterogeneity

To compare heterogeneity within and between subsets of specimens, we used means of correlation coefficients and jackknife estimates as follows. Determine the 2000 genes with the highest variance in log10(RPM) values across all specimens. Let v_i denote the log10(RPM) values for those 2000 genes for the i^{th} specimen and let $c(i, j)$ denote the Pearson correlation coefficient between v_i and v_j. Given T, a subset of the set of pairs of specimens, we let

$$M_T = \underset{(i,j)\in T}{\text{mean}}(\text{atanh}(c(i, j))).$$

Let s_T be the jackknife estimator of the standard deviation of M_T, where the jackknife is with respect to specimens (not pairs of specimens). We then call $\tanh(M_T)$ the "mean correlation coefficient" and define its 95% confidence interval to be $\tanh(M_T \pm s_T\Phi^{-1}(0.975))$, where Φ is the cumulative distribution function of the standard normal distribution. Given two subsets of the set of pairs of specimens, T and U, to compute a p-value for the null hypothesis that the mean of M_T is the same as the mean of M_U, we let

$$p = 2\left(1 - \Phi\left(\left|M_T - M_U\right| / \sqrt{s_T^2 + s_U^2}\right)\right).$$

To consider whether there's a significant difference between the heterogeneity in cell lines and CTCs, we let T be (i, j) such that $i > j$ and specimens i and j are cells from the same cell line and let U be (i, j) such that $i > j$ and specimens i and j are CTCs from the same patient. To consider whether there's a significant difference between the within-patient heterogeneity and the between-patient heterogeneity, we let T be (i, j) such that $i > j$ and specimens i and j are CTCs from the same patient and we let U be (i, j) such that $i > j$ and specimens i and j are CTCs from different patients.

Differential gene expression

Supervised differential gene expression was performed for the datasets shown in Fig. S5 and Table S4. For each RNA-seq dataset, we first filtered out genes for which the 0.9 quantile of RPM values was less than 10. For each microarray dataset, we first filtered out genes for which the 0.9 quantile of unlogged expression units per million was less than 10. A t-test assuming equal variance in the two classes was then performed for each gene on the log10(RPM) values for the RNA-seq datasets and on the GEO-provided expression values for the microarray datasets. The resulting p-values were used to create False Discover Rate (FDR) estimates by the Benjamini-Hochberg (BH) method. A gene was considered differentially expressed if its FDR estimate was less than 0.1 and its fold-change was greater than 2.

Gene set enrichment

Enrichment of signaling pathways in the differentially expressed genes was determined by performing a hypergeometric test for gene sets in the Pathway Interaction Database (PID) (*15*). When considering multiple gene sets, the resulting p-values were used to estimate FDR by BH. When determining pathways differentially expressed in CTCs versus primary tumors but not in metastatic tumors (Fig. 2C and 2D), to be conservative

in pathways we identified as uniquely enriched in CTCs, we used an FDR threshold of 0.1 for the CTC versus primary tumors comparison and 0.25 for the metastatic versus primary tumors comparisons.

GSEA version gsea2-2.0.14 was run first on the PID gene sets from version 4.0 of MSigDB (*35*) to generate hypotheses (Fig. 3B, upper panel) and later on specific gene sets to test hypotheses (Fig. 3B, lower panels and Fig. 4D). For right panels of Fig. 4D, we considered samples in GEO GSE52169 to be resistant and GR-high if their title began with "Res - top 50th percentile of GR expressers" or "Res - top 75th percentile of GR expressers." Those whose title began with "Res - Low GR" we considered to be resistant and GR-low.

Androgen receptor (AR) splice variants

To look for evidence of the AR splice variants discussed in Egan et al. (*1*), we consulted Lu and Luo (*17*) for genomic locations of the cryptic exons. We then added the splice variants found in Figure 3 of Egan et al. (*1*) to the transcriptome we had used for aligning and re-aligned. We then submitted the resulting new alignments to cufflinks (*33*) to quantify the different AR splice variants. We found that the 3'-biased nature of our reads caused cufflinks to output very wrong interpretations since cufflinks interprets a lack of reads in a location as evidence against any splice variant that should have reads at that location. So, we decided to only look for positive evidence of AR splice variants. We counted reads spanning exons 4 and 8 or spanning exons 8 and 9 (see Figure 1 of Lu and Luo (*17*) as evidence of AR^{v567es} (AR-V12). We normalized these counts by the total number of reads that spanned exons in that specimen. We counted reads aligning to cryptic exon CE3 to be evidence of AR-V7 and reads aligning to cryptic exons CE4 or CE1 to be evidence of AR-V1, AR-V3 or AR-V4. These counts of alignments to cryptic exons were normalized by the total number of aligned reads for that specimen.

KLK3 splice variants

To look for evidence of KLK3 splice variants we added the splice variants found in Figure 6 of Kurlender et al. (*23*) to the transcriptome we had used for aligning and then re-aligned. We counted reads overlapping the introns in that figure as evidence of the splice variants that contain sequence from those introns as indicated in the figure (after noting that the second variant labeled NA in the figure has since been named NM_001030047 and the third variant labeled NA in the figure has since been named NM_001030048). These counts of alignments to introns were normalized by the total number of uniquely aligned reads for that specimen.

AR mutations

To look in our single-cell RNA sequencing data for evidence of known prostate-related mutations in the AR, we downloaded the Androgen Receptor Gene Mutations Database (*16*) as available at http://androgendb.mcgill.ca on June 12, 2014. We filtered the database as follows. We kept only those entries with the word "Prostate" in the "Phenotype" column. We knew that our alignment had yielded no insertions or deletions in the AR, so we kept only those entries for which the "Mutation type" column was "Substitut.". We then kept only those entries for which the "To nucleotide" column was

">A", ">C", ">G", or ">T" and for which the "nucleotide position" field was present. We also fixed the record with accession number 568 to have "nucleotide position" equal to 2688 and "From nucleotide" set to "2688G". We then removed records that had the same "nucleotide position" as previous records. Finally, we added the F876L mutation (*19, 20*) (which in NM_000044.2 (the version of AR used in the database) is at amino acid 877 and is a T -> C substitution at nucleotide 3744).

For each mutation in the database and each single-cell specimen, we counted how many reads aligned to the position, how many were wild-type, and how many were the "To nucleotide" from the database. In order to determine which mutations were statistically significant, we needed an estimate of the error rate of our sequencing procedure. Since the AR is on the X chromosome and we are only considering single cells, we expected the reads at a particular location to be almost all wild-type or almost all not wild-type. Indeed, we found this to be the case. Only two location/specimen pairs had a percentage of wild-type reads between 10% and 85%. The 3068 other location/specimen pairs had a percentage of wild-type reads less than 10% or greater then 85%. We assumed, therefore, that the location/specimen pairs with percentage of wild-type reads greater than 85% were, in fact, wild-type and that any non-wild-type read was an error. This gave us an error rate estimate of 0.0012. For each location/specimen pair, we then did a one-sided binomial test with alternative hypothesis being that the probability of getting the substitution listed in the database is greater than 0.0012. We adjusted all the resulting p-values for multiple hypothesis testing using the Holms method. We concluded there was a mutation at those location/specimen pairs for which the adjusted p-value was less than 0.05 and the percentage of reads that matched the mutation in the database was greater than 90%.

Metagene computation

If we let $x_1, x_2, \ldots, x_m$ be the log10(RPM) values of the UP genes of a signature and let $y_1, y_2, \ldots, y_n$ be the log10(RPM) values of the DOWN genes of that signature, we define the metagene to be $(x_1 + x_2 + \ldots + x_m - y_1 - y_2 - \ldots - y_n)/(m+n)$. The UP and DOWN genes of the signatures for which we computed metagenes are given in Table S7.

P-values for Group A vs. Group B

The "CTC" p-values were computed by a two-sided t-test with Welch approximation to the degrees of freedom applied to the log10(RPM) values of Group A specimens versus those of Group B specimens. The "patient" p-values were determined by fitting the mixed effects model

$$e_{i,j} = \beta_0 + \beta_1 I_i + b_i + \varepsilon_{i,j},$$

where $e_{i,j}$ is the log10(RPM) value of the jth specimen from the ith patient, I_i is 0 if the ith patient is in Group A and 1 otherwise, $b_i \sim N(0, \sigma_b^2)$ and $\varepsilon_{i,j} \sim N(0, \sigma^2)$. The "patient" p-value was defined as the two-sided p-value for the null hypothesis $\beta_1 = 0$ as determined by the lme function of the R package nlme.

P-values for KLK3 splice variants in primary tumors vs. CTCs
For each sample, we summed the counts described in the "KLK3 splice variants" paragraph above and then normalized the sum by the total number of uniquely aligned reads. "CTC" p-values and "patient" p-values were then computed as in the "P-values for Group A vs. Group B" paragraph above.

RNA In-Situ Hybridization (RNA-ISH)

RNA-ISH in prostate tumor tissues
RNA in situ Hybridization (RNA-ISH) was performed using the Affymetrix ViewRNA ISH Tissue Assay Kit (2-plex). Briefly, paraffin-embedded tissue blocks were freshly cut and frozen at -80°C until staining. Upon removal from the freezer, slides were baked for 1 hr at 60°C. Slides were treated with Histo-Clear to remove paraffin. Tissue sections were pretreated in pretreatment buffer solution for 10 min at 95°C and digested with protease for 10 min, before being fixed at RT in 5% formaldehyde. Target probe sets were applied and hybridized to the tissue by incubating for 2 hr at 40°C. Type 1 WNT5A (VA1-12202) was used at 1:50, and Type 6 probes KRT8, KRT18, and KLK3 (when used) (VA6-11560, VA6-11561, VA6-13505) pooled each at 1:200. Signal was amplified through the sequential hybridization of PreAmplifier and Amplifer QT mixes to the target probe set. Target mRNA molecules were detected by applying Type 6 Label Probe with Fast Blue substrate and Type 1 Label Probe with Fast Red substrate. Tissue was counterstained with Gill's Hematoxylin for 10 sec at RT. DAPI (Invitrogen, D3571; 3.0 μg/ml) staining was performed for 1 min. Slides were imaged on the Aperio microscopy system within 1 week of staining to maintain a digital pathology archive of specimens.

RNA-ISH in circulating tumor cells
Isolated CTCs were centrifuged onto poly-L-lysine coated glass slides (Sigma Life Sciences, P0425) for 5 minutes at 800 rpm using Shandon EZ Megafunnels (A78710001). Slides were dried for 10 minutes, fixed with 4% PFA for 10 minutes and washed with 1xPBS for 10 minutes before dehydration and storage in 100% ethanol at -20 degrees Celsius until staining procedure. ViewRNA ISH Cell Assay Kit (Affymetrix, Santa Clara, CA) was used to stain CTC slides. Cells were permeabilized using Detergent Solution QC for 5 minutes at room temperature (RT). RNA was unmasked using Protease QS (1:2000 dilution) for 10 minutes at RT. Type 1 probes for WNT5A (VA1-12202), WNT7B (VA1-16571) and Type 6 probes for KRT8 (VA6-11560), KRT18 (VA6-11561), KRT19 (VA6-10947), KLK3 (VA6-63528), FOLH1 (VA6-11578), EPCAM (VA6-13003) were hybridized to target mRNA for 3 hours at 40°C. Signal amplification was achieved through sequential hybridization of Pre-Amplifier molecules, Amplifier molecules, and fluorescently conjugated Label Probe oligonucleotides. Cells were stained with DAPI (Invitrogen, D3571; 5 μg/ml) for 1 min at RT. Slides were then scanned on the BioView automated fluorescent imaging platform for quantification and analysis.

Cell line experiments

Prostate cancer cell lines (LNCaP, VCaP, PC3, DU145) were obtained from ATCC after authentication by short tandem repeat profiling, and maintained as recommended. Drug treatment experiments were performed using 1-10 μM enzalutamide (Selleckchem), 1 nM R1881 (Perkin-Elmer), or dimethyl sulfoxide (DMSO). Sequenced LNCaP cells labeled LNCaP.R or LNCaP.D were cultured for 3 days in medium containing 10% charcoal-stripped FBS (Invitrogen), and treated with R1881 or DMSO as a vehicle control for 24 hours. The enzalutamide-resistant cell line LN_EnzR was generated by prolonged (4 months) *in vitro* selection in the presence of 1 μM enzalutamide. Non-canonical Wnt ligands (*WNT4*, *WNT5A*, *WNT7B*, and *WNT11*) were overexpressed in LNCaP cells using lentiviral constructs. WNT4, WNT5a, WNT7b, WNT11 plasmids were purchased from Addgene (*36, 37*) (35873, 35874, 35878, 35885), and cloned into pLX301 (Addgene 25895) through Gateway Cloning (Life Technologies). pLX301-Wnt plasmids together with packaging plasmids were transfected into 293T cells using Lipofectamine 2000 (Life Technologies). Lentivirus was collected 48 and 72 hours later. LNCaP cells were infected with lentivirus in the presence of 8mg/ml polybrene overnight. Stable cell pools were selected in growth medium containing 2 mg/mL puromycin for 1 week.

siRNA
Knockdown experiments of endogenous *WNT5A* and *WNT7B* gene expression in cells were performed using siRNA. ON-TARGETplus siRNAs against *WNT5A*, *WNT7B*, and control siRNAs were purchased from GE Dharmacon.

Western blots
Wnt5a (C27E8) antibodies were purchased from Cell Signaling. Antibodies against Wnt7b (ab155313) and Wnt11 (ab96730) were purchased from Abcam. Antibodies against GAPDH (MAB374) were acquired from Millipore. Goat anti-rabbit or anti-mouse antibodies conjugated to IRDye 800CW were used as secondary antibodies (Cell Signaling) and detected by Li-cor Odyssey CLX Infrared Imaging System.

Primers and quantitative real-time PCR
Total RNA was extracted using RNeasy Micro Kit (Qiagen). 1μg of RNA was used to generate cDNA using superscript III First Strand synthesis system (Life Technologies). Reactions were amplified and analyzed in triplicate using the ABI 7500 Real-Time PCR System. The following primers are listed in the below table:

WNT4_F	TCTGACAACATCGCCTACG
WNT4_R	CGTCTTTACCTCACAGGAGC
WNT5A_F	ATTCTTGGTGGTCGCTAGGTA
WNT5A_R	CGCCTTCTCCGATGTACTGC
WNT7B_F	TTTCTCTGCTTTGGCGTCC
WNT7B_R	TACTGGCACTCGTTGATGC
WNT11_F	AGCCAATAAACTGATGCGTC
WNT11_R	ACAGGTATCGGGTCTTGAG
GAPDH_F	GGTCTCCTCTGACTTCAACA
GAPDH_R	GTGAGGGTCTCTCTCTTCCT

Cell growth and colony formation assay

For proliferation assays, subconfluent cells were plated in triplicate for each time point at a density of 2,000 cells per well of 96-well plates 24 hours after siRNA transfection. The fold increase in cell number was measured by the CellTiter-Glo Luminescent Cell Viability Assay (Promega). For colony formation assays, cells were plated in triplicate at a density of 10,000 cells per well of 12-well plates in the presence of 1μM, 3μM or 10μM Enzalutamide (Selleckchem), and grown for 21 days before fixing and staining with crystal violet (Sigma-Aldrich). Fresh medium containing enzalutamide was changed twice a week.

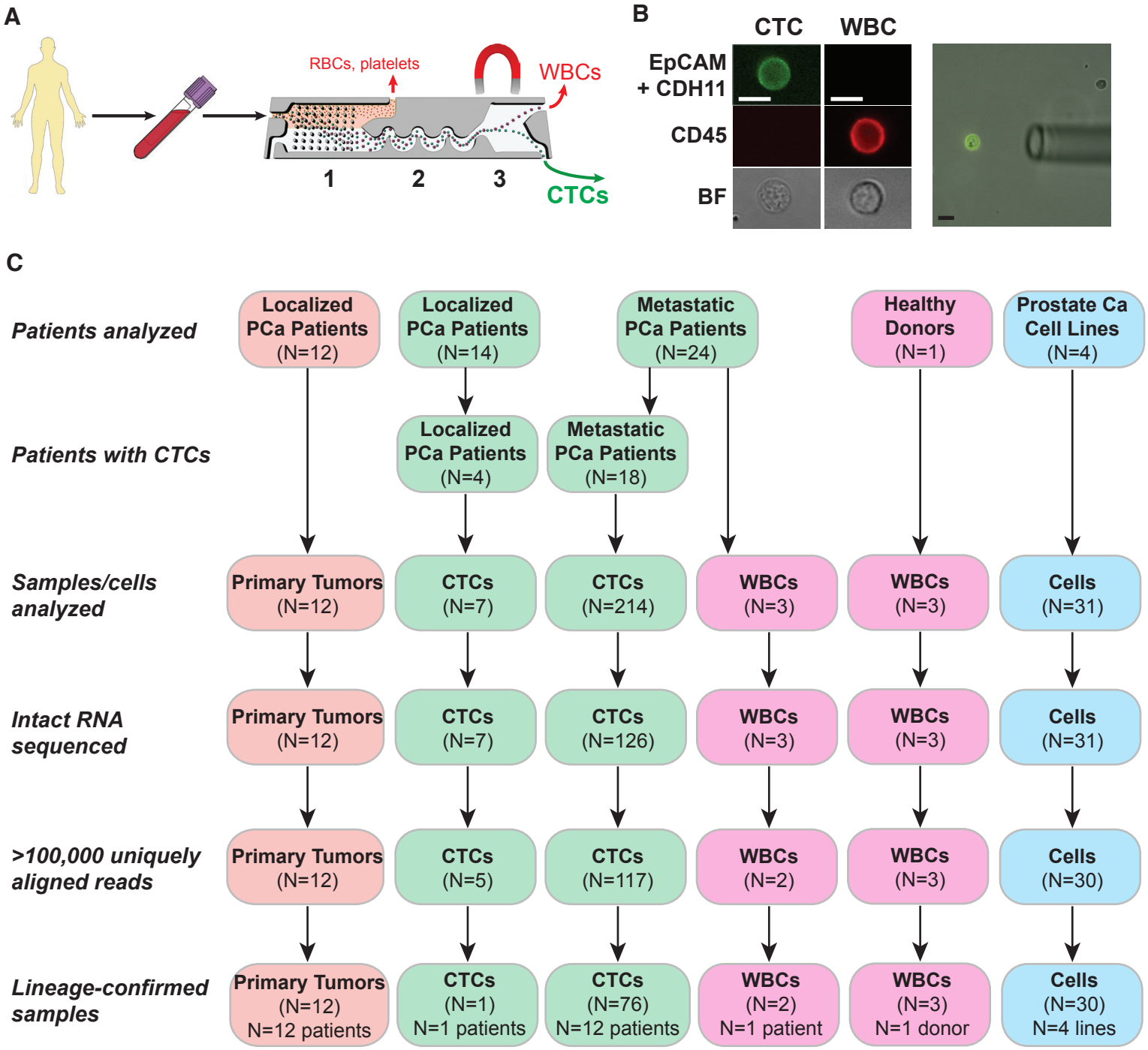

Fig. S1. Experimental workflow for single CTC RNA-sequencing studies. **(A)** Schematic of integrated microfluidic system (CTC-iChip) to deplete hematopoietic cells from whole blood and isolate circulating tumor cells (CTCs). The three microfluidic components of the system are depicted, including (i) hydrodynamic sorting to enrich for nucleated cells (CTCs and WBCs), (ii) inertial focusing to align all nucleated cells within a single streamline for efficient sorting, and (iii) magnetophoresis to remove leukocytes tagged with immunomagnetic beads. **(B)** Immunofluorescence images of a CTC stained with antibodies against both EpCAM and CDH11 (green), and a leukocyte (WBC) stained with antibody against CD45 (red). Bright field (BF) image of the CTC and WBC. Right panel depicts a CTC being isolated using a micromanipulator needle. Scale bars = 10 μm. **(C)** Flow chart of samples analyzed in this study. For CTC samples, patients were analyzed for the presence of CTCs by immunofluorescence microscopy as above, and single CTCs were micromanipulated and processed for RNA sequencing. Lineage-confirmed CTCs were defined as those that met stringent pre-specified thresholds for expression of prostate cancer-specific markers and low expression of leukocyte markers (see Fig. S2B, Results, and Methods).

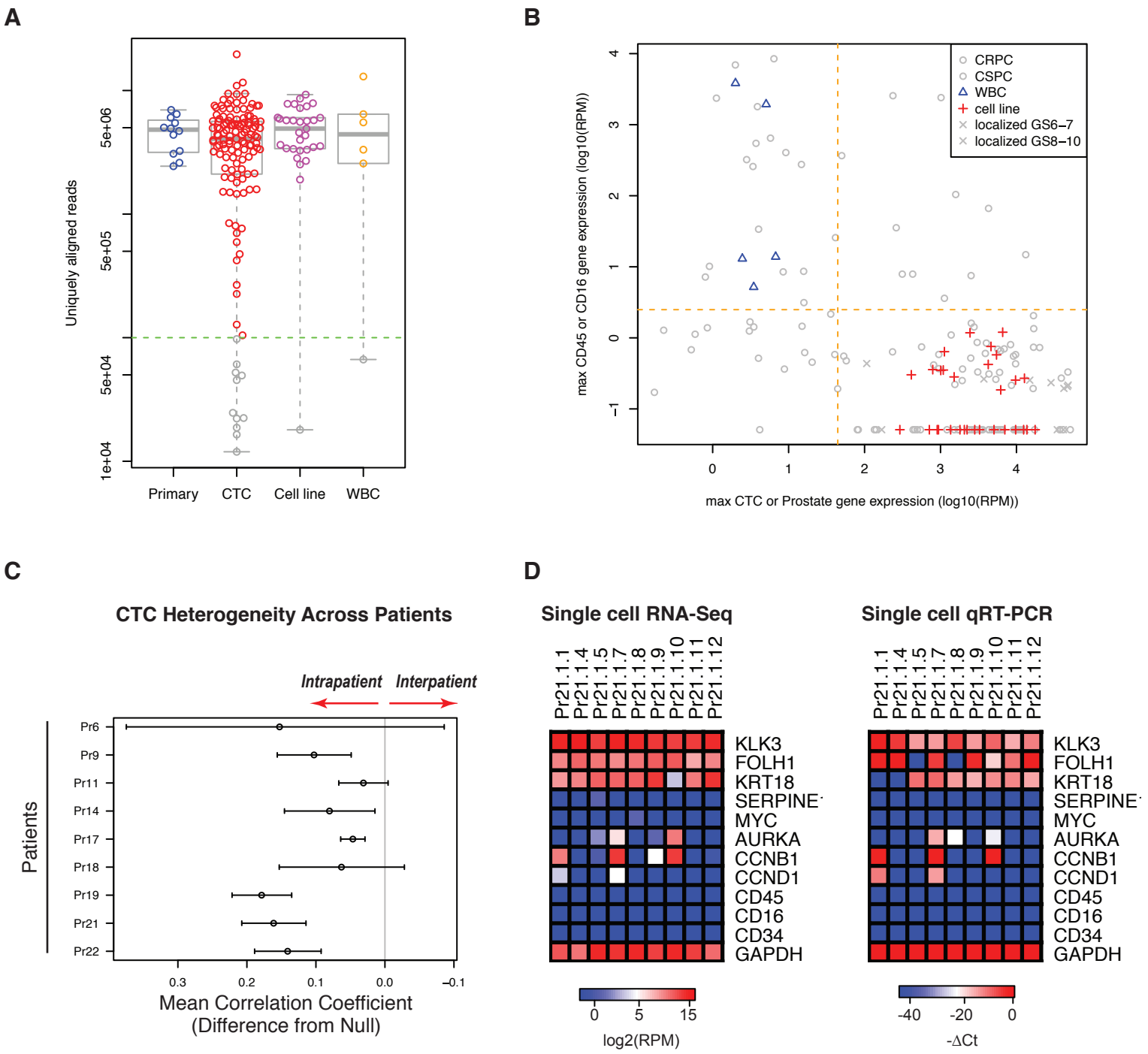

Fig. S2. RNA-sequencing of single CTCs, primary prostate tumors, cell lines, and leukocytes. **(A)** Uniquely aligned RNA-sequencing reads for primary prostate tumors, single candidate CTCs, prostate cancer cell lines, and leukocytes. Dotted line represents the cutoff value of 100,000 uniquely aligned reads, and samples below this threshold were not further analyzed. **(B)** Stringent expression thresholds used to define lineage-confirmed CTCs. Maximum log10(RPM) expression of CTC or prostate specific markers (KRT7, KRT8, KRT18, KRT19, EPCAM, AR, KLK3, FOLH1, and AMACR) are plotted against leukocyte markers (CD45 and CD16). Dashed lines are thresholds defined by the relative expression of these markers in leukocytes and prostate cancer cell lines. CTCs in the lower right quadrant were defined as lineage-confirmed CTCs. See Methods for details. **(C)** CTC heterogeneity across patients, illustrated by the difference between the mean correlation coefficients within patients (intrapatient) and between patients (interpatient) (see Fig. 1, B and C). **(D)** Validation of single cell RNA-seq data using an independent method (single cell multiplex qRT-PCR) in a subset of isolated single prostate CTCs with a panel of selected genes (prostate-specific genes, leukocyte genes, and cell cycle genes).

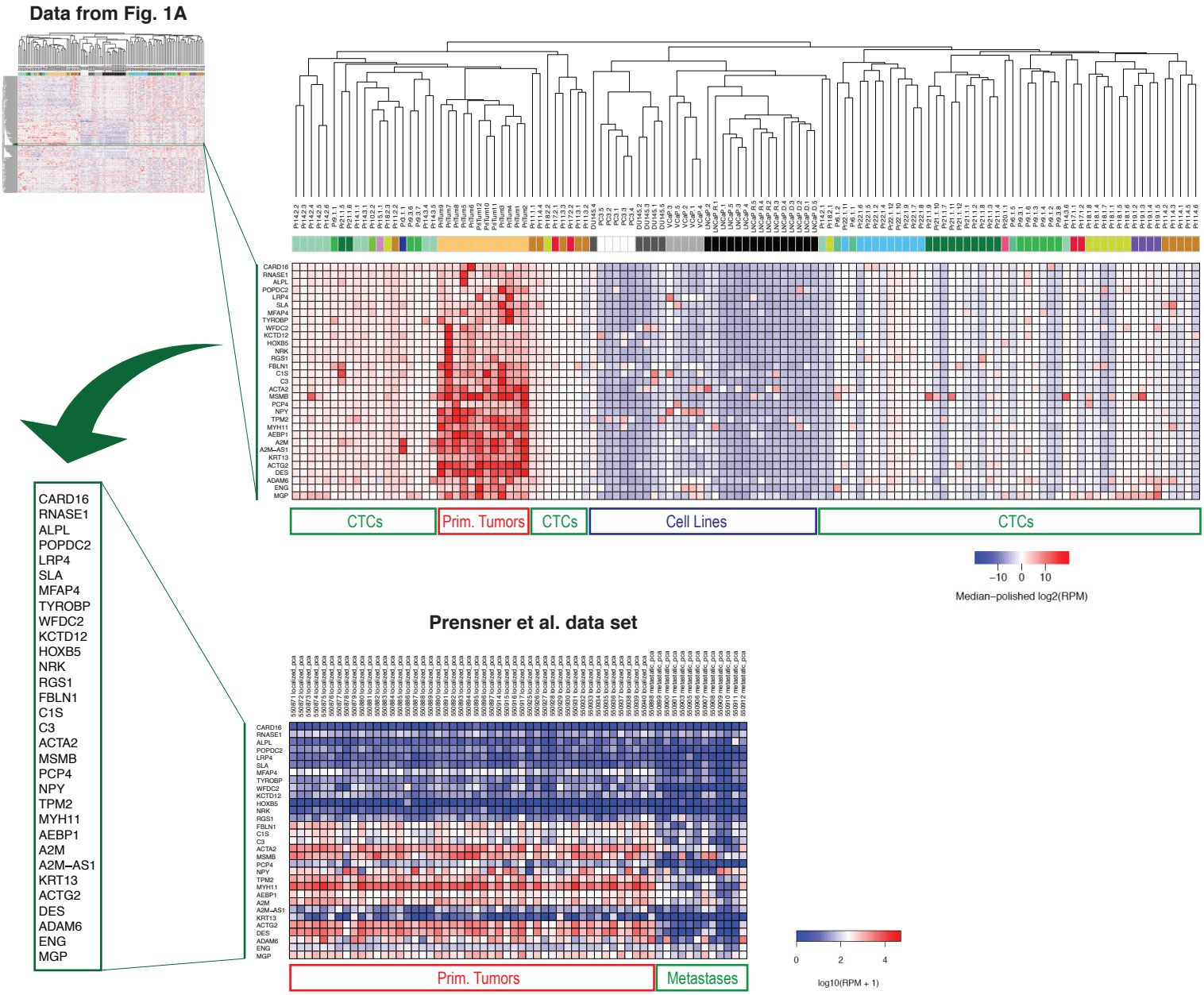

Fig. S3. Confirmation of selected gene expression profiles using an independent RNA-seq data set. Top panel, magnified view of the heatmap from Fig. 1A, revealing a set of genes that are highly upregulated in primary tumors. Bottom panel, expression profiles of these same genes in a previously published RNA-seq data set (dbGaP dataset phs000443.v1.p1) that included primary and metastatic prostate tumors (34).

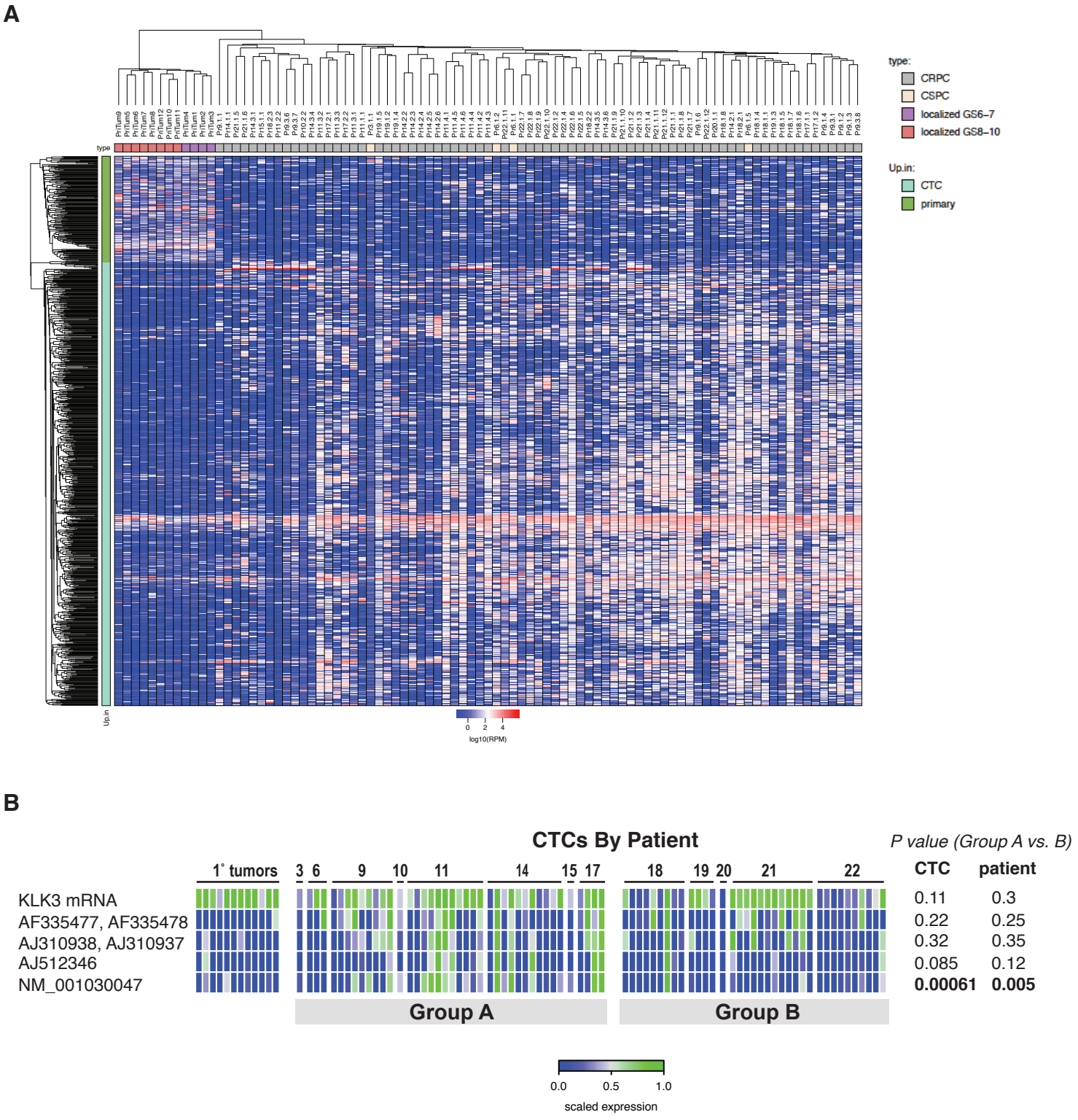

Fig. S4. (A) Comparison of prostate CTCs and primary prostate tumors by unsupervised hierarchical clustering. CRPC, castration-resistant prostate cancer; CSPC, castration-sensitive prostate cancer; GS, Gleason score. **(B)** Heat map depicting KLK3 splice variants in radical prostatectomy specimens, prostate CTCs from enzalutamide-naïve patients (Group A), and prostate CTCs from patients who had radiographic or biochemical progression of disease while receiving treatment with enzalutamide (Group B). Numbers at top of heatmap represent ID numbers (Pr numbers) for patients from which each CTC is derived.

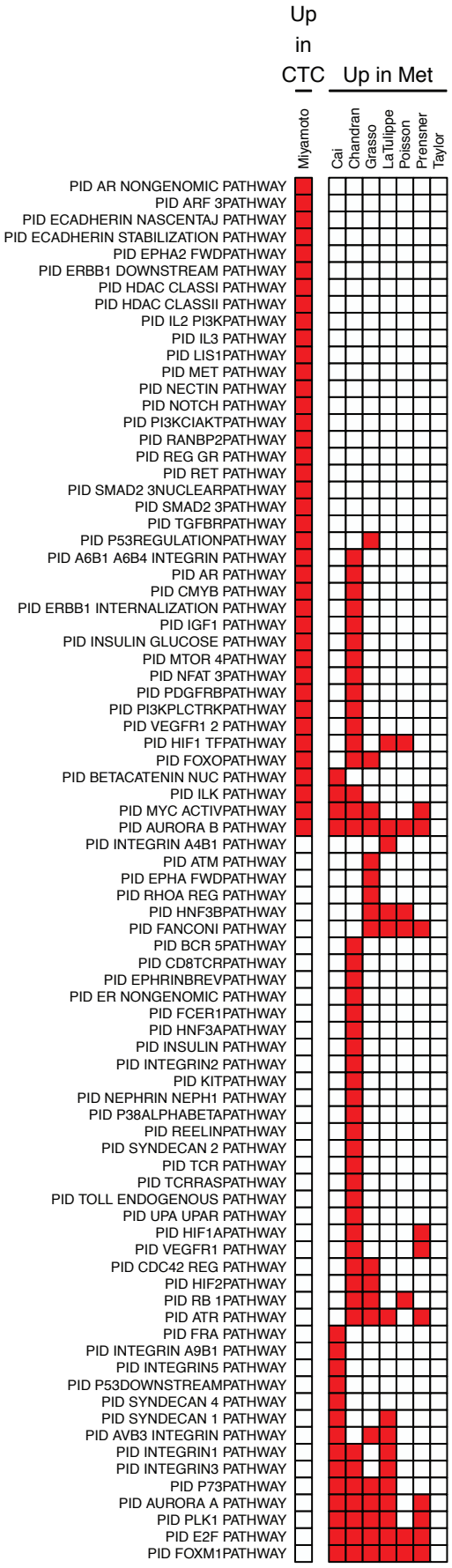

Fig. S5. Heatmap showing PID pathways enriched in prostate CTCs compared to primary tumors in the current study (Miyamoto), and PID pathways enriched in metastatic tumors compared to primary tumors in seven other datasets (see Table S4 and Methods).

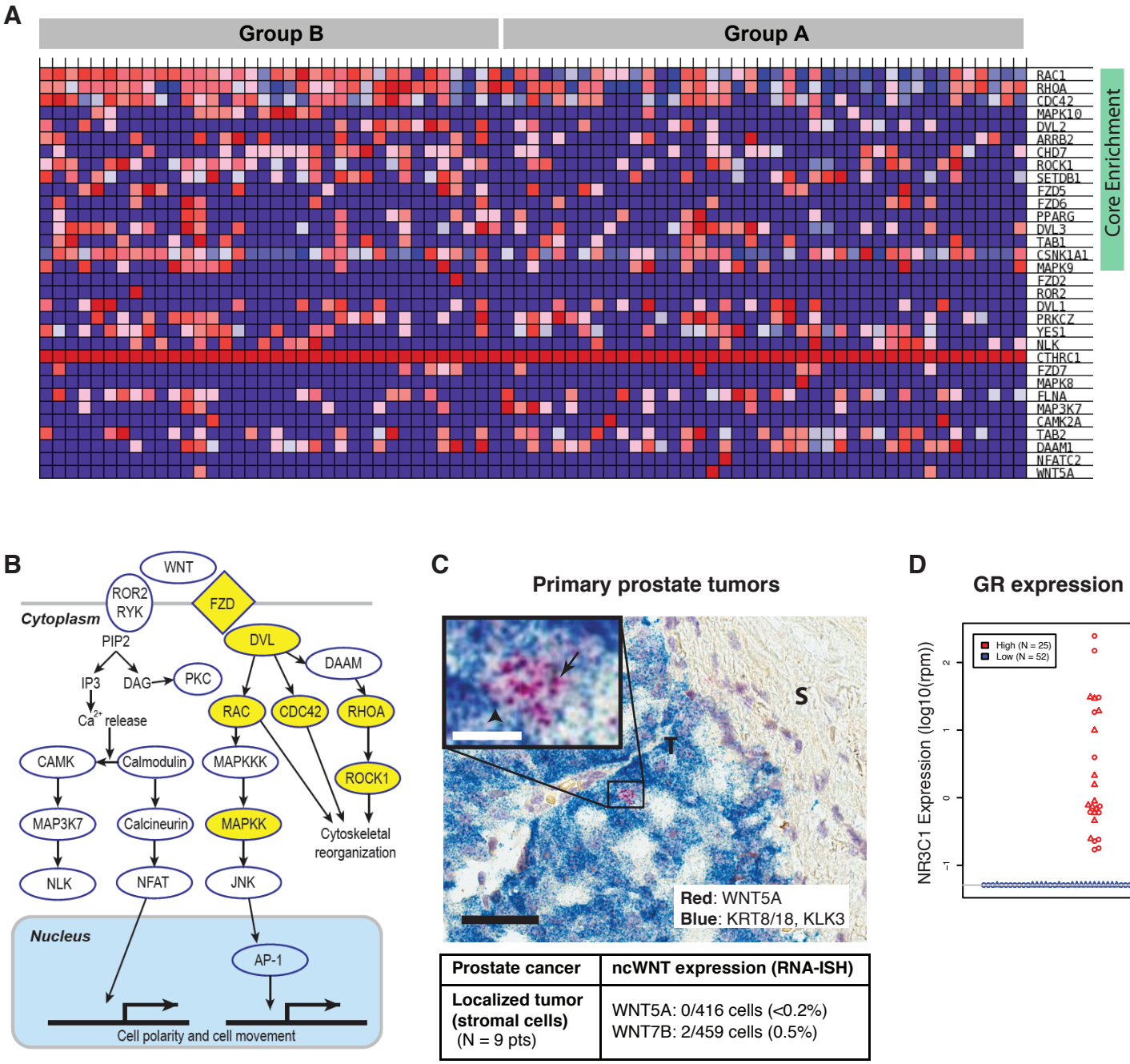

Prostate cancer	ncWNT expression (RNA-ISH)
Localized tumor (stromal cells) (N = 9 pts)	WNT5A: 0/416 cells (<0.2%) WNT7B: 2/459 cells (0.5%)

Fig. S6. Comparison of CTCs from Group A patients (enzalutamide-naïve) and Group B patients (progression while on enzalutamide). **(A)** Heat map corresponding to GSEA plot (Fig. 3B) showing enrichment of PID non-canonical Wnt pathway in CTCs from Group B compared to Group A patients, with Core Enrichment genes identified. **(B)** Non-canonical Wnt signaling pathway. Components of the pathway enriched in Group B compared to Group A based on GSEA analysis are highlighted in yellow. **(C)** Representative micrograph of RNA-in situ hybridization assay in primary prostate tumors, probing for WNT5A (red dots), and CK8, CK18, and KLK3 (blue dots). WNT7B probe was used in adjacent tissue sections (see Fig. 3C). T, tumor; S, stroma. 40x magnification, black scale bar = 50 µm. Inset, high magnification, white scale bar = 10 µm. **(D)** NR3C1 (GR gene) expression in single cell prostate CTC RNA-seq data.

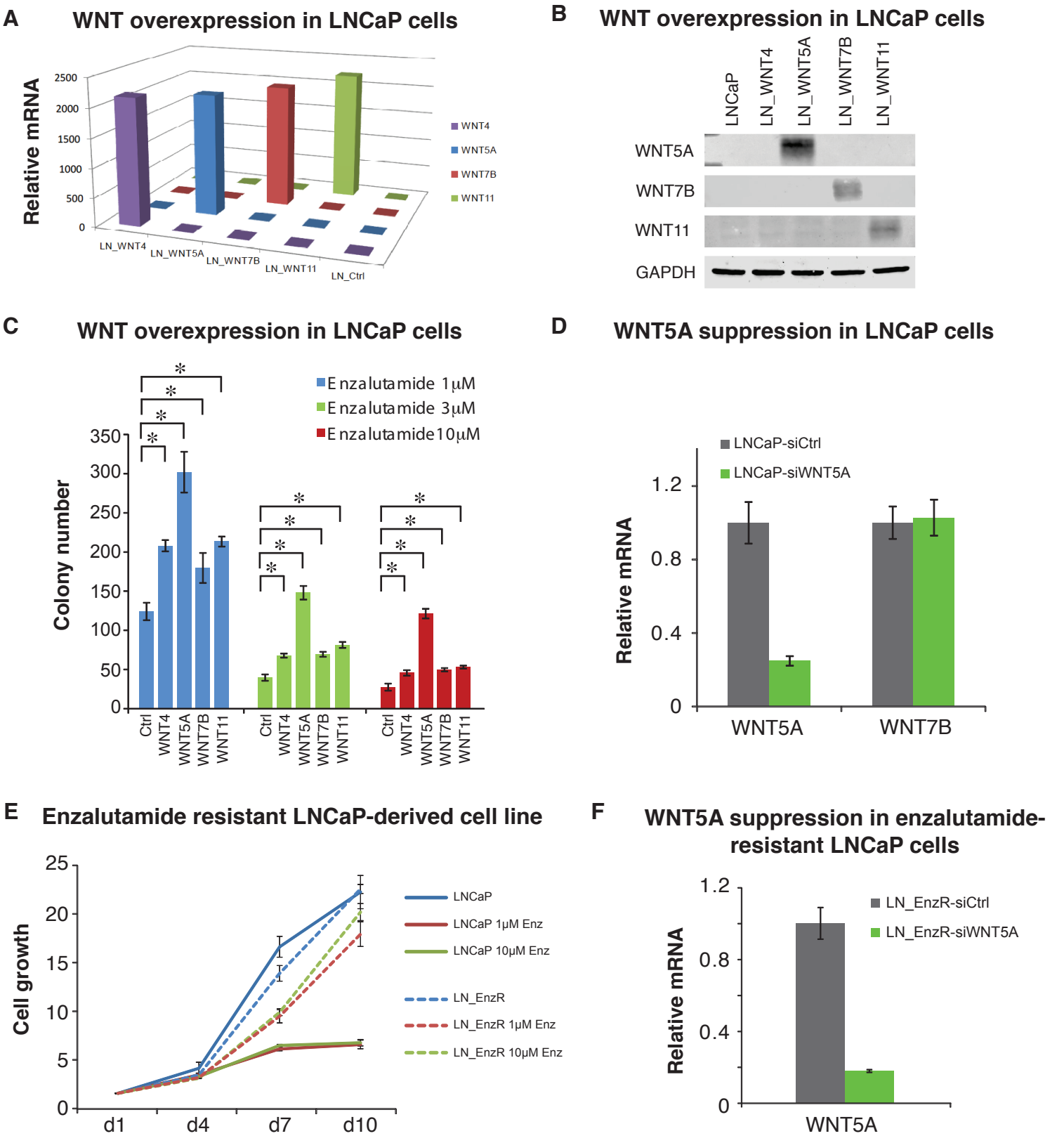

Fig. S7. Overexpression and knockdown of non-canonical (nc) Wnt in prostate cancer cell lines. **(A)** Stable ectopic expression of ncWnt ligands WNT4, WNT5A, WNT7B, WNT11 in LNCaP cells, quantified by qRT-PCR. **(B)** Western blot showing stable expression of WNT5A, WNT7B, WNT11 in LNCaP cells. No specific WNT4 antibody was available for the analysis. **(C)** Ectopic expression of ncWnts in LNCaP cells increases cell survival in the presence of different concentrations of enzalutamide. **(D)** Efficient knockdown of WNT5A in LNCaP cells using siRNA quantified by qRT-PCR. mRNA levels of WNT7B is not affected. **(E)** Growth curve demonstrating that the LNCaP-derived enzalutamide-resistant LN_EnzR cells shows continued growth in the presence of 1μM and 10μM enzalutamide, relative to control LNCaP cells. **(F)** Efficient knockdown of WNT5A in LN_EnzR cells quantified by qRT-PCR. Each experiment (C-F) was performed ≥3 times. Data are presented as mean +/- SD.

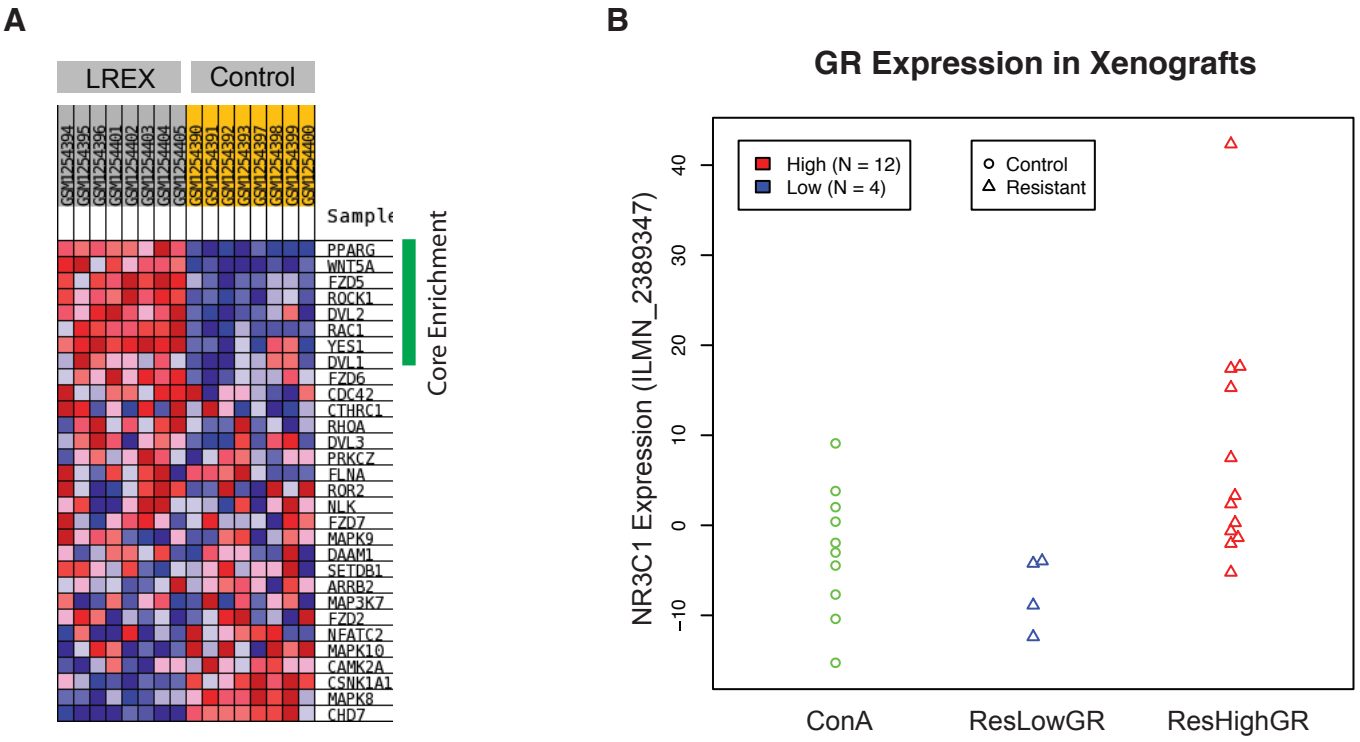

Fig. S8. GR expression in mouse xenografts. **(A)** Heat map corresponding to GSEA plot (Fig. 4D) showing ncWnt pathway enrichment in mouse xenografts derived from enzalutamide-resistant LREX' cells (29) compared to control LNCaP cells, with Core Enrichment genes identified. **(B)** NR3C1 (GR gene) expression in mouse xenograft microarray data from GEO GSE52169 (29).

Table S1 | Patient CTC Samples

Patient	Stage	Disease status at time of CTC collection	PSA (ng/mL)	No. cells picked	No. cells sequenced	No. lineage-confirmed CTCs	Group	Response to enzalutamide	Prior Treatments
Pr1	loc.	CSPC, pre-treatment	10.0	1	1	0	-	-	none
Pr2	loc.	CSPC, pre-treatment	6.8	2	2	0	-	-	none
Pr3	loc.	CSPC, pre-treatment	8.5	2	2	1	A	enzalutamide-naïve	none
Pr4	loc.	CSPC, pre-treatment	10.1	2	2	0	-	-	none
Pr5	met.	CSPC, pre-treatment	144.1	4	3	0	-	-	none
Pr6	met.	CSPC, pre-treatment	207.8	9	5	3	A	enzalutamide-naïve	none
Pr7	met.	CSPC, pre-treatment	34.7	3	2	0	-	-	none
Pr8	met.	CSPC, pre-treatment	7.3	5	5	0	-	-	none
Pr9	met.	CRPC, on abiraterone	93.9	32	17	9	A	enzalutamide-naïve	ADT
Pr10	met.	CRPC, on abiraterone	445.5	8	6	1	A	enzalutamide-naïve	ADT, doc, cabo
Pr11	met.	CRPC, on abiraterone	1504.0	27	15	11	A	enzalutamide-naïve	ADT, bic, metformin, keto, cabo, doc
Pr12	met.	CRPC, on abiraterone	0.2	3	2	0	-	-	ADT
Pr13	met.	CRPC, on abiraterone	0.2	2	2	0	-	-	ADT
Pr14	met.	CRPC, on abiraterone	365.6	20	13	11	A	enzalutamide-naïve	ADT
Pr15	met.	CRPC, on docetaxel	43.0	4	2	1	A	enzalutamide-naïve	ADT, abi
Pr16	met.	CRPC, on Phase I drug†	87.7	8	6	0	-	-	ADT, metformin, keto, doc, abi, cabaz
Pr17	met.	CRPC, on cabazitaxel	384.9	7	4	4	A	enzalutamide-naïve	ADT, doc, abi
Pr18	met.	CRPC, on enzalutamide	311.3	27	13	9	B	Rad. progression	ADT, sipT, metformin, cabo, doc
Pr19	met.	CRPC, on enzalutamide	349.4	9	5	4	B	Rad. and PSA progression	ADT, abi, doc
Pr20	met.	CRPC, on enzalutamide	94.0	4	2	1	B	Rad. and PSA progression	ADT, doc, abi
Pr21	met.	CRPC, on enzalutamide*	4573.0	18	12	12	B	PSA progression	ADT, doc, abi, cabaz
Pr22	met.	CRPC, on enzalutamide	219.1	24	12	10	B	Rad. and PSA progression	ADT, abi
			Total:	**221**	**133**	**77**			

Legend: ADT, androgen deprivation therapy; abi, abiraterone; bic, bicalutamide; cabaz, cabazitaxel; cabo, cabozantinib; CRPC, castration-resistant prostate cancer; CSPC, castration-sensitive prostate cancer; doc, docetaxel; ket, ketoconazole; loc., localized; met., metastatic; PSA, serum prostate-specific antigen at time of CTC collection; Rad., radiographic; sipT, sipuleucel-T; †E7050 and E7080; *started enzalutamide on the day of the CTC blood draw.

Table S2 | Primary Tumor Samples

Patient	Stage	Clinical status	PSA (ng/mL)	Gleason score	T Stage
PriTum1	localized	CSPC	4.6	3+3=6	pT2c
PriTum2	localized	CSPC	5	3+3=6	pT2c
PriTum3	localized	CSPC	10.8	5+4=9	pT3ab
PriTum4	localized	CSPC	7	3+4=7	pT2c
PriTum5	localized	CSPC	13	5+4=9	pT3a
PriTum6	localized	CSPC	12.9	5+4=9	pT3a
PriTum7	localized	CSPC	6.7	5+4=9	pT3ab
PriTum8	localized	CSPC	10.7	4+4=8	pT3a
PriTum9	localized	CSPC	16.7	5+4=9	pT3a
PriTum10	localized	CSPC	8.6	4+5=9	pT3ab
PriTum11	localized	CSPC	4.96	4+5=9	pT3a
PriTum12	localized	CSPC	4.4	4+3=7	pT2c

Legend: PSA, serum prostate-specific antigen; CSPC, castration-sensitive prostate cancer

Supplementary Excel Tables

Table S3. Genes differentially expressed between CTCs and primary prostate tumors. "Up in CTC" tab – 711 genes enriched in CTCs. "Up in Primary" tab – 173 genes enriched in primary tumors.

Table S4. Data sets used in the differential gene expression and pathway analyses comparing metastatic and primary prostate tumors (see Figs. 2C and S5).

Table S5. Androgen receptor mutation analysis in prostate CTCs, primary tumors, and prostate cancer cell lines.

Table S6. Androgen receptor splice variant analysis in prostate CTCs and primary tumors.

Table S7. Pathway signatures used for metagene analyses in this study (see Fig. 3A).

Supplementary References

32. H. Hieronymus, J. Lamb, K. N. Ross, X. P. Peng, C. Clement, A. Rodina, M. Nieto, J. Du, K. Stegmaier, S. M. Raj, K. N. Maloney, J. Clardy, W. C. Hahn, G. Chiosis, T. R. Golub, Gene expression signature-based chemical genomic prediction identifies a novel class of HSP90 pathway modulators. *Cancer Cell* **10**, 321–330 (2006).

33. C. Trapnell, A. Roberts, L. Goff, G. Pertea, D. Kim, D. R. Kelley, H. Pimentel, S. L. Salzberg, J. L. Rinn, L. Pachter, Differential gene and transcript expression analysis of RNA-seq experiments with TopHat and Cufflinks. *Nat. Protoc.* **7**, 562–578 (2012).

34. J. R. Prensner, M. K. Iyer, O. A. Balbin, S. M. Dhanasekaran, Q. Cao, J. C. Brenner, B. Laxman, I. A. Asangani, C. S. Grasso, H. D. Kominsky, X. Cao, X. Jing, X. Wang, J. Siddiqui, J. T. Wei, D. Robinson, H. K. Iyer, N. Palanisamy, C. A. Maher, A. M. Chinnaiyan, Transcriptome sequencing across a prostate cancer cohort identifies *PCAT-1*, an unannotated lincRNA implicated in disease progression. *Nat. Biotechnol.* **29**, 742–749 (2011).

35. A. Subramanian, P. Tamayo, V. K. Mootha, S. Mukherjee, B. L. Ebert, M. A. Gillette, A. Paulovich, S. L. Pomeroy, T. R. Golub, E. S. Lander, J. P. Mesirov, Gene set enrichment analysis: A knowledge-based approach for interpreting genome-wide expression profiles. *Proc. Natl. Acad. Sci. U.S.A.* **102**, 15545–15550 (2005).

36. R. Najdi, K. Proffitt, S. Sprowl, S. Kaur, J. Yu, T. M. Covey, D. M. Virshup, M. L. Waterman, A uniform human Wnt expression library reveals a shared secretory pathway and unique signaling activities. *Differentiation* **84**, 203–213 (2012).

37. X. Yang, J. S. Boehm, X. Yang, K. Salehi-Ashtiani, T. Hao, Y. Shen, R. Lubonja, S. R. Thomas, O. Alkan, T. Bhimdi, T. M. Green, C. M. Johannessen, S. J. Silver, C. Nguyen, R. R. Murray, H. Hieronymus, D. Balcha, C. Fan, C. Lin, L. Ghamsari, M. Vidal, W. C. Hahn, D. E. Hill, D. E. Root, A public genome-scale lentiviral expression library of human ORFs. *Nat. Methods* **8**, 659–661 (2011).

ELSEVIER

CrossMark

Urologic Oncology: Seminars and Original Investigations 34 (2016) 490–501

UROLOGIC ONCOLOGY

Seminar article

Cell-free and circulating tumor cell–based biomarkers in men with metastatic prostate cancer: Tools for real-time precision medicine?

David T. Miyamoto, M.D., Ph.D.[a,b,d,*], Richard J. Lee, M.D., Ph.D.[a,c,d]

[a] *Massachusetts General Hospital Cancer Center, Boston, MA*
[b] *Department of Radiation Oncology, Massachusetts General Hospital, Boston, MA*
[c] *Department of Medicine, Massachusetts General Hospital, Boston, MA*
[d] *Harvard Medical School, Boston, MA*

Received 21 May 2016; received in revised form 3 September 2016; accepted 7 September 2016

Abstract

The recent expansion of therapeutic options for the treatment of metastatic prostate cancer highlights the need for precision medicine approaches to enable the rational selection of appropriate therapies for individual patients. In this context, circulating biomarkers in the peripheral blood are attractive as readily accessible tools for predicting and monitoring therapeutic response. In the case of circulating tumor cells and circulating tumor DNA, they may also serve as a noninvasive means of assessing molecular aberrations in tumors at multiple time points before and during therapy. These so-called "liquid biopsies" can provide a snapshot view of tumor molecular architecture and may enable clinicians to monitor the molecular status of tumors as they evolve during treatment, thus allowing for individualized precision therapeutic decisions for patients over time. In this review, we outline recent progress in the field of circulating biomarkers in metastatic prostate cancer and evaluate their potential for enabling this vision of real-time precision medicine.

Keywords: Prostate cancer; CTCs; ctDNA; Circulating biomarkers; AR

Introduction

Prostate cancer remains the second leading cause of cancer-related death in men in the United States, with an estimated 26,120 deaths in 2016 [1]. The past 6 years have seen the expansion of therapies that improve overall survival (OS) for men with metastatic castration-resistant prostate cancer (mCRPC), with other promising drugs in development [2]. However, all of these drugs ultimately have limited efficacy, and primary or acquired resistance to therapy is a significant problem. Monitoring the effectiveness of individual therapies in patients with mCRPC is a uniquely difficult problem because of the high prevalence of bone metastases, which are difficult to quantitate. There exists a need for accurate biomarkers to monitor and predict clinical response in prostate cancer, and thus enable a precision medicine approach to personalizing treatment for the individual patient. A biomarker that can reliably substitute for OS as a surrogate end point would also be useful in the design of clinical trials investigating novel therapies, especially in a disease with a growing number of available life-prolonging treatments.

A biomarker is defined as "a characteristic that is objectively measured and evaluated as an indicator of normal biological processes, pathogenic processes, or pharmacologic responses to a therapeutic intervention" [3]. A biomarker can thus provide a clinical measurement for a specific clinical context that may correlate with patient outcomes (*prognostic* biomarker) or likelihood of response to a specific therapy (*predictive* biomarker). In many cancers, tissue biomarkers based on the molecular analysis of primary or metastatic tumors have prognostic or predictive value. However, 90% of men with mCRPC have bone metastases, and tissues from metastatic bone lesions are difficult to reliably obtain and often do not reflect the evolving biology of tumors before and after treatment [4]. Therefore, in

* Corresponding author. Tel.: +1-617-726-5866; fax: +1-617-726-3603.
E-mail addresses: dmiyamoto@mgh.harvard.edu, dmiyamoto@partners.org (D.T. Miyamoto).

http://dx.doi.org/10.1016/j.urolonc.2016.09.001
1078-1439/

the setting of metastatic prostate cancer, circulating biomarkers in the peripheral blood are particularly appealing, as they may be assessed noninvasively and repeatedly throughout therapy.

The most widely used circulating biomarker in the care of men with prostate cancer is prostate-specific antigen (PSA, also known as kallikrein-3), a serine protease produced by normal and cancerous prostate epithelial cells. Although characterized as a tumor marker, PSA is produced by normal prostate cells and by other organs in men and women and is therefore not specific for cancer, gland, or sex [5]. Most but not all prostate cancers are associated with elevated serum PSA level. PSA is regulated by circulating androgens, and its gene expression depends on activation of the androgen receptor (AR). Androgen deprivation therapy is typically associated with a decrease in serum PSA level, as well as improvement in disease-related symptoms and measurable metastatic disease. In the setting of mCRPC, PSA levels have prognostic value as an independent risk factor for mortality, and posttreatment changes in PSA level may reflect changes in tumor burden for some mCPRC therapies (reviewed in detail in Ref. [6]). However, posttreatment PSA level change has failed to satisfy the definition of a surrogate for OS for multiple therapies with varied mechanisms of action for mCRPC [7–9]. Accordingly, no therapy for prostate cancer has been approved solely based on an observed posttreatment decline in serum PSA level. This review will focus on alternative circulating biomarkers that have been proposed and studied in recent years.

Perhaps the most promising of these alternative circulating biomarkers are circulating tumor cells (CTCs) and cell-free DNA (cfDNA), so-called "liquid biopsies" that involve the noninvasive sampling and analysis of tumor-derived cells or nucleic acids in the peripheral blood [10,11]. Indeed, these approaches may not only enable the monitoring of treatment responses but may also provide detailed molecular information about their tumors that can predict response or resistance to specific treatments, and thus guide patients toward the appropriate next lines of therapy. This concept has become increasingly relevant in prostate cancer given our increased level of molecular understanding of prostate cancer through next-generation sequencing studies [12]. In this review, we provide an overview of published data regarding circulating biomarkers for men with mCRPC, with a focus on liquid biopsy approaches, their prognostic and predictive value (Table 1), and their potential to guide patient care.

Circulating tumor cells

CTCs are cancer cells that have been shed from primary or metastatic tumor deposits into the peripheral blood [13–15] and are genetically representative of the primary and metastatic tumors [16–19]. A total of 2 key limitations of CTC analyses include the rarity of CTCs, estimated at one cell per billion normal blood cells and the challenging prospect of reliable detection and isolation of these cells. In general, CTC detection strategies include (1) enrichment from blood cells by positively selecting CTCs using antibodies directed against an epithelial cell surface protein, (2) enrichment from blood cells by size-based separation, (3) depletion of blood cells using red blood cell lysis or depletion of common leukocyte antigen (CD45)–expressing leukocytes or both, and (4) CTC identification using immunofluorescence for specific proteins among a spread of the nucleated cells remaining in peripheral blood after red blood cell lysis. Details of the varied approaches to CTC isolation have been described recently in other reviews [13–15,20]. As the only Food and Drug Administration (FDA)–cleared CTC detection technology, the CellSearch assay (Veridex, USA) relies on magnetic beads coated with anti-EpCAM antibodies to capture CTCs, followed by confirmation as epithelial cells by positive expression of cytokeratin (CK)-8, CK-18, and CK-19 proteins and lack of CD45 expression by immunofluorescence staining [21]. This platform has several limitations, including its inability to capture mesenchymal CTCs that do not express EpCAM [22]. Other technologies have been developed to enable the capture of a more comprehensive range of CTC phenotypes, including the Epic Sciences platform and the negative selection–based CTC-iChip [23,24]. However, CellSearch has been the primary CTC detection platform used for large-scale patient studies that have assessed CTCs as a biomarker in mCRPC. These studies, described in more detail later, show that enumeration of CTCs correlates with clinical end points including survival and may thus serve as a prognostic biomarker (Table 1).

CTC enumeration

The prospective study that led to FDA clearance of prognostic use of the CellSearch assay in prostate cancer, IMMC38, demonstrated that CTCs are an independent predictor of OS [25]. This prospective study enrolled 276 patients with progressive mCRPC who were starting a new chemotherapy regimen. CTCs were evaluated in blood samples taken before treatment and monthly after initiation of therapy. Patients were categorized as having "unfavorable" ($\geq$5 CTCs in 7.5 ml of blood) or "favorable" ($<$5 CTCs in 7.5 ml of blood) CTC counts. IMMC38 met its primary end point, demonstrating that unfavorable posttreatment CTC counts were associated with shorter median OS when compared with favorable CTC counts (9.5 months vs. 20.7 months, hazard ratio [HR] = 4.5, $P < 0.0001$). Unfavorable pretreatment counts were also associated with decreased median OS (11.5 vs. 21.7 months). Additionally, patients who converted from unfavorable baseline CTC counts to favorable posttreatment CTC counts had improved median OS (from 6.8–21.3 months); conversely, those who converted from favorable to unfavorable CTC counts had reduced median OS (from $>$26 to 9.3 months). CTC abundance was a better predictor of OS than posttreatment changes in serum PSA levels at all time points.

Table 1
Prognostic and predictive value of individual circulating biomarkers in mCRPC from selected publications

Biomarker	Trial	Correlation	Clinical notes	Prognostic or predictive value	References
CTCs	IMMC38	HR = 4.5 $P < 0.0001$	Unfavorable postchemotherapy CTC count associated with shorter OS	Prognostic	[25]
		HR = 3.3 $P < 0.0001$	Unfavorable prechemotherapy CTC count associated with shorter OS	Prognostic	[25]
	SWOG S0421	HR = 2.74 $P = 0.001$	Favorable predocetaxel CTC count associated with longer OS	Prognostic	[29]
		HR = 2.55 $P = 0.041$	Any increase in CTCs after 1 cycle of docetaxel associated with shorter OS	Prognostic	[29]
	COU-AA-301	HR = 1.19 $P < 0.0001$	Unfavorable preabiraterone CTC count associated with shorter OS	Prognostic	[32]
LDH	IMMC38	HR = 6.44 $P < 0.0001$	Higher prechemotherapy LDH associated with shorter OS	Prognostic	[26]
	COU-AA-301	HR = 2.98 $P < 0.0001$	Higher preabiraterone LDH associated with shorter OS	Prognostic	[32]
PSA	COU-AA-301	HR = 1.04 $P = 0.1797$	PSA was not associated with OS	N/A	[32]
	COU-AA-302	HR = 1.14 $P < 0.0001$	Baseline PSA level associated with OS	Prognostic	[92]
AR-V7 in CTCs		HR = 6.9 $P = 0.002$	Detectable AR-V7 associated with shorter OS on enzalutamide	Predictive	[58]
		HR = 12.7 $P = 0.006$	Detectable AR-V7 associated with shorter OS on abiraterone	Predictive	[58]
		P = NS	Detectable AR-V7 was not associated with primary resistance to docetaxel or cabazitaxel	N/A	[63,64]
		HR = 0.24 $P = 0.035$	Detectable AR-V7 predicted superior OS with taxanes relative to AR inhibitors	Predictive	[66]
TMPRSS2-ERG in CTCs		P = NS	Detectable *TMPRSS2-ERG* did not predict response to abiraterone	N/A	[77]
Telomerase in CTCs	SWOG S0421	HR = 1.14 $P = 0.001$	Telomerase activity in live CTCs associated with shorter OS	Prognostic	[86]
cfDNA		HR = 0.34 $P = 0.032$	Increased cfDNA associated with worse OS in men starting taxane chemotherapy	Prognostic	[53]
AR copy number or mutation in ctDNA		$P = 0.0026$	*AR* copy number variation associated with worse OS	Prognostic	[72]
		HR = 7.33 $P = 1.3 \times 10^{-9}$	Presence of *AR* gain or mutation in ctDNA before abiraterone associated with worse OS	Predictive	[71]
		HR = 2.92 $P = 0.001$	Presence of *AR* gain or mutation in ctDNA before enzalutamide associated with worse PFS	Predictive	[75]

A reanalysis of the IMMC38 trial data focused on the patients receiving first-line chemotherapy, and evaluating CTC counts as a continuous variable, rather than favorable vs. unfavorable risk categories, as well as other pretreatment and posttreatment variables including lactate dehydrogenase levels (LDH) [26]. Increased LDH expression has previously been shown to be associated with worse prognosis in mCRPC [27]. In IMMC38, higher baseline LDH concentrations (HR = 6.44), CTC counts (HR = 1.58), and serum PSA level (HR = 1.26) were significantly associated with shorter OS. During therapy, only baseline LDH and CTC counts at the specific timepoint, and not PSA levels or other markers, were associated with survival. These data suggested that CTC abundance combined with baseline LDH could provide a more accurate intermediate end point for clinical trials than posttreatment PSA level

change. Other studies using CellSearch have similarly identified serum LDH concentration and CTC counts as independent prognostic factors in mCRPC [28].

CTC enumeration has been evaluated prospectively as an intermediate end point in several published clinical trials. SWOG S0421 was a phase III double-blind, randomized placebo-controlled trial evaluating patients with mCRPC starting first-line docetaxel chemotherapy with or without atrasentan [29]. Atrasentan did not improve OS in this trial [30]. Baseline favorable vs. unfavorable CTC counts measured on the CellSearch platform were associated with better OS (26 vs. 13 months, HR = 2.74, $P = 0.001$). Any increase in CTC counts after one cycle of docetaxel was significantly associated with worse OS (HR = 2.55), whereas falling CTC counts exhibited a nonsignificant trend toward improved OS [29]. These data suggest that rising CTC counts during docetaxel chemotherapy may be used for clinical decision making to change therapy.

COU-AA-301 was a phase III, double-blind, randomized placebo-controlled trial that demonstrated an OS benefit for abiraterone acetate in 1,195 men with mCRPC who had previously received docetaxel [31]. COU-AA-301 was the first phase III trial to prospectively define a secondary objective evaluating whether CellSearch-based CTC enumeration could be used as a surrogate efficacy-response biomarker of OS [32]. The final analysis included 711 subjects with CTC and LDH data at week 12. Abiraterone treatment (HR = 0.70, $P < 0.0001$), baseline LDH concentration (HR = 2.98, $P < 0.0001$), and CTC count (HR = 1.19, $P < 0.0001$) were prognostic for survival, although PSA level was not (HR = 1.04, $P = 0.1797$) [33]. A "CTC biomarker panel," comprising CTC count and LDH level, categorized subjects as low risk (CTCs $\leq$ 4 cells per 7.5 ml of blood, any LDH), intermediate risk (CTCs $\geq$ 5, LDH $\leq$ 250 U/l), and high risk (CTCs $\geq$ 5, LDH $>$ 250 U/l). The CTC biomarker panel discriminated survival time and satisfied the 4 Prentice criteria for surrogacy [34], unlike CTC count or LDH as individual variables [32]. These prospective, phase III data from SWOG S0421 and COU-AA-301 are encouraging and require validation by ongoing, independent phase III clinical trials.

Circulating tumor DNA

It has long been appreciated that cell-free fragments of DNA circulate in the blood after being shed by lysed and apoptotic cells [35,36]. These fragments are estimated to be 140 to 180 base pairs long, corresponding to nucleosome-protected DNA [37]. In healthy individuals, the amount of cfDNA in the blood is thought to be relatively low, approximately in the range of 0 to 50 ng/ml of blood [38,39]. However, cfDNA levels can be higher in certain conditions including inflammation, exercise, or tissue injury, and in patients with cancer, the quantity is often several fold higher and highly variable, in the range of 50 to 5,000 ng/ml [38,39]. The portion of cfDNA in patients that is derived from tumors, termed circulating tumor DNA (ctDNA), represents a small fraction of the total circulating nucleic acid burden, with a variable range from $<0.1\%$ to $>10\%$ of DNA molecules [40]. As many cancers harbor tumor-specific somatic alterations that are not present in normal cells, ctDNA detection represents a potentially highly specific approach to cancer detection, despite representing a small fraction of cfDNA. The number of circulating mutant gene fragments corresponding to tumor-specific somatic mutations can be very small compared with the number of normal circulating DNA fragments, sometimes less than 0.01% [40], and there are significant challenges associated with detecting these low-frequency mutations, especially given the high variability in signal. Nevertheless, using novel sensitive detection techniques, the relative quantity of ctDNA in individual patients with cancer has been shown to correlate with tumor burden and treatment responses over time [20,40].

Many ultrasensitive techniques have been developed to detect and quantitate ctDNA, and these have been reviewed in detail recently [20,36]. These techniques include mutation-specific real-time or end point polymerase chain reaction (PCR) [36], as well as digital PCR approaches [41], including BEAMing [42] and Droplet Digital PCR [43,44]. More recently, next-generation sequencing approaches have been used to detect and quantify rare mutations in ctDNA, either by PCR or hybridization-based capture of specific genomic loci [45] followed by massively parallel sequencing to detect relevant sequence alterations [46–48]. Many of these analyses target multiple exons of key genes, but they have also been extended to enable whole-exome analyses [49], as well as detection of chromosomal aberrations and copy number changes at the whole-genome level [50,51]. Although a shallow sequencing depth of 0.1$\times$ coverage may be sufficient for the analysis of copy number changes at the whole-genome level, a greater sequencing depth of approximately 50$\times$ coverage is often necessary for the in-depth analysis of structural rearrangements and mutations [51]. Thus, given the costs and time required for next-generation sequencing at high coverage, the sequencing strategy may be altered depending on the specific clinical application, with the use of whole-genome sequencing at a low sequencing depth to detect copy number changes, and the use of a more targeted deep sequencing approach to identify specific gene breakpoints or mutations.

ctDNA burden

Similar to CTC enumeration, measurement of cfDNA and ctDNA burden in the peripheral blood has been correlated with overall tumor burden and potentially

prognosis. One study examined both CTCs and cfDNA in the plasma from 81 patients with prostate cancer [52]. Plasma cfDNA levels were approximately 2 to 3 times higher in metastatic compared with patients with localized prostate cancer (median 562 vs. 186 ng/ml, $P = 0.03$), in comparison with healthy men who had a median of 21 ng/ml of plasma cfDNA. Allelic imbalances representative of ctDNA, detected using a PCR panel of microsatellite markers, were found in 45% and 59% of patients with localized disease and those with metastatic disease, respectively. In addition, a significant association was noted between the number of CTCs, detected using an epithelial immunospot assay, and allelic imbalance frequencies at markers corresponding to genes encoding demantin, CDKN2/p16, and BRCA1 [52]. Thus, the quantitation of both ctDNA and CTCs may provide similar information regarding tumor burden.

Other studies have suggested that cfDNA concentration may be a useful prognostic biomarker to predict outcomes after treatment of mCRPC. In a retrospective study of 59 men with mCRPC starting taxane-based chemotherapy, cfDNA concentration was found to be an independent predictor of OS on multivariate analysis (HR = 0.34, $P = 0.032$) [53]. A threshold of 55 ng/ml cfDNA was significantly associated with a worse PSA response to therapy, with a $<30\%$ decline from baseline ($P = 0.005$) [53]. Other studies also suggest a correlation between changes in plasma cfDNA content and response to chemotherapy, although many of these studies are limited by small sample size and retrospective study designs [54].

Molecular analysis of liquid biopsies

Perhaps the most promising applications of CTCs and ctDNA are molecular analyses that can inform the rational selection of appropriate therapies for patients. In the treatment of a patient with mCRPC, alterations in AR may provide the most immediately actionable information regarding the choice between AR-targeted therapies or non–AR-targeted therapies such as cytotoxic chemotherapy. The reactivation of AR signaling despite androgen deprivation therapy that occurs during the evolution of castration resistance underlies the rationale for therapies that target AR signaling, such as abiraterone and enzalutamide [55]. However, alterations in the *AR* gene may be associated with resistance to therapy, including *AR* gene amplification, point mutations in *AR*, and *AR* mRNA splice variants [55]. For example, the F876L mutation in the ligand-binding domain of AR leads to enzalutamide resistance [56,57], and the AR-V7 mRNA splice variant, which lacks a functional ligand-binding domain and is thus constitutively active, is linked to resistance to abiraterone and enzalutamide, as discussed later [58]. Liquid biopsy methods have the potential to detect the presence of such AR alterations in tumors, as well as assess for dynamic changes in AR activity in response to therapies in real time. It is possible that such assessment of the molecular status of AR may guide the monitoring and application of AR-targeted therapies.

AR alterations in CTCs

Several studies have demonstrated the feasibility of detecting *AR* alterations in CTCs isolated from patients with prostate cancer. Fluorescence in situ hybridization has been used to characterize copy number amplification of *AR* in CTCs from patients with mCRPC [59,60]. *AR* mutations have also been detected in CTCs. For example, one study identified *AR* mutations in 20 of 35 patients with mCRPC in CTCs isolated using the CellSearch system, including 19 missense mutations, 5 deletions, 1 insertion, and 2 silent mutations [61]. Another study evaluated the simultaneous detection of *AR* point mutations and the AR-V7 splice variant in CTCs using qPCR and DNA sequencing in 47 patients with prostate cancer starting a new line of therapy [62]. Of 37 patients with detectable CTCs, 19 (51%) harbored *AR* alterations, including 17 with AR-V7, one with a T878A mutation, and one with both AR-V7 and an H875Y mutation. Although these studies demonstrate the feasibility of using CTCs to noninvasively detect *AR* alterations in patients with mCRPC, they are limited by their lack of clinical correlations to demonstrate predictive value and clinical use.

The presence of the AR-V7 splice variant in CTCs has been evaluated as a potential predictive biomarker associated with resistance to enzalutamide and abiraterone in mCRPC [58]. In a prospective study of 31 enzalutamide-treated patients and 31 abiraterone-treated patients, 39% and 19%, respectively, had detectable AR-V7 in CTCs before initiation of therapy. CTCs were isolated by EpCAM positive selection, and AR-V7 expression was analyzed using a qRT-PCR assay. Patients in the enzalutamide cohort who were positive for AR-V7 had shorter duration of PSA level response (progression-free survival [PFS] 1.4 vs. 6.0 months, $P < 0.001$), clinical or radiographic PFS (2.1 vs. 6.1 months, $P < 0.001$), and OS (5.5 months vs. not reached, $P = 0.002$), compared with patients without detectable AR-V7. Similar results were seen in the abiraterone cohort, where AR-V7-positive patients had lower PSA level response rates (0% vs. 68%, $P = 0.004$), shorter duration of PSA level response (1.3 months vs. not reached, $P < 0.001$), clinical or radiographic PFS (2.3 months vs. not reached, $P < 0.001$), and OS (10.6 months vs. not reached, $P = 0.006$) [58]. In contrast with AR-targeted therapies, the presence of AR-V7 in CTCs pretreatment was not associated with resistance to docetaxel or cabazitaxel in patients with mCRPC starting chemotherapy [63,64]. A follow-up study of a small cohort of 14 patients showed that AR-V7 can be monitored serially and that longitudinal AR-V7 dynamics may reflect tumor responses [65]. In addition, in a separate cross-sectional cohort study of 161 patients starting therapy with either AR inhibitors or

taxanes, the presence of detectable AR-V7 protein in CTCs pretherapy using the Epic Sciences platform was associated with superior OS with taxanes relative to AR inhibitors (HR = 0.24, $P = 0.035$), thus confirming the aforementioned findings [66]. However, other reports indicate that the expression of AR-V7 in CTCs does not necessarily preclude a response to abiraterone or enzalutamide, thus cautioning against systematic denial of AR-targeted therapies to these patients [67]. Together, these results indicate that larger prospective validation studies are necessary to further evaluate AR-V7 in CTCs as a predictive biomarker that may guide patients away from AR-targeted therapies and toward cytotoxic chemotherapy.

Approaches have been developed to directly measure AR activity in CTCs as a dynamic biomarker to predict and monitor responses to therapy. The AR protein translocates to the nucleus in response to activation of AR signaling, and the cytoplasmic (as opposed to nuclear) localization of AR in CTCs from patients with mCRPC receiving taxane chemotherapy has been shown to correlate with treatment response [68]. A method to dynamically measure downstream effects of AR signaling in prostate CTCs has also been described, using relative levels of PSA and prostate-specific membrane antigen (PSMA) proteins, which are consistently up-regulated or down-regulated, respectively, by AR activity [69]. These and other studies suggest the potential use of assessing dynamic signaling pathways in prostate CTCs to predict treatment response to AR-targeted therapies, although further evaluation of these approaches are required in prospective clinical trials.

AR alterations in ctDNA

Serial interrogation of ctDNA can detect the emergence of *AR* alterations over time in patients with mCRPC treated with AR-targeted therapies. In recent studies, serial sampling of plasma and tumors from patients with mCRPC has demonstrated a temporal association between clinical progression on abiraterone and the emergence of *AR* mutations [70,71]. In a study of plasma DNA from 97 men with mCRPC, the emergence of *AR* mutations (T878A or L702H) was observed in 13% of patients with disease progression on abiraterone, despite a stable *AR* copy number throughout therapy [71]. Furthermore, patients with *AR* gain or mutations detected in their ctDNA before abiraterone therapy (45%) were 4.9 times less likely to have a >50% decline in PSA level and significantly worse OS (HR = 7.33, $P = 1.3 \times 10^{-9}$) and PFS (HR = 3.73, $P = 5.6 \times 10^{-7}$) rates [71]. On multivariate analysis accounting for other clinical factors including serum LDH, altered *AR* status remained the only significant predictor of OS and PFS rates. Another study analyzed cfDNA to examine *AR* copy number variations together with *CYP17A1* copy number variations in serum cfDNA from 53 patients with CRPC starting abiraterone. Both *AR* and *CYP17A1* gene gains were associated with a significantly lower PFS and OS on univariate analysis, whereas on multivariate analysis, performance status, PSA level decline, *AR* copy number variation, and DNA concentration were associated with OS [72]. These data suggest that evaluation of plasma ctDNA for *AR* alterations may be useful for identifying patients with primary resistance to abiraterone.

Similar to the abiraterone findings, in a retrospective cohort of 39 patients with mCRPC commencing enzalutamide therapy, alterations in *AR* (copy number increase or an exon 8 mutation or both) in pretreatment ctDNA were associated with adverse outcomes, including lower rates of PSA level decline ≥30% (and a trend toward lower rates of PSA level decline ≥50%), and shorter time to radiographic/clinical progression [73]. *AR* gene aberrations were observed in 19 of 39 patients (49%), including 14 with copy number increase and 5 with *AR* mutations (H874Y [$n = 2$], E893K, M895V, and T877A). In a subsequent study, the authors modified their sequencing and data analysis approaches and were able to identify 4 additional single *AR* mutations and 5 mutation combinations associated with mCRPC, with experimental validation of gain-of-function effects [74]. A similar study of 65 patients with mCRPC demonstrated that the detection of *AR* amplification, 2 or more mutations in *AR*, and *RB* loss in cfDNA were associated with worse PFS during treatment with enzalutamide [75]. Together, these studies indicate the promise of ctDNA analyses to evaluate *AR* copy number variations and *AR* mutations to predict outcomes after AR-targeted therapies. As with AR CTC assays, however, these methods require prospective validation in large clinical trials before they may be routinely applied in the clinic.

Detection of other molecular alterations

Other genetic alterations have been successfully detected in prostate CTCs, including loss of *PTEN* [60], amplification of *MYC* [59], and the *TMPRSS2-ERG* chromosomal translocation that is seen in half of patients with prostate cancer [60,76]. Regarding *TMPRSS2-ERG*, small studies indicate approximately 70% concordance between the presence of this genetic aberration in CTCs and the primary tumor [60,76]. Although *TMPRSS2-ERG* fusion status can be determined in CTCs, its presence did not predict response to abiraterone treatment in a study of 41 patients with mCRPC [77]. Recent technologic advances have also enabled genome-wide analyses of CTCs, such as whole-exome sequencing to map the mutational landscape of mCRPC [18], and single-cell whole-transcriptome RNA-seq to identify pathways potentially associated with anti-androgen resistance including noncanonical Wnt signaling [78]. Although these studies demonstrate the use of CTC analyses to detect known and novel molecular alterations in mCRPC, their value as prognostic or predictive biomarkers remains an area of active investigation.

Similarly, sequencing of cfDNA has been used to identify a range of other molecular alterations. Heitzer et al. [51] performed whole-genome sequencing from plasma in 5 patients with CRPC and 4 patients with castration-sensitive disease and were able to identify multiple copy number aberrations including losses in 8p and gains in 8q, as well as the *TMPRSS2-ERG* rearrangement. Methylated glutathione S-transferase 1 (mGSTP1) levels in plasma cfDNA have been prospectively evaluated as a prognostic biomarker in men with mCRPC starting chemotherapy [79]. Detectable mGSTP1 in ctDNA at baseline was associated with worse OS and a decrease in plasma mGSTP1 after one cycle of chemotherapy was associated with PSA level response [79]. However, additional larger prospective studies are necessary to validate these findings.

Insights into intratumoral heterogeneity

Prostate cancer is known to be a heterogeneous entity, with prostate glands often harboring multiple foci of disease [80]. Recent deep sequencing studies have demonstrated the existence of divergent cancer clones within primary tumors [81], and metastatic lesions in men with mCRPC likely arise through polyclonal seeding of divergent clones [82], although some studies suggest that driver lesions are conserved in metastatic lesions within individuals [83]. This substantial intratumoral heterogeneity indicates the potential for tumor misclassification when relying on a single-tumor biopsy in mCRPC, as molecular signatures may differ considerably depending on the clonal origin of the lesion that was biopsied. In this context, the molecular analysis of CTCs and ctDNA may be advantageous compared with individual tumor biopsies, because these circulating materials are shed from multiple different metastatic lesions and thus may be more representative of the genetic composition of the total metastatic burden.

Single-cell analyses of CTCs isolated from men with prostate cancer demonstrate considerable intracellular heterogeneity consistent with the known intratumoral heterogeneity of prostate cancer. In a single-cell RNA-seq study of 77 intact CTCs isolated from 13 patients, single CTCs displayed considerable heterogeneity in their transcriptional profiles, including expression of multiple different *AR* mRNA splice variants across different single cells from the same patient [78]. Nevertheless, unsupervised hierarchical clustering analyses showed strong clustering of single CTCs according to their patient of origin, suggesting higher diversity between patients compared with within individual patients. Similar levels of single CTC heterogeneity were observed in AR signaling patterns in patients with mCRPC, assessed through relative protein expression levels of PSA and PSMA [69].

CTC morphology has also been shown to be significantly heterogeneous, and potentially related to patient disease status. In a study of CTCs isolated from 57 patients with prostate cancer with either no metastases, nonvisceral metastases, or visceral metastases, 3 distinct subpopulations of CTCs were noted with different nuclear sizes, and CTCs with "very small nuclei" were found to be strongly associated with visceral metastases [84]. Interestingly, another study identified unique morphologic characteristics in CTCs from patients with neuroendocrine prostate cancer, including smaller morphology, abnormal nuclear and cytoplasmic features, and lower CK and AR expression [85].

Serial analyses of plasma cfDNA have also enabled characterization of heterogeneity in tumor clone dynamics reflective of treatment response and disease progression in prostate cancer. In a study of 16 *ERG*-rearrangement–positive patients, targeted deep sequencing of plasma DNA to detect deletions of 21p22, 8p21, and 10q23 in serial blood samples revealed surprisingly dynamic clonal architectural heterogeneity, where relative frequencies of these common deletions were found to be continuously changing over time [70]. Of note, in several cases, initially dominant deletions became subclonal after therapy, and then reemerged as dominant clones at subsequent time points, suggesting that independent tumor clones from distinct metastases are differentially represented in the peripheral circulation in a dynamic fashion. This complex clonal heterogeneity may originate either from multiple different clones from different tumor foci or potentially from genetically altered daughter clones arising from a single cell of origin.

CTCs or ctDNA

Both CTCs and ctDNA have the potential to be useful for the noninvasive sampling of tumors from the peripheral blood, but the question arises as to which is better suited for clinical applications and which is closer to routine clinical implementation. The relative quantities of each of these circulating biomarkers are correlated with prognosis in mCRPC, likely owing to their reflection of overall tumor burden. Furthermore, both approaches enable the noninvasive molecular analyses of tumors, including the assessment of *AR* and other molecular alterations. However, as they have orthogonal strengths and weaknesses, CTCs and ctDNA may ultimately serve as *complementary* biomarkers in the management of mCRPC (Table 2). ctDNA may be better suited for the detection of actionable mutations, whereas CTCs are more appropriate for analyses of RNA expression, protein cellular localization, intracellular heterogeneity, and establishment of long-term tumor cell cultures.

Plasma ctDNA has the advantage of generally being easier and less costly to isolate compared with CTCs and thus may be suitable for large-scale serial analyses of tumor-specific mutations in patients. Coupled with the increasing availability and decreasing costs of next-generation sequencing platforms, ctDNA analyses may soon become straightforward to implement into routine

Table 2
Potential complementary clinical applications of CTCs and ctDNA in prostate cancer

Application	CTCs		cfDNA/ctDNA	
	Example	References	Example	References
Measure of tumor burden	Prognostic value: baseline CTC measurement	[25,29,32]	Prognostic value: quantification of cfDNA concentration	[53]
	Predictive value: posttreatment change in CTCs	[25,29]	Predictive value: quantification of change in cfDNA	[54]
Detection of DNA/RNA alterations	Copy number alterations of *AR*	[59,60]	Gain of *AR* copy number	[71–73,75]
	Mutations in *AR* (RNA)	[61,62]	Mutations in *AR* (DNA)	[70,71,73–75]
	Presence of *AR* mRNA splice variants (e.g., *AR-V7*)	[58,63,64,67,78]	–	–
	Detection of translocations (e.g., *TMPRSS2-ERG*)	[60,76,77]	Detection of translocations (e.g., *TMPRSS2-ERG*)	[51]
	Whole-exome sequencing	[18]	Whole-genome sequencing	[51]
	–	–	Detection of methylated cfDNA (e.g., *GSTP1*)	[79]
Evaluation of intracellular heterogeneity	Single-cell RNA-seq of CTCs	[78]	Dynamic changes in specific deletions (e.g., 21p22, 8p21, and 10q23)	[70]
	Heterogeneity of CTC morphology	[84]	N/A	–
Protein localization	AR subcellular localization	[68]	N/A	–
	AR-V7 protein detection and localization	[66]	N/A	–
Protein measures of cellular activity	AR activity assessed by relative PSA and PSMA levels	[69]	N/A	–
	Telomerase activity	[86]	N/A	–
	Ki-67 as a measure of proliferation	[76]	N/A	–
Establishment of cultures	Organoids from CTCs	[88]	N/A	–

clinical practice and clinical trials. However, these platforms for the most part have not yet been standardized, and new tools for ctDNA detection and computational analyses continue to emerge at a rapid pace. A continuing challenge for the use of ctDNA as an analytical tool is the low yield of total cfDNA and the often low percentage of ctDNA among the cfDNA present in the blood of patients. In cfDNA samples without detectable mutations or DNA copy number changes, it is often impossible to distinguish between the actual absence of these changes (true negative) and insufficient yield of ctDNA (false negative). In addition, the specific detection of copy number losses as opposed to gains is particularly challenging in the setting of low ctDNA fractions and may require ctDNA fractions as high as 10% [51]. The ctDNA fraction tends to correlate with tumor burden, as suggested in studies that reveal a strong relationship between the presence of tumor-derived cfDNA and a CTC count ≥ 5 cells [73]. Thus, further improvements in the specific isolation and sensitive detection of the ctDNA fraction are necessary to enable the application of this technology to a wider spectrum of patients with varying tumor burden.

In contrast to ctDNA, the isolation of CTCs tends to be more resource intensive, given the technical challenges of isolating rare and fragile cells from the blood. An advantage of CTC enumeration is the existence of an FDA-cleared standardized platform for CTC enumeration (CellSearch), with a large number of patients prospectively studied using this platform to demonstrate the value of CTCs as a prognostic biomarker and a surrogate end point in clinical trials. Interestingly, despite the wealth of prospective data supporting its use as a prognostic marker, CTC enumeration with or without other markers such as LDH has not seen widespread adoption in routine clinical practice. Indeed, although these tests can help a clinician predict how well a patient would do, they do not provide information regarding whether an alternative form of therapy may be more appropriate for a given patient. Thus, there is a critical need for *predictive* biomarkers that can provide actionable information and influence patient clinical management, in contrast to *prognostic* markers such as CTC enumeration.

The recent demonstration of the potential value of detecting the AR-V7 splice variant in CTCs to predict resistance to AR-targeted therapies suggests that the molecular analysis of CTCs may provide such predictive biomarkers. However, such detailed analyses that go beyond enumeration often require more advanced CTC isolation technologies, many of which are not standardized or widely

available. Nevertheless, access to intact CTCs enables a variety of analyses not possible with ctDNA, including RNA-based analyses such as the detection of *AR* mRNA splice variants and whole-transcriptome RNA-seq and protein-based analyses including AR localization and PSA/PSMA expression, as described earlier. Other analyses that require intact cells include assessment of the marker of proliferation Ki-67, which in a pilot study exhibited widely variable expression in prostate CTCs (1%–81%), with a higher proliferative index associated with mCRPC [76]. The detection of telomerase activity in live CTCs has been shown to be prognostic of OS in a large subgroup of the prospective SWOG 0421 trial (HR = 1.14, $P = 0.001$) [86]. The analysis of intact CTCs also enables the direct study of intracellular heterogeneity regarding cellular morphology and genetic profiles, which may itself be of prognostic value. Perhaps the ultimate application of isolated CTCs is the establishment of CTC cultures for the purpose of individualized testing of drug susceptibility in vitro [87]. Pilot studies have demonstrated that culture of CTCs isolated from patients with mCRPC is possible using conditions optimized for 3D organoid growth [88], although further optimization of culture conditions is necessary to enable successful culture of samples from patients with lower CTC burden.

In addition to CTCs and ctDNA, an emerging category of potential circulating biomarkers includes extracellular vesicles such as exosomes and oncosomes, which are secreted by normal and cancer cells [89]. These 50- to 200-nm vesicles contain proteins and RNA molecules derived from the membrane and cytoplasm of their donor cells and are thought to function as regulators of cell-to-cell communication through transfer of biologically active components [90]. Proteins such as the multidrug resistance protein 1 (MDR1/ABCB1) have been found to be potentially higher in serum exosomes isolated from men with docetaxel-resistant prostate cancer [91]. Further exploration of circulating extracellular vesicles as potential biomarkers in mCRPC is warranted, although much remains to be done regarding standardization of isolation procedures, the development of robust assays, and their prospective validation in clinical trials.

Conclusions

Identifying biomarkers to help clinicians prescribe effective therapies while sparing patients the side effects of treatments that are unlikely to be beneficial remains an important unmet medical need in the care of patients with prostate cancer. Circulating biomarkers such as CTCs and ctDNA hold promise as readily accessible sources of tumor-derived material that may serve as prognostic or predictive biomarkers. This approach has been likened to a liquid biopsy that would be amenable to repetitive evaluations during the course of therapy, providing information about tumor burden as reflected by the number of CTCs or quantity of ctDNA, as well as a window into the molecular architecture of tumors as they evolve during treatment. CTC enumeration has been demonstrated to serve as a reliable prognostic biomarker in mCRPC and a potential surrogate end point for clinical trials, especially in combination with LDH. Beyond enumeration, the molecular characterization of CTCs and the analysis of ctDNA can provide actionable information regarding the presence of *AR* splice variants and *AR* mutations in patients and the corresponding likelihood of resistance to AR-targeted therapies. Such assays require rigorous standardization of analytic methodology and validation in large-scale, prospective clinical trials before they can be incorporated into routine clinical care. It can be envisioned that other liquid biopsy assays would be developed in the future to match men with mCRPC with appropriate targeted therapies based on molecular characteristics of their tumors, such as deficiencies in DNA damage response pathways with PARP inhibitors or mutations in *PIK3CA* with PI3K pathway inhibitors. Indeed, technologies for the molecular characterization of both CTCs and ctDNA continue to improve at a rapid pace, and we are moving closer to using these liquid biopsies to tailor treatment for individual patients in real time.

Acknowledgments

This work was supported by the Department of Defense (DTM) (Grant no. W81XWH-12-1-0153) and the Prostate Cancer Foundation (D.T.M. and R.J.L.). R.J.L. has received research funding from Janssen.

References

[1] Siegel RL, Miller KD, Jemal A. Cancer statistics, 2016. CA Cancer J Clin 2016;66:7–30.
[2] Mateo J, Carreira S, Sandhu S, Miranda S, Mossop H, Perez-Lopez R, et al. DNA-repair defects and olaparib in metastatic prostate cancer. N Engl J Med 2015;373:1697–708.
[3] Biomarkers Definitions Working Group. Biomarkers and surrogate endpoints: preferred definitions and conceptual framework. Clin Pharmacol Ther 2001;69:89–95.
[4] Saylor PJ, Lee RJ, Smith MR. Emerging therapies to prevent skeletal morbidity in men with prostate cancer. J Clin Oncol 2011;29:3705–14.
[5] Lovgren J, Valtonen-Andre C, Marsal K, Lilja H, Lundwall A. Measurement of prostate-specific antigen and human glandular kallikrein 2 in different body fluids. J Androl 1999;20:348–55.
[6] Armstrong AJ, Eisenberger MA, Halabi S, Oudard S, Nanus DM, Petrylak DP, et al. Biomarkers in the management and treatment of men with metastatic castration-resistant prostate cancer. Eur Urol 2012;61:549–59.
[7] Halabi S, Armstrong AJ, Sartor O, de Bono J, Kaplan E, Lin CY, et al. Prostate-specific antigen changes as surrogate for overall survival in men with metastatic castration-resistant prostate cancer treated with second-line chemotherapy. J Clin Oncol 2013;31:3944–50.
[8] Kantoff PW, Higano CS, Shore ND, Berger ER, Small EJ, Penson DF, et al. Sipuleucel-T immunotherapy for castration-resistant prostate cancer. N Engl J Med 2010;363:411–22.
[9] Petrylak DP, Ankerst DP, Jiang CS, Tangen CM, Hussain MH, Lara PN Jr., et al. Evaluation of prostate-specific antigen declines for

surrogacy in patients treated on SWOG 99–16. J Natl Cancer Inst 2006;98:516–21.
[10] Heitzer E, Auer M, Ulz P, Geigl JB, Speicher MR. Circulating tumor cells and DNA as liquid biopsies. Genome Med 2013;5:73.
[11] Alix-Panabieres C, Pantel K. Clinical applications of circulating tumor cells and circulating tumor DNA as liquid biopsy. Cancer Discov 2016;6:479–91.
[12] Robinson D, Van Allen EM, Wu YM, Schultz N, Lonigro RJ, Mosquera JM, et al. Integrative clinical genomics of advanced prostate cancer. Cell 2015;161:1215–28.
[13] Miyamoto DT, Sequist LV, Lee RJ. Circulating tumour cells-monitoring treatment response in prostate cancer. Nat Rev Clin Oncol 2014;11:401–12.
[14] Li J, Gregory SG, Garcia-Blanco MA, Armstrong AJ. Using circulating tumor cells to inform on prostate cancer biology and clinical utility. Crit Rev Clin Lab Sci 2015;52:191–210.
[15] Alix-Panabieres C, Pantel K. Challenges in circulating tumour cell research. Nat Rev Cancer 2014;14:623–31.
[16] Fehm T, Sagalowsky A, Clifford E, Beitsch P, Saboorian H, Euhus D, et al. Cytogenetic evidence that circulating epithelial cells in patients with carcinoma are malignant. Clin Cancer Res 2002;8:2073–84.
[17] Heitzer E, Auer M, Gasch C, Pichler M, Ulz P, Hoffmann EM, et al. Complex tumor genomes inferred from single circulating tumor cells by array-CGH and next-generation sequencing. Cancer Res 2013; 73:2965–75.
[18] Lohr JG, Adalsteinsson VA, Cibulskis K, Choudhury AD, Rosenberg M, Cruz-Gordillo P, et al. Whole-exome sequencing of circulating tumor cells provides a window into metastatic prostate cancer. Nat Biotechnol 2014;32:479–84.
[19] Shaffer DR, Leversha MA, Danila DC, Lin O, Gonzalez-Espinoza R, Gu B, et al. Circulating tumor cell analysis in patients with progressive castration-resistant prostate cancer. Clin Cancer Res 2007;13:2023–9.
[20] Haber DA, Velculescu VE. Blood-based analyses of cancer: circulating tumor cells and circulating tumor DNA. Cancer Discov 2014;4:650–61.
[21] FDA Clearance Document for Veridex LLC. CellSearch(TM) Circulating Tumor Cell Kit. Premarket notification—expanded indications for use—metastatic prostate cancer. February 26, 2008. Available at: http://accessdata.fda.gov/cdrh_docs/pdf7/K073338 [accessed 28.01.14].
[22] Armstrong AJ, Marengo MS, Oltean S, Kemeny G, Bitting RL, Turnbull JD, et al. Circulating tumor cells from patients with advanced prostate and breast cancer display both epithelial and mesenchymal markers. Mol Cancer Res 2011;9:997–1007.
[23] Marrinucci D, Bethel K, Kolatkar A, Luttgen MS, Malchiodi M, Baehring F, et al. Fluid biopsy in patients with metastatic prostate, pancreatic and breast cancers. Phys Biol 2012;9:016003.
[24] Ozkumur E, Shah AM, Ciciliano JC, Emmink BL, Miyamoto DT, Brachtel E, et al. Inertial focusing for tumor antigen-dependent and -independent sorting of rare circulating tumor cells. Sci Transl Med 2013;5:179ra47.
[25] de Bono JS, Scher HI, Montgomery RB, Parker C, Miller MC, Tissing H, et al. Circulating tumor cells predict survival benefit from treatment in metastatic castration-resistant prostate cancer. Clin Cancer Res 2008;14:6302–9.
[26] Scher HI, Jia X, de Bono JS, Fleisher M, Pienta KJ, Raghavan D, et al. Circulating tumour cells as prognostic markers in progressive, castration-resistant prostate cancer: a reanalysis of IMMC38 trial data. Lancet Oncol 2009;10:233–9.
[27] Halabi S, Small EJ, Kantoff PW, Kattan MW, Kaplan EB, Dawson NA, et al. Prognostic model for predicting survival in men with hormone-refractory metastatic prostate cancer. J Clin Oncol 2003;21: 1232–7.
[28] Goodman OB Jr., Fink LM, Symanowski JT, Wong B, Grobaski B, Pomerantz D, et al. Circulating tumor cells in patients with castration-resistant prostate cancer baseline values and correlation with prognostic factors. Cancer Epidemiol Biomarkers Prev 2009;18:1904–13.
[29] Goldkorn A, Ely B, Quinn DI, Tangen CM, Fink LM, Xu T, et al. Circulating tumor cell counts are prognostic of overall survival in SWOG S0421: a phase III trial of docetaxel with or without atrasentan for metastatic castration-resistant prostate cancer. J Clin Oncol 2014;32:1136–42.
[30] Quinn DI, Tangen CM, Hussain M, Lara PN Jr., Goldkorn A, Moinpour CM, et al. Docetaxel and atrasentan versus docetaxel and placebo for men with advanced castration-resistant prostate cancer (SWOG S0421): a randomised phase 3 trial. Lancet Oncol 2013;14: 893–900.
[31] de Bono JS, Logothetis CJ, Molina A, Fizazi K, North S, Chu L, et al. Abiraterone and increased survival in metastatic prostate cancer. N Engl J Med 2011;364:1995–2005.
[32] Scher HI, Heller G, Molina A, Attard G, Danila DC, Jia X, et al. Circulating tumor cell biomarker panel as an individual-level surrogate for survival in metastatic castration-resistant prostate cancer. J Clin Oncol 2015;33:1348–55.
[33] Scher HI, Heller G, Molina A, Kheoh TS, Attard G, Moreira J, et al. Evaluation of circulating tumor cell (CTC) enumeration as an efficacy response biomarker of overall survival (OS) in metastatic castration-resistant prostate cancer (mCRPC): planned final analysis (FA) of COU-AA-301, a randomized, double-blind, placebo-controlled, phase III study of abiraterone acetate (AA) plus low-dose prednisone (P) post docetaxel. J Clin Oncol 2011;29(Suppl):LBA4517.
[34] Prentice RL. Surrogate endpoints in clinical trials: definition and operational criteria. Stat Med 1989;8:431–40.
[35] Stroun M, Lyautey J, Lederrey C, Olson-Sand A, Anker P. About the possible origin and mechanism of circulating DNA apoptosis and active DNA release. Clin Chim Acta 2001;313:139–42.
[36] Heitzer E, Ulz P, Geigl JB. Circulating tumor DNA as a liquid biopsy for cancer. Clin Chem 2015;61:112–23.
[37] Fan HC, Blumenfeld YJ, Chitkara U, Hudgins L, Quake SR. Analysis of the size distributions of fetal and maternal cell-free DNA by paired-end sequencing. Clin Chem 2010;56:1279–86.
[38] Leon SA, Shapiro B, Sklaroff DM, Yaros MJ. Free DNA in the serum of cancer patients and the effect of therapy. Cancer Res 1977;37:646–50.
[39] Perkins G, Yap TA, Pope L, Cassidy AM, Dukes JP, Riisnaes R, et al. Multi-purpose utility of circulating plasma DNA testing in patients with advanced cancers. PLoS One 2012;7:e47020.
[40] Diehl F, Schmidt K, Choti MA, Romans K, Goodman S, Li M, et al. Circulating mutant DNA to assess tumor dynamics. Nat Med 2008; 14:985–90.
[41] Vogelstein B, Kinzler KW. Digital PCR. Proc Natl Acad Sci U S A 1999;96:9236–41.
[42] Dressman D, Yan H, Traverso G, Kinzler KW, Vogelstein B. Transforming single DNA molecules into fluorescent magnetic particles for detection and enumeration of genetic variations. Proc Natl Acad Sci U S A 2003;100:8817–22.
[43] Hindson BJ, Ness KD, Masquelier DA, Belgrader P, Heredia NJ, Makarewicz AJ, et al. High-throughput droplet digital PCR system for absolute quantitation of DNA copy number. Anal Chem 2011;83: 8604–10.
[44] Pekin D, Skhiri Y, Baret JC, Le Corre D, Mazutis L, Salem CB, et al. Quantitative and sensitive detection of rare mutations using droplet-based microfluidics. Lab Chip 2011;11:2156–66.
[45] Thompson JD, Shibahara G, Rajan S, Pel J, Marziali A. Winnowing DNA for rare sequences: highly specific sequence and methylation based enrichment. PLoS One 2012;7:e31597.
[46] Kinde I, Wu J, Papadopoulos N, Kinzler KW, Vogelstein B. Detection and quantification of rare mutations with massively parallel sequencing. Proc Natl Acad Sci U S A 2011;108:9530–5.
[47] Forshew T, Murtaza M, Parkinson C, Gale D, Tsui DW, Kaper F, et al. Noninvasive identification and monitoring of cancer mutations by targeted deep sequencing of plasma DNA. Sci Transl Med 2012; 4:136ra68.

[48] Newman AM, Bratman SV, To J, Wynne JF, Eclov NC, Modlin LA, et al. An ultrasensitive method for quantitating circulating tumor DNA with broad patient coverage. Nat Med 2014;20: 548–54.
[49] Murtaza M, Dawson SJ, Tsui DW, Gale D, Forshew T, Piskorz AM, et al. Non-invasive analysis of acquired resistance to cancer therapy by sequencing of plasma DNA. Nature 2013;497:108–12.
[50] Leary RJ, Sausen M, Kinde I, Papadopoulos N, Carpten JD, Craig D, et al. Detection of chromosomal alterations in the circulation of cancer patients with whole-genome sequencing. Sci Transl Med 2012;4:162ra54.
[51] Heitzer E, Ulz P, Belic J, Gutschi S, Quehenberger F, Fischereder K, et al. Tumor-associated copy number changes in the circulation of patients with prostate cancer identified through whole-genome sequencing. Genome Med 2013;5:30.
[52] Schwarzenbach H, Alix-Panabieres C, Muller I, Letang N, Vendrell JP, Rebillard X, et al. Cell-free tumor DNA in blood plasma as a marker for circulating tumor cells in prostate cancer. Clin Cancer Res 2009;15:1032–8.
[53] Kienel A, Porres D, Heidenreich A, Pfister D. cfDNA as a prognostic marker of response to taxane based chemotherapy in patients with prostate cancer. J Urol 2015;194:966–71.
[54] Kwee S, Song MA, Cheng I, Loo L, Tiirikainen M. Measurement of circulating cell-free DNA in relation to 18F-fluorocholine PET/CT imaging in chemotherapy-treated advanced prostate cancer. Clin Transl Sci 2012;5:65–70.
[55] Watson PA, Arora VK, Sawyers CL. Emerging mechanisms of resistance to androgen receptor inhibitors in prostate cancer. Nat Rev Cancer 2015;15:701–11.
[56] Balbas MD, Evans MJ, Hosfield DJ, Wongvipat J, Arora VK, Watson PA, et al. Overcoming mutation-based resistance to antiandrogens with rational drug design. eLife 2013;2:e00499.
[57] Joseph JD, Lu N, Qian J, Sensintaffar J, Shao G, Brigham D, et al. A clinically relevant androgen receptor mutation confers resistance to second-generation antiandrogens enzalutamide and ARN-509. Cancer Discov 2013;3:1020–9.
[58] Antonarakis ES, Lu C, Wang H, Luber B, Nakazawa M, Roeser JC, et al. AR-V7 and resistance to enzalutamide and abiraterone in prostate cancer. N Engl J Med 2014;371:1028–38.
[59] Leversha MA, Han J, Asgari Z, Danila DC, Lin O, Gonzalez-Espinoza R, et al. Fluorescence in situ hybridization analysis of circulating tumor cells in metastatic prostate cancer. Clin Cancer Res 2009;15:2091–7.
[60] Attard G, Swennenhuis JF, Olmos D, Reid AH, Vickers E, A'Hern R, et al. Characterization of ERG, AR and PTEN gene status in circulating tumor cells from patients with castration-resistant prostate cancer. Cancer Res 2009;69:2912–8.
[61] Jiang Y, Palma JF, Agus DB, Wang Y, Gross ME. Detection of androgen receptor mutations in circulating tumor cells in castration-resistant prostate cancer. Clin Chem 2010;56:1492–5.
[62] Steinestel J, Luedeke M, Arndt A, Schnoeller TJ, Lennerz JK, Wurm C, et al. Detecting predictive androgen receptor modifications in circulating prostate cancer cells. Oncotarget 2015. [Epub ahead of print].
[63] Antonarakis ES, Lu C, Luber B, Wang H, Chen Y, Nakazawa M, et al. Androgen receptor splice variant 7 and efficacy of taxane chemotherapy in patients with metastatic castration-resistant prostate cancer. JAMA Oncol 2015;1:582–91.
[64] Onstenk W, Sieuwerts AM, Kraan J, Van M, Nieuweboer AJ, Mathijssen RH, et al. Efficacy of cabazitaxel in castration-resistant prostate cancer is independent of the presence of AR-V7 in circulating tumor cells. Eur Urol 2015;68:939–45.
[65] Nakazawa M, Lu C, Chen Y, Paller CJ, Carducci MA, Eisenberger MA, et al. Serial blood-based analysis of AR-V7 in men with advanced prostate cancer. Ann Oncol 2015;26:1859–65.
[66] Scher HI, Lu D, Schreiber NA, Louw J, Graf RP, Vargas HA, et al. Association of AR-V7 on circulating tumor cells as a treatment-specific biomarker with outcomes and survival in castration-resistant prostate cancer. JAMA Oncol 2016. [Epub ahead of print].
[67] Bernemann C, Schnoeller TJ, Luedeke M, Steinestel K, Boegemann M, Schrader AJ, et al. Expression of AR-V7 in circulating tumour cells does not preclude response to next generation androgen deprivation therapy in patients with castration resistant prostate cancer. Eur Urol 2016. [Epub ahead of print].
[68] Darshan MS, Loftus MS, Thadani-Mulero M, Levy BP, Escuin D, Zhou XK, et al. Taxane-induced blockade to nuclear accumulation of the androgen receptor predicts clinical responses in metastatic prostate cancer. Cancer Res 2011;71:6019–29.
[69] Miyamoto DT, Lee RJ, Stott SL, Ting DT, Wittner BS, Ulman M, et al. Androgen receptor signaling in circulating tumor cells as a marker of hormonally responsive prostate cancer. Cancer Discov 2012;2:995–1003.
[70] Carreira S, Romanel A, Goodall J, Grist E, Ferraldeschi R, Miranda S, et al. Tumor clone dynamics in lethal prostate cancer. Sci Transl Med 2014;6:254ra125.
[71] Romanel A, Gasi Tandefelt D, Conteduca V, Jayaram A, Casiraghi N, Wetterskog D, et al. Plasma AR and abiraterone-resistant prostate cancer. Sci Transl Med 2015;7:312re10.
[72] Salvi S, Casadio V, Conteduca V, Burgio SL, Menna C, Bianchi E, et al. Circulating cell-free AR and CYP17A1 copy number variations may associate with outcome of metastatic castration-resistant prostate cancer patients treated with abiraterone. Br J Cancer 2015;112:1717–24.
[73] Azad AA, Volik SV, Wyatt AW, Haegert A, Le Bihan S, Bell RH, et al. Androgen receptor gene aberrations in circulating cell-free DNA: biomarkers of therapeutic resistance in castration-resistant prostate cancer. Clin Cancer Res 2015;21:2315–24.
[74] Lallous N, Volik SV, Awrey S, Leblanc E, Tse R, Murillo J, et al. Functional analysis of androgen receptor mutations that confer anti-androgen resistance identified in circulating cell-free DNA from prostate cancer patients. Genome Biol 2016;17:10.
[75] Wyatt AW, Azad AA, Volik SV, Annala M, Beja K, McConeghy B, et al. Genomic alterations in cell-free DNA and enzalutamide resistance in castration-resistant prostate cancer. JAMA Oncol 2016. [Epub ahead of print].
[76] Stott SL, Lee RJ, Nagrath S, Yu M, Miyamoto DT, Ulkus L, et al. Isolation and characterization of circulating tumor cells from patients with localized and metastatic prostate cancer. Sci Transl Med 2010;2:25ra3.
[77] Danila DC, Anand A, Sung CC, Heller G, Leversha MA, Cao L, et al. TMPRSS2-ERG status in circulating tumor cells as a predictive biomarker of sensitivity in castration-resistant prostate cancer patients treated with abiraterone acetate. Eur Urol 2011;60:897–904.
[78] Miyamoto DT, Zheng Y, Wittner BS, Lee RJ, Zhu H, Broderick KT, et al. RNA-Seq of single prostate CTCs implicates noncanonical Wnt signaling in antiandrogen resistance. Science 2015;349:1351–6.
[79] Mahon KL, Qu W, Devaney J, Paul C, Castillo L, Wykes RJ, et al. Methylated glutathione S-transferase 1 (mGSTP1) is a potential plasma free DNA epigenetic marker of prognosis and response to chemotherapy in castrate-resistant prostate cancer. Br J Cancer 2014;111:1802–9.
[80] Andreoiu M, Cheng L. Multifocal prostate cancer: biologic, prognostic, and therapeutic implications. Hum Pathol 2010;41:781–93.
[81] Cooper CS, Eeles R, Wedge DC, Van Loo P, Gundem G, Alexandrov LB, et al. Analysis of the genetic phylogeny of multifocal prostate cancer identifies multiple independent clonal expansions in neoplastic and morphologically normal prostate tissue. Nat Genet 2015;47:367–72.
[82] Gundem G, Van Loo P, Kremeyer B, Alexandrov LB, Tubio JM, Papaemmanuil E, et al. The evolutionary history of lethal metastatic prostate cancer. Nature 2015;520:353–7.
[83] Kumar A, Coleman I, Morrissey C, Zhang X, True LD, Gulati R, et al. Substantial interindividual and limited intraindividual genomic diversity among tumors from men with metastatic prostate cancer. Nat Med 2016;22:369–78.
[84] Chen JF, Ho H, Lichterman J, Lu YT, Zhang Y, Garcia MA, et al. Subclassification of prostate cancer circulating tumor cells by nuclear

size reveals very small nuclear circulating tumor cells in patients with visceral metastases. Cancer 2015;121:3240–51.

[85] Beltran H, Jendrisak A, Landers M, Mosquera JM, Kossai M, Louw J, et al. The Initial detection and partial characterization of circulating tumor cells in neuroendocrine prostate cancer. Clin Cancer Res 2016;22:1510–9.

[86] Goldkorn A, Ely B, Tangen CM, Tai YC, Xu T, Li H, et al. Circulating tumor cell telomerase activity as a prognostic marker for overall survival in SWOG 0421: a phase III metastatic castration resistant prostate cancer trial. Int J Cancer 2015;136:1856–62.

[87] Yu M, Bardia A, Aceto N, Bersani F, Madden MW, Donaldson MC, et al. Cancer therapy. Ex vivo culture of circulating breast tumor cells for individualized testing of drug susceptibility. Science 2014;345:216–20.

[88] Gao D, Vela I, Sboner A, Iaquinta PJ, Karthaus WR, Gopalan A, et al. Organoid cultures derived from patients with advanced prostate cancer. Cell 2014;159:176–87.

[89] Junker K, Heinzelmann J, Beckham C, Ochiya T, Jenster G. Extracellular vesicles and their role in urologic malignancies. Eur Urol 2016;70:323–31.

[90] Di Vizio D, Kim J, Hager MH, Morello M, Yang W, Lafargue CJ, et al. Oncosome formation in prostate cancer: association with a region of frequent chromosomal deletion in metastatic disease. Cancer Res 2009;69:5601–9.

[91] Kato T, Mizutani K, Kameyama K, Kawakami K, Fujita Y, Nakane K, et al. Serum exosomal P-glycoprotein is a potential marker to diagnose docetaxel resistance and select a taxoid for patients with prostate cancer. Urol Oncol 2015;33:385.e15-e20.

[92] Ryan CJ, Smith MR, Fizazi K, Saad F, Mulders PF, Sternberg CN, et al. Abiraterone acetate plus prednisone versus placebo plus prednisone in chemotherapy-naive men with metastatic castration-resistant prostate cancer (COU-AA-302): final overall survival analysis of a randoomised, double-blind, placebo-controlled phase 3 study. Lancet Oncol 2015;16:152–60.

Review

For reprint orders, please contact: reprints@futuremedicine.com

Biomarkers in Medicine

The promise of circulating tumor cells for precision cancer therapy

William L Hwang[1,2], Katie L Hwang[2,3] & David T Miyamoto*[,1,2]

[1]Department of Radiation Oncology, Massachusetts General Hospital, Boston, MA 02114, USA

[2]Massachusetts General Hospital Cancer Center, Boston, MA 02114, USA

[3]Medical Scientist Training Program, Harvard Medical School, Boston, MA 02115, USA

*Author for correspondence:
Tel.: +1 617 726 5866;
Fax: +1 617 726 3603;
dmiyamoto@mgh.harvard.edu

The rapidly growing array of therapeutic options in cancer requires informative biomarkers to guide the rational selection and precision application of appropriate therapies. Circulating biomarkers such as circulating tumor cells have immense potential as noninvasive, serial 'liquid biopsies' that may be more representative of the complete spectrum of a patient's individual malignancy than spatially and temporally restricted tumor biopsies. In this review, we discuss the current state-of-the-art in the isolation and molecular characterization of circulating tumor cells as well as their utility in a wide range of clinical applications such as prognostics, treatment monitoring and identification of novel therapeutic targets and resistance mechanisms to enable real-time adjustments in the clinical management of cancer.

First draft submitted: 15 July 2016; Accepted for publication: 27 September 2016; Published online: 7 December 2016

Keywords: cancer • circulating tumor cells (CTCs) • precision therapy • predictive marker • prognostic marker

The evolving landscape of cancer therapy creates an urgent need for minimally invasive biomarkers to facilitate early detection, prognosis and prediction of therapeutic response and resistance to enable highly adaptable, real-time precision therapy [1]. The conventional gold standard of using single biopsies of the primary tumor to inform all downstream therapeutic decisions may no longer be adequate given increasing evidence of significant spatial and temporal heterogeneity in tumors [2], especially when placed under the selection pressure of various treatments. Moreover, serial biopsies are often impractical, morbid and technically challenging.

In this review, we focus on the emerging role of circulating tumor cells (CTCs), which can be serially obtained from minimally invasive blood draws or 'liquid biopsies'. CTCs are cancer cells that have been shed into the peripheral circulation from primary or metastatic tumors [3,4]. The first reported observation of CTCs was in 1869 by Australian pathologist Thomas Ashworth at the autopsy of a patient with metastatic cancer [5]. By comparing the morphology of circulating cells with those from different cancerous lesions, Ashworth came to the prescient conclusion that 'cells identical with those of the cancer itself being seen in the blood may tend to throw some light upon the mode of origin of multiple tumors existing in the same person' [5]. Indeed, molecular analyses of CTCs may be superior to individual tumor biopsies because these circulating cells likely provide a sampling of different regions of the primary tumor as well as metastatic deposits, and therefore are more likely to capture the genetic heterogeneity of a patient's cancer.

While cell-free circulating tumor DNA (ctDNA) is an important, complementary biomarker to CTCs, it has been reviewed extensively elsewhere and will not be discussed in this review [4,6]. Moreover, although ctDNA may in some cases be more reliably

Future Medicine part of fsg

isolated from patients than CTCs [7], they are largely limited to genomic mutational analysis. In contrast, CTC analysis can provide a wealth of other information including cell morphology, immunocytochemical phenotype, presence of important epitopes, presence of multiple mutations within a single cell to decode tumor heterogeneity and map clonal evolution, and genomic mutational analysis combined with epigenetic/transcriptomic/proteomic/metabolomic profiling. CTC analyses may also enable determination of the functional relevance of novel targets for therapeutic inhibition, and provide an unprecedented opportunity to dissect the biology of metastasis. Additional emerging blood-based biomarkers such as exosomes and platelets are discussed elsewhere and are also beyond the scope of this review [8–10].

Biology of CTCs

CTCs originate from cells within primary or metastatic tumors that acquire the ability to invade through the basement membrane and tissue stroma to enter the bloodstream/lymphatics, a process that is hypothesized to involve epithelial-to-mesenchymal transition (EMT) [11]. Furthermore, only a subset of CTCs have the tumorigenic potential to form distant metastatic deposits [12], which are ultimately responsible for up to 90% of cancer deaths [13]. Understanding the biology of CTCs can provide insights into the evolution of malignancy, development of metastases and identification of exploitable targets for treatment.

Epithelial–mesenchymal transition & metastasis

EMT is a normal process in embryogenesis and wound healing, but in cancer, it is a process whereby epithelial tumor cells are believed to lose their apical-basal polarization and cell–cell adhesions to take on a mesenchymal phenotype with a motile cytoskeleton that enables them to invade through adjacent tissue [14]. Epithelial markers include epithelial cell adhesion molecule (EpCAM) and cytokeratins, whereas mesenchymal markers include vimentin, N-cadherin and O-cadherin, among others. The reason that positive selection approaches for CTC capture generally use epithelial markers is because mesenchymal markers such as vimentin are also expressed on blood cells.

CTCs expressing mesenchymal markers are more frequently found in advanced cancers than early-stage disease, indicating a likely association between EMT and disease progression [15]. Furthermore, a spectrum of breast cancer CTCs spanning a mixed epithelial–mesenchymal phenotype was identified by RNA FISH, with an increase in the representation of the mesenchymal phenotype during disease progression and a decrease during disease regression, further suggesting mesenchymal CTCs are associated with metastatic progression [16]. Interestingly, metastases often resemble the predominantly epithelial primary tumor, implying that cells may transition from epithelial to mesenchymal phenotypes to migrate, but then revert back to an epithelial state at distant sites (mesenchymal–epithelial transition), which recapitulates the process in organ development [17,18]. Tumor cells that have undergone partial EMT (intermediate phenotype) may have the highest plasticity to adapt to the conditions present at secondary sites [19].

However, it is not as simple as concluding that mesenchymal-type CTCs all have the capability of generating metastases [20]. Indeed, it has been hypothesized that only a small fraction of tumor cells have metastatic capability-adaptations to survive passage through the circulation and generate metastases [21,22]. This subset of cells likely overlaps with cancer stem cells, which have properties of adult stem cells (self-renewal and multipotency), as well as a mesenchymal phenotype as discussed previously, and are capable of initiating tumors when injected into immunocompromised mice [23–25]. These metastatic stem and mesenchymal-like cells should be represented in the CTC population, and identifying and studying their properties in isolation, culture and preclinical animal models would enable a better understanding of these unique cancer-driving cells and increase the odds of eradicating them.

Blood samples depleted of leukocytes from metastatic breast cancer patients have been used to generate CTC-derived xenografts in immunocompromised mice, but the process is highly inefficient. In one study, xenografts with multiorgan metastases were only successful when there were >1000 CTCs per 7.5 ml of blood, measured using the CellSearch® platform (Janssen Diagnostics, Raritan, NJ, USA; discussed in detail below) [26]. This was the first confirmation of a tumorigenic subpopulation of CTCs, which by flow cytometry was characterized as $CD45^-$ $EpCAM^+$ $CD44^+$ $CD47^+$ $c\text{-}MET^+$ [26]. Another similar study on breast cancer uncovered $EpCAM^-$ CTCs with tumorigenic properties, causing brain metastases [27]. A group from Manchester, UK recently created a non-small-cell lung cancer (NSCLC) CTC-derived xenograft using blood samples that were devoid of CTCs when using the CellSearch platform; size-based CTC enrichment revealed abundant heterogeneous CTCs, of which 80% expressed the mesenchymal marker vimentin, demonstrating that the absence of epithelial CTCs does not preclude the generation of CTC-derived xenografts [28]. Using an orthotopic mouse model of colorectal cancer that reliably produces metastases and CTCs, Scholch and colleagues cultured the CTCs and

demonstrated their tumorigenic capacity upon re-injection into mice [12]. Reverse transcription PCR expression profiling of these CTCs revealed reduced expression of cell–cell adhesion genes such as *claudin-7* and *CD166*, and increased expression of stem cell markers such as *DLG7* and *BMI1* relative to bulk tumor cells derived from hepatic metastases.

Circulating tumor microemboli (CTM) are defined as a cluster of three or more CTCs that circulate together [29]. The presence of heterotypic tumor stroma (fibroblasts, platelets, leukocytes, endothelial cells, pericytes) increases viability of tumor cells within CTM and confers an early growth advantage to metastatic colonies [30], which is supported by the observation that CTM injected into mice have a higher probability of seeding distant metastases than single CTCs [31–33]. Lung cancer CTCs clustered as CTM were found to be nonproliferative (based on absence of Ki-67 expression), but up to 62% of single cells had high Ki-67 expression, suggesting that tumor cells within CTM are in a state of cell-cycle arrest, which may contribute to chemotherapy resistance and enhanced cell survival, resulting in worse prognosis [29].

Recent genomic studies challenge the conventional model that each metastasis arises from a single malignant cell, and instead reveal that metastases can be composed of multiple genetically distinct clones [33–35]. Cheung and colleagues used multicolor lineage tracing to demonstrate that polyclonal seeding by CTM is a frequent mechanism in a breast cancer mouse model, accounting for >90% of metastases [36]. Expression of the epithelial cytoskeletal protein, keratin 14 (K14) plays a critical role in this process since depletion of K14 abrogates distant metastases, suggesting that $K14^+$ epithelial tumor cell clusters disseminate collectively to colonize distant organs. In an elegant study from the University of California San Francisco, Headley and colleagues developed an intravital two-photon lung imaging model in mice to directly observe the arrival of CTCs and subsequent host immune interaction [37]. They found that tumor microemboli form in the capillaries within minutes of CTC arrival and then remain attached to the lung vasculature or migrate along the vessels. Interestingly, waves of different myeloid cell derivatives were seen to interact with these CTC microemboli, ingesting them and accumulating in the lung interstitium. While recruited neutrophils and monocytes/macrophages are important to establishing the early metastatic niche, the less abundant lung dendritic cells mediate potent antimetastatic effects.

Evolution & heterogeneity

Reliable detection of mutations plays an important role in personalized therapy selection, since mutations in genes encoding therapeutic targets or downstream signaling proteins can affect drug efficacy. For example, mutations in EGFR affect anti-EGFR therapy in lung cancer and mutations in KRAS, a protein downstream of EGFR, block efficacy of anti-EGFR therapy in colorectal cancer [38,39]. It can be informative to compare CTC and matched biopsy profiles to determine the degree of overlap or disparity. Furthermore, sequencing analysis of single CTCs circumvents leukocyte contamination and can potentially provide a more global view of cancer heterogeneity than spatially limited biopsies. Single-cell DNA sequencing of CTCs has revealed intra- and inter-patient genetic heterogeneity as well as discordance with primary tumors, metastatic deposits and changes after treatment [38,40–41]. However, most copy number variations and mutations found in CTCs (>80%) can be traced back to either primary or metastatic tumors [42,43]. These initial findings suggested that serial CTC analyses during cancer treatment could potentially guide real-time precision therapy by providing a snapshot of the genetic evolution of a patient's particular cancer and allowing identification of genetic vulnerabilities. For example, the EGFR T790M mutation is acquired by some EGFR-mutant NSCLC as they become resistant to selective tyrosine kinase inhibitors (TKIs), making the newer third-generation TKIs necessary. Sundaresan and colleagues found that combined CTC- and ctDNA-based genotyping detected T790M in 35% of patients in whom concurrent biopsy was negative or indeterminate [44], thereby identifying a population of patients in whom liquid biopsies demonstrably improved real-time precision therapy.

To elucidate the phenotypic diversity of CTCs with regard to differential gene expression profiles, several groups have undertaken single-cell RNA sequencing [45–49]. Powell and colleagues identified two major CTC subgroups in breast cancer patients, one with elevated expression of metastasis-associated genes and the other with increased expression of EMT-associated genes [45]. Using single-cell transcriptomics, Miyamoto and colleagues identified two androgen receptor (AR) independent mechanisms for antiandrogen resistance in prostate cancer: noncanonical Wnt signaling and activation of glucocorticoid receptor signaling [49,50]. Additional examples will be discussed in the 'Clinical application' section.

Capture & characterization of CTCs

The reliable capture of CTCs from whole blood is challenging due to their scarcity, estimated at approximately one CTC per 10^7 leukocytes per ml of blood [18]. Numerous approaches for their isolation have been devised, which can be loosely grouped into the fol-

lowing categories: immunomagnetic capture (both positive and negative selection); physical separation; high-throughput microscopy; and functional selection [51–53] (Figure 1). The sensitivity and specificity of CTC detection vary for different methods. The most commonly used blood volume in clinical CTC studies is 7.5 ml. Assuming an underlying Poisson distribution, the probability of detecting at least 1 CTC in 7.5 ml of whole blood from a patient with a total of 500 CTCs is approximately 50% [54].

Recently, integrated microfluidic platforms with increased automation incorporating sample preparation and image processing with immunohistochemistry, flow cytometry or DNA/RNA FISH have been reported [55]. While technologies designed to isolate single CTCs can often detect CTMs as well, there have also been efforts toward the specific capture of CTMs [56].

Immunomagnetic capture

Enrichment of CTCs by immunomagnetic capture is the most established strategy. The paradigm of this approach is CellSearch, which uses ferromagnetic beads coated with anti-EpCAM antibodies to enrich for EpCAM-expressing epithelial-type CTCs and then performs a second selection step based on morphology, expression of cytokeratins and absence of leukocyte common antigen (CD45) [57]. To date, CellSearch is the only CTC-capture system that has been extensively validated and deployed in large clinical trials, leading to US FDA clearance [58] as a prognostic tool in metastatic breast, prostate and colorectal cancer [59–61]. Other platforms utilizing EpCAM positive selection of CTCs have been developed including magnetic rods [62], a medical wire that enriches CTCs directly from a peripheral vein [63] and microfluidic chips [64–67]. Non-EpCAM positive selection (e.g., cytokeratins, EGFR, CD19) and negative selection (e.g., CD45) techniques have been demonstrated [66,68–70]. Capturing CTCs using rationally designed aptamer cocktails in a microfluidic platform was recently described [71]. Despite the successful and varied implementation of immunomagnetic capture, the common reliance on expression of epithelial markers such as EpCAM and cytokeratins omits mesenchymal-type CTCs, which are thought to be fundamentally important for metastasis. Hence, there has recently been increased interest in technologies that utilize marker-independent isolation methods.

Physical separation

The primary advantage of label-free approaches is avoiding the selective enrichment of CTC subgroups with particular immunocytochemical features, which enables isolation of nonepithelial CTCs. Several physical differences between CTCs and leukocytes can be exploited. Size-based filtration harnesses the fact that CTCs tend to be larger than leukocytes [72–74]. CTCs typically have higher membrane capacitance than leukocytes, in large part because of greater total surface area, allowing for their isolation by dielectrophoresis field-flow fractionation [75]. Finally, CTCs are more rigid than leukocytes because of increased nuclear to cytoplasmic ratio (as indicated by the length of time required for them to pass through a microfluidic constriction); hence, using tapered microfluidic constrictions and diagonal oscillatory flow, the resultant ratcheting effect produces distinct flow paths for CTCs, leukocytes and erythrocytes (Figure 1) [76,77].

High-throughput microscopy

Another unbiased, label-free approach has been developed by Epic Sciences (CA, USA) in which CTCs undergo no enrichment other than erythrocyte lysis, are plated on multiple slides, and then identified against a background of excess leukocytes by high-throughput immunofluorescence microscopy [78–80] (Figure 1). This platform was recently used by Scher and colleagues to demonstrate that CTC expression of AR-V7 in patients with metastatic castrate-resistant prostate cancer is associated with longer survival on taxane chemotherapy as opposed to AR-targeted therapies [81].

Functional selection

The Vita-Assay™ (Vitatex, NY, USA) method identifies CTCs based on preferential adhesion of invasive CTCs to a tissue or tumor microenvironment mimic (cell adhesion matrix or CAM), which has been shown to enrich viable CTCs from blood up to 1,000,000-fold [82,83]. Moreover, CAM-captured CTCs can ingest the CAM itself such that the use of fluorescent-labeled CAM allows for direct visualization of cancer cell invasion (Figure 1).

For additional information on the various approaches available for the capture and analysis of CTCs, we refer the reader to comprehensive reviews on this topic [3,52–53,84].

Clinical application of CTCs

Among the many potential clinical applications for CTCs, we will focus on early detection; prognosis and treatment decisions based on CTC enumeration and molecular characterization; monitoring the efficacy of treatment; dynamic identification of therapeutic targets and resistance mechanisms to make real-time changes in clinical management; and direct targeting of CTCs as a therapeutic strategy to eliminate the putative metastatic subpopulation (Figure 2).

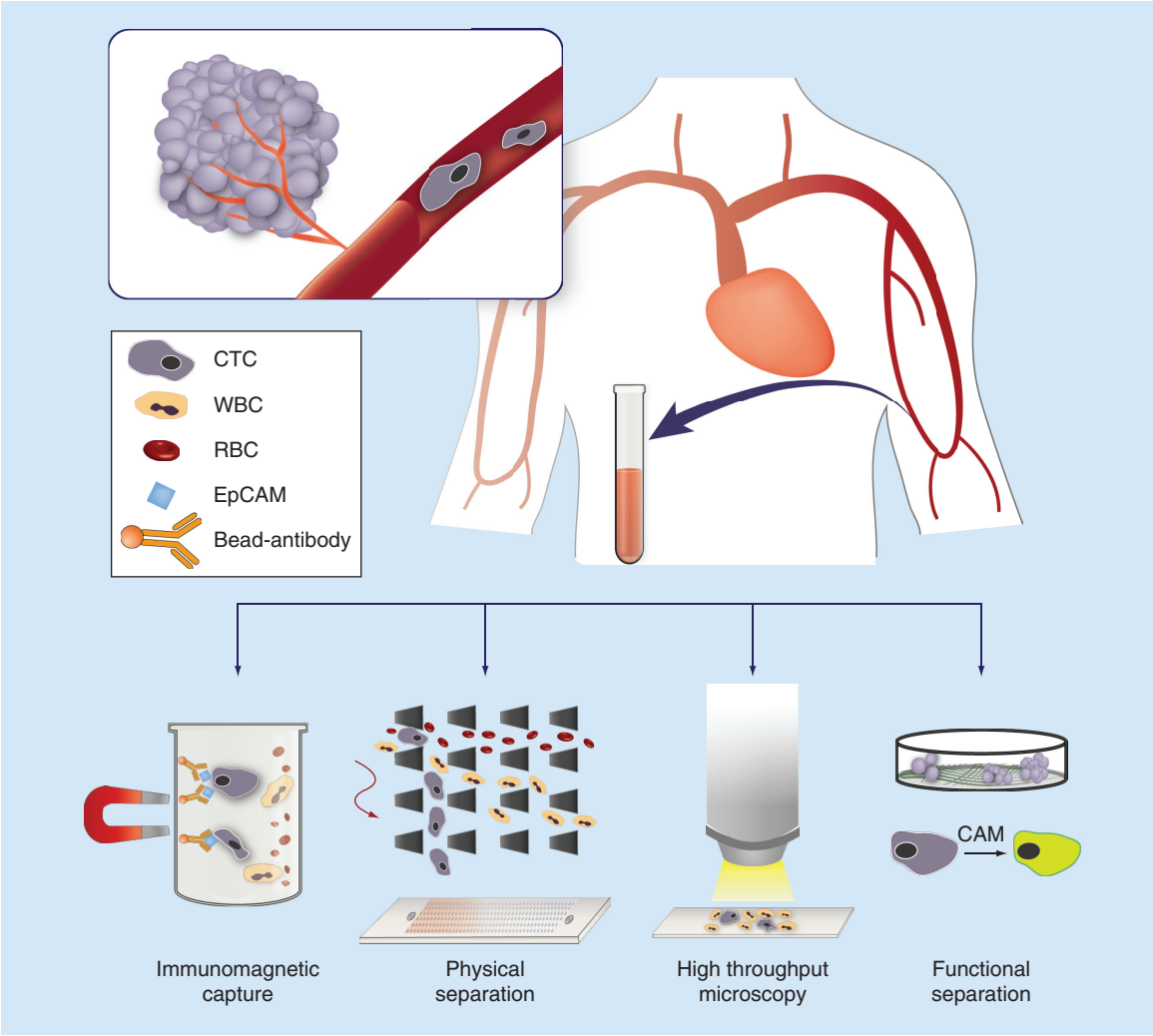

Figure 1. Capture of circulating tumor cells. Circulating tumor cells (CTCs) can be enriched from blood samples, or 'liquid biopsies' based on their biological and physical properties. (Left panel) Immunomagnetic capture utilizes antibodies against specific CTC surface markers such as epithelial cell adhesion molecule (EpCAM). (Left-Middle panel) Separation of CTCs from other blood cells can also be accomplished through differences in physical properties, such as size, deformability and capacitance. Application of an oscillating flow gradient across a microfluidic chip with tapered constrictions separates cell types based on rigidity. (Right-middle panel) High-throughput microscopy of nucleated blood cells with fluorescent antibody staining allows for CTCs to be detected and isolated. (Right panel) Functional separation of CTCs can be achieved based on their viability in selective cell culture conditions or ability to attach to and invade extracellular matrix. In the Vita-Assay™ method depicted, CTCs preferentially attach to and ingest a fluorescently labeled cell adhesion matrix (CAM), which enables direct visualization by fluorescent microscopy.

Early detection

While early detection of cancer by CTCs is hampered by limited sensitivity and specificity, there have been some successful applications to date, and more are anticipated with improvements in capture and detection technologies discussed above. For example, CTCs were found in 3% of chronic obstructive pulmonary disease patients without clinically detectable lung cancer compared with 0% of healthy and smoking controls [85]. These CTC-positive individuals were monitored annually by low-dose spiral CT, and lung nodules were detected 1–4 years after CTC detection, leading to prompt surgical resection and histopathologic diagnosis of early-stage lung cancer. The Breast Early Screening Test study obtained 8 ml of blood in 144 women presenting for breast biopsy due to a mammogram BIRADS score (breast imaging reporting and data system) of at least 3, and CTC detection was performed with antimammoglobin immunocytochemistry (positive if at least one CTC detected) [86]. While the CTC

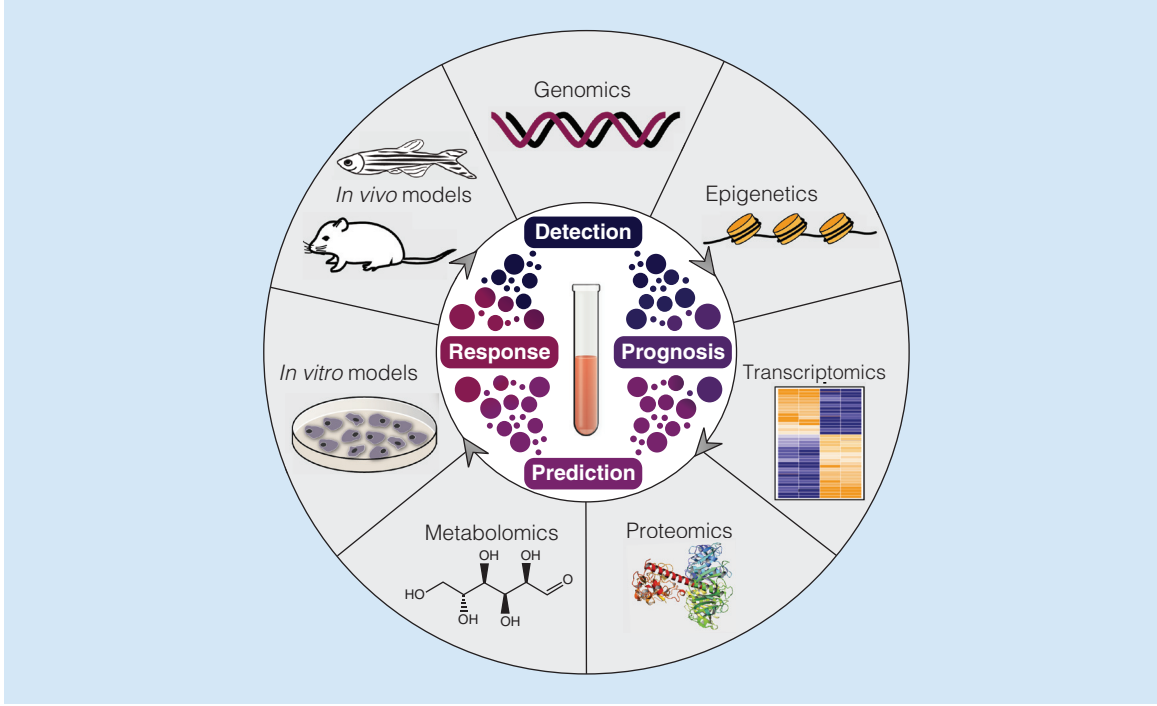

Figure 2. Clinical application of circulating tumor cells. The broad range of applications for circulating tumor cells (CTCs) in clinical decision making are illustrated schematically. Multidimensional molecular characterization of CTCs (outer ring) enables a cycle of utilizing CTCs for early detection, prognosis, prediction of targets/resistance, monitoring of treatment response and detection of tumor evolution/recurrence (inner ring).

screening test detected 87% of invasive cancers, it only detected 50% of *in situ* cancers and none of the intraductal cancers.

Prognosis

Many studies have demonstrated that enumeration of CTCs using the FDA-cleared CellSearch platform before, during and after various systemic therapies has prognostic value for a wide range of malignancies. The majority of studies have focused on the metastatic setting, due to the overall higher yield of CTCs [87]. CTCs above a certain threshold (typically on the order of one to five CTCs per 7.5 ml of blood, except 50 CTCs per 7.5 ml of blood for small-cell lung cancer) at any time point or the lack of a sufficient decrease in CTCs after treatment were associated with worse prognosis in terms of progression-free survival (PFS) and overall survival (OS) for metastatic breast cancer [59,88–91], prostate cancer [60,92–93], colorectal cancer [61], NSCLC [94], small cell lung cancer (SCLC) [29,95], gastric cancer [96] and neuroendocrine tumors [97] among others. In many cases, CTCs are a superior prognostic indicator to conventional tumor markers. For example, CTC enumeration improved the prognostication of metastatic breast cancer when added to full clinicopathologic predictive models, whereas serum tumor markers (CEA, CA15–3) did not, despite the fact that these serum markers are frequently used in clinical practice [98]. The presence of CTM may portend an even worse prognosis compared with the presence of CTCs alone [99,100].

More recently, the improvement in detection technologies has shifted more attention to localized cancers. The presence of any CTCs (≥1) is associated with unfavorable outcomes in a number of primary malignancies, including breast cancer [90,101–103], bladder cancer [104,105], liver cancer [106], NSCLC [107], head and neck squamous cell carcinoma (HNSCC) [108] and cholangiocarcinoma [109]. In contrast, results to date are inconsistent for a handful of other localized malignancies such as prostate cancer [110,111] and colorectal cancer [112,113]. Another anticipated use of CTC enumeration is in the selection of patients with early-stage cancer who are most likely to benefit from adjuvant therapy.

Molecular analyses of CTCs and CTM can yield distinct prognostic information beyond enumeration alone. Bulfoni and colleagues identified four CTC subpopulations in breast cancer patients: epithelial, epithelial–mesenchymal, mesenchymal and negative [114]. The presence of CTCs coexpressing epithelial and mesenchymal markers was associated with significantly poorer PFS and OS [114]. In metastatic melanoma, the presence of CTM with high expres-

sion of SOX10, CD100 and TRF2 was an independent predictor of shorter survival from time of diagnosis regardless of treatment strategy [115]. Vimentin- and Ki67-positive CTCs are associated with increased mortality in metastatic castration resistant prostate cancer (mCRPC) [116]. Moreover, the combination of stem-like gene expression and CTC enumeration improved prediction of docetaxel treatment efficacy and OS in mCRPC patients [117]. Barbazan and colleagues found that overexpression of nonreceptor guanine nucleotide exchange factors in CTCs isolated from metastatic colorectal cancer was associated with a shorter PFS, implying that hyperactivation of G-protein signaling may be a critical event during metastatic progression [118]. Interestingly, the presence of epithelial-like but not mesenchymal-like CTCs correlated with poorer survival in pancreatic adenocarcinoma; moreover, CTCs with partial EMT phenotype (cytokeratin and vimentin positive) were associated with earlier recurrence [119].

Treatment monitoring

CTC counts have also been used as a surrogate marker of efficacy in clinical trials. For example, a Phase I study of LY2606368, a checkpoint kinase 1 inhibitor, in patients with advanced solid tumors, used CTCs as a measure of pharmacodynamics [120]. In another Phase I study investigating apatorsen, an antisense inhibitor targeting heat shock protein 27, in mCRPC and other advanced cancers, CTC enumeration was used as evidence of single-agent activity [121]. Meulendijks and colleagues undertook a multicenter, Phase II study on the feasibility of bevacizumab, docetaxel, oxaliplatin, and capecitabine (B-DOC) chemotherapy for patients with advanced HER2-negative, previously untreated, gastric or gastroesophageal adenocarcinoma and found that CTC enumeration was prognostic in patients treated with B-DOC [122]. In the Phase III trial COU-AA-301, abiraterone was found to prolong OS for patients with mCRPC who had previously received chemotherapy [123]. One of the secondary objectives in this study was to evaluate whether CTC enumeration by CellSearch was a suitable surrogate biomarker of treatment efficacy and OS. Remarkably, Scher and colleagues found on multivariate analysis that a biomarker panel encompassing CTC number and LDH level were prognostic for survival and could be used to risk stratify patients, whereas changes in prostate-specific antigen (PSA) serum levels, currently used in clinical practice to assess therapeutic efficacy, were not relevant [124].

An increase in CTCs from favorable to unfavorable levels after chemotherapy is associated with shorter OS in several cancer types, including mCRPC [60,93]. When such a finding is detected, a switch to another therapy may be warranted, although in a trial with metastatic breast cancer patients, an early switch from one cytotoxic chemotherapeutic agent to another for patients with an increase in CTCs did not improve OS [125]. Notably, this may not reflect a failure of screening by CTCs *per se*, but rather may be an indication that we need more effective treatments for these patients; indeed, one can only optimize decision making up to the asymptote defined by the maximum efficacy of the therapy itself. NCT01710605 is an ongoing trial of hormone receptor (HR) positive, metastatic breast cancer patients randomized to first-line treatment with chemotherapy or endocrine therapy based on CTC count versus clinician decision. In the CTC count arm, patients with high CTC counts (≥5 per 7.5 ml blood) receive chemotherapy, whereas those with low CTC counts receive endocrine therapy first. The study is designed to show noninferiority of the CTC arm for PFS and superiority of the CTC arm from a medicoeconomics standpoint.

Beyond systemic therapies, CTCs may also play an important role in monitoring the impact of locoregional cancer interventions. Some studies have shown that surgical manipulation can dislodge CTCs and increase CTC levels in the peripheral blood with the presence of CTM associated with unfavorable outcomes [126] while others have not [127]. Nevertheless, 'no-touch' isolation techniques for certain tumor resections have been developed and proposed as a way to reduce CTC shedding into the circulation [128], although no prospective data on the efficacy of such techniques are currently available.

Similarly, radiotherapy (RT) mediated CTC shedding has also been reported. NSCLC patients treated with RT may release CTCs with elevated γ-H2AX into the circulation, indicating their DNA damage and viability, and provides a rationale for potentially reducing the number of viable CTCs and subsequent treatment failure rate by modulating RT fractionation or by co-administering systemic therapies [129]. As with systemic therapies, CTC enumeration before, during and after RT seems to be reflective of treatment efficacy [130,131]. The mechanism of CTC shedding after local therapy, whether surgery or RT, is not well understood though vascular disruption may play a role.

Therapeutic targets & resistance mechanisms

In addition to serving as prognostic biomarkers, the molecular analysis of CTCs can also open the door to a wealth of additional information that can help identify new therapeutic targets and resistance mechanisms to

guide real-time precision therapy. In the following, we provide representative examples in breast and prostate cancers.

Metastatic breast cancer patients with estrogen receptor (ER) positive primary tumors have been shown to frequently have ER-negative CTCs, which may escape endocrine therapy [132]. To address this issue, Paoletti and colleagues developed a multiparameter CTC-endocrine therapy index based on CTC enumeration and CTC expression of ER, BCL2, HER2 and Ki67 that may improve prediction of resistance to endocrine therapy in patients with HR-positive metastatic breast cancer and is currently undergoing a prospective trial [133]. In a similar vein, Reijm and colleagues developed an eight-gene mRNA expression profile in CTCs to predict the response to first-line aromatase inhibitors in metastatic breast cancer [134].

HER2-amplification is seen in approximately 20% of primary breast cancers and there is increasing evidence that CTCs and metastatic deposits have disparate HER2 statuses compared with the primary tumor in more than 30% of cases [135]. This has led to multicenter trials investigating whether these discordant patients still benefit from HER2-specific therapies [136,137]. For example, the ongoing DETECT III study is enrolling patients with metastatic breast cancer treated with up to three chemotherapy lines for metastatic disease who are found to have $HER2^+$ CTCs (HER2 status of primary tumor and metastatic lesions must be negative) and randomizing them to standard therapy (chemotherapy or endocrine therapy) versus standard therapy plus lapatinib, a dual TKI that interrupts the HER2/neu and EGFR pathways [138]. Resistance to HER2-targeted therapies is often secondary to activation of the PI3K pathway (e.g., mutations in *PIK3CA* gene) and can be detected in CTCs [139–141].

Immune checkpoint inhibitors are highly efficacious in a subpopulation of patients with advanced malignancies, but due to their cost and toxicity, there is a critical need for predictive biomarkers to discriminate responders from nonresponders. PD-L1 is frequently expressed on CTCs in HR-positive, HER2-negative breast cancer and may provide an approach for further clinical trials as a prospective predictive biomarker [142,143].

mCRPC is defined by disease progression despite androgen-deprivation therapy. Next-generation AR-targeted therapies have activity in mCRPC, including enzalutamide and abiraterone, but some patients unfortunately do not benefit. In prostate cancer, PSA and prostate-specific membrane antigen (PSMA) are upregulated following AR activation and suppression, respectively. PSA/PSMA-based measurements can serve as surrogates for AR signaling in CTCs, and may help predict the response to AR-targeted therapies [144]. Mutations or amplification of the AR can cause resistance to androgen-deprivation therapy and are detectable in CTCs [145]. Moreover, recent studies have shown that mRNA expression of *AR-V7*, a truncated mRNA splice variant of *AR* that lacks the ligand-binding domain but remains constitutively active, in CTCs may predict failure of treatment with enzalutamide and abiraterone [146,147], but retained sensitivity to cytotoxic taxanes such as docetaxel [81,148–150]. In addition, a point mutation (F876L) in the ligand-binding domain of AR confers resistance to enzalutamide [151,152]. Although these results require validation in larger prospective trials, they do suggest that detection of *AR-V7* and *AR* mutations in CTCs can serve as predictive biomarkers that portend poor response to AR-targeted therapies and may prompt clinicians to initiate cytotoxic chemotherapy earlier.

Beyond modifications of the AR, other genomic and transcriptomic alterations have been detected in prostate CTCs including loss of *PTEN* [153], amplification of *MYC* [154] and the *TMPRSS2-ERG* chromosomal translocation [153,155]. TMPRSS2-ERG expression in peripheral CTCs does not predict response to abiraterone treatment [156] but interestingly does predict resistance to docetaxel and may be useful in treatment selection to avoid possible toxicities in refractory patients [157]. Moving beyond genetic analysis, Miyamoto and colleagues harnessed single-cell transcriptomics to identify activation of noncanonical Wnt signaling as a potential non-AR mechanism for antiandrogen resistance [49].

CTC-directed therapies

Among the CTCs is a putative metastatic subpopulation, so the CTCs themselves may serve as a promising therapeutic target. Platelets are thought to promote metastasis by protecting CTCs from immune elimination and promoting their arrest at the endothelium, supporting CTC extravasation into secondary sites. TNF-related apoptosis-inducing ligand (TRAIL) is a cytokine known to induce apoptosis specifically in tumor cells. Using synthetic silica particles functionalized with activated platelet membrane with surface conjugation of TRAIL or platelets genetically modified to express surface-bound TRAIL, Li and colleagues demonstrated selective killing of cancer cells *in vitro* and a significant metastatic reduction in mouse models of prostate and breast cancer metastasis [158,159]. This is the first demonstration of a Trojan-horse approach to neutralize CTCs and attenuate

metastasis. In a similar fashion, Wayne and colleagues used nanoscale liposomes conjugated with E-selectin adhesion protein and Apo2L/TRAIL that attach to the surface of leukocytes to rapidly clear viable CTCs and prevent the spontaneous formation and growth of metastatic tumors in an orthotopic xenograft model of prostate cancer [160].

Rather than target endogenous CTCs for destruction, Dondossola and colleagues exploited the self-seeding ability of CTCs to colonize distant organs and form metastases or reinfiltrate primary tumors by engineering cancer cells to release murine TNF [161]. Systemic administration of TNF-expressing tumor cells was associated with decreased growth of both primary tumors and metastatic colonies in immunocompetent mice. This novel proof of concept study demonstrated that genetically modified CTCs can act as targeted vectors to deliver anticancer agents.

Conclusion & future perspective

The majority of biomarkers currently used to guide ongoing treatment decisions in cancer are based on the analysis of primary and metastatic tumor biopsies. However, cancer is constantly evolving at the molecular level, especially under the selection pressure of various treatments, yielding a tremendous amount of spatial and temporal heterogeneity, which is unlikely to be captured by a spatially and temporally limited biopsy. An attractive alternative is the concept of serial 'liquid biopsies' in which peripheral blood is sampled throughout the course of disease to enable molecular analysis of CTCs, which are shed by both primary and metastatic tumors and may be more representative of the total breadth of disease. A wide range of applications using CTCs have already been demonstrated, including illuminating the fundamental processes of epithelial–mesenchymal transition and metastasis, providing prognostic information in numerous malignancies, monitoring treatment efficacy and identifying new therapeutic targets and resistance mechanisms to enable real-time modifications in clinical management.

Over the next decade, we envision the increased clinical adoption of new transformative technologies utilizing CTCs and other circulating tumor biomarkers such as cell-free DNA and exosomes to enable real-time precision medicine. Integrated microfluidic platforms for combined enrichment, detection, analysis of CTCs are on the horizon. Another area of expected growth is in single-CTC multiomics analysis. CTC analysis at the DNA and RNA levels may have a considerable impact on increasing our understanding of the molecular evolution of cancer (Figure 2). Most of the information obtained to date has been targeted based on known cancer pathways, which has the advantage of lower cost and dropout rate; however, complementary untargeted omics approaches will enable more unbiased discovery. Other salient forms of information can be gleaned from individual CTCs, including epigenetics, proteomics and metabolomics. Single-CTC methylation analysis was recently demonstrated by Huang and colleagues, indicating at a gross level that DNA was hypomethylated and RNA was hypermethylated [162,163]. Along similar lines, methylation patterns in ctDNA has been used to identify tissue-specific cell death [164], and ctDNA detection of aberrant promoter methylation in a six-gene panel has been used for diagnosing breast cancer [165]. Concurrent multiomics analysis of single CTCs in a highly automated and multiplexed fashion using microfluidics and barcoding technology could augment lineage tracing and dissection of the genetic and epigenetic contributions to CTC cell state and dynamics (via the transcriptome readout) [166]. Integrated genome and transcriptome sequencing has recently been achieved in single cells [167,168] as has combined transcriptome and methylome sequencing [169].

CTC cultures [170], organoids [171] and xenografts [172] will facilitate additional testing for therapeutic targets and drug susceptibility to guide real-time therapeutic decisions (Figure 2). The concept of a co-clinical platform would be extremely powerful as each patient could have a personalized CTC-derived xenograft animal avatar at each stage of disease to enable direct testing of potential therapies before administration to the patient [173,174]. One of the challenges that will need to be overcome is the current inefficiency of the process, with hundreds to thousands of CTCs required to establish a cell line or xenograft, which limits the approach to patients with advanced disease.

CTCs represent a powerful, multifaceted tool that can help uncover fundamental principles of cancer biology in the laboratory and provide ongoing therapeutic guidance in the clinic; the journey to unlocking its full potential has only just begun.

Financial & competing interests disclosure

This work was supported by the Department of Defense (DT Miyamoto), Prostate Cancer Foundation (DT Miyamoto) and NIH T32G007753 Training Grant (KL Hwang). The authors have no other relevant affiliations or financial involvement with any organization or entity with a financial interest in or financial conflict with the subject matter or materials discussed in the manuscript apart from those disclosed.

No writing assistance was utilized in the production of this manuscript.

Executive summary

Biology of circulating tumor cells

- Circulating tumor cells (CTCs) originate from cells within primary or metastatic tumors that acquire the ability to invade through the basement membrane and tissue stroma to enter the bloodstream/lymphatics, a process that is hypothesized to involve epithelial-to-mesenchymal transition.
- It is thought that only a small fraction of tumor cells have metastatic capability and CTCs provide an accessible window into this fundamental tumorigenic process, including the epithelial–mesenchymal transition.
- The use of CTCs has led to evidence that metastases are composed of multiple genetically distinct clones likely secondary to polyclonal seeding by CTCs and circulating tumor microemboli and the interplay between host immune cells at the metastatic site and arriving CTCs has been directly observed using intravital two-photon microscopy.
- Genomic and transcriptomic analysis of single CTCs can provide a global view of cancer heterogeneity, disease evolution and tumor biology. Comparing CTC and matched biopsy profiles for the degree of overlap/heterogeneity provides complementary information to guide therapeutic decision-making.

Capture & characterization of CTCs

- The reliable capture of CTCs from whole blood is challenging due to their scarcity, estimated at approximately one CTC per 10^7 leukocytes per ml of blood.
- Immunomagnetic capture uses antibodies directed toward epithelial markers (positive selection) or leukocyte markers (negative selection) and includes the only US FDA-cleared CTC enrichment technology, CellSearch.
- Label-free physical separation of CTCs from hematological cells harnesses the larger size, higher membrane capacitance and increased rigidity of CTCs compared with leukocytes and has the benefit of not enriching for CTC subgroups with specific immunocytochemical features.
- CTCs undergo no enrichment other than erythrocyte lysis, are plated on multiple slides, and then identified against a background of excess leukocytes by high-throughput immunofluorescence microscopy.
- Functional selection of CTCs captures viable CTCs that are capable of growing in culture and invading cell adhesion matrix.

Clinical application of CTCs

- Early detection is generally hampered by low sensitivity, though the prediction of lung cancer development in chronic obstructive pulmonary disease patients has been demonstrated.
- Enumeration of CTCs represents the simplest and most cost-effective level of analysis, and has been shown to provide nonredundant prognostic information for early-stage and metastatic cancers. Moreover, CTC counts can contribute to ongoing therapeutic monitoring, with a persistence or increase in counts motivating a change in treatment.
- Molecular analysis of CTCs provides prognostic information beyond enumeration alone, and importantly, is capable of uncovering new therapeutic targets and resistance mechanisms to optimize precision therapy for individual patients.
- Researchers have validated CTC expression profiles that can predict response to hormone therapy in breast cancer patients. Moreover, the hormone receptor and HER2/neu status of CTCs is often discordant with that of the primary/metastatic biopsy specimen and there is increasing evidence that applying targeted therapies based on the information gleaned from CTCs can improve clinical outcomes.
- In prostate cancer, prostate-specific antigen- and prostate-specific membrane antigen-based measurements can serve as surrogates for androgen receptor (AR) signaling in CTCs, which may help predict the outcome of AR-targeted therapy. Expression of *AR-V7*, a truncated mRNA splice variant of *AR* that lacks the ligand-binding domain but remains constitutively active, in CTCs may predict failure of AR-targeted therapy with enzalutamide and abiraterone but retained sensitivity to taxanes such as docetaxel.
- Surgical manipulation and radiotherapy can dislodge CTCs and increase CTC levels in the peripheral blood, but the clinical significance of this observation is not known.
- Given the putative metastatic CTC subpopulation, there has been recent attention toward targeting CTCs therapeutically. Approaches to date include particles, liposomes or platelets expressing TRAIL to induce CTC apoptosis and engineering CTCs to release TNF such that upon reinjection they home to primary/metastatic tumors and induce massive apoptosis.

References

Papers of special note have been highlighted as:• of interest; •• of considerable interest

1 Haber DA, Gray NS, Baselga J. The evolving war on cancer. *Cell* 145(1), 19–24 (2011).

2 Marusyk A, Almendro V, Polyak K. Intra-tumour heterogeneity: a looking glass for cancer? *Nat. Rev. Cancer* 12(5), 323–334 (2012).

3 Miyamoto DT, Sequist LV, Lee RJ. Circulating tumour cells-monitoring treatment response in prostate cancer.

Nat. Rev. Clin. Oncol. 11(7), 401–412 (2014).

4 Alix-Panabières C, Pantel K. Clinical applications of circulating tumor cells and circulating tumor DNA as liquid biopsy. *Cancer Discov.* 6(5), 479–491 (2016).

5 Ashworth TR. A case of cancer in which cells similar to those in the tumours were seen in the blood after death. *Aust. Med. J.* 14, 146–147 (1869).

6 Ma M, Zhu H, Zhang C, Sun X, Gao X, Chen G. 'Liquid biopsy'-ctDNA detection with great potential and challenges. *Ann. Transl. Med.* 3(16), 235 (2015).

7 Dawson S-J, Tsui DWYYW, Murtaza M *et al.* Analysis of circulating tumor DNA to monitor metastatic breast cancer. *N. Engl. J. Med.* 368(13), 1199–209 (2013).

8 Melo SA, Luecke LB, Kahlert C *et al.* Glypican-1 identifies cancer exosomes and detects early pancreatic cancer. *Nature* 523(7559), 177–182 (2015).

9 Hoshino A, Costa-Silva B, Shen T-L *et al.* Tumour exosome integrins determine organotropic metastasis. *Nature* 527(7578), 329–335 (2015).

10 Best MG, Sol N, Kooi I *et al.* RNA-Seq of tumor-educated platelets enables blood-based pan-cancer, multiclass, and molecular pathway cancer diagnostics. *Cancer Cell* 28(5), 666–676 (2015).

11 Vincent-Salomon A, Thiery JP. Host microenvironment in breast cancer development: epithelial–mesenchymal transition in breast cancer development. *Breast Cancer Res.* 5(2), 101–106 (2003).

12 Schölch S, García SA, Iwata N *et al.* Circulating tumor cells exhibit stem cell characteristics in an orthotopic mouse model of colorectal cancer. *Oncotarget* 7(19), 27232–27242 (2016).

13 Weitz J, Koch M, Debus J, Höhler T, Galle PR, Büchler MW. Colorectal cancer. *Lancet* 365(9454), 153–165 (2005).

14 Kalluri R, Weinberg RA. The basics of epithelial–mesenchymal transition. *J. Clin. Invest.* 119(6), 1420–1428 (2009).

15 Kallergi G, Papadaki MA, Politaki E, Mavroudis D, Georgoulias V, Agelaki S. Epithelial to mesenchymal transition markers expressed in circulating tumour cells of early and metastatic breast cancer patients. *Breast Cancer Res.* 13(3), R59 (2011).

16 Yu M, Bardia A, Wittner BS *et al.* Circulating breast tumor cells exhibit dynamic changes in epithelial and mesenchymal composition. *Science* 339, 580–584 (2013).

17 Stark K, Vainio S, Vassileva G, McMahon AP. Epithelial transformation of metanephric mesenchyme in the developing kidney regulated by Wnt-4. *Nature* 372(6507), 679–683 (1994).

18 Krebs MG, Metcalf RL, Carter L, Brady G, Blackhall FH, Dive C. Molecular analysis of circulating tumour cells-biology and biomarkers. *Nat. Rev. Clin. Oncol.* 11(3), 129–144 (2014).

19 Tam WL, Weinberg RA. The epigenetics of epithelial–mesenchymal plasticity in cancer. *Nat. Med.* 19(11), 1438–1449 (2013).

20 Massagué J, Obenauf AC. Metastatic colonization by circulating tumour cells. *Nature* 529(7586), 298–306 (2016).

21 Fidler IJ. The pathogenesis of cancer metastasis: the 'seed and soil' hypothesis revisited. *Nat. Rev. Cancer* 3, 453–458 (2003).

22 Chaffer CL, Weinberg RA. A perspective on cancer cell metastasis. *Science* 331(6024), 1559–1564 (2011).

23 Al-Hajj M, Wicha MS, Benito-Hernandez A, Morrison SJ, Clarke MF. Prospective identification of tumorigenic breast cancer cells. *Proc. Natl Acad. Sci. USA* 100(7), 3983–3988 (2003).

24 Singh SK, Clarke ID, Terasaki M *et al.* Identification of a cancer stem cell in human brain tumors. *Cancer Res.* 63(18), 5821–5828 (2003).

25 Ricci-Vitiani L, Pallini R, Biffoni M *et al.* Tumour vascularization via endothelial differentiation of glioblastoma stem-like cells. *Nature* 468(7325), 824–828 (2010).

26 Baccelli I, Schneeweiss A, Riethdorf S *et al.* Identification of a population of blood circulating tumor cells from breast cancer patients that initiates metastasis in a xenograft assay. *Nat. Biotechnol.* 31(6), 539–44 (2013).

27 Zhang L, Ridgway LD, Wetzel MDA *et al.* The identification and characterization of breast cancer CTCs competent for brain metastasis. *Sci. Transl. Med.* 5(180), 180ra48 (2013).

28 Morrow CJ, Trapani F, Metcalf RL, Bertolini G, Hodgkinson CL. Tumourigenic non-small-cell lung cancer mesenchymal circulating tumour cells: a clinical case study. *Ann. Oncol.* 27(6), 1155–1160 (2016).

29 Hou JM, Krebs MG, Lancashire L *et al.* Clinical significance and molecular characteristics of circulating tumor cells and circulating tumor microemboli in patients with small-cell lung cancer. *J. Clin. Oncol.* 30(5), 525–532 (2012).

30 Duda DG, Duyverman AM, Kohno M *et al.* Malignant cells facilitate lung metastasis by bringing their own soil. *Proc. Natl Acad. Sci. USA* 107(50), 21677–21682 (2010).

31 Fidler IJ. The relationship of embolic homogeneity, number, size and viability to the incidence of experimental metastasis. *Eur. J. Cancer* 9(3), 223–227 (1973).

32 Topal B, Roskams T, Fevery J, Penninckx F. Aggregated colon cancer cells have a higher metastatic efficiency in the liver compared with nonaggregated cells: an experimental study. *J. Surg. Res.* 112(1), 31–37 (2003).

33 Aceto N, Bardia A, Miyamoto DT *et al.* Circulating tumor cell clusters are oligoclonal precursors of breast cancer metastasis. *Cell* 158(5), 1110–1122 (2014).

34 Maddipati R, Stanger BZ. Pancreatic cancer metastases harbor evidence of polyclonality. *Cancer Discov.* 5(10), 1086–1097 (2015).

35 Gundem G, Van Loo P, Kremeyer B *et al.* The evolutionary history of lethal metastatic prostate cancer. *Nature* 520(7547), 353–357 (2015).

36 Cheung KJ, Padmanaban V, Silvestri V *et al.* Polyclonal breast cancer metastases arise from collective dissemination of keratin 14-expressing tumor cell clusters. *Proc. Natl Acad. Sci.* 113(7), E854–E863 (2016).

37 Headley MB, Bins A, Nip A *et al.* Visualization of immediate immune responses to pioneer metastatic cells in the lung. *Nature* 531(7595), 513–517 (2016).

• **Developed a murine intravital two-photon lung imaging model to directly observe the arrival of fluorescently labeled circulating tumor cells (CTCs) and their interaction with the host immune system. Discovered**

that tumor microemboli form within minutes of CTC arrival and remain attached to the lung vasculature where waves of different myeloid cell derivatives interact with the circulating tumor microemboli in a competitive manner, including prometastatic neutrophils/monocytes/macrophages and antimetastatic dendritic cells.

38 Gasch C, Bauernhofer T, Pichler M *et al.* Heterogeneity of epidermal growth factor receptor status and mutations of KRAS/PIK3CA in circulating tumor cells of patients with colorectal cancer. *Clin. Chem.* 59(1), 252–260 (2013).

39 Mostert B, Jiang Y, Sieuwerts AM *et al.* KRAS and BRAF mutation status in circulating colorectal tumor cells and their correlation with primary and metastatic tumor tissue. *Int. J. Cancer* 133(1), 130–141 (2013).

40 Fabbri F, Carloni S, Zoli W *et al.* Detection and recovery of circulating colon cancer cells using a dielectrophoresis-based device: KRAS mutation status in pure CTCs. *Cancer Lett.* 335(1), 225–231 (2013).

41 De Luca F, Rotunno G, Salvianti F *et al.* Mutational analysis of single circulating tumor cells by next generation sequencing in metastatic breast cancer. *Oncotarget* 7(18), 26107–26119 (2016).

42 Heitzer E, Auer M, Gasch C *et al.* Complex tumor genomes inferred from single circulating tumor cells by array-CGH and next-generation sequencing. *Cancer Res.* 73(10), 2965–2975 (2013).

43 Jiang R, Lu Y, Ho H *et al.* A comparison of isolated circulating tumor cells and tissue biopsies using whole-genome sequencing in prostate cancer. *Oncotarget* 6(42), 44781–44793 (2015).

44 Sundaresan TK, Sequist LV, Heymach JV *et al.* Detection of T790M, the acquired resistance EGFR mutation, by tumor biopsy versus noninvasive blood-based analyses. *Clin. Cancer Res.* 22(5), 1103–1110 (2015).

45 Powell AA, Talasaz AAH, Zhang H *et al.* Single cell profiling of circulating tumor cells: transcriptional heterogeneity and diversity from breast cancer cell lines. *PLoS ONE* 7(5), e33788 (2012).

46 Ramsköld D, Luo S, Wang Y *et al.* Full-length mRNA-Seq from single-cell levels of RNA and individual circulating tumor cells. *Nat. Biotechnol.* 30(8), 777–782 (2012).

47 Cann GM, Gulzar ZG, Cooper S *et al.* mRNA-Seq of single prostate cancer circulating tumor cells reveals recapitulation of gene expression and pathways found in prostate cancer. *PLoS ONE* 7(11), e49144 (2012).

48 Ting DT, Wittner BS, Ligorio M *et al.* Single-cell RNA sequencing identifies extracellular matrix gene expression by pancreatic circulating tumor cells. *Cell Rep.* 8(6), 1905–1918 (2014).

49 Miyamoto DT, Zheng Y, Wittner BS *et al.* RNA-Seq of single prostate CTCs implicates noncanonical Wnt signaling in antiandrogen resistance. *Science* 349(6254), 1351–1356 (2015).

•• **Using single-cell RNA sequencing, the authors discovered that activation of noncanonical Wnt signaling (ectopic expression of Wnt5a) was a novel, nonandrogen receptor mediated mechanism underlying resistance to antiandrogen therapy.**

50 Arora VK, Schenkein E, Murali R *et al.* Glucocorticoid receptor confers resistance to antiandrogens by bypassing androgen receptor blockade. *Cell* 155(6), 1309–1322 (2013).

51 Andree KC, van Dalum G, Terstappen LWMM *et al.* Challenges in circulating tumor cell detection by the CellSearch system. *Mol. Oncol.* 10(3), 395–407 (2016).

52 Gabriel MT, Calleja LR, Chalopin A, Ory B, Heymann D. Circulating tumor cells: a review of non-EpCAM-based approaches for cell enrichment and isolation. *Clin. Chem.* 62(4), 571–581 (2016).

53 Green BJ, Saberi Safaei T, Mepham A, Labib M, Mohamadi RM, Kelley SO. Beyond the capture of circulating tumor cells: next-generation devices and materials. *Angew. Chem. Int. Ed. Engl.* 55(4), 1252–1265 (2016).

54 Tibbe AGJ, Craig Miller M, Terstappen LWMM. Statistical considerations for enumeration of circulating tumor cells. *Cytom. Part A* 71(A), 154–162 (2007).

55 Gogoi P, Sepehri S, Zhou Y *et al.* Development of an automated and sensitive microfluidic device for capturing and characterizing circulating tumor cells (CTCs) from clinical blood samples. *PLoS ONE* 11(1), e0147400 (2016).

56 Sarioglu AF, Aceto N, Kojic N *et al.* A microfluidic device for label-free, physical capture of circulating tumor cell clusters. *Nat. Methods* 12(7), 685–691 (2015).

57 Allard WJ, Matera J, Miller MC *et al.* Tumor cells circulate in the peripheral blood of all major carcinomas but not in healthy subjects or patients with nonmalignant diseases. *Clin. Cancer Res.* 10, 6897–6904 (2005).

58 Veridex LLC. CellSearch(TM) circulating tumor cell kit. Premarket notification – expanded indications for use – metastatic prostate cancer. (2008). www.accessdata.fda.gov/

59 Cristofanilli M, Stopeck A, Matera J *et al.* Circulating tumor cells, disease progression, and survival in metastatic breast cancer. *N. Engl. J. Med.* 351(8), 781–791 (2004).

•• **Seminal prospective trial of 177 patients with metastatic breast cancer that showed patients with at least five CTCs per 7.5 ml blood before or after treatment had shorter progression-free survival (PFS) and overall survival (OS), paving the way for US FDA approval of CTC enumeration using CellSearch in metastatic breast cancer.**

60 de Bono JS, Scher HI, Montgomery RB *et al.* Circulating tumor cells predict survival benefit from treatment in metastatic castration-resistant prostate cancer. *Clin. Cancer Res.* 14(19), 6302–6309 (2008).

•• **Prospective trial of 276 patients with castration-resistant prostate cancer (CRPC) that showed patients with at least five CTCs per 7.5 ml blood (unfavorable) before or after treatment had shorter OS and CTC counts were a better predictor of OS than prostate-specific antigen decrement at all time points, and led to FDA approval of CellSearch for castration resistant prostate cancer. Moreover, patients with unfavorable baseline CTC counts who converted to favorable CTC counts after treatment had significantly improved prognosis whereas those who went the other way had poorer prognosis.**

61 Cohen SJ, Punt CJA, Iannotti N *et al.* Relationship of circulating tumor cells to tumor response, progression-free survival, and overall survival in patients with metastatic colorectal cancer. *J. Clin. Oncol.* 26(19), 3213–3221 (2008).

•• **Prospective trial of 430 patients with metastatic colorectal cancer, which found that patients with unfavorable baseline or post-therapy CTC counts (≥3 CTCs per 7.5 ml blood) had significantly poorer PFS and OS, and conversion of baseline unfavorable CTC counts to favorable with treatment correlated with longer PFS and OS compared with those who did not change groups. These results led to FDA approval of CellSearch for metastatic colorectal cancer.**

62 Talasaz AH, Powell AA, Huber DE *et al.* Isolating highly enriched populations of circulating epithelial cells and other rare cells from blood using a magnetic sweeper device. *Proc. Natl Acad. Sci. USA* 106(10), 3970–3975 (2009).

63 Saucedo-Zeni N, Mewes S, Niestroj R *et al.* A novel method for the *in vivo* isolation of circulating tumor cells from peripheral blood of cancer patients using a functionalized and structured medical wire. *Int. J. Oncol.* 41(4), 1241–1250 (2012).

64 Nagrath S, Sequist LV, Maheswaran S *et al.* Isolation of rare circulating tumour cells in cancer patients by microchip technology. *Nature* 450(7173), 1235–1239 (2007).

65 Stott SL, Hsu C-HC-H, Tsukrov DI *et al.* Isolation of circulating tumor cells using a microvortex-generating herringbone-chip. *Proc. Natl Acad. Sci. USA* 107(35), 18392–18397 (2010).

66 Ozkumur E, Shah AM, Ciciliano JC *et al.* Inertial focusing for tumor antigen-dependent and -independent sorting of rare circulating tumor cells. *Sci. Transl. Med.* 5(179), 179ra47 (2013).

67 Tang M, Wen C, Wu L *et al.* Lab on a Chip system for the efficient capture and *in situ* identification of circulating tumor cells. *Lab Chip* 16, 1214–1223 (2016).

68 Saliba A-E, Saias L, Psychari E *et al.* Microfluidic sorting and multimodal typing of cancer cells in self-assembled magnetic arrays. *Proc. Natl Acad. Sci. USA* 107(33), 14524–14529 (2010).

69 Zieglschmid V, Hollmann C, Gutierrez B *et al.* Combination of immunomagnetic enrichment with multiplex RT-PCR analysis for the detection of disseminated tumor cells. *Anticancer Res.* 25(3 A), 1803–1810 (2005).

70 Wang Z, Wu W, Wang Z *et al. Ex vivo* expansion of circulating lung tumor cells based on one-step microfluidics-based immunomagnetic isolation. *Analyst* 141, 3621–3625 (2016).

71 Zhao L, Tang C, Xu L *et al.* Enhanced and differential capture of circulating tumor cells from lung cancer patients by microfluidic assays using aptamer cocktail. *Small* 12(8), 1072–1081 (2016).

72 Vona G, Estepa L, Béroud C *et al.* Impact of cytomorphological detection of circulating tumor cells in patients with liver cancer. *Hepatology* 39(3), 792–797 (2004).

73 Hou HW, Warkiani ME, Khoo BL *et al.* Isolation and retrieval of circulating tumor cells using centrifugal forces. *Sci. Rep.* 3, 1259 (2013).

74 Warkiani ME, Khoo BL, Wu L *et al.* Ultra-fast, label-free isolation of circulating tumor cells from blood using spiral microfluidics. *Nat. Protoc.* 11(1), 134–148 (2016).

75 Gascoyne PR, Noshari J, Anderson TJ, Becker FF. Isolation of rare cells from cell mixtures by dielectrophoresis. *Electrophoresis* 30(8), 1388–1398 (2009).

76 Shaw Bagnall J, Byun S, Begum S *et al.* Deformability of tumor cells versus blood cells. *Sci. Rep.* 5, 18542 (2015).

77 Park ES, Jin C, Guo Q *et al.* Continuous flow deformability-based separation of circulating tumor cells using microfluidic ratchets. *Small* 12(14), 1909–1919 (2016).

78 Werner SL, Graf RP, Landers M *et al.* Analytical validation and capabilities of the epic CTC platform: enrichment-free circulating tumour cell detection and characterization. *J. Circ. Biomarkers* 4(3), doi:10.5772/60725 (2015).

79 Marrinucci D, Bethel K, Kolatkar A *et al.* Fluid biopsy in patients with metastatic prostate, pancreatic and breast cancers. *Phys. Biol.* 9, 1–9 (2012).

80 Cho EHE, Wendel M, Luttgen M *et al.* Characterization of circulating tumor cell aggregates identified in patients with epithelial tumors. *Phys. Biol.* 9, 1–13 (2012).

81 Scher HI, Lu D, Schreiber NA *et al.* Association of AR-V7 on circulating tumor cells as a treatment-specific biomarker with outcomes and survival in castration-resistant prostate cancer. *JAMA Oncol.* doi:10.1001/jamaoncol.2016.1828 (2016) (Epub ahead of print).

82 Lu J, Fan T, Zhao Q *et al.* Isolation of circulating epithelial and tumor progenitor cells with an invasive phenotype from breast cancer patients. *Int. J. Cancer* 126(3), 669–683 (2010).

83 Tulley S, Zhao Q, Dong H, Pearl ML, Chen W. Vita-Assay™ method of enrichment and identification of circulating cancer cells/circulating tumor cells (CTCs). *Methods Mol. Biol.* 1406, 107–119 (2006).

84 Lianidou ES, Markou A. Circulating tumor cells in breast cancer: detection systems, molecular characterization, and future challenges. *Clin. Chem.* 57(9), 1242–1255 (2011).

85 Ilie M, Hofman V, Long-Mira E *et al.* 'Sentinel' circulating tumor cells allow early diagnosis of lung cancer in patients with chronic obstructive pulmonary disease. *PLoS ONE* 9(10), 4–10 (2014).

86 Murray NP, Miranda R, Ruiz A, Droguett E. Diagnostic yield of primary circulating tumor cells in women suspected of breast cancer: the BEST (Breast Early Screening Test) study. *Asian Pac J. Cancer Prev.* 16(5), 1929–1934 (2015).

87 Miller MC, Doyle GV, Terstappen LWMM. Significance of circulating tumor cells detected by the CellSearch system in patients with metastatic breast colorectal and prostate cancer. *J. Oncol.* 2010, 617421 (2010).

88 Lv Q, Gong L, Zhang T *et al.* Prognostic value of circulating tumor cells in metastatic breast cancer: a systemic review and meta-analysis. *Clin. Transl. Oncol.* 18(3), 322–330 (2016).

89 Shiomi-Mouri Y, Kousaka J, Ando T *et al.* Clinical significance of circulating tumor cells (CTCs) with respect to optimal cut-off value and tumor markers in advanced/metastatic breast cancer. *Breast Cancer* 23(1), 120–127 (2016).

90 Lu Y-J, Wang P, Wang X, Peng J, Zhu Y-W, Shen N. The significant prognostic value of circulating tumor cells in triple-negative breast cancer: a meta-analysis. *Oncotarget* doi:10.18632/oncotarget.8156 (2016) (Epub ahead of print).

91 Zhang L, Riethdorf S, Wu G *et al.* Meta-analysis of the prognostic value of circulating tumor cells in breast cancer. *Clin. Cancer Res.* 18(20), 5701–5710 (2012).

92 Scher HI, Jia X, de Bono JS *et al.* Circulating tumour cells as prognostic markers in progressive, castration-resistant prostate cancer: a reanalysis of IMMC38 trial data. *Lancet Oncol.* 10(3), 233–239 (2009).

93 Goldkorn A, Ely B, Quinn DI *et al.* Circulating tumor cell counts are prognostic of overall survival in SWOG S0421: A Phase III trial of docetaxel with or without atrasentan for metastatic castration-resistant prostate cancer. *J. Clin. Oncol.* 32(11), 1136–1142 (2014).

94 Krebs MG, Sloane R, Priest L *et al.* Evaluation and prognostic significance of circulating tumor cells in patients with non-small-cell-lung cancer. *J. Clin. Oncol.* 29(12), 1556–1563 (2011).

95 Cheng Y, Liu X, Fan Y *et al.* Circulating tumor cell counts/change for outcome prediction in patients with extensive-stage small-cell-lung cancer. *Future Oncol.* 12(6), 789–799 (2016).

96 Li Y, Gong J, Zhang Q *et al.* Dynamic monitoring of circulating tumour cells to evaluate therapeutic efficacy in advanced gastric cancer. *Br. J. Cancer* 114(2), 138–145 (2016).

97 Khan MS, Kirkwood AA, Tsigani T *et al.* Early changes in circulating tumor cells are associated with response and survival following treatment of metastatic neuroendocrine neoplasms. *Clin. Cancer Res.* 22(1), 79–85 (2016).

98 Bidard F-C, Peeters DJ, Fehm T *et al.* Clinical validity of circulating tumour cells in patients with metastatic breast cancer: a pooled analysis of individual patient data. *Lancet Oncol.* 15(4), 406–414 (2014).

99 Mu Z, Wang C, Ye Z *et al.* Prospective assessment of the prognostic value of circulating tumor cells and their clusters in patients with advanced-stage breast cancer. *Breast Cancer Res. Treat.* 154(3), 563–571 (2015).

100 Chang M-C, Chang Y-T, Chen J-Y *et al.* Clinical significance of circulating tumor microemboli as a prognostic marker in patients with pancreatic ductal adenocarcinoma. *Clin. Chem.* 62(3), 505–513 (2016).

101 Rack B, Schindlbeck C, Jückstock J *et al.* Circulating tumor cells predict survival in early average-to-high risk breast cancer patients. *J. Natl Cancer Inst.* 106(5), dju066 (2014).

102 Hall CS, Karhade MG, Bowman Bauldry JB *et al.* Prognostic value of circulating tumor cells identified before surgical resection in nonmetastatic breast cancer patients. *J. Am. Coll. Surg.* doi:10.1016/j.jamcollsurg.2016.02.021 (2016) (Epub ahead of print).

103 Janni W, Rack B, Terstappen LW *et al.* Pooled analysis of the prognostic relevance of circulating tumor cells in primary breast cancer. *Clin. Cancer Res.* 22(10), 2583–2593 (2016).

104 Rink M, Chun FK, Dahlem R *et al.* Prognostic role and HER2 expression of circulating tumor cells in peripheral blood of patients prior to radical cystectomy: a prospective study. *Eur. Urol.* 61(4), 810–817 (2012).

105 Gazzaniga P, de Berardinis E, Raimondi C *et al.* Circulating tumor cells detection has independent prognostic impact in high-risk non-muscle invasive bladder cancer. *Int. J. Cancer* 135, 1978–1982 (2014).

106 Schulze K, Gasch C, Staufer K *et al.* Presence of EpCAM-positive circulating tumor cells as biomarker for systemic disease strongly correlates to survival in patients with hepatocellular carcinoma. *Int. J. Cancer* 133(9), 2165–2171 (2013).

107 Bayarri-Lara C, Ortega FG, Cueto Ladrón de Guevara A *et al.* Circulating tumor cells identify early recurrence in patients with non-small-cell lung cancer undergoing radical resection. *PLoS ONE* 11(2), e0148659 (2016).

108 Wu XL, Tu Q, Faure G, Gallet P, Kohler C, Bittencourt Mde C. Diagnostic and prognostic value of circulating tumor cells in head and neck squamous cell carcinoma: a systematic review and meta-analysis. *Sci. Rep.* 6, 20210 (2016).

109 Yang JD, Campion MB, Liu MC *et al.* Circulating tumor cells are associated with poor overall survival in patients with cholangiocarcinoma. *Hepatology* 63(1), 148–158 (2016).

110 Thalgott M, Rack B, Horn T *et al.* Detection of circulating tumor cells in locally advanced high-risk prostate cancer during neoadjuvant chemotherapy and radical prostatectomy. *Anticancer Res.* 35(10), 5679–5685 (2015).

111 Meyer CP, Pantel K, Tennstedt P *et al.* Limited prognostic value of preoperative circulating tumor cells for early biochemical recurrence in patients with localized prostate cancer. *Urol. Oncol.* 34(5), e11–e16 (2016).

112 Denève E, Riethdorf S, Ramos J *et al.* Capture of viable circulating tumor cells in the liver of colorectal cancer patients. *Clin. Chem.* 59(9), 1384–1392 (2013).

113 Hinz S, Röder C, Tepel J *et al.* Cytokeratin 20 positive circulating tumor cells are a marker for response after neoadjuvant chemoradiation but not for prognosis in patients with rectal cancer. *BMC Cancer* 15(1), 953 (2015).

114 Bulfoni M, Gerratana L, Del Ben F *et al.* In patients with metastatic breast cancer the identification of circulating tumor cells in epithelial-to-mesenchymal transition is associated with a poor prognosis. *Breast Cancer Res.* 18(1), 30 (2016).

115 Long E, Ilie M, Bence C *et al.* High expression of TRF2, SOX10, and CD10 in circulating tumor microemboli detected in metastatic melanoma patients. A potential impact for the assessment of disease aggressiveness. *Cancer Med.* 5(6), 1022–1030 (2016).

116 Lindsay CR, Le Moulec S, Billiot F *et al.* Vimentin and Ki67 expression in circulating tumour cells derived from castrate-resistant prostate cancer. *BMC Cancer* 16(1), 168 (2016).

117 Chang K, Kong Y, Dai B, Ye D, Qu Y, Wang Y. Combination of circulating tumor cell enumeration and tumor marker detection in predicting prognosis and treatment effect in metastatic castration-resistant prostate cancer. *Oncotarget* 6(39), 41825–41836 (2015).

118 Barbazan J, Dunkel Y, Li H *et al.* Prognostic impact of modulators of g proteins in circulating tumor cells from

patients with metastatic colorectal Cancer. *Sci. Rep.* 6, 22112 (2016).

119 Poruk KE, Valero V, Saunders T *et al.* Circulating tumor cell phenotype predicts recurrence and survival in pancreatic Adenocarcinoma. *Ann. Surg.* doi:10.1097/SLA.0000000000001600 (2016) (Epub ahead of print).

120 Hong D, Infante J, Janku F *et al.* Phase I Study of LY2606368, a checkpoint kinase 1 inhibitor, in patients with advanced cancer. *J. Clin. Oncol.* 34(15), 1764–1771 (2016).

121 Chi K, Yu EY, Jacobs C *et al.* A Phase 1 dose-escalation study of apatorsen (OGX-427), an antisense inhibitor targeting heat shock protein 27 (Hsp27), in patients with castration resistant prostate cancer and other advanced cancers. *Ann. Oncol.* 27, 1116–1122 (2016).

122 Meulendijks D, De Groot JWB, Los M *et al.* Bevacizumab combined with docetaxel, oxaliplatin, and capecitabine, followed by maintenance with capecitabine and bevacizumab, as first-line treatment of patients with advanced HER2-negative gastric cancer: a multicenter Phase II study. *Cancer* 122(9), 1434–1443 (2016).

123 de Bono JS, Logothetis CJ, Molina A *et al.* Abiraterone and increased survival in metastatic prostate cancer. *N. Engl. J. Med.* 364(21), 1995–2005 (2011).

124 Scher HI, Heller G, Molina A *et al.* Circulating tumor cell biomarker panel as an individual-level surrogate for survival in metastatic castration-resistant prostate cancer. *J. Clin. Oncol.* 33(12), 1348–1355 (2015).

•• **COU-AA-301, a Phase III trial that demonstrated an increase in OS with abiraterone in metastatic castration-resistant prostate cancer, was the first Phase III trial to prospectively evaluate a secondary objective on whether CTC enumeration by CellSearch could serve as a surrogate biomarker for treatment efficacy and OS. Multivariate analysis led to a biomarker panel consisting of CTC count and LDH level, which was used to risk stratify patients. Interestingly, prostate-specific antigen was not a significant prognostic factor.**

125 Smerage JB, Barlow WE, Hortobagyi GN *et al.* Circulating tumor cells and response to chemotherapy in metastatic breast cancer: SWOG S0500. *J. Clin. Oncol.* 32(31), 3483–3489 (2014).

•• **Prior trials had noted that patients who remain in the unfavorable CTC count group after treatment may benefit from a change in therapeutic strategy – a hypothesis that was tested in SWOG S0500. Metastatic breast cancer patients with a persistent unfavorable level of CTCs after one cycle of chemotherapy were randomized to remain on the same therapeutic agent or to switch to a different chemotherapy. There was no difference in OS observed though CTC counts were strongly prognostic; this result does not necessarily imply a failure in the predictive power of CTC enumeration but more likely indicates that more effective therapies are needed.**

126 Sawabata N, Funaki S, Hyakutake T, Shintani Y, Fujiwara A, Okumura M. Perioperative circulating tumor cells in surgical patients with non-small-cell lung cancer: does surgical manipulation dislodge cancer cells thus allowing them to pass into the peripheral blood? *Surg. Today* doi:10.1007/s00595–016–1318–4 (2016) (Epub ahead of print).

127 Charitoudis G, Schuster R, Joussen AM, Keilholz U, Bechrakis NE. Detection of tumour cells in the bloodstream of patients with uveal melanoma: influence of surgical manipulation on the dissemination of tumour cells in the bloodstream. *Br. J. Ophthalmol.* 100(4), 468–472 (2016).

128 Kuroki T, Eguchi S. No-touch isolation techniques for pancreatic cancer. *Surg. Today* doi:10.1007/s00595–016–1317–5 (2016) (Epub ahead of print).

129 Martin OA, Anderson RL, Russell PA *et al.* Mobilization of viable tumor cells into the circulation during radiation therapy. *Int. J. Radiat. Oncol.* 88(2), 395–403 (2014).

130 Dorsey JF, Kao GD, MacArthur KM *et al.* Tracking viable circulating tumor cells (CTCs) in the peripheral blood of non-small-cell lung cancer (NSCLC) patients undergoing definitive radiation therapy: pilot study results. *Cancer* 121(1), 139–149 (2015).

131 Lowes LE, Lock M, Rodrigues G *et al.* The significance of circulating tumor cells in prostate cancer patients undergoing adjuvant or salvage radiation therapy. *Prostate Cancer Prostatic Dis.* 18, 358–364 (2015).

132 Babayan A, Hannemann J, Spotter J, Muller V, Pantel K, Joosse SA. Heterogeneity of estrogen receptor expression in circulating tumor cells from metastatic breast cancer patients. *PLoS ONE* 8(9), e75038 (2013).

133 Paoletti C, Muñiz MC, Thomas DG *et al.* Development of circulating tumor cell-endocrine therapy index in patients with hormone receptor-positive Breast Cancer. *Clin. Cancer Res.* 21(11), 2487–2498 (2015).

134 Reijm EA, Sieuwerts AM, Smid M *et al.* An 8-gene mRNA expression profile in circulating tumor cells predicts response to aromatase inhibitors in metastatic breast cancer patients. *BMC Cancer* 16(123), 1–9 (2016).

135 Fehm T, Muller V, Aktas B *et al.* HER2 status of circulating tumor cells in patients with metastatic breast cancer: A prospective, multicenter trial. *Breast Cancer Res. Treat.* 124(2), 403–412 (2010).

136 Riethdorf S, Fritsche H, Müller V *et al.* Detection of circulating tumor cells in peripheral blood of patients with metastatic breast cancer: a validation study of the CellSearch system. *Clin. Cancer Res.* 13(3), 920–928 (2007).

137 Ignatiadis M, Rothé F, Chaboteaux C *et al.* HER2-positive circulating tumor cells in breast cancer. *PLoS ONE* 6(1), e15624 (2011).

138 Schramm A, Friedl TWP, Schochter F *et al.* Therapeutic intervention based on circulating tumor cell phenotype in metastatic breast cancer: concept of the DETECT study program. *Arch. Gynecol. Obstet.* 293(2), 271–281 (2016).

139 Neves RPL, Raba K, Schmidt O *et al.* Genomic high-resolution profiling of single CKpos/CD45neg flow-sorting purified circulating tumor cells from patients with metastatic breast cancer. *Clin. Chem.* 60(10), 1290–1297 (2014).

140 Pestrin M, Salvianti F, Galardi F *et al.* Heterogeneity of PIK3CA mutational status at the single cell level in circulating tumor cells from metastatic breast cancer patients. *Mol. Oncol.* 9(4), 749–757 (2015).

141 Polzer B, Medoro G, Pasch S *et al.* Molecular profiling of single circulating tumor cells with diagnostic intention. *EMBO Mol. Med.* 6(11), 1371–1386 (2014).

142 Mazel M, Jacot W, Pantel K *et al.* Frequent expression of PD-L1 on circulating breast cancer cells. *Mol. Oncol.* 9(9), 1773–1782 (2015).

143 David R. PD-L1 expression by circulating breast cancer cells. *Lancet Oncol.* 16(7), e321 (2015).

144 Miyamoto DT, Lee RJ, Stott SL *et al.* Androgen receptor signaling in circulating tumor cells as a marker of hormonally responsive prostate cancer. *Cancer Discov.* 2(11), 995–1003 (2012).

145 Jiang Y, Palma JF, Agus DB, Wang Y, Gross ME. Detection of androgen receptor mutations in circulating tumor cells in castration-resistant prostate cancer. *Clin. Chem.* 56(9), 1492–1495 (2010).

146 Antonarakis ES, Lu C, Wang H *et al.* AR-V7 and resistance to enzalutamide and abiraterone in prostate cancer. *N. Engl. J. Med.* 371(11), 1028–1038 (2014).

• **AR-V7 is a splice variant of the androgen receptor that lacks the ligand-binding domain targeted by enzalutamide and abiraterone, but remains constitutively active as a transcription factor. The authors were able to detect AR-V7 in CTCs from metastatic castration-resistant prostate cancer patients using qRT-PCR and showed that the presence of this splice variant in CTCs was a predictive marker of therapeutic resistance to enzalutamide and abiraterone.**

147 Steinestel J, Luedeke M, Arndt A *et al.* Detecting predictive androgen receptor modifications in circulating prostate cancer cells. *Oncotarget* doi:10.18632/oncotarget.3925 (2015) (Epub ahead of print).

148 Thadani-Mulero M, Portella L, Sun S *et al.* Androgen receptor splice variants determine taxane sensitivity in prostate cancer. *Cancer Res.* 74(8), 2270–2282 (2014).

149 Antonarakis ES, Lu C, Luber B *et al.* Androgen receptor splice variant 7 and efficacy of taxane chemotherapy in patients with metastatic castration-resistant prostate cancer. *JAMA Oncol.* 1(5), 582–591 (2015).

150 Onstenk W, Sieuwerts AM, Kraan J *et al.* Efficacy of cabazitaxel in castration-resistant prostate cancer is independent of the presence of AR-V7 in circulating tumor cells. *Eur. Urol.* 68(6), 939–945 (2015).

151 Balbas MD, Evans MJ, Hosfield DJ *et al.* Overcoming mutation-based resistance to antiandrogens with rational drug design. *Elife* 2, e00499 (2013).

152 Joseph JD, Lu N, Qian J *et al.* A clinically relevant androgen receptor mutation confers resistance to second-generation antiandrogens enzalutamide and ARN-509. *Cancer Discov.* 3(9), 1020–1029 (2013).

153 Attard G, Swennenhuis JF, Olmos D *et al.* Characterization of ERG, AR and PTEN gene status in circulating tumor cells from patients with castration-resistant prostate cancer. *Cancer Res.* 69(7), 2912–2918 (2009).

154 Leversha MA, Han J, Asgari Z *et al.* Fluorescence *in situ* hybridization analysis of circulating tumor cells in metastatic prostate cancer. *Clin. Cancer Res.* 15(6), 2091–2097 (2009).

155 Stott SL, Lee RJ, Nagrath S *et al.* Isolation and characterization of circulating tumor cells from patients with localized and metastatic prostate cancer. *Sci. Transl. Med.* 2(25), 25ra23 (2010).

156 Danila DC, Anand A, Sung CC *et al.* TMPRSS2-ERG Status in circulating tumor cells as a predictive biomarker of sensitivity in castration-resistant prostate cancer patients treated with abiraterone acetate. *Eur. Urol.* 60(5), 897–904 (2011).

157 Reig O, Marin-Aguilera M, Carrera G *et al.* TMPRSS2-ERG in blood and docetaxel resistance in metastatic castration-resistant prostate cancer. *Eur. Urol.* doi:10.1016/j.eururo.2016.02.034 (2016) (Epub ahead of print).

158 Li J, Sharkey CC, Wun B, Liesveld JL, King MR. Genetic engineering of platelets to neutralize circulating tumor cells. *J. Control. Release* 228, 38–47 (2016).

159 Li J, Ai Y, Wang L *et al.* Targeted drug delivery to circulating tumor cells via platelet membrane-functionalized particles. *Biomaterials* 76, 52–65 (2016).

160 Wayne EC, Chandrasekaran S, Mitchell MJ *et al.* TRAIL-coated leukocytes that prevent the bloodborne metastasis of prostate cancer. *J. Control. Release* 223, 215–223 (2016).

161 Dondossola E, Dobroff AS, Marchiò S *et al.* Self-targeting of TNF-releasing cancer cells in preclinical models of primary and metastatic tumors. *Proc. Natl Acad. Sci. USA* 113(8), 2223–2228 (2016).

• **Proof of concept study demonstrating the use of genetically modified CTCs to deliver anticancer agents. The authors exploited the self-seeding ability of CTCs by engineering them to release murine TNF such that they home to and reinfiltrate primary tumors and metastatic deposits to elicit apoptosis of cancer cells, thereby decreasing the tumor burden in immunocompetent mice.**

162 Huang W, Qi C-B, Lv S-W *et al.* Determination of DNA and RNA epigenetic modifications in circulating tumor cells by mass spectrometry. *Anal. Chem.* 88, 1378–1384 (2015).

163 Lianidou ES. Gene expression profiling and DNA methylation analyses of CTCs. *Mol. Oncol.* 10(3), 431–442 (2016).

164 Lehmann-Werman R, Neiman D, Zemmour H *et al.* Identification of tissue-specific cell death using methylation patterns of circulating DNA. *Proc. Natl Acad. Sci. USA* 113(13), e1826–e1834 (2016).

165 Shan M, Yin H, Li J *et al.* Detection of aberrant methylation of a six-gene panel in serum DNA for diagnosis of breast cancer. *Oncotarget* 7(14), 18485–18494 (2016).

166 Macosko EZ, Basu A, Satija R *et al.* Highly parallel genome-wide expression profiling of individual cells using nanoliter droplets. *Cell* 161(5), 1202–1214 (2015).

167 Macaulay IC, Haerty W, Kumar P *et al.* G&T-seq: parallel sequencing of single-cell genomes and transcriptomes. *Nat. Methods* 12(6), 519–522 (2015).

168 Dey SS, Kester L, Spanjaard B, Bienko M, van Oudenaarden A. Integrated genome and transcriptome sequencing of the same cell. *Nat. Biotechnol.* 33(3), 285–289 (2015).

169 Angermueller C, Clark SJ, Lee HJ *et al.* Parallel single-cell sequencing links transcriptional and epigenetic heterogeneity. *Nat. Methods* 13(3), 229–232 (2016).

170 Yu M, Bardia A, Aceto N *et al. Ex vivo* culture of circulating breast tumor cells for individualized testing of drug susceptibility. *Science* 345(6193), 216–220 (2014).

171 Gao D, Vela I, Sboner A *et al.* Organoid cultures derived from patients with advanced prostate cancer. *Cell* 159(1), 176–187 (2014).

172 Williams ES, Rodriguez-Bravo V, Rodriquez-Bravo V *et al.* Generation of prostate cancer patient derived xenograft models from circulating tumor cells. *J. Vis. Exp.* 105, 53182 (2015).

173 Malaney P, Nicosia SV, Dave V. One mouse, one patient paradigm: new avatars of personalized cancer therapy. *Cancer Lett.* 344(1), 1–12 (2014).

174 Lunardi A, Pandolfi PP. A co-clinical platform to accelerate cancer treatment optimization. *Trends Mol. Med.* 21(1), 1–5 (2015).

Single-Cell Analysis of Circulating Tumor Cells as a Window into Tumor Heterogeneity

David T. Miyamoto,[1,2] David T. Ting,[1,3] Mehmet Toner,[4,5] Shyamala Maheswaran,[1,4] and Daniel A. Haber[1,3,6]

[1]*Massachusetts General Hospital Cancer Center, Boston, Massachusetts 02114*

[2]*Department of Radiation Oncology, Massachusetts General Hospital and Harvard Medical School, Boston, Massachusetts 02114*

[3]*Department of Medicine, Massachusetts General Hospital and Harvard Medical School, Boston, Massachusetts 02114*

[4]*Department of Surgery, Massachusetts General Hospital and Harvard Medical School, Boston, Massachusetts 02114*

[5]*Center for Engineering in Medicine, Massachusetts General Hospital and Shriners Hospitals for Children, Charlestown, Massachusetts 02129*

[6]*Howard Hughes Medical Institute, Chevy Chase, Maryland 20815*

Correspondence: dhaber@mgh.harvard.edu

Recent advances in microfluidic approaches have enabled the efficient isolation and detailed molecular characterization of circulating tumor cells (CTCs) in the peripheral blood of patients with cancer. Single-cell molecular analyses of CTCs reveal a tremendous degree of intracellular heterogeneity in CTC populations, reflective of heterogeneity across different patients as well as the underlying heterogeneity of tumors within each individual patient. These studies have enabled the identification of heterogeneous drug resistance mechanisms that can coexist in treatment refractory tumors. CTC analyses also enable serial noninvasive monitoring in patients and can capture the emergence of tumor heterogeneity over time, whether due to tumor evolution through genetic instability or through cellular plasticity. The presence and extent of intratumoral heterogeneity as revealed through the study of CTCs have important clinical implications for understanding and predicting the development of treatment resistance in a variety of solid tumors and for formulating appropriate therapeutic strategies in the effective treatment of cancer.

Major advances in our molecular understanding of cancer have led to the development of effective new therapies that target tumor-specific genetic alterations, often resulting in profound responses in subsets of patients with specific oncogenic drivers in their tumors (Haber et al. 2011; Hyman et al. 2017). However, acquired resistance to therapy remains a pressing problem, and the emergence of resistant subclones within heterogeneous tumors represents a significant barrier to the effective treatment of cancer. Detailed next-generation sequencing studies have showed dramatic spatial and temporal heterogeneity in metastatic and primary tumors from individual patients (Gerlinger et al. 2012; Wu et al. 2012), but such analyses present technical and logistical challenges to routine clinical implementation, particularly for cancers that frequently metastasize to the bone, brain, or lungs. Tumor heterogeneity is especially difficult to study in patients with multiple metastases, because capturing the full range of relevant tumor clones would require invasive biopsies of multiple different individual sites of metastatic disease. Furthermore, traditional tissue biopsies sample only a small portion of a tumor, and thus the range of clones within a heterogeneous tumor may not be fully represented.

The sampling of tumor cells that circulate in the peripheral blood, or "circulating tumor cells" (CTCs), provides an elegant solution to the study of tumor heterogeneity, because CTCs may be a more representative sample of invasive tumor cell populations derived from heterogeneous tumors in multiple sites within an individual patient. In addition, the ability to sample cells in the blood noninvasively at multiple time points allows for the longitudinal study of tumor evolution over time. Recent advances in microfluidic engineering have made possible the development of novel platform technologies that efficiently isolate rare CTCs at the single-cell level, thus enabling the study of single CTCs to gain insights into tumor heterogeneity and treatment resistance in a variety of cancers.

MICROFLUIDIC ISOLATION OF CIRCULATING TUMOR CELLS

Although the existence of circulating populations of tumor cells in the peripheral blood was first posited in 1869 (Ashworth 1869), the isolation and study of CTCs has been a challenging endeavor because of their rarity

Published by Cold Spring Harbor Laboratory Press; doi: 10.1101/sqb.2016.81.031120

and fragility. In the past several years, a variety of methods and technologies have been developed to isolate and enumerate CTCs. In this concise review, we focus on microfluidic CTC isolation technologies that were developed in our laboratories; other CTC isolation technologies have been reviewed in detail elsewhere (Alix-Panabieres and Pantel 2014, 2016; Haber and Velculescu 2014; Miyamoto et al. 2014; Li et al. 2015). In collaboration with our bioengineering colleagues at the Massachusetts General Hospital, we developed a series of microfluidic devices aimed at the gentle and efficient isolation of CTCs from blood. The first- and second-generation microfluidic devices, the $^{\mu p}$CTC-Chip and the ^{HB}CTC-Chip, process blood through microfluidic channels and rely on the physical capture and immobilization of CTCs onto microfluidic surfaces coated with antibodies directed against tumor-specific cell surface antigens (Nagrath et al. 2007; Stott et al. 2010). The third-generation device, the CTC-iChip, is a tumor antigen-independent CTC isolation technology based on the concept of negative depletion, in which leukocytes, erythrocytes, platelets, and noncellular objects are removed from the blood, resulting in the enrichment of an untagged population of CTCs (Ozkumur et al. 2013; Karabacak et al. 2014). Because the CTC-iChip enables the efficient, gentle isolation of intact, untagged CTCs in suspension, it has allowed for detailed single-cell molecular analyses of CTCs from cancer patients and mouse models, thus revealing new insights into tumor heterogeneity at the single-cell level.

The microfluidic CTC-iChip uses three integrated sequential steps, consisting of continuous deterministic lateral displacement for size-based separation of CTCs and leukocytes from whole blood, inertial focusing for precise alignment of cells in a microchannel, and microfluidic magnetophoresis for removal of leukocytes prebound to magnetic beads labeled with anti-CD45, anti-CD16, and anti-CD66b antibodies (Karabacak et al. 2014). This tumor antigen-independent purification method enables the isolation of CTCs without assumptions regarding the nature of cell surface epitopes present on the tumor cells. Using the integrated microfluidic CTC-iChip, up to 10^7 cells per second can be sorted, enabling the sensitive, efficient, and high-throughput isolation of CTCs. The purity of CTCs within the enriched product ranges between 0.01% and 10%, depending on the burden of CTCs present in the patient's circulation. Importantly, CTCs isolated using this method are intact and untagged and amenable to a variety of downstream biological and molecular analyses including immunofluorescence, RNA-in situ hybridization, single-cell RNA-seq, and in vitro culture (Ozkumur et al. 2013; Aceto et al. 2014; Ting et al. 2014; Yu et al. 2014; Miyamoto et al. 2015). These sensitive analyses are possible because the gentle microfluidic enrichment processes of the CTC-iChip preserves the integrity and viability of isolated cells, in contrast to other methods that require cellular fixation and antibody-mediated binding of magnetic beads to cell membrane epitopes. Of note, our single CTC RNA-seq studies suggest that approximately one-half of CTCs have RNA at various stages of degradation even when isolated using this gentle microfluidic method, indicating that many cells in the circulation are nonviable (Ting et al. 2014; Miyamoto et al. 2015). Nevertheless, the quality and integrity of RNA in CTCs isolated using the CTC-iChip are well-preserved compared with prior methods, thus enabling single-cell RNA expression analyses, including the study of intracellular heterogeneity.

INSIGHTS INTO INTRATUMOURAL HETEROGENEITY THROUGH CTCs

Prostate Cancer

Prostate cancer is a heterogeneous entity, with primary tumors that are frequently multifocal and arise from divergent cancer clones (Andreoiu and Cheng 2010; Cooper et al. 2015). Metastases in prostate cancer are likely established through polyclonal seeding of divergent clones (Gundem et al. 2015), although some studies point to the conservation of driver lesions in metastatic lesions within individuals (Kumar et al. 2016). Consistent with substantial intratumoral heterogeneity, we observed through single-cell immunofluorescence analysis heterogeneous and varying degrees of androgen receptor (AR) signaling in CTCs from patients with castration-resistant prostate cancer (CRPC), in striking contrast to relatively homogeneous CTC populations with activated AR signaling in patients with untreated prostate cancer (Miyamoto et al. 2012). Similar levels of heterogeneity have been observed in prostate CTCs with respect to cellular morphologic criteria, related to disease status and cell differentiation state (Chen et al. 2015; Beltran et al. 2016). Single-cell RNA-seq of CTCs isolated from CRPC patients revealed a tremendous degree of heterogeneity in expression profiles, both in CTC populations from individual patients and across different patients (Miyamoto et al. 2015). Indeed, upon unsupervised hierarchical clustering of transcriptional profiles, the mean correlation coefficient for single CTCs from individual patients was significantly lower than the mean correlation coefficient of single cells from prostate cancer cell lines, and it was similar to that of single cells across multiple different cell lines, suggesting a much higher level of heterogeneity in CTCs. Nevertheless, these single CTCs clustered based on their patient of origin, indicative of shared transcriptional programs among CTCs derived from any given individual patient.

Heterogeneity at the single CTC level was also observed in the acquisition of varied mechanisms of resistance to AR-targeted therapies (Miyamoto et al. 2015). In an analysis of specific molecular aberrations in CTCs, including previously reported AR splice variants and AR mutations (Antonarakis et al. 2014; Robinson et al. 2015), we noted that single CTCs from individual patients expressed remarkable heterogeneity in their expression of different AR splice variants. More than half of patients had multiple CTCs expressing different AR splice variants, and about one of six single CTCs had expression of multiple different AR splice variants simultaneously.

Through the analysis of transcriptional differences between CTCs from patients who were resistant to the antiandrogen therapy enzalutamide compared with patients who were enzalutamide naïve, we identified two AR-independent pathways associated with resistance to enzalutamide: we confirmed the previously reported activation of glucocorticoid receptor (GR) (Arora et al. 2013) and discovered elevated noncanonical Wnt (ncWnt) signaling, finding that both of these resistance pathways were activated in different subsets of cells. Thus, we found that complex and heterogeneous drug resistance mechanisms exist in advanced prostate cancer, as revealed by the study of heterogeneous populations of CTCs. The degree of heterogeneity observed in CTCs in CRPC patients is consistent with intratumoral heterogeneity observed in patients with advanced metastatic prostate cancer, suggestive of the polyclonal seeding of divergent clones (Lohr et al. 2014; Gundem et al. 2015; Jiang et al. 2015), and is reflective of the variety of molecular alterations that may occur in parallel in tumor cells during disease progression and the development of resistance to therapy.

Pancreatic Cancer

We observed similar intracellular heterogeneity in single CTCs isolated from the genetically engineered *LSL-Kras^{G12D}, Trp53$^{flox/flox\ or\ +}$, Pdx1-Cre* (KPC) mouse model of pancreatic cancer (Bardeesy et al. 2006; Ting et al. 2014). Although the genetic driver mutations were identical in CTCs from different mice because of their shared genetic background, there was nevertheless a significant level of heterogeneity observed within CTCs, with specific clustering of CTCs derived from different animals (Ting et al. 2014). These findings suggest the potential importance of somatically acquired genetic and epigenetic changes in defining the heterogeneity of CTC populations, despite a shared genetic background.

In the KPC pancreatic cancer mouse model, we noted three subsets of CTCs: a major "classical CTC" group with strong expression of epithelial markers, a group with enrichment of platelet markers, and a group associated with proliferation signatures (Ting et al. 2014). Notably, although the classical CTCs showed clear loss of the epithelial marker E-cadherin (*Cdh1*) consistent with epithelial-to-mesenchymal transition (EMT), they did not lose expression of other epithelial markers such as cytokeratins, and they showed heterogeneous expression of mesenchymal genes across single cells. Thus, many classical CTCs appear to be arrested in a biphenotypic EMT state. Nevertheless, they also showed great diversity in their transcriptional programs, including expression of cancer stem cell markers *Aldh1a1* and *Aldh1a2* in some cells, and surprising enrichment of extracellular matrix (ECM) transcripts in many CTCs. Indeed, this finding of ECM gene expression in CTCs was recapitulated in human pancreatic, breast, and prostate cancer patients, with enrichment of the core matrisome protein *SPARC* in 100% of pancreatic CTCs. Together, these studies of CTCs in the KPC genetic mouse model showed substantial intracellular heterogeneity in CTCs from mice despite a conserved genetic background and strong expression of ECM transcripts in a majority of pancreatic CTCs, suggestive of a remarkable ability of CTCs to make their own contributions to tumor stromal remodeling and establishment of a hospitable microenvironment at metastatic sites.

Breast Cancer

Considerable heterogeneity has also observed in single CTCs from breast cancer patients using a variety of methods, including microfluidic transcriptional profiling, targeted mutation detection, and next-generation sequencing (Powell et al. 2012; Deng et al. 2014; De Luca et al. 2016). We used an RNA-in situ hybridization (ISH) assay to observe a spectrum of expression of epithelial and mesenchymal markers in single breast CTCs (Yu et al. 2013), ranging from exclusively epithelial to exclusively mesenchymal CTCs, as well as CTCs in an intermediate state with dual expression of epithelial and mesenchymal markers, similar to the biphenotypic EMT state identified in the pancreatic cancer mouse model (Ting et al. 2014). Interestingly, the EMT features of CTCs varied according to histological subtype of breast cancer, where CTCs from ER^+/PR^+ and $HER2^+$ cancers were predominantly epithelial, and CTCs from triple-negative ($ER^-/PR^-/HER2^-$) breast cancer were predominantly mesenchymal. Examination of changes in EMT states before and after systemic therapy suggested that patients who responded to therapy showed a decrease in CTC numbers and/or a proportional decrease in mesenchymal compared with epithelial markers, and that those with progressive disease despite therapy showed an increase in mesenchymal markers in CTCs post-treatment. Thus, the EMT status of CTCs may serve as a potential biomarker of therapeutic response, with the degree of heterogeneity of cells reflective of their susceptibility to treatment.

Progressive disease in cancer patients is often accompanied by the appearance of multicellular clusters of CTCs (Molnar et al. 2001; Cho et al. 2012), and the presence of these CTC clusters in breast cancer patients is associated with a worse overall survival (Aceto et al. 2014). A detailed examination of CTC clusters in mouse models revealed that they have a critical role as mediators of cancer metastasis, because they have a higher propensity for seeding metastatic disease compared with single CTCs in circulation (Fidler 1973; Liotta et al. 1976; Aceto et al. 2014). Of note, cellular tagging and mixing studies in mice showed that nearly all CTC clusters were derived from oligoclonal precursor cells, indicative of their heterogeneous composition and origin (Aceto et al. 2014). Nevertheless, RNA-seq expression studies of breast cancer patient-derived single CTCs and CTC clusters showed a strong clustering pattern by patient of origin, and a high level of concordance in expression patterns between matched CTC clusters and

single CTCs from individual breast cancer patients, with the exception of a few candidate cluster-related genes including XBP1, AGR2, HER3, and plakoglobin (Aceto et al. 2014). Indeed, knockdown of plakoglobin in mouse models suppressed CTC cluster formation and development of metastases, pointing to an important role of this protein in tumor dissemination. Thus, two distinct populations of CTCs appear to coexist in the circulation, including single CTCs and CTC clusters with much higher metastatic potential, derived from oligoclonal precursor cells representative of the inherent heterogeneity of the primary tumor.

MONITORING TUMOR EVOLUTION AND HETEROGENEITY WITH CTCs

Although the evolution of tumors in response to initially effective targeted therapies has become increasingly appreciated, either through the selection of rare preexisting subclonal populations or through molecular tumor evolution (Hata et al. 2016), the routine sampling of tumors at multiple time points remains a major technical challenge. CTCs provide a uniquely accessible mechanism to perform noninvasive serial sampling of tumors over time, and hence they could prove revolutionary in monitoring tumor evolution in patients undergoing treatments. Although circulating tumor DNA (ctDNA) is another type of "liquid biopsy" that may be used to assess for the emergence of specific tumor mutations (Bardelli and Pantel 2017), tumor evolution occurs not just through genetic changes, but also from phenotypic changes through epigenetic cellular plasticity (Fig. 1). Such functional changes cannot be easily ascertained using ctDNA but rather require the use of functional assays in live tumor cells. Thus, the analysis of CTCs, CTC-derived cell lines, and patient-derived xenograft models are invaluable tools in the study of tumor evolution.

In breast cancer, the emergence of HER2 expressing subpopulations has been observed in CTCs from patients with initially $HER2^-$ tumors after exposure to multiple courses of therapy (Fehm et al. 2010; Lindstrom et al. 2012). Analysis of CTCs in such patients revealed discrete $HER2^+$ and $HER2^-$ subpopulations, which had the ability to interconvert spontaneously when maintained in culture (Jordan et al. 2016). Thus, a dynamic equilibrium of $HER2^+$ and $HER2^-$ cell populations exist within a heterogeneous tumor cell population, driven by spontaneous interconversion between these phenotypes. $HER2^+$ CTCs were more rapidly proliferative with activation of multiple receptor tyrosine kinase pathways, whereas $HER2^-$ CTCs showed resistance to cytotoxic chemotherapy and activation of Notch and DNA damage pathways. These two cell populations had comparable tumor initiating potential and similar expression of the stem cell marker *ALDH1*, suggesting that an underlying cellular

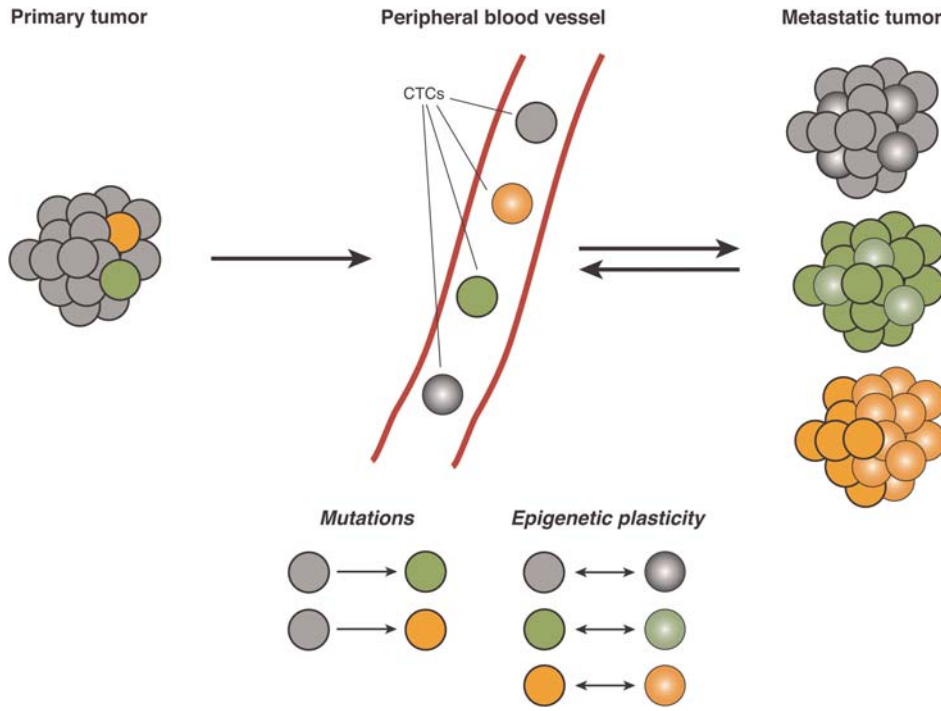

Figure 1. Schematic of heterogeneous tumors giving rise to circulating tumor cells (CTCs). CTCs arise from intravasation of cancer cells into peripheral blood vessels from primary or metastatic tumors. Single-cell heterogeneity can arise from genetic mutations (represented by gray circles becoming green or orange circles) or from epigenetic plasticity (represented by circles converting into spheres, and the reverse conversion of spheres to circles). Mutations and epigenetic changes can also occur simultaneously in the same cancer cell (represented by green and orange circles converting into green and orange spheres). Metastatic tumors may consist of heterogeneous groups of cancer cells that have undergone changes because of any combination of mutations, epigenetic plasticity, or both.

plasticity leads to disease progression and drug resistance in breast cancer, rather than preexisting drug-resistant subclones in a hierarchical cancer stem-cell model.

Whether resistant subclones arise within heterogeneous tumors through genetic instability or through cellular plasticity, their emergence portends the development of therapeutic resistance. The early detection of resistant subclonal populations may allow the early implementation of combination therapies that simultaneously target multiple different oncogenic pathways before a dominant resistant clone emerges. This strategy requires careful repeated monitoring of patients while on treatment, which may be accomplished using serial CTC analyses. In addition, the deployment of aggressive treatments earlier in the disease course before tumor evolution, such as adjuvant therapy following local therapy, may become an increasingly important approach guided by the monitoring of patients through CTC analyses.

CONCLUSION

In the new world of precision oncology, the development of novel therapeutics and diagnostics often merge with one another and are codependent. The emergence of heterogeneity in evolving tumors suggests the inadequacy of a "one-size-fits-all" approach to cancer therapy and necessitates the development of sophisticated molecular tests to guide the precision selection of appropriate therapeutic strategies. The driving force for the effective use of new targeted therapies is novel diagnostic strategies to identify the presence of specific molecular lesions in tumors, but at the same time there is no impetus to develop such diagnostic tests until clear therapeutic options have been developed that make these molecular lesions worth uncovering. This coevolution model in oncology is unprecedented and requires the integrated development of therapeutics and diagnostics at the levels of discovery, validation, and practical implementation in the clinic. Ultimately, the careful application of CTC-based diagnostic tools may help overcome treatment resistance mediated by tumor heterogeneity by guiding the rational selection and application of effective new targeted therapies.

ACKNOWLEDGMENTS

This work was supported by grants from the Prostate Cancer Foundation (D.T.M., D.A.H., S.M., M.T.), Charles Evans Foundation (D.A.H.), Department of Defense (D.T.M., D.T.T.), Howard Hughes Medical Institute (D.A.H.), Burroughs Wellcome Fund (D.T.T.), National Institute of Biomedical Imaging and Bioengineering (NIBIB) EB008047 (M.T.), and the MGH-Johnson & Johnson Center for Excellence in CTC Technologies (M.T., S.M.).

REFERENCES

Aceto N, Bardia A, Miyamoto DT, Donaldson MC, Wittner BS, Spencer JA, Yu M, Pely A, Engstrom A, Zhu H, et al. 2014. Circulating tumor cell clusters are oligoclonal precursors of breast cancer metastasis. *Cell* **158:** 1110–1122.

Alix-Panabieres C, Pantel K. 2014. Challenges in circulating tumour cell research. *Nat Rev Cancer* **14:** 623–631.

Alix-Panabieres C, Pantel K. 2016. Clinical applications of circulating tumor cells and circulating tumor DNA as liquid biopsy. *Cancer Discov* **6:** 479–491.

Andreoiu M, Cheng L. 2010. Multifocal prostate cancer: Biologic, prognostic, and therapeutic implications. *Hum Pathol* **41:** 781–793.

Antonarakis ES, Lu C, Wang H, Luber B, Nakazawa M, Roeser JC, Chen Y, Mohammad TA, Chen Y, Fedor HL, et al. 2014. AR-V7 and resistance to enzalutamide and abiraterone in prostate cancer. *N Engl J Med* **371:** 1028–1038.

Arora VK, Schenkein E, Murali R, Subudhi SK, Wongvipat J, Balbas MD, Shah N, Cai L, Efstathiou E, Logothetis C, et al. 2013. Glucocorticoid receptor confers resistance to antiandrogens by bypassing androgen receptor blockade. *Cell* **155:** 1309–1322.

Ashworth TR. 1869. A case of cancer in which cells similar to those in the tumors were seen in the blood after death. *Aust Med J* **14:** 146–149.

Bardeesy N, Aguirre AJ, Chu GC, Cheng KH, Lopez LV, Hezel AF, Feng B, Brennan C, Weissleder R, Mahmood U, et al. 2006. Both p16(Ink4a) and the p19(Arf)-p53 pathway constrain progression of pancreatic adenocarcinoma in the mouse. *Proc Natl Acad Sci* **103:** 5947–5952.

Bardelli A, Pantel K. 2017. Liquid biopsies, what we do not know (yet). *Cancer Cell* **31:** 172–179.

Beltran H, Jendrisak A, Landers M, Mosquera JM, Kossai M, Louw J, Krupa R, Graf RP, Schreiber NA, Nanus DM, et al. 2016. The initial detection and partial characterization of circulating tumor cells in neuroendocrine prostate cancer. *Clin Cancer Res* **22:** 1510–1519.

Chen JF, Ho H, Lichterman J, Lu YT, Zhang Y, Garcia MA, Chen SF, Liang AJ, Hodara E, Zhau HE, et al. 2015. Subclassification of prostate cancer circulating tumor cells by nuclear size reveals very small nuclear circulating tumor cells in patients with visceral metastases. *Cancer* **121:** 3240–3251.

Cho EH, Wendel M, Luttgen M, Yoshioka C, Marrinucci D, Lazar D, Schram E, Nieva J, Bazhenova L, Morgan A, et al. 2012. Characterization of circulating tumor cell aggregates identified in patients with epithelial tumors. *Phys Biol* **9:** 016001.

Cooper CS, Eeles R, Wedge DC, Van Loo P, Gundem G, Alexandrov LB, Kremeyer B, Butler A, Lynch AG, Camacho N, et al. 2015. Analysis of the genetic phylogeny of multifocal prostate cancer identifies multiple independent clonal expansions in neoplastic and morphologically normal prostate tissue. *Nat Genet* **47:** 367–372.

De Luca F, Rotunno G, Salvianti F, Galardi F, Pestrin M, Gabellini S, Simi L, Mancini I, Vannucchi AM, Pazzagli M, et al. 2016. Mutational analysis of single circulating tumor cells by next generation sequencing in metastatic breast cancer. *Oncotarget* **7:** 26107–26119.

Deng G, Krishnakumar S, Powell AA, Zhang H, Mindrinos MN, Telli ML, Davis RW, Jeffrey SS. 2014. Single cell mutational analysis of PIK3CA in circulating tumor cells and metastases in breast cancer reveals heterogeneity, discordance, and mutation persistence in cultured disseminated tumor cells from bone marrow. *BMC Cancer* **14:** 456.

Fehm T, Muller V, Aktas B, Janni W, Schneeweiss A, Stickeler E, Lattrich C, Lohberg CR, Solomayer E, Rack B, et al. 2010. HER2 status of circulating tumor cells in patients with metastatic breast cancer: A prospective, multicenter trial. *Breast Cancer Res Treat* **124:** 403–412.

Fidler IJ. 1973. The relationship of embolic homogeneity, number, size and viability to the incidence of experimental metastasis. *Eur J Cancer* **9:** 223–227.

Gerlinger M, Rowan AJ, Horswell S, Larkin J, Endesfelder D, Gronroos E, Martinez P, Matthews N, Stewart A, Tarpey P, et al. 2012. Intratumor heterogeneity and branched evolution revealed by multiregion sequencing. *N Engl J Med* **366:** 883–892.

Gundem G, Van Loo P, Kremeyer B, Alexandrov LB, Tubio JM, Papaemmanuil E, Brewer DS, Kallio HM, Hognas G, Annala M, et al. 2015. The evolutionary history of lethal metastatic prostate cancer. *Nature* **520:** 353–357.

Haber DA, Velculescu VE. 2014. Blood-based analyses of cancer: Circulating tumor cells and circulating tumor DNA. *Cancer Discov* **4:** 650–661.

Haber DA, Gray NS, Baselga J. 2011. The evolving war on cancer. *Cell* **145:** 19–24.

Hata AN, Niederst MJ, Archibald HL, Gomez-Caraballo M, Siddiqui FM, Mulvey HE, Maruvka YE, Ji F, Bhang HE, Krishnamurthy Radhakrishna V, et al. 2016. Tumor cells can follow distinct evolutionary paths to become resistant to epidermal growth factor receptor inhibition. *Nat Med* **22:** 262–269.

Hyman DM, Taylor BS, Baselga J. 2017. Implementing genome-driven oncology. *Cell* **168:** 584–599.

Jiang R, Lu YT, Ho H, Li B, Chen JF, Lin M, Li F, Wu K, Wu H, Lichterman J, et al. 2015. A comparison of isolated circulating tumor cells and tissue biopsies using whole-genome sequencing in prostate cancer. *Oncotarget* **6:** 44781–44793.

Jordan NV, Bardia A, Wittner BS, Benes C, Ligorio M, Zheng Y, Yu M, Sundaresan TK, Licausi JA, Desai R, et al. 2016. HER2 expression identifies dynamic functional states within circulating breast cancer cells. *Nature* **537:** 102–106.

Karabacak NM, Spuhler PS, Fachin F, Lim EJ, Pai V, Ozkumur E, Martel JM, Kojic N, Smith K, Chen PI, et al. 2014. Microfluidic, marker-free isolation of circulating tumor cells from blood samples. *Nat Protoc* **9:** 694–710.

Kumar A, Coleman I, Morrissey C, Zhang X, True LD, Gulati R, Etzioni R, Bolouri H, Montgomery B, White T, et al. 2016. Substantial interindividual and limited intraindividual genomic diversity among tumors from men with metastatic prostate cancer. *Nat Med* **22:** 369–378.

Li J, Gregory SG, Garcia-Blanco MA, Armstrong AJ. 2015. Using circulating tumor cells to inform on prostate cancer biology and clinical utility. *Crit Rev Clin Lab Sci* **52:** 191–210.

Lindstrom LS, Karlsson E, Wilking UM, Johansson U, Hartman J, Lidbrink EK, Hatschek T, Skoog L, Bergh J. 2012. Clinically used breast cancer markers such as estrogen receptor, progesterone receptor, and human epidermal growth factor receptor 2 are unstable throughout tumor progression. *J Clin Oncol* **30:** 2601–2608.

Liotta LA, Saidel MG, Kleinerman J. 1976. The significance of hematogenous tumor cell clumps in the metastatic process. *Cancer Res* **36:** 889–894.

Lohr JG, Adalsteinsson VA, Cibulskis K, Choudhury AD, Rosenberg M, Cruz-Gordillo P, Francis JM, Zhang CZ, Shalek AK, Satija R, et al. 2014. Whole-exome sequencing of circulating tumor cells provides a window into metastatic prostate cancer. *Nat Biotechnol* **32:** 479–484.

Miyamoto DT, Lee RJ, Stott SL, Ting DT, Wittner BS, Ulman M, Smas ME, Lord JB, Brannigan BW, Trautwein J, et al. 2012. Androgen receptor signaling in circulating tumor cells as a marker of hormonally responsive prostate cancer. *Cancer Discov* **2:** 995–1003.

Miyamoto DT, Sequist LV, Lee RJ. 2014. Circulating tumour cells-monitoring treatment response in prostate cancer. *Nat Rev Clin Oncol* **11:** 401–412.

Miyamoto DT, Zheng Y, Wittner BS, Lee RJ, Zhu H, Broderick KT, Desai R, Fox DB, Brannigan BW, Trautwein J, et al. 2015. RNA-Seq of single prostate CTCs implicates noncanonical Wnt signaling in antiandrogen resistance. *Science* **349:** 1351–1356.

Molnar B, Ladanyi A, Tanko L, Sreter L, Tulassay Z. 2001. Circulating tumor cell clusters in the peripheral blood of colorectal cancer patients. *Clin Cancer Res* **7:** 4080–4085.

Nagrath S, Sequist LV, Maheswaran S, Bell DW, Irimia D, Ulkus L, Smith MR, Kwak EL, Digumarthy S, Muzikansky A, et al. 2007. Isolation of rare circulating tumour cells in cancer patients by microchip technology. *Nature* **450:** 1235–1239.

Ozkumur E, Shah AM, Ciciliano JC, Emmink BL, Miyamoto DT, Brachtel E, Yu M, Chen PI, Morgan B, Trautwein J, et al. 2013. Inertial focusing for tumor antigen-dependent and -independent sorting of rare circulating tumor cells. *Sci Transl Med* **5:** 179ra147.

Powell AA, Talasaz AH, Zhang H, Coram MA, Reddy A, Deng G, Telli ML, Advani RH, Carlson RW, Mollick JA, et al. 2012. Single cell profiling of circulating tumor cells: Transcriptional heterogeneity and diversity from breast cancer cell lines. *PLoS One* **7:** e33788.

Robinson D, Van Allen EM, Wu YM, Schultz N, Lonigro RJ, Mosquera JM, Montgomery B, Taplin ME, Pritchard CC, Attard G, et al. 2015. Integrative clinical genomics of advanced prostate cancer. *Cell* **161:** 1215–1228.

Stott SL, Hsu CH, Tsukrov DI, Yu M, Miyamoto DT, Waltman BA, Rothenberg SM, Shah AM, Smas ME, Korir GK, et al. 2010. Isolation of circulating tumor cells using a microvortex-generating herringbone-chip. *Proc Natl Acad Sci* **107:** 18392–18397.

Ting DT, Wittner BS, Ligorio M, Vincent Jordan N, Shah AM, Miyamoto DT, Aceto N, Bersani F, Brannigan BW, Xega K, et al. 2014. Single-cell RNA sequencing identifies extracellular matrix gene expression by pancreatic circulating tumor cells. *Cell Rep* **8:** 1905–1918.

Wu X, Northcott PA, Dubuc A, Dupuy AJ, Shih DJ, Witt H, Croul S, Bouffet E, Fults DW, Eberhart CG, et al. 2012. Clonal selection drives genetic divergence of metastatic medulloblastoma. *Nature* **482:** 529–533.

Yu M, Bardia A, Wittner BS, Stott SL, Smas ME, Ting DT, Isakoff SJ, Ciciliano JC, Wells MN, Shah AM, et al. 2013. Circulating breast tumor cells exhibit dynamic changes in epithelial and mesenchymal composition. *Science* **339:** 580–584.

Yu M, Bardia A, Aceto N, Bersani F, Madden MW, Donaldson MC, Desai R, Zhu H, Comaills V, Zheng Z, et al. 2014. Cancer therapy. Ex vivo culture of circulating breast tumor cells for individualized testing of drug susceptibility. *Science* **345:** 216–220.